A Sheffield Hallam University thesis

ProQuest Number: 10697200

ProQuest 10697200

Advanced Applications of Numerical Modelling Techniques for Clay Extruder Design

Saravanakumar Kandasamy

A thesis submitted in partial fulfilment of the requirements of Sheffield Hallam University for the degree of Master of Philosophy

April-2013

Acknowledgement

Preface

A major portion of the research work discussed in this report was completed through Knowledge Transfer Partnership **(KTP)** programme **(Ref.No:KTP007670),** between Sheffield Hallam University (SHU), United Kingdom (U.K) and Craven Fawcett Limited **(C.F Ltd)** - a part of Group Rhodes Limited, U.K.

KTP is a U.K government initiated programme intended to support mainly the small and medium scale business sectors in the U.K. It focuses on improving their business prospects, either by solving any technological or management issues existing in their business structure or to improve their product quality and introduce new products. The main aim is to increase the competitiveness and create healthy business prospects within the economy. The required objectives of a KTP programme will be achieved by establishing a short term partnership between a Higher Educational Institution and a company registered in the U.K. The aim and objectives of the project will be defined clearly by the members of participating organisation and will be achieved through a working member, called an Associate.

Established in the year 1836, Sheffield Hallam University is one among the top 50 higher education institutions in the U.K, to undertake research works in the subject of engineering. It has dedicated research institutions and lab facilities for carrying out world class research works under the supervision of academic experts from various areas of mechanical and materials engineering. It also possesses a dedicated team of academics and experts to support industrial partnership based projects and research works in the field of engineering.

Craven Fawcett Limited, established in the year 1843, is a subsidiary company of Group Rhodes Limited. It specialises in design and manufacturing of clay working machines, which has its application mainly in heavy clay structural ceramics industry. The range of products offered by them includes box feeders, grinding mills, mixers, conveyors and extruders. Being an ISO 9001 certified organisation and a well reputed company in U.K

and worldwide, it places a greater emphasis on design, and material selection for the components of their products, optimising the production process and time and improving the quality and efficiency of their products. Combined de-airing type (Vacuum type) extruder is a specialised product of C.F Ltd. and being a market leader in this segment, the management has a keen interest in introducing and using advanced computer aided techniques such as Computational Fluid Dynamics and Finite Element Analysis to improve their current designs and to fast track the development of new extruders and its components. Through this they are intended to achieve a better and energy efficient extruders, for the use of ceramic industries. Since the company did not have any experience and expertise available in-house to accomplish this, a KTP programme was established and the research work was undertaken to meet the required objectives. This report summarises the research work undertaken and accomplishments towards the company's intended requirement.

Abstract

Ceramic materials play a vital role in our day to day life. Recent advances in research, manufacture and processing techniques and production methodologies have broadened the scope of ceramic products such as bricks, pipes and tiles, especially in the construction industry. These are mainly manufactured using an extrusion process in auger extruders. During their long history of application in the ceramic industry, most of the design developments of extruder systems have resulted from expensive laboratory-based experimental work and field-based trial and error runs. In spite of these design developments, the auger extruders continue to be energy intensive devices with high operating costs. Limited understanding of the physical process involved in the process and the cost and time requirements of lab-based experiments were found to be the major obstacles in the further development of auger extruders.

An attempt has been made herein to use Computational Fluid Dynamics (CFD) and Finite Element Analysis (FEA) based numerical modelling techniques to reduce the costs and time associated with research into design improvement by experimental trials. These two techniques, although used widely in other engineering applications, have rarely been applied for auger extruder development. This had been due to a number of reasons including technical limitations of CFD tools previously available. Modern CFD and FEA software packages have much enhanced capabilities and allow the modelling of the flow of complex fluids such as clay.

This research work presents a methodology in using Herschel-Bulkley's fluid flow based CFD model to simulate and assess the flow of clay-water mixture through the extruder and the die of a vacuum de-airing type clay extrusion unit used in ceramic extrusion. The extruder design and the operating parameters were varied to study their influence on the power consumption and the extrusion pressure. The model results were then validated using results from experimental trials on a scaled extruder which seemed to be in reasonable agreement with the former. The modelling methodology was then extended to full-scale industrial extruders. The technical and commercial

suitability of using light weight materials to manufacture extruder components was also investigated. The stress and deformation induced on the components, due to extrusion pressure, was analysed using FEA and suitable alternative materials were identified. A cost comparison was then made for different extruder materials. The results show potential of significant technical and commercial benefits to the ceramic industry.

Contents

List of figures

XI

XIII

XVI

List of tables

1.1 Bricks

Ceramic products like bricks, pipes and tiles have been used extensively in the construction industry for many years. The demand for ceramic products especially bricks have rapidly increased over the past few decades due to the excessive growth in population. This burgeoning demand has opened up a huge market potential for ceramic industries to thrive upon. In order to utilise the market potential to its full capacity, the brick industry needs to overcome some key challenges like better and efficient production methods, reduction of energy usage during manufacturing and reduced impact on environment through sustainable operation. The ceramic industry, compared to its predecessors has made significant and laudable changes in terms of production techniques and machines used. The modern industry is incorporated with completely automated production process and looks entirely different from how it was in the olden days. Energy efficiency in its operation is still an arduous task that needs to be accomplished. It requires an integrated effort from all the entities embedded in its entire supply chain, which includes raw material suppliers, other major systems and equipment providers. Brick industry, being energy intensive, faces an increasing pressure from the government and environmental organisations for reducing its environmental impact, by cutting down its energy consumption and emissions. This in turn has increased the scope for further research works in this field and a definite need to identify key areas in the brick manufacturing process and improve their performance.

1.2 Aim

The main aim of this research work is to assess and improve the design of auger extruders used in clay extrusion process using computational fluid dynamics (CFD) and Finite Element Analysis (FEA).

1.3 Objectives

The main objectives of this research work includes,

- Conduct a thorough literature search on previously completed research works in the clay extrusion process.

2

- Investigate suitable CFD techniques to model the clay extrusion process.
- Analyse the flow parameters like pressure and velocity for various designs and operating conditions.
- Assess the performance of the clay extruder with changes in design.
- Investigate alternate designs and materials to improve the performance of the extruders and reduce their capital costs.
- Experimentally validate the results obtained from the applied CFD modelling technique.

1.4 Research methodology

The objectives of this research work were achieved in three stages:

1. The first stage was dedicated to the use of computational methods for determining the extrusion pressure and the power requirement of extruders for various design and operational parameters.
2. The focus in the second stage was on experimental tests to assess the performance of a miniature scaled extruder. The results obtained from the experiments were used to validate the computational methodology used in first stage.
3. The third stage of this research focused on using FEA to predict the stresses induced on extruder components during the process of extrusion, for various materials. It also looked at the costs and technical benefits that could be achieved by using alternate materials.

1.5 Previous works

A similar effort was made by Jonathan Headley in 2009 and Alex Poyser in 2011, MSc. students at Sheffield Hallam University. In their work, both of them have used CFD techniques to study the flow characters of the clay and water system during the process of extrusion and assessed the performance of extruders. A detailed review of their works and the results obtained are discussed in Chapter-2.

1.6 Thesis outline

This report is divided into five chapters suitably to give the reader a clear picture about the need for design improvements of extruders used in brick industries and the use of CFD, FEA based numerical modelling technique to accomplish that.

A brief introduction is presented in Chapter 1, detailed review of existing research in the modelling of extruders, experimental studies and clay rheology is presented in Chapter-2. Experimental validation of the numerical modelling approach and assessing the performance and flow parameters of extruders and clay extrusion process using the CFD technique is presented in Chapter 3. Assessing mechanically induced stresses using FEA technique, potential alternative cost effective and light weight materials for improving the efficiency of extruders is presented in Chapter 4. Conclusions and suggestions for the future research work in this area are presented in Chapter 5.

A brief review on the prospect of brick industries and brick manufacturing process is presented in Appendix C.

Design, functional and process requirements of vacuum type de-airing extruder and the association of flow parameters to the performance of the system is reviewed in Appendix D.

Chapter-2   Review of existing work for ceramic extrusion

2.1 Introduction

The aim of this chapter is to provide a comprehensive review of scientific works undertaken by academic researchers and industrial professionals, focused on studying the flow parameters of clay and assess the performance of extruders using numerical and empirical methods. The results obtained and conclusions drawn from their studies are presented and discussed. The review is based on three key areas that are necessary to build and simulate a CFD model successfully; that includes numerical modelling methods for simulating clay extrusion or a ceramic shaping process, experimental studies conducted to assess key performance variables (like extrusion pressure) involved in ceramic shaping process and works related to rheological characters of clay-water system.

Even though there are different types of mechanical systems, which are termed as extruders, were used in the process of shaping, discussed briefly in Appendix- D, henceforth in this report the term extruders commonly refer to auger extruders, unless and until specified. The extruder system considered for this research work is vacuum type de-airing extruder, falls under the category of stiff extruders used in the heavy clay structural ceramic industries.

Due to the limitation in the availability of published works, that specifically discuss the simulation of the extrusion process and design assessment of extruders using CFD based numerical modelling technique, most of the work discussed here do not have direct relation to this research work. However it presents the reader with various scientific approaches and methods that were used and how significant those works were to the methodology used and results obtained from the numerical modelling approach undertaken through this research work.

2.2 Modelling and simulation of extruder system

Zhang et al. (2011) have investigated the process of clay extrusion in a de-airing type extruder, using CFD technique. In their research work they investigated the velocity of the clay material, during the process of extrusion, along the entire length of the auger and have assessed the variation of clay

6

velocity along the radial and longitudinal direction within the extruder chamber. They have also studied the effect of varying moisture contents and the auger speed on the velocity of the clay within the extruder chamber. In their work they have used a Bingham Fluid model to represent the flow physics of clay and water mixture and have assumed the flow process to be isothermal and laminar. The effect of gravity and inertial force were not accounted for in their model. Using a 3-D model with an unstructured T-grid mesh, they have solved their model in FLUENT-CFD solver and have presented their results.

It is understood from their work that the velocity of clay particles varies both along the longitudinal and radial directions of an extruder chamber, during the process of extrusion and also depends upon the moisture condition of the clay.

They have also predicted from their model that the velocity of clay near the wall zones (both at the hub's outer edge and barrel's inner edge) is almost zero and the maximum value is observed in the middle (area between hub and the barrel); which is demonstrated by the formation of an oval shaped pattern for the velocity of clay at different sections of the auger.

The formation of the secondary flow zone (a circular flow pattern), as discussed by them- demonstrates the plastic and elastic properties possessed by the clay during extrusion. The change from elastic zone to plastic zone is subjected to shear force experienced from the extruder components.

They have concluded from their study that the radial velocity is an important component for the mixing and plasticity of the material and the axial velocity is important for discharge rate. They have also mentioned that both these velocity components are influenced by the moisture content in the clay material used.

Hedley (2009) attempted to study the flow of clay through full scale de-airing type vacuum extruders using CFD technique. In his work he has used a 3-D, multiphase laminar flow approach and Herschel-Bulkley's fluid model to define the flow physics of the clay. He has assessed the dynamic pressure

developed during extrusion and velocity of clay in the direction of extrusion; with respect to various pitch length and speed of auger. He has used unstructured T-grid mesh elements to mesh the components of extruder and solved the model using FLUENT solver. In order to achieve a good quality mesh and avoid complexity while meshing the geometry, he has used a simplified geometry (uniform rectangular cross section) for the auger and neglected the effects of barrel and liner geometry. Using a constant density value for the clay material, the model has been solved with the effect of gravity. From his work it is understood that the pressure during extrusion rises gradually from the inlet of the auger and reaches a maximum value at a certain length of the auger and further down along the length of the auger the pressure reduces as the material approaches the exit area, as shown in Figure 2-1.
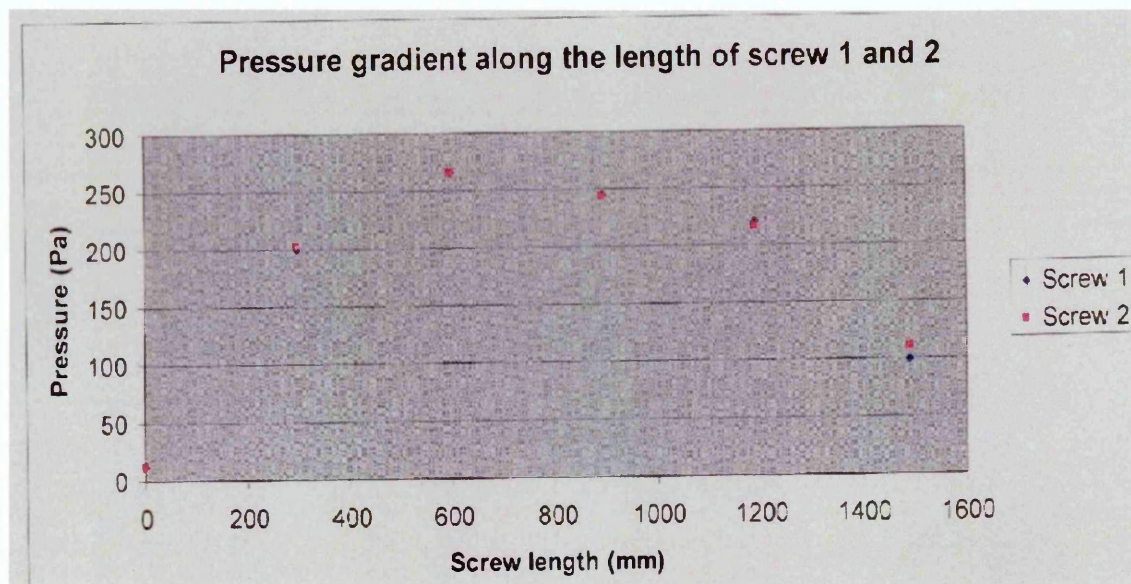
Figure 2-1 Extrusion pressure at various length of extruder

[Source: Hedley, 2009]

Also the dynamic pressure varies at different sections of auger with respect to the change in pitch length and speed of auger, as shown in Figure 2-2 and 2-3.

8
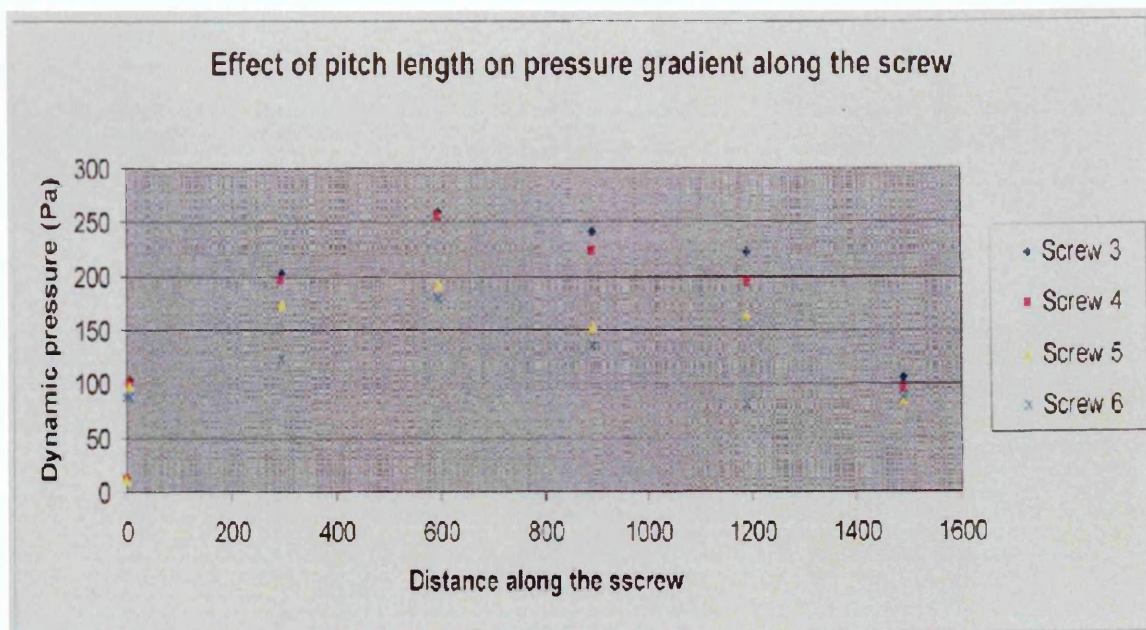
Figure 2-2 Dynamic pressure at various length of extruder
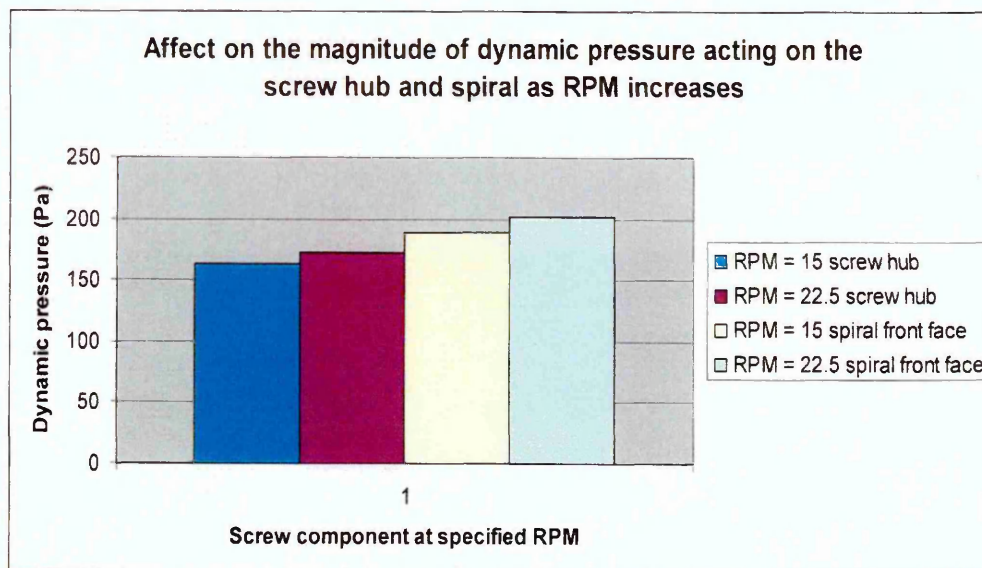
[Source: Hedley, 2009]

Figure 2-3 Dynamic pressure variation with respect to auger speed

[Source: Hedley, 2009]

The same trend was observed in the velocity as well, shown in Figure 2-4.
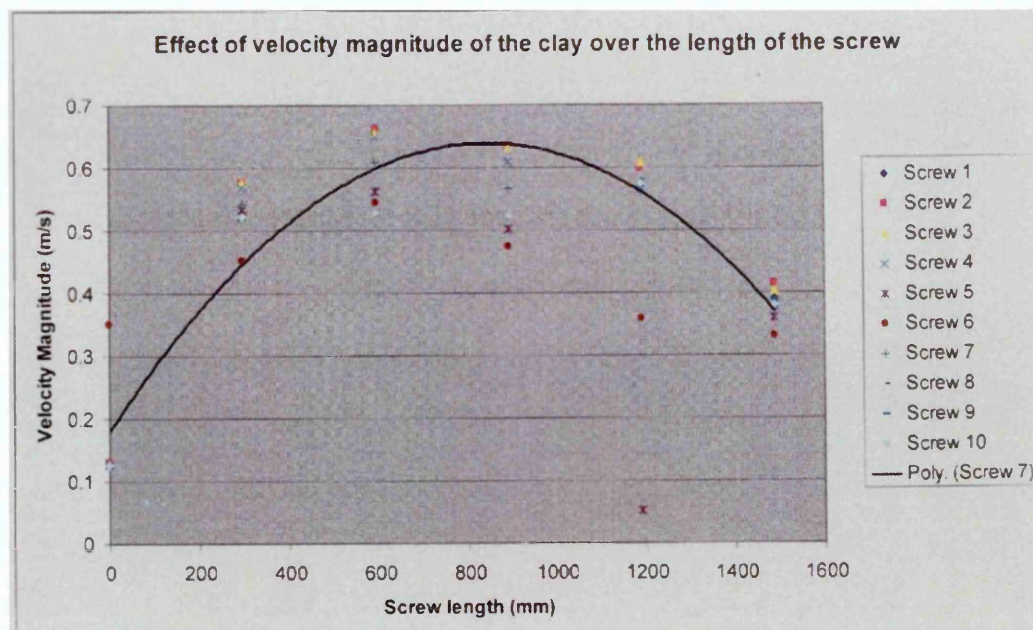
Figure 2-4 Clay velocity at various lengths of extruder

[Source: Hedley, 2009]

The results and discussions presented in his work, clearly indicates that the dynamic pressure and the velocity of clay observed during extrusion is influenced by the pitch length and speed of the auger.

Poyser (2011) attempted to use CFD technique to assess the performance of lab-scale model of an extruder system. Using a 3-D steady state, single phase laminar flow model approach with Herschel-Bulkley's fluid model for clay, he has assessed the performance of the scaled extruder. In his model, he has used unstructured T-grid mesh to discretize the geometry and Fluent-CFD solver to solve the model. From the results obtained through his work, he has suggested that the use of unsteady state method in CFD modelling could help to gain a better understanding of the flow process within an extruder system.

Händle (2007) has discussed about the application of simulation in ceramics. He has reviewed about numerical simulation of ceramic extrusion using CFD technique, and has presented various governing equations that typically represent the flow physics of ceramic materials. The author proposes that the ceramic material exhibits visco-plastic behaviour and is expected to take

the form of either a Bingham or Casson model. Figure 2-5 shows typical viscosity profiles of materials that follow the above mentioned fluid models.
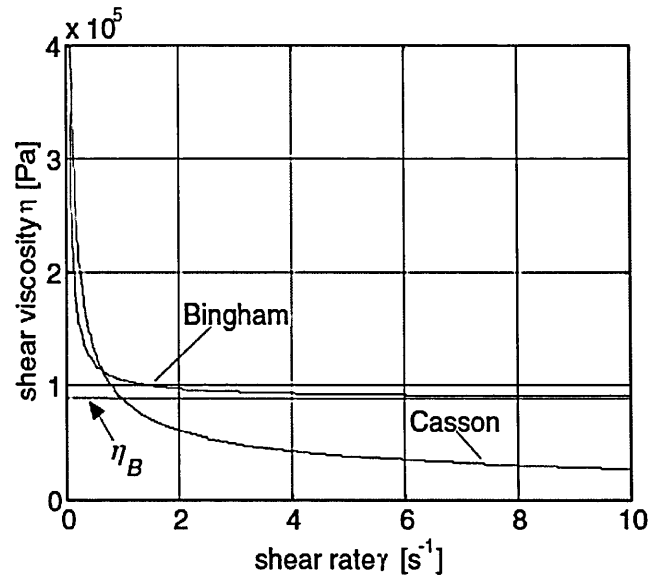
Figure 2-5 Viscosity profile for Bingham and Casson model fluids

[Source: Händle, 2007]

[Note: Unit for Shear viscosity is Pa.s, it is misprinted as Pa in the above picture]

Continuity equations for mass, momentum and energy, proposed by the authors are based on incompressible, Bingham fluid model. The reason for including the energy equation in the numerical model is because the viscosity of ceramic material is temperature dependent. He recommends that the accurate definition of ceramic material properties like density, viscosity and specific heat capacity at constant volume and specific heat conductivity is a vital part in ceramic extrusion process simulation.

Bouzakis et al. (2008) have investigated the stress distribution on the surface of a die mandrel, during the process of extrusion, using experimental and numerical modelling techniques. Using Finite Element Method (FEM) based numerical simulation (DEFORM); they have assessed the clay sliding velocity; various stress elements and its distribution on the surface of the mandrel. They have also compared the results obtained with the experimental results. Figure 2-6 shows the investigated model and results obtained.

11
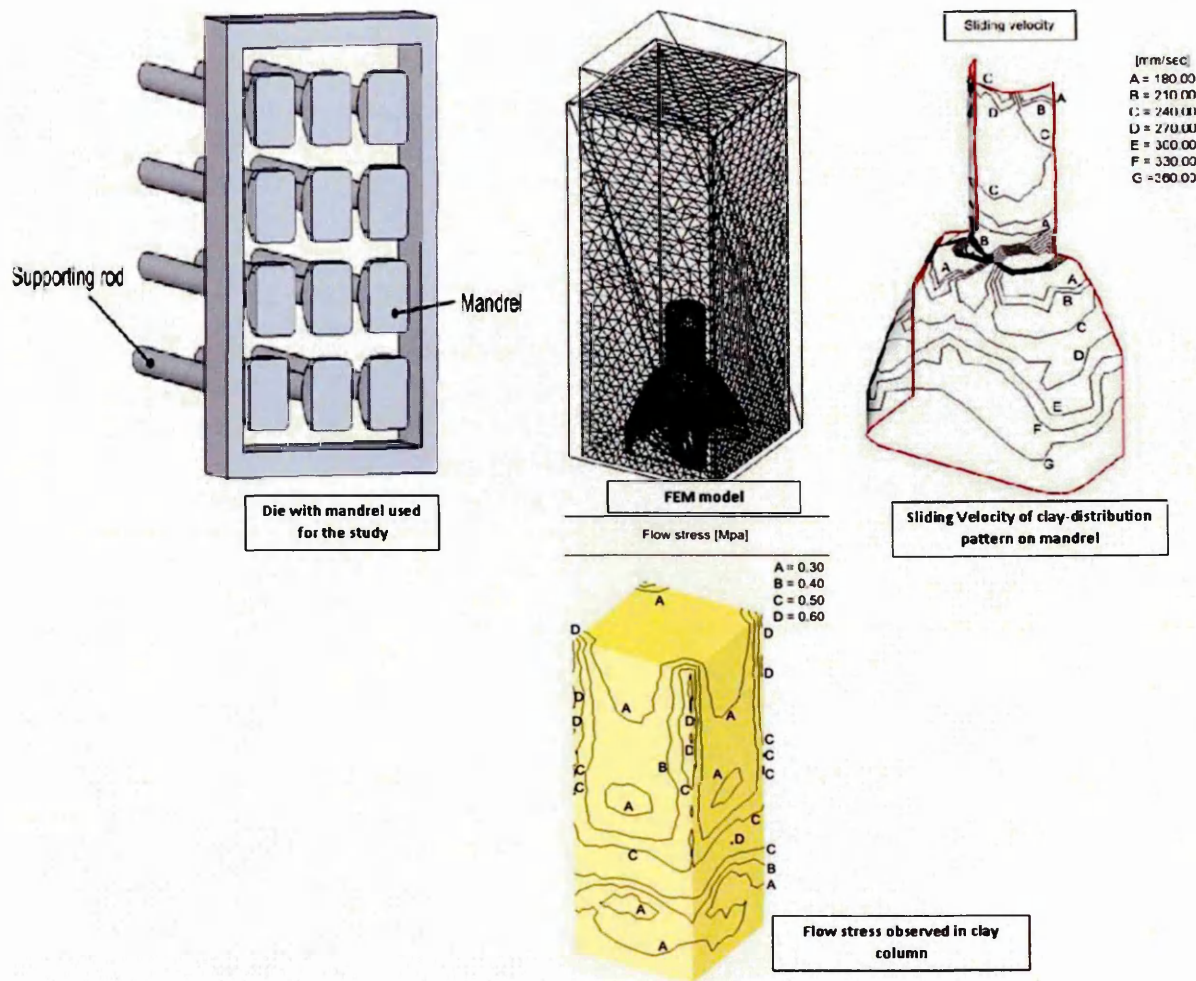
Figure 2-6 Stress induced on die mandrel during wet clay extrusion

[Source: Bouzakis et al. (2008)]

Through the experimental and numerical model results, they have derived a characteristic equation that represents the rigid- viscoplastic behaviour of wet clay, observed during extrusion. Based on the assumptions they made to include the frictional factor during extrusion, they suggests that the flow pattern of the rigid viscoplastic material like clay, is not effected by the friction on the wall surfaces and the stress induced on the die wall depends on the speed of extrusion .

Doltsinis and Schimmler (1998), using FEM, have investigated the process of ram extrusion used in making ceramic tubular components. In their work, considering the ceramic paste to be a viscous compressible fluid, they have developed a suitable numerical model to represent the flow features of the material. Using an analytical approach to determine material parameters

required for the numerical model they have predicted the flow velocity of the material within the barrel, die and the tool. By applying the developed FE model to an actual industrial scale system and through the results obtained, they have concluded that the FEA is adequate enough to represent the flow of such viscous materials and such computational methods can be used for modelling ceramic extrusion process to a higher degree of appropriateness.

Discussion:-

The efforts undertaken by professionals in various scientific communities, to apply numerical modelling and simulation as a tool to model the clay extrusion process, clearly indicates that there is an indisputable need for such tools in the ceramic industries. With the availability of wide range of fluid flow models and modelling techniques that are suitable, as illustrated above, there is inadequate evidence on the applicability of a particular numerical modelling technique and methodology suitable for auger extrusion process. Though **Zhang et al. (2011), Hedley (2009), Poyser (2011),** have attempted to use CFD to model the auger extrusion process and assess the performance of an extruder, their methodology does not really account for all the major features of an auger extrusion process. For instance, in all their work, the material density is considered to be a constant, which is not true in a real scenario. Also they have not given much importance to the clearance volume between the auger and the barrel in their model, which is considered to have a major influence on the extrusion pressure and the material flow.

The modelling technique and methodology used in this research work has taken into consideration of additional factors like change in density, temperature and temperature dependant properties that influences the process of extrusion and performance of an extruder. A detailed description about the CFD modelling approach undertaken in this research is presented in Chapter 3.

2.3 Design and performance evaluation of extruders

Johnson (1962) studied the design parameters of variable pitch or variable volume augers that influence the performance of an extruder system used in sewer pipe production using experimental methods. Combining both

13

geometrical and experimental methods, he has analysed the influence of auger diameter, pitch and conditions of raw material on the extruder performance. He has proposed that the determination of Displacement Volume Ratio (DVR) (function of pitch of the auger) of augers using mathematical methods is a significant approach in studying and comparing their performance.

The result obtained through his work indicates that the volumetric efficiency of a variable extruder increases when the size of the extrudate increases, even if the type of clay remains the same. He suggests that the efficiency of an extruder system depends on extrusion pressure, clay particle size and design modifications to the pitch and diameter of an auger. Suitable considerations to these parameters at the design stage could result in a more efficient system.

Lund et al. (1962) have studied the operating characteristics of augers used in pipe clay extrusion, with respect to various design parameters at specific moisture content of clay. In their work they have assessed the performance of constant and variable pitch augers. They have also determined the validity of scaled extruder results when extrapolating it to a full scale system. Based on the design data available for the augers used in production and using an empirical approach, they have designed experimental augers and assessed their performance. Using the approach of calculating DVR value to compare the performance of auger system, as discussed by **Johnson (1962)** and by employing a special device to maintain the consistency of the clay, they have assessed the extrusion rate, power consumption; die pressure and internal radial barrel pressure for constant and variable pitch auger systems. Figure 2-7 shows the effect of varying the displacement volume on the performance characters of augers for a constant pitch auger and Figure 2-8 shows the characteristic curves of the various experimental augers used in their study.
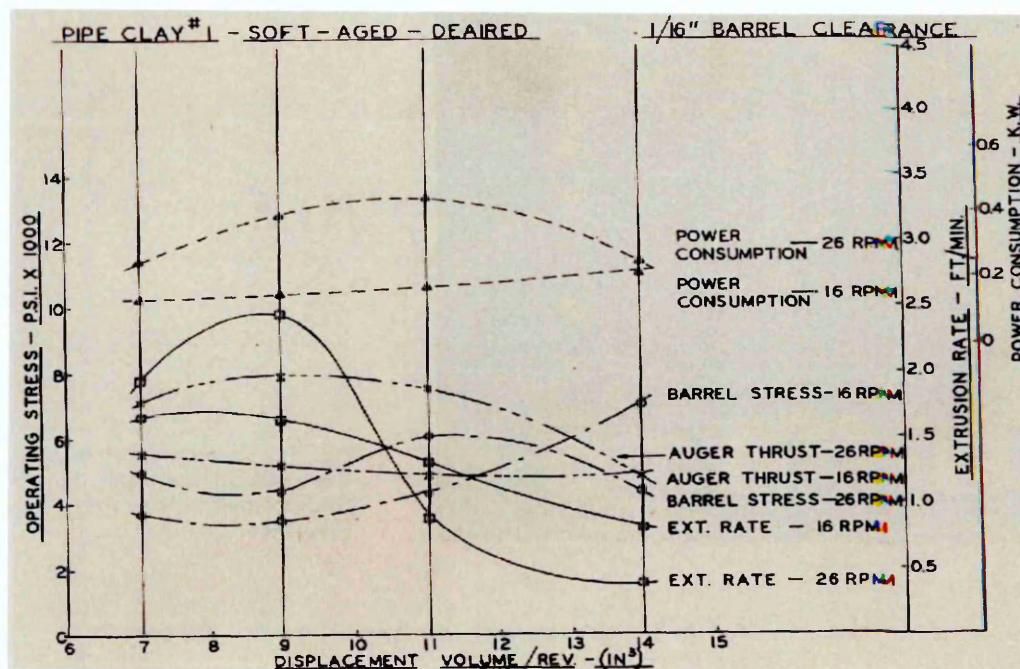
Figure 2-7 Effect of auger pitch variation on extruder performance

[Source: Lund et al. (1962)]
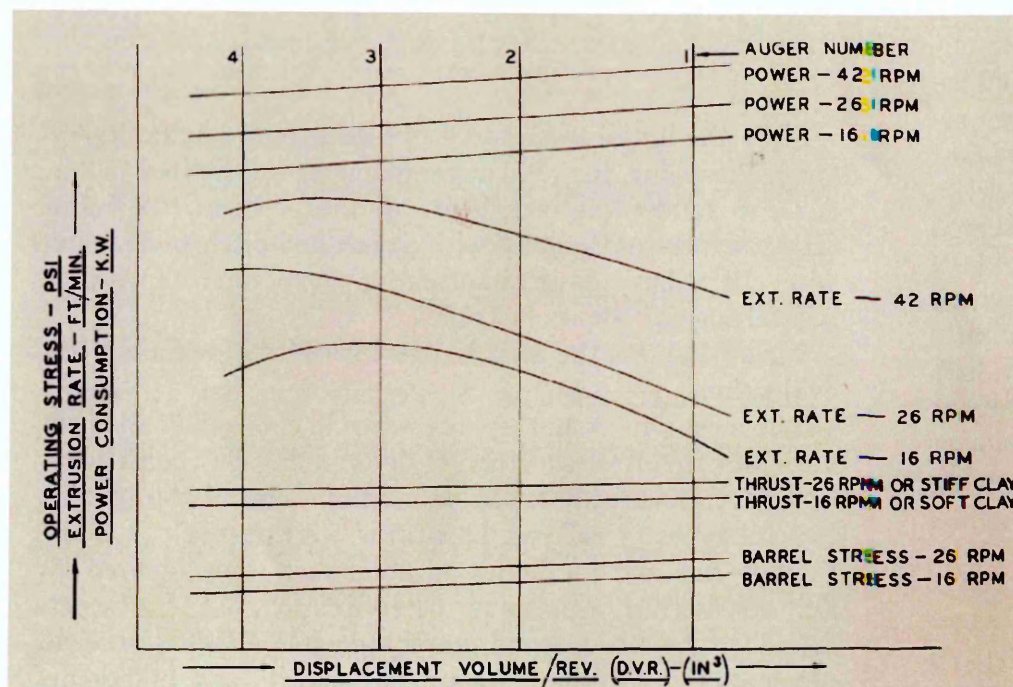
Figure 2-8 Performance characteristics profile for a typical auger

[Source: Lund et al. (1962)]

From the results obtained through their work on constant pitch auger, it is understood that the increase in auger speed and decrease in DVR (pitch) increases the extrusion rate. Also that power consumption is a function of

auger speed and clay consistency. Barrel stress increases with increase in auger speed, clay stiffness and clay particle size.

The results obtained through their work on variable pitch auger indicate that the extrusion rate for a variable volume or variable pitch auger is higher than that of a constant pitch auger. Also the compression ratio (ratio of change in volume between successive auger flights) of variable pitch auger influences the extrusion rate. They have also noted that changes in the tip volume of an auger also influence the extrusion rate.

In both the cases, they have noted that extruding clay with smaller particle size resulted in an increased extrusion rate and better flow character, compared to extruding clay with large particle size. This also confirms to the suggestion by **Norton (1954)**.

Seanor and Schweizer (1962) have investigated about mechanical and physical factors that affect auger design and its performance. They have suggested that the co-efficient of friction is an important factor that has significant effect on auger's performance. Also in order to have a better flow, the clay contacting surface in an auger should be sufficiently sloped to achieve better sliding for the clay, which enhances its flow. Hence they believed that reducing the pitch of auger will reduce the co-efficient of friction and will lessen the augers performance. This contradicts the above discussed results, presented by **Lund, et al. (1962)**. They had also postulated suitable design modifications for the leading face of an auger (working face of an auger which is subjected to stress and wear is called the leading face of an auger), to enhance the performance of a new auger and increase its life, right from installation. Since they did not validate their suggestions with any experimental results and also the co-efficient of friction varies with respect to clay stiffness, clay material and auger material, it is hard to include it at the earlier stages when designing an auger.

They have also studied the effect of adding half pitch augers or wings or half flights, to the tip of main auger system. Through investigating the performance of the extruder system by having single, double and triple wings at the end of the main auger, they have suggested that having wings in the

16

tip ensures smooth and uniform feeding of clay to the die section from extruder and ensures uniform pressure distribution over the entire area of die, as shown in Figure 2-9. Also an auger with three wings performs more efficiently than augers with single and double wings, when it is ensured that the die is mounted properly.
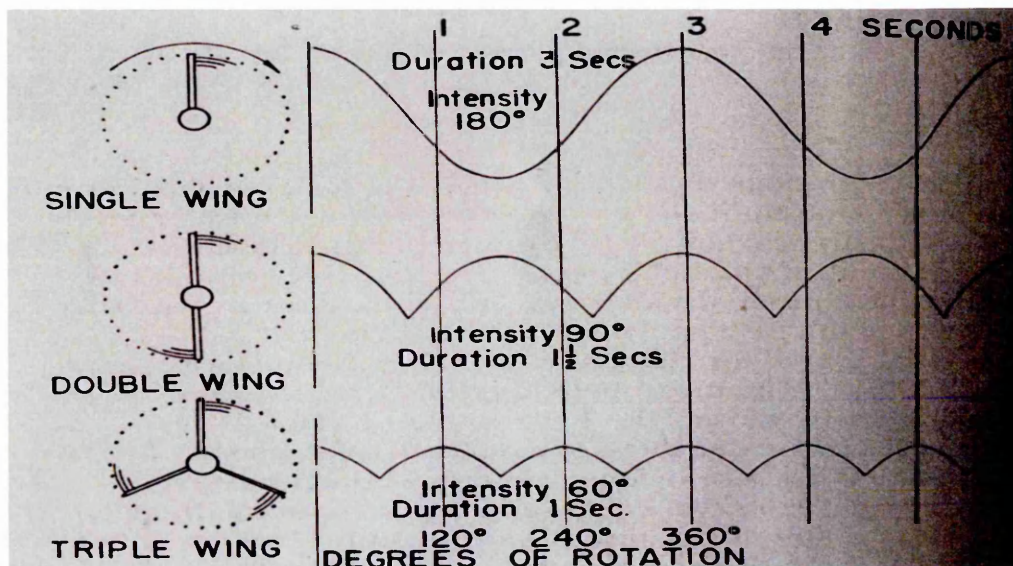
Figure 2-9 Pressure waves experienced in auger with half flights

[Source: Seanor and Schweizer, 1962]

Parks and Hill (1959) have developed mathematical equations for the purpose of designing augers and die for extrusion application. Through performing experiments in clay like plastic material with specific moisture content, they have developed a mathematical representation for calculating extrusion rate for auger and die section. They have also mentioned that the extruder system comprising the barrel, auger and die, is divided into different zones based on the functions they perform at different stages of extrusion process and the pressure during extrusion varies across each of these zones, as shown in Figure 2-10.

17
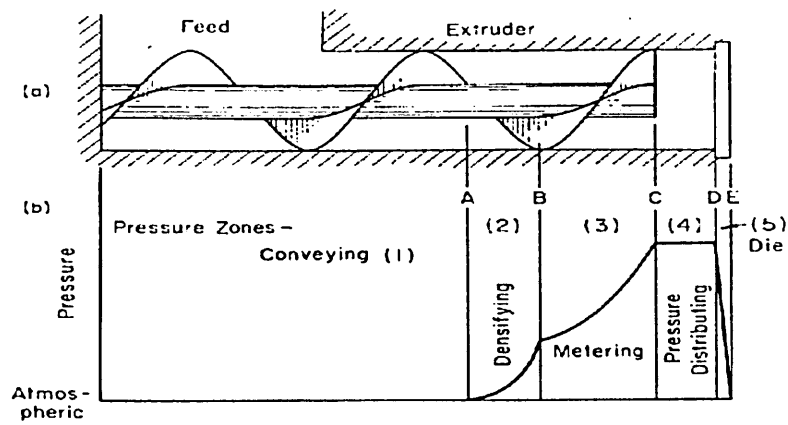
Figure 2-10 Typical pressure distribution in an extruder

[Source: Parks and Hill, 1959]

It is understood from their mathematical model that the extrusion rate at auger section is a function of outside diameter of auger, depth of auger channel, helix angle, clay material and speed of auger. Whereas the extrusion rate at die section is a function of pressure and it has linear relation as shown in Figure 2-11.
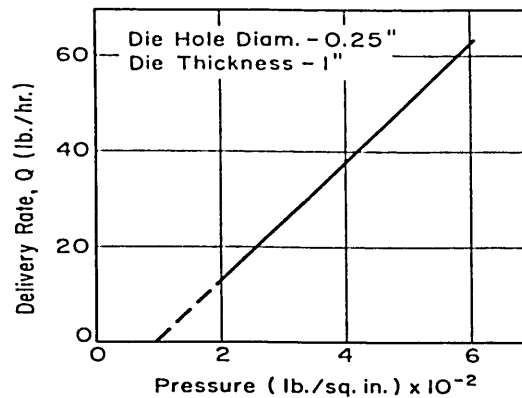
Figure 2-11 Effect of extrusion rate on die pressure

[Source: Parks and Hill, 1959]

It is clearly understood from their results that the pressure increases as the extrusion rate increases in the die section. They suggests that, though this linear relationship curve was not obtained for an actual clay material, but still it holds a good representation of what happens in clay extruding augers.

Händle (2007) suggests that the pressure developed within the extruder and die has greater influence on the quality of extruded product and performance

18

of extruder. He has discussed the effects of changing geometric, process and operating parameters on the extrusion or pressure developed during an extrusion process. The results presented by him show, under normal circumstances the pressure profile for an extruder system will be like as shown in Figure 2-12.
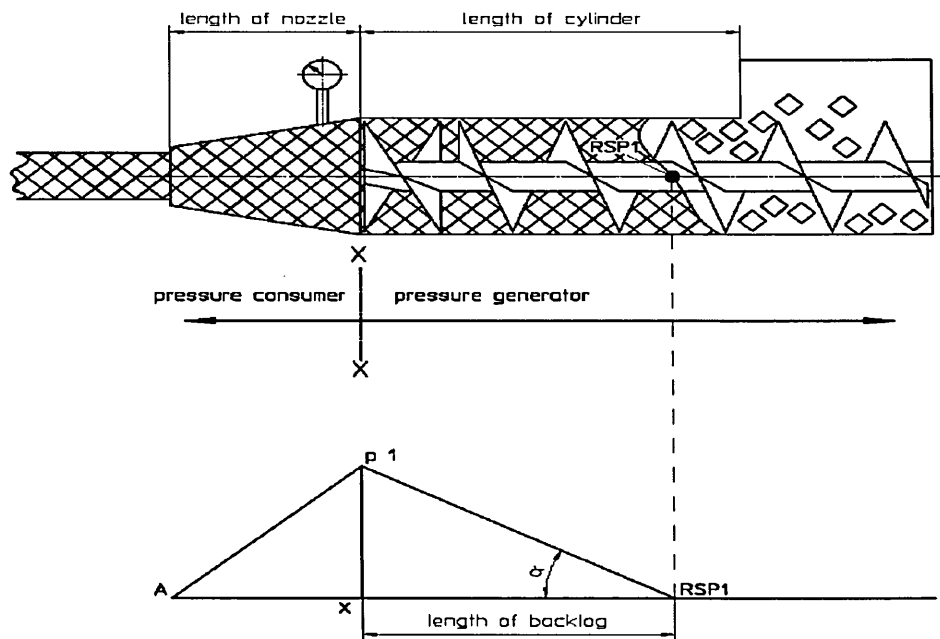
Figure 2-12 Forming pressure profile under normal condition

[Source: Händle, 2007]

As mentioned earlier it is clear that the pressure within the extruder unit rises gradually from a lower value to a peak value at a certain length of auger and then it gradually decreases within die section to attain ambient conditions. The author describes these functions as pressure generator and pressure consumer. It is also understood from the above figure that the maximum extrusion pressure is experienced at the tip of the extruder. This pressure profile is similar to the other theories about extrusion pressure proposed by other authors, whose works were discussed earlier in this chapter.

According to him, modification to clay moisture content, die (nozzle) geometry and feed rate has a significant effect in the extrusion pressure formation and distribution within the extruder and die system. The various pressure profile observed for such changes, suggested by him is shown from Figure 2-13 to 2-16.
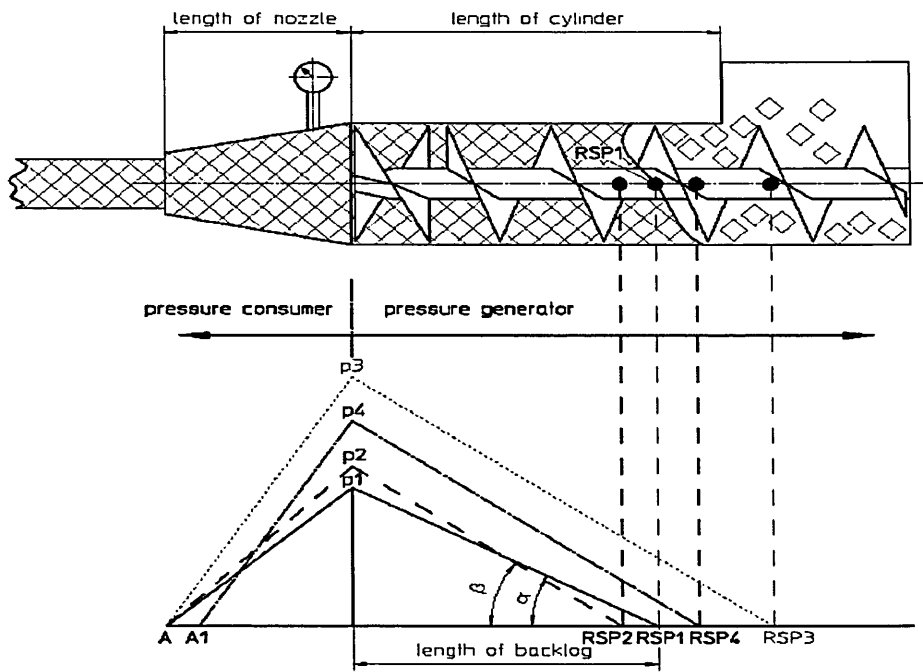
Figure 2-13 Effect of increasing clay stiffness on extrusion pressure
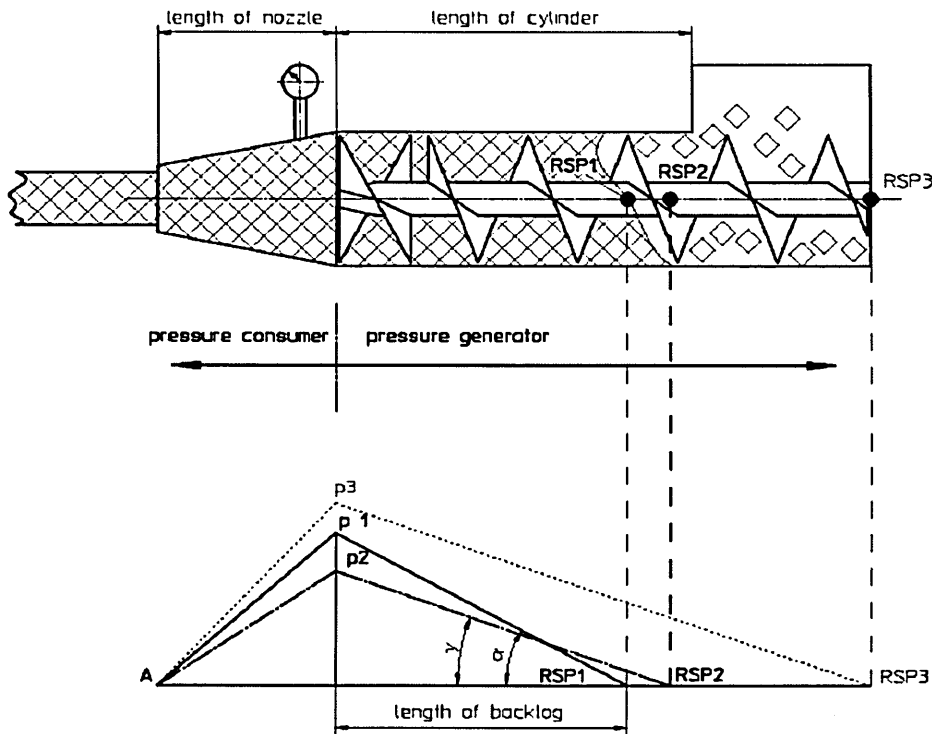
[Source: Händle, 2007]

Figure 2-14 Effect of decreasing clay stiffness on extrusion pressure

[Source: Händle, 2007]

20
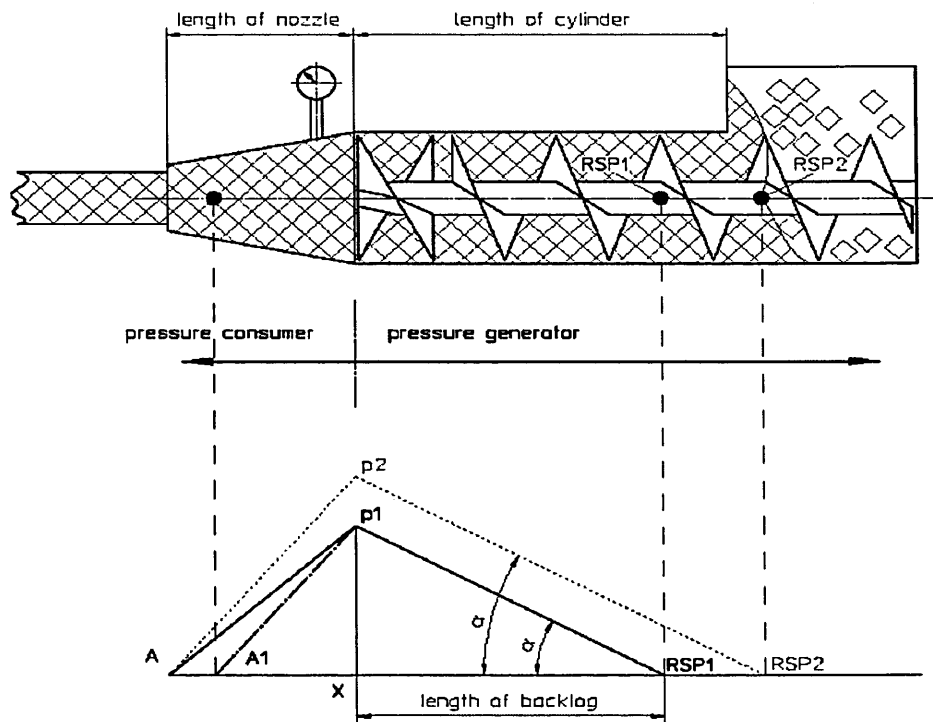
Figure 2-15 Effect of changing die geometry on extrusion pressure
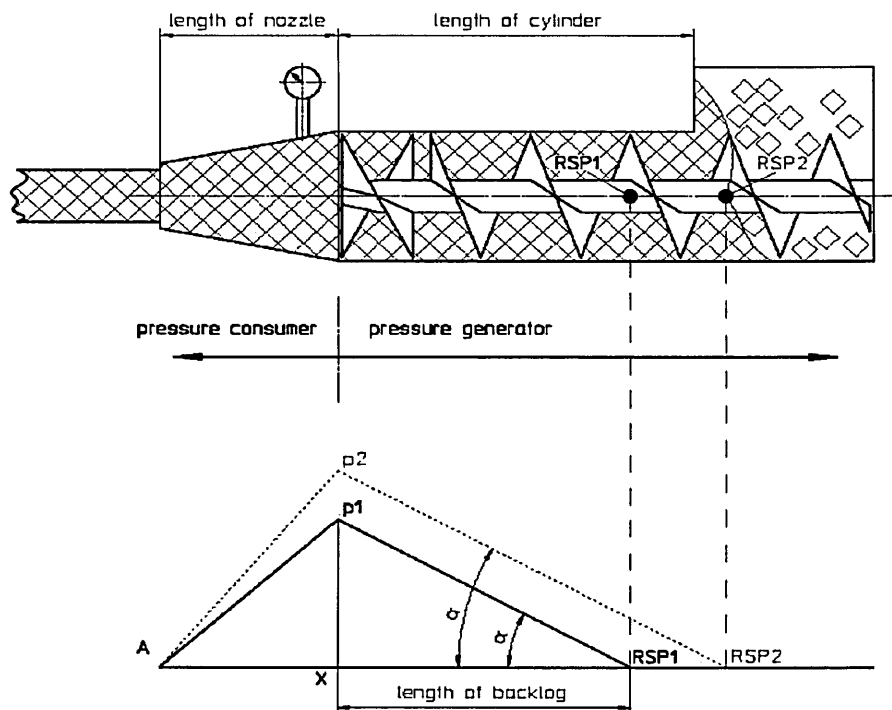
[Source: Händle, 2007]

Figure 2-16 Effect of changing feed rate on extrusion pressure

[Source: Händle, 2007]

21

The effects of changing process, operating and design parameters on the extrusion pressure, as discussed by **Händle (2007),** clearly indicates that the performance of an extruder system depends on one or more independent variables. It is also evident that the process of experimental analysis, to study the effect of each such change consumes time and resource.

Kocserhà and Kristàly (2010) have theoretically and experimentally investigated the effect of die shape on the performance of an extruder system and on the quality of extrudate. They have used a Bingham fluid model for representing the flow parameters of clay in their theoretical evaluation. They suggest that the optimization of extruder component geometries or rotation speed of the auger have beneficial effects on extrudate quality and power consumption. They also suggest that the extrusion pressure depends on rheology of the clay. The plastic flow character of clay throughout the entire cross section of the die is considered as an important factor to avoid crack formation that occurs during lateral processing of the extrudate. The results obtained from their work for a specific clay water mixture proportion demonstrates, a) the effect of die shape on extrusion pressure and power consumption at different auger speeds, shown in Figure 2-17, b) the effect of die shape on the physical properties of extrudate, shown in Figure 2-18.

| Extrusion pressure Vs Auger speed for various die shapes | Power consumption Vs Auger speed for various die shapes |
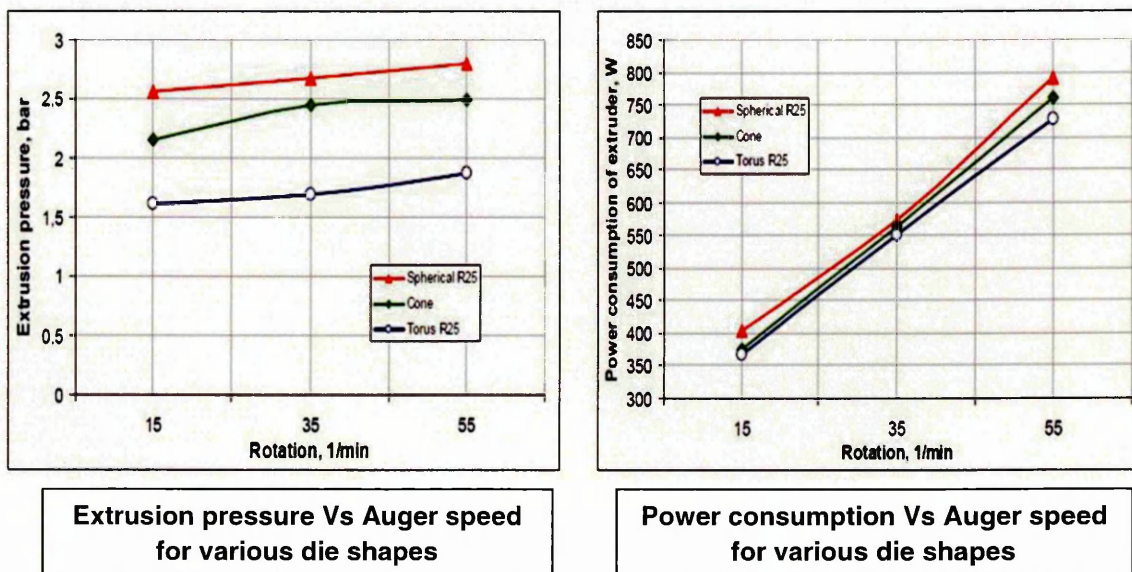
Figure 2-17 Effect of die shape on extrusion pressure and power

[Source: Kocserhà and Kristàly , 2010]

22
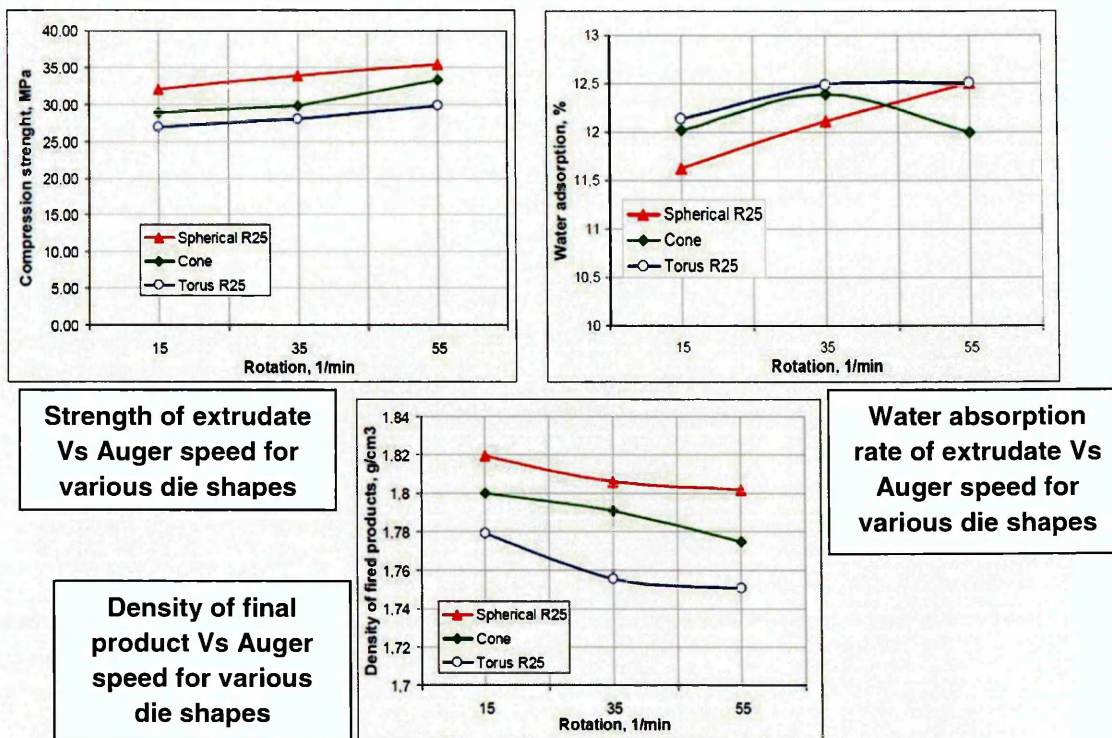
Figure 2-18 Effect of die shape on quality of extruded product

[Source: Kocserhà and Kristàly, 2010]

It is understood form their work that any change made to the geometrical parameters of the extruder components not only affects the performance of the extruder, but also the physical characters of the product.

Discussion:-

The work undertaken and the results obtained by various authors, as presented above, clearly illustrates that an optimised design of extruder components, die and material properties of clay plays a vital role in determining the performance of an extruder system. Most of their works focused to determine the optimised design requirement has resulted from time and cost consuming experimental works and none of them considered using computer based modelling techniques to reduce cost and time. However the valuable results and suggestions for various design changes, acquired from their work, were used to justify the results obtained from the computer based modelling work presented in this report.

23

2.4 Clay-Water rheology

The rheological properties of clay-water system, has been a subject of interest in different fields of engineering for many years, that includes for example soil, civil engineering, and ceramics etc. A number of research works have been undertaken to develop mathematical models to predict and understand the flow physics of clay-water system. Some of those key works and significant findings were useful in choosing a suitable flow model used in the CFD modelling work undertaken through this research work and are discussed here.

Amin et al. (2009) have discussed their experimental work on optimizing the mixing variables that influences the rheology of clay sewer pipe paste (Aswan clay-found in Upper Egypt). In their work they have clearly illustrated the effect of water content in a clay water system on the viscosity, as a function of shear rate, shown in Figure 2-19.
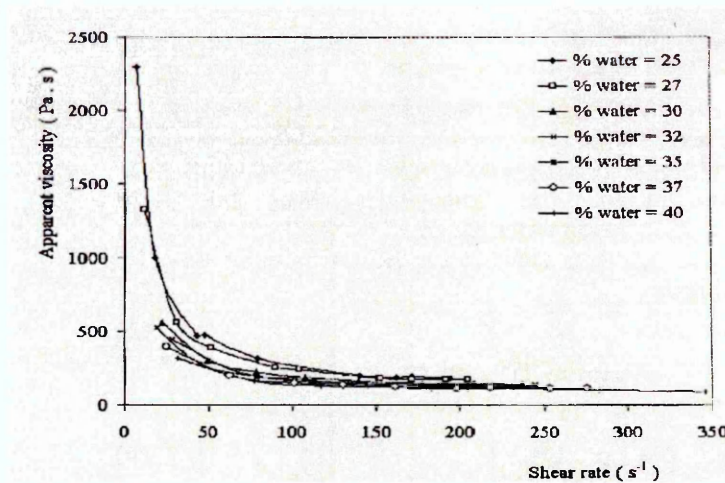
Figure 2-19 Viscosity of pure clay sewer paste
[Source: Amin et al, 2009)]

The result obtained by them is for a pure clay water mixture, with the particle size of 0.2 mm. They suggest that additives like grog or any adhesive to the pure form of clay will alter the above shown results. Also the mathematical model that fits well to predict the above shown results, as suggested by them is the Bingham model (Equation 2.1).

$$\tau = k.\dot{\gamma} + \tau_0 - -2.1$$

24

Where, τ= shear stress (Pascal), $\dot{\gamma}$ = strain rate (s^{-1}), k= consistency index (Pa.s^n), τ_0= yield stress (Pascal). (When τ> τ_0 flow & τ< τ_0 solid)

The values of the constants k and τ_0 are said to vary with respect to water content. The results obtained from their work indicates that when the clay is soft (more water content), it tends to yield quicker and the viscosity attains a lower value in less time, compared to stiffer clays. Also the value of k and τ_0 dictates the initial viscosity values and the flow curves of a fluid based on Bingham model.

Ormsby and Marcus (1963) have discussed the variation of clay viscosity with respect to the size of clay particle. Through their work they have noticed that the flow curve for various types of clays varies with respect to particle size, even when the amount of moisture is maintained to the same level. They suggest that when clay added with 50% of water to the weight, 1) behaves like a Newtonian fluid for particle size with 44-10, 10-5, 5-2 micron fractions, 2) behaves like a pseudoplastic fluid for 1-0.5 and 0.5-0.25 micron fractions and 3) like a dilatant fluid for 2-1 micron fractions. They have also observed dilatant behaviour for clay water mixture, even at lower percentage of water content. It is clear from their work that one should account for the particle size of clays as well, while determining or choosing a value for the variables associated with the rheology of clay.

Al-Zahrani (1997) has developed a generalised mathematical model to predict the viscosity as a function of shear rate for non-Newtonian fluids. He claims that the model is suitable to predict the behaviour of shear thinning fluids like clay water, polymer melts, paints and paper pulps etc. and is better than the traditionally used Power law and Herschel-Bulkley's model. The mathematical models proposed by him are shown in Equation 2.2 and 2.3.

$$\tau = B\left|\left(\frac{\dot{\gamma} + A}{A}\right)^n - 1\right| - -2.2$$

$$\tau = B\left[1 - \left(\frac{\dot{\gamma} - A}{A}\right)^n\right]^{1/n} - -2.3$$

Where, τ= shear stress (Pa), A, B= Constants, n=model index and $\dot{\gamma}$= shear rate (s^{-1})

The results obtained by using his model to predict the viscosity of a gelex polymer fluid is shown in Figure 2-20.
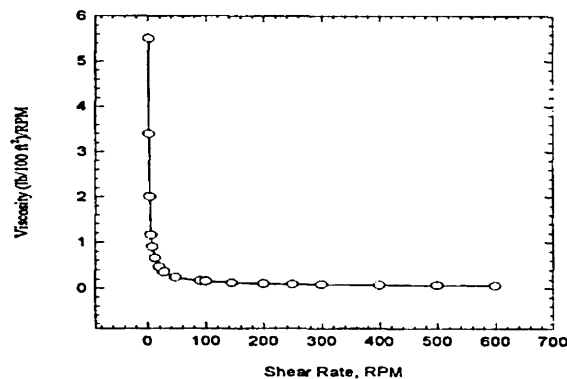
Figure 2-20 Viscosity profile of a typical shear thinning fluid

[Source: Zahrani, 1997]

He claims that the predicted result using his model is accurate when compared to the experimental results and suggests it to be an alternate and improved approach to Herschel-Bulkley's model. The key things to be noted from his work includes, the viscosity profile of a shear thinning fluid as a function of shear rate and suggestion about the suitability of Herschel-Bulkley's model in predicting the shear thinning fluid rheology.

Maciel et al. (2009) have studied the physical and rheological properties of Kaolinite clay and water mixture using Herschel-Bulkley's model. They suggest that material, like clay-water mixtures, could be well represented by Herschel-Bulkley's viscoplastic non-linear rheological model. Their study was focused to develop behaviour laws for predicting the flow behaviour of mud found in torrential lavas. Based on the experimental and mathematical model results obtained from their work, they suggest that the flow characters of Kaolinite clay and water systems predicted using Herschel- Bulkley's model was in good agreement with the measured values. They also suggest that Herschel-Bulkley's model is better for predicting the yield stress (deformation of the fluids) experienced at lower shear rates than the Bingham model, which is good for fluids yield at high shear rate.

Nelson and Andrews (1959) have experimentally investigated the forces required to shear plastic clay (Florida Kaolin), both within its own structure and at clay-metal surface interface. They suggest that, in addition to the basic factors like type of clay material and water content, the shearing of plastic clay is also influenced by pressure distributed within the clay and speed of rotation of metal surface that comes in contact with the clay. Results obtained through their investigation indicate that the pressure distribution in a clay water system is a function of yield value and the force required to shear plastic clay increases with increase in pressure to a certain extent and remains constant. It also increases with the speed of the metal surface with which the clay encounters.

Mahajan and Budhu (2008) have proposed an analytical model to determine shear viscosity of clay-water system (Kaolin clay), using Casson's Model. They suggest that it is applicable for mixtures with very low water content. The results obtained through their work indicate that the shear viscosity reduces with increase in percentage of water content. They also suggest that the accurate prediction of viscosity of clay water system using numerical model depends on the rheological model used.

Andrade et al. (2010) have developed a mathematical model for evaluating the clay plasticity. Comparing their model with experimental results, they had confirmed that their model gives a more accurate approach in obtaining the plasticity for wide range of ceramic materials, with different mineral and moisture content. From the results obtained through their work, it is understood that the plasticity value of clay varies with respect to its mineral contents, even if the moisture content remains the same.

Discussion:-

It is evident from the above information that the flow physics of clay-water system have been studied for many years. The research activities undertaken and results obtained clearly indicate that the flow characteristic of clay-water system varies with respect to the type of clay, additives, particle size and moisture content. It also influences the performance of the machine that it encounters. From various mathematical models used to represent

highly viscous materials like clay water mixture, the choice of an appropriate numerical model, that suits the problem of investigation, depends upon experimental and availability of other resources.

2.5 Conclusion

Thus a review of previously completed works relevant to the subject of interest in this research was presented in this chapter. The various methodologies used, results obtained, their advantages and disadvantages were briefed clearly for further understanding and also to acquire substantial validation to the methodology and modelling technique used in this research work.

Chapter-3   CFD modelling of clay extruder

3.1 Introduction

This chapter presents a brief review about the basic classification of fluids and available numerical models for modelling the viscosity of non-Newtonian fluids (exhibited by the clay-water mixture). It also reviews the basics about CFD modelling technique. The CFD modelling approach used in this research work is discussed, explaining the background concepts involved in modelling various physical processes involved in the clay extrusion. Experimental validation of the modelling approach, results obtained from various CFD simulations along with the evaluation of performance characters for various design and operating conditions of the extruder are presented and discussed.

3.2 Fundamental classification of fluids

Fundamental classification of fluids includes *Gases-* substances that deform under shear stress and *Liquids-* substances that continuously deform under shear stresses. The dependency of continuous deformation of liquids subjected to shear stress is an inherent property of the substance and this has led to further classification of fluids,

1. ***Newtonian fluids:*** The fluids that have a constant viscosity or deform linearly to the applied shear stress, as shown in Figure 3-1, are called Newtonian fluids.

<table>
<tr><td>A</td><td>B</td></tr>
<tr><td>Shear stress vs. Strain rate</td><td>Viscosity vs. Strain rate</td></tr>
</table>
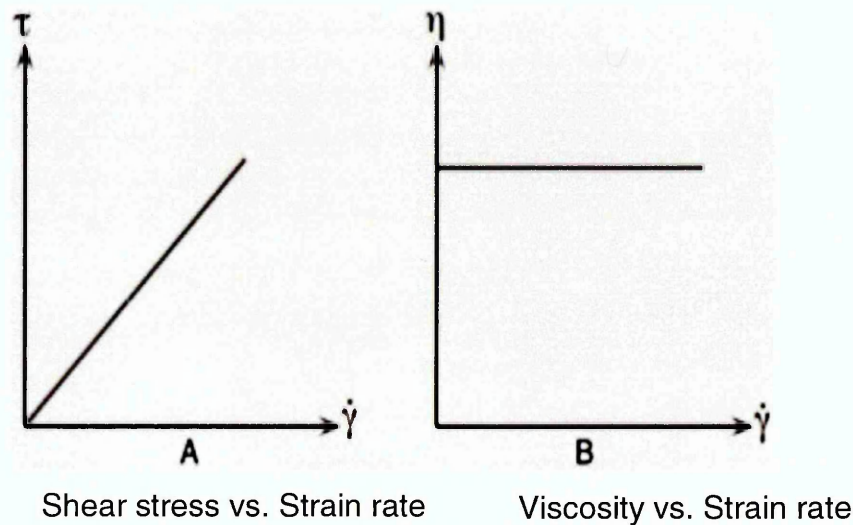
Figure 3-1 Newtonian fluids

[Source: Brookfield Engineering, 2010]

Newtonian fluids are commonly agreed to obey the Navier-Stokes equation and the best curve fit mathematical model, accepted and used widely to describe the flow of such substances is shown in Equation 3-1.

$$\tau = \mu \frac{du}{dy} = \mu * \dot{\gamma} - -3.1$$

Where μ= Shear viscosity (Pa.s), $\frac{du}{dy}$ or $\dot{\gamma}$ = Rate of shear (s^{-1})

2. **Non-Newtonian fluids:** Fluids that do not obey the basic principles of Newtonian fluids are commonly described as non-Newtonian fluids. The flow of such liquids is subjected to shear stress and is influenced by more than one factor under certain circumstances. There are various types of such fluids that exist in nature. The three basic categories under which these types of fluids are grouped include a) time independent non-Newtonian fluids, b) Time dependant non-Newtonian fluids, and c) Visco-elastic fluids.

a. **Time-Independent non-Newtonian fluids:** The rate of shear for such type non-Newtonian fluids depends only on the instantaneous value of the shear stress and is independent of time. It is also referred as non-Newtonian viscous fluids **[Wilkinson,1960]**.Depending on the function of rate of shear to the applied shear stress, the different types of fluids grouped under this category includes I) Pseudoplastic fluids or Shear-thinning fluids II) Visco-Plastic fluids or Bingham plastics III) Dilatant fluids or Shear thickening fluids.

Pseudoplastic fluids: In such fluids, the rate of shear is not linear to the applied shear stress, the viscosity decreases with increase in shear rate and it becomes linear only at a very high shear rate, as shown in Figure 3-2.
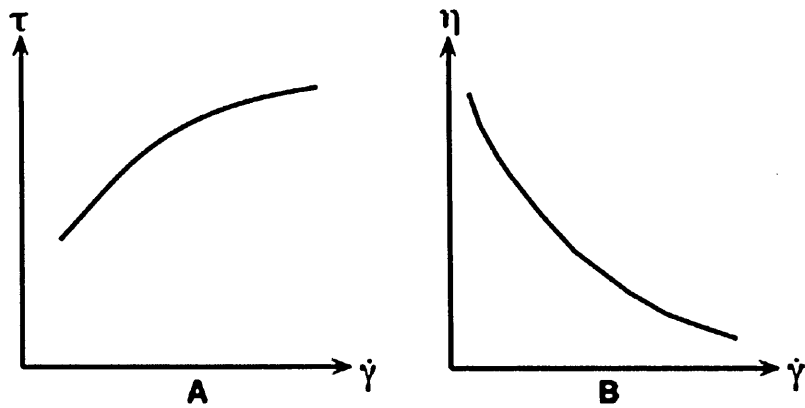
Shear stress vs. Strain rate   Viscosity vs. Strain rate

Figure 3-2 Pseudoplastic fluids

[Source: Brookfield Engineering, 2010]

The viscosity values are termed as Zero shear viscosity and infinite shear viscosity. The mathematical models that best describes the behaviour of such fluids include,

Power law model$= \tau = k\dot{\gamma}^n$ $- -3.2$

Where k = Flow consistency index ($Pa.s^n$), n=power law index (<1 for shear thinning fluids)

Carreau Model$= \dfrac{\mu - \mu_\infty}{\mu_0 - \mu_\infty} = \left[1 + \left(\lambda * \dfrac{du}{dy}\right)^2\right]^{(n-1)/2}$ $- -3.3$

Cross model$= \dfrac{\mu - \mu_\infty}{\mu_0 - \mu_\infty} = \dfrac{1}{1 + (\lambda\dot{\gamma}_{xy})}$ $- -3.4$

Where μ_0, μ_∞= Zero and infinite shear viscosity (Pa.s), λ = time constant, n=flow index.

The other, not widely used models include the Prandtl, Eyring, Powell-Eyring and Williamson.

Viscoplastic fluids: These type of fluids when subjected to shear stress will start to flow only after a certain value of stress is reached. This value is commonly described as yield stress and beyond this value the flow could be linear or non-linear as shown in Figure 3-3.

32

Strain rate vs. Shear stress   Viscosity vs. Strain rate
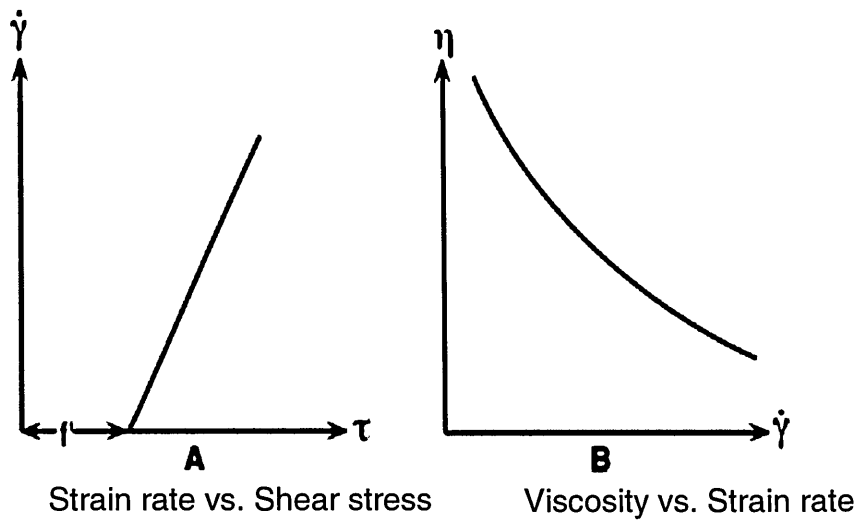
Figure 3-3 Visco plastic fluids

[Source: Brookfield Engineering, 2010]

Viscoplastic fluids that have a linear profile after the minimum yield stress are called as Bingham plastic fluids. Mathematical models commonly used to describe the behaviour of such fluids include,

Bingham plastic model=$\tau - \tau_0 = K\dot{\gamma}$ — −3.5

Herschel-Bulkley's model= $\tau = \tau_0 + k\dot{\gamma}^n$ — −3.6

Where τ_0=minimum yield stress threshold (Pa),

And, Cross model-another type of recommended mathematical model, for studying the behaviour of such fluids.

Dilatant fluids: It is similar to Pseudoplastic fluids **[Wilkinson 1960]**. In this type of fluids, the fluid viscosity increases with rate of shear, as shown in Figure 3-4. Clay slurries, candy compounds and sand-water mix are few examples.

33

A   B
Shear stress vs. Strain rate   Viscosity vs. Strain rate
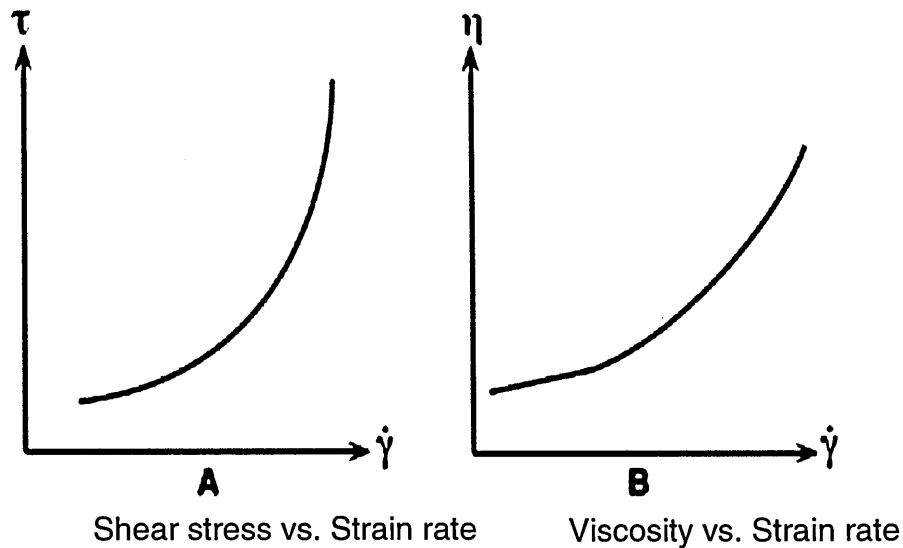
Figure 3-4 Dilatant fluids

[Source: Brookfield Engineering, 2010]

It is suggested that even power law model could be used to model such fluids, with flow index value greater than unity **[Wilkinson 1960]**.

b. ***Time-dependent non-Newtonian fluids:*** The rate of shear and shear stress, for such type of non-Newtonian fluids, are functions of time. Such type of complex fluids is further divided into a) Thixotropic fluids- characterised by decreasing apparent viscosity or shear stress with respect to time, when subjected to constant rate of shear. As shown in Figure 3-5. b) Rheopectic fluids - characterised by increasing apparent viscosity or shear stress with time, when subjected to constant rate of shear. As shown in Figure 3-6.
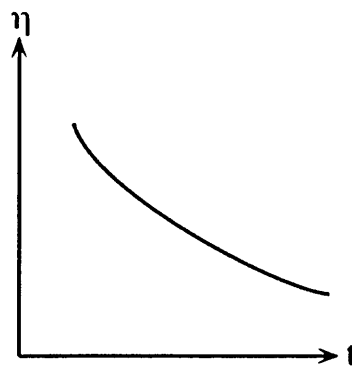
Figure 3-5 Thixotropic fluids

[Source: Brookfield Engineering, 2010]

34
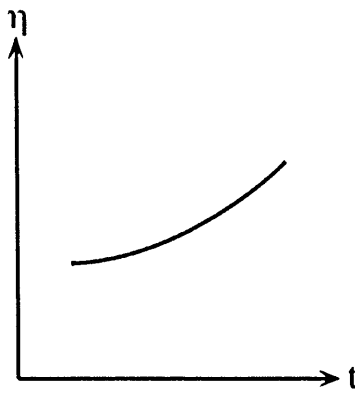
Figure 3-6 Rheopectic fluids

[Source: Brookfield Engineering, 2010]

c. **Visco-elastic fluids:** This type of fluids exhibits both elastic characters like solids and viscous character like fluids, as shown in Figure 3-7.
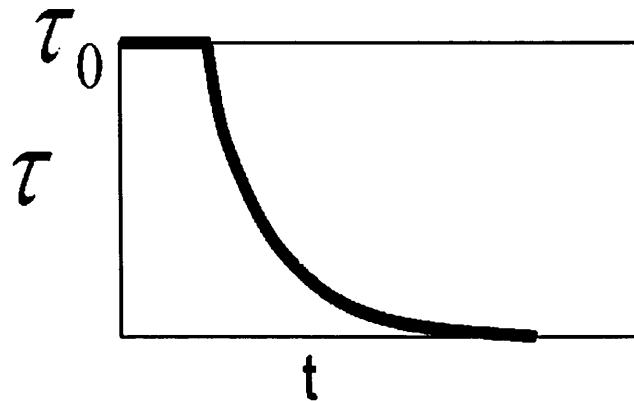
Figure 3-7 Visco-elastic fluids

[Source: Brookfield Engineering, 2010]

The suggested mathematical model that represents the behaviour of such fluids is Maxwell's model, shown in Equation 3.7.

$$\dot{\gamma} = {}^{\tau}/_{\mu_0} + {}^{\dot{\tau}}/_{G} - -3.7$$

Where, G = rigidity modulus (Pa), $\dot{\tau}$= Rate of shear stress (Pa).

Through the knowledge gained from the classification of fluids, basic working principle of extruders and various scientific works completed previously, it is sensible to consider the clay-water system as a non-Newtonian fluid and exhibits a Visco-plastic fluid or shear thinning fluid character. Its behaviour could be summarised as, the mixture when subjected to a shear force does not deforms readily until it reaches as particular value and this value is

35

termed as the minimum yield stress threshold. Once this value is attained, it continuously deforms under the action of shear stress to the extent where the viscosity reduces to a very low value and remains constant (at this point the fluid is set to have reached the Newtonian fluid flow regime). Herschel-Bulkley's model, discussed above along with other available mathematical models for non-Newtonian fluids, which includes the functions representing both yield stress region and constant viscosity region, proves to be the best suitable model for clay like materials. Due to its extensive use in various fields for studying clay-water rheology and recommended for CFD modelling of clay like materials [**Ansys-Fluent 12.0 user's guide 2010**], in this research work it was decided to use Herschel-Bulkley's fluid model to simulate the process of clay extrusion and assess the performance of extruder using CFD.

3.3 Process of CFD modelling

There are three different types of numerical modelling techniques commonly used in engineering applications: a) Finite Difference Methods (FDM) b) Finite Element Method (FEM) and c) Finite Volume Method (FVM). The fundamental difference between all these techniques is based on the way a functional variable is represented and with the process of discretisation [**Versteeg and Malalasekera 1995**]. CFD is one of the computational techniques used for solving internal and external fluid flow problems and associated heat transfer phenomenon. The three common equations involved in any CFD model are equations for conservation of mass, momentum and energy. Irrelevant to the nature of problem, these equations will always be included in the model; additional equations in the model will depend upon the nature of the problem investigated. The various types of flow physics that can be modelled and investigated using CFD is shown in Figure 3-8.
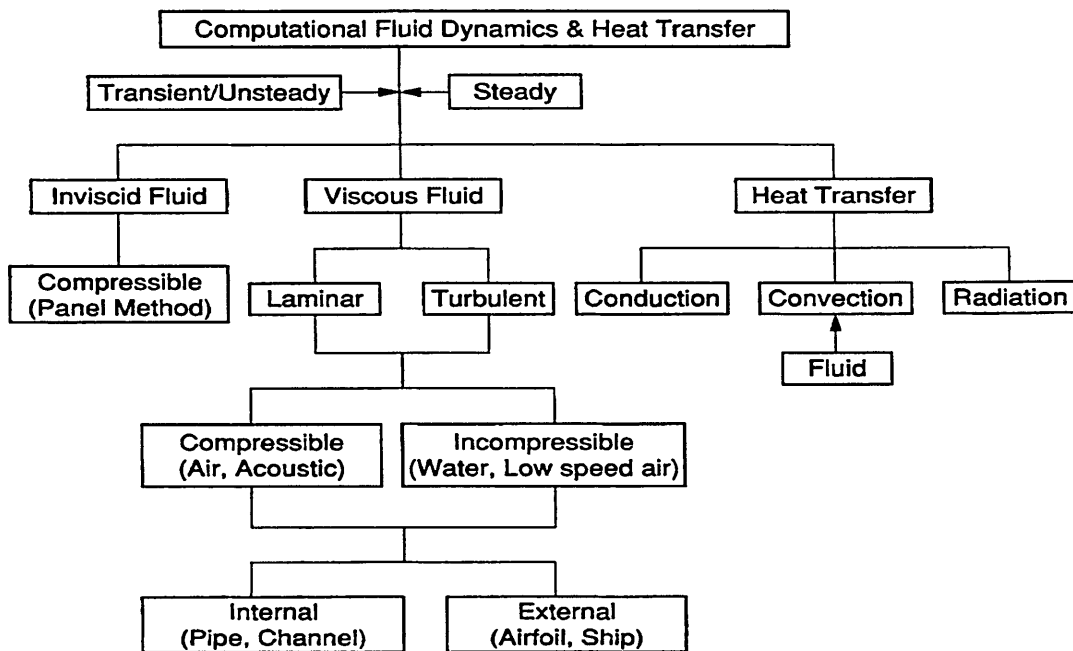
Figure 3-8 Flow physics features in CFD

[Source: Jiyuan Tu et al, 2013]

Major steps involved in any CFD modelling process includes,

1) Pre-processing: Generating suitable CAD geometry to represent the domain or domains of interest and meshing. Meshing is defined as discretizing the domain or the CAD geometry into suitable finite number of volumes using any standard mesh generating software. GAMBIT and ICEM-CFD are some of commonly used meshing software. In this stage, the physical and chemical phenomenon to be modelled and boundary conditions will be defined. The boundary conditions can be even defined or altered in the next step of the modelling process. Gambit was used for meshing the extruder geometries investigated in this research.

2) Solver setting: A suitably meshed geometry will then be imported to a solver, where appropriate numerical techniques, flow equations and variables for solving the problem will be defined. This is required for solving the physical or chemical phenomenon of a flow process defined earlier. Examples of commercially available solvers for the application of CFD problems includes FLUENT, STAR-CD, CFX, FLOW 3D, PHOENICS and

FEMLAB and all these solvers are based on FVM technique. In this research work the extruder model was solved using Ansys- FLUENT 12.0.

3) Post-processing: The primary function in a post processing stage is reviewing the results obtained from the solver. For example pressure, velocity and temperature distribution in a flow regime. Recent advancements in the capability of computer graphics, has enhanced this process and proves to be more useful tool in communicating the results of a solved flow problem to end users.

A flow diagram that briefs the various stages involved in a complete CFD analysis is shown in Figure 3-9.
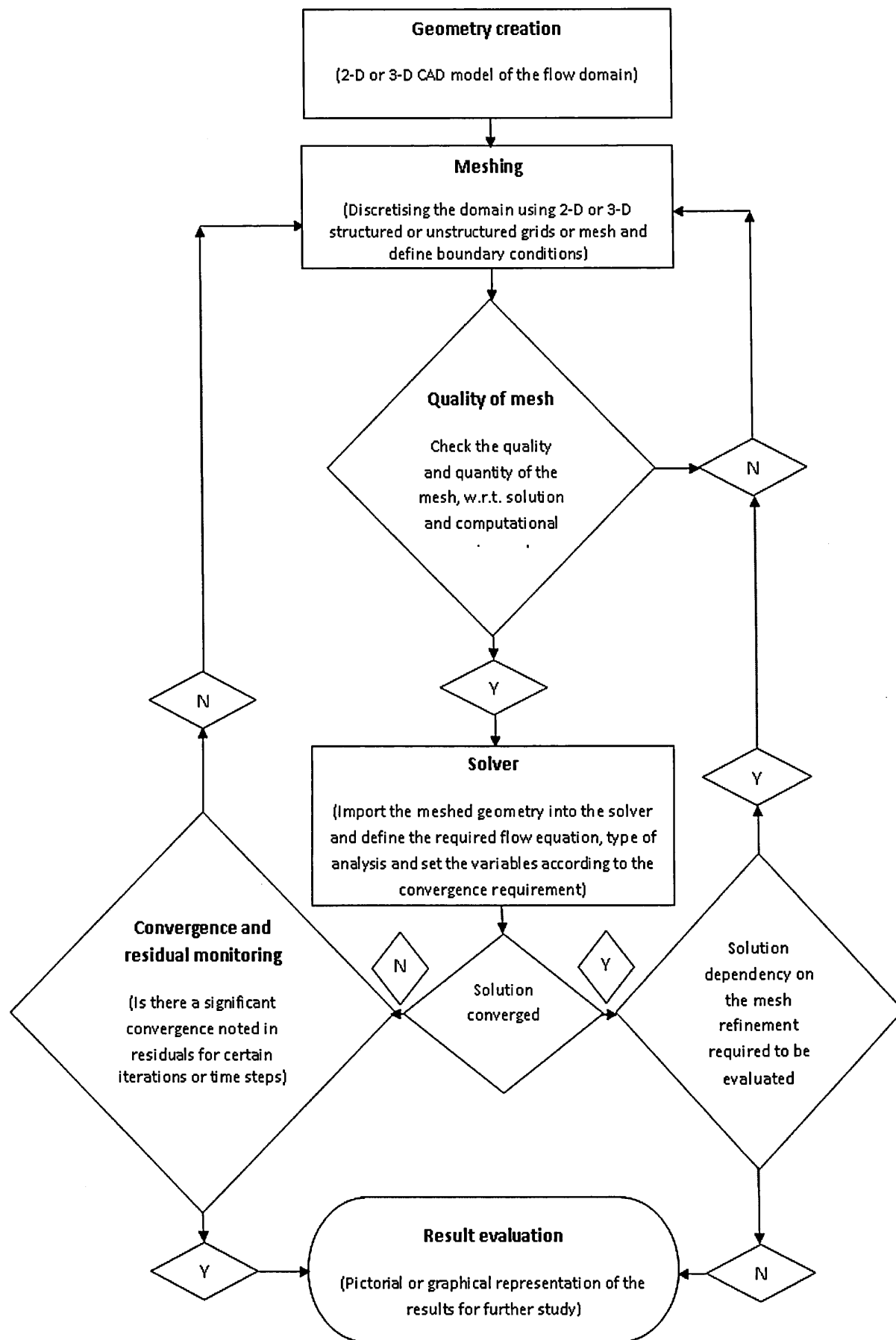
Figure 3-9 CFD modelling process flow diagram

3.4 CFD modelling of extruder

The methodology used to set up the flow problem of clay extrusion and assess the performance of an extruder in the CFD solver is described below in this section. The process of set up remains the same for all the CFD analysis discussed in this report.

3.4.1 Geometry creation

The various standard sizes of extruders designed and manufactured by C.F limited, for the process of ceramic extrusion (mainly bricks) is provided in Table 3-1.

Machine	Size (Extruder diameter)
CENTRIM	406.40 mm (~16 inch)
CENTEX	430 mm (~16 inch) , 500 mm (~19.68 inch)
60F	422.27 mm (~16.625 inch)
90BD	488.95 mm (~19.25 inch)

Table 3-1 Craven Fawcett extruders for brick making

The Centex series of extruders are the most widely used extruder system by many of C.F customers. Considering the feasibility in obtaining any valuable field based data to validate the numerical model investigated in this research, it was considered to be sensible approach to model and assess the performance of CENTEX type machines. Hence the various sizes of full scale extruders from CENTEX series, considered for the investigation includes 430 mm, 500 mm and 600 mm. The 600 mm extruder is an extended version of the 500 mm extruder, targeted for higher productivity rate. Proposed for a specific requirement, it was the first of its kind that the company were intending to manufacture and the design engineers were very keen to obtain performance comparison data with respect to its predecessors. So the 600 mm extruder was also included in this numerical modelling work and its performance was assessed and compared.

The domains of interest include barrel liner, auger with shaft (collectively called as extruder) and die. The required 3-D geometry of the components was created using Autodesk-Inventor and Pro-Engineer Wildfire.

3.4.2 Geometry discretisation

The 3-D CAD model of the extruder geometries created in the above step were discretised using Gambit. The different types of surface mesh elements available in Gambit are Quad-generates only quadrilateral elements; Tri-generates only triangular elements, Quad-Tri-generates quadrilateral and triangular elements at the required areas. The different types of surface mesh schemes available in Gambit are Map- generates structured grid of mesh elements, Sub-map- generates a structured grid of mesh elements in a suitably converted unmappable face, Pave-generates structured or unstructured mesh elements, Tri-Primitive-generates mapped quadrilateral elements and Wedge primitive- generates a triangular mesh element for wedge shaped elements. The different types of volume mesh elements available in Gambit include Hex, Hex/Wedge, Tet/Hybrid and types of volume mesh schemes include Map. Sub-map, Tet-Primitive, Cooper, Stairstep, T-grid and Hexa core **[Gambit-2, 2001]**.

The option of treating the entire geometry as a single volume and generating a uniformly distributed mesh with suitable size was considered to be a complex process, due to the nature of the shape of various components. Hence the system was sub divided into different zones namely, 1) Auger volume-I, 2) Auger volume-II, 3) Clearance volume, 4) Die /Mouth piece, 5) Liner volume. As discussed earlier, based on the available computing power and solution requirement, unstructured volume mesh with 4-node tetra-hedral mesh elements and t-grid hybrid meshing scheme was used for meshing the auger, die and liner geometry, and a structured hex mesh for the clearance volume. The various fluid volumes along with the mesh generated for a 430 mm extruder, used for the investigation, are shown below.

1) Auger volume-1: Fluid volume around the auger shaft, shown in Figure 3-10.
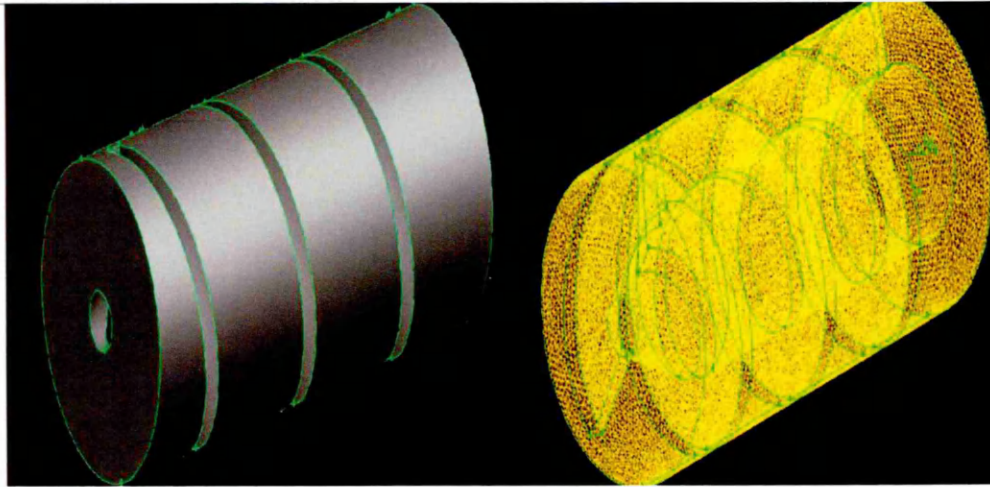
Figure 3-10 430 mm extruder- Auger volume-1

2) *Auger volume-2:* Solid volume around the auger shaft, shown in Figure 3-11.
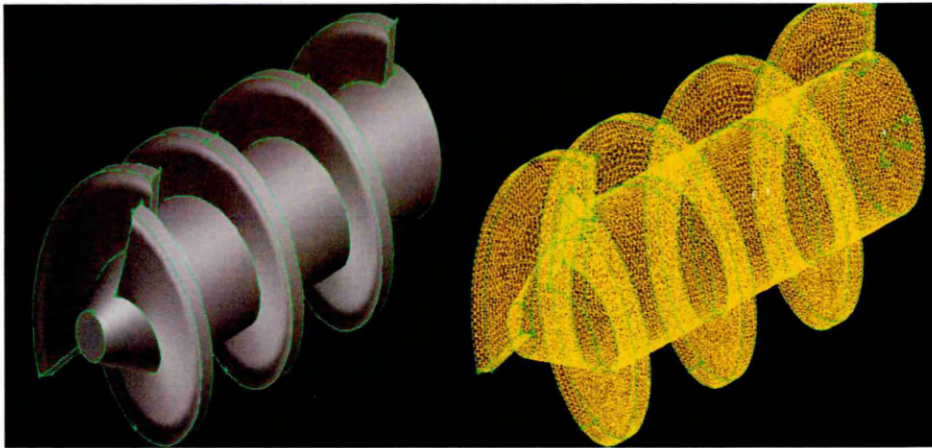
Figure 3-11 430 mm extruder- Auger volume-2

3) *Clearance volume*: Small gap between the auger shaft and the liners, shown in Figure 3-12. A structured hexahedral mesh was generated for this volume.
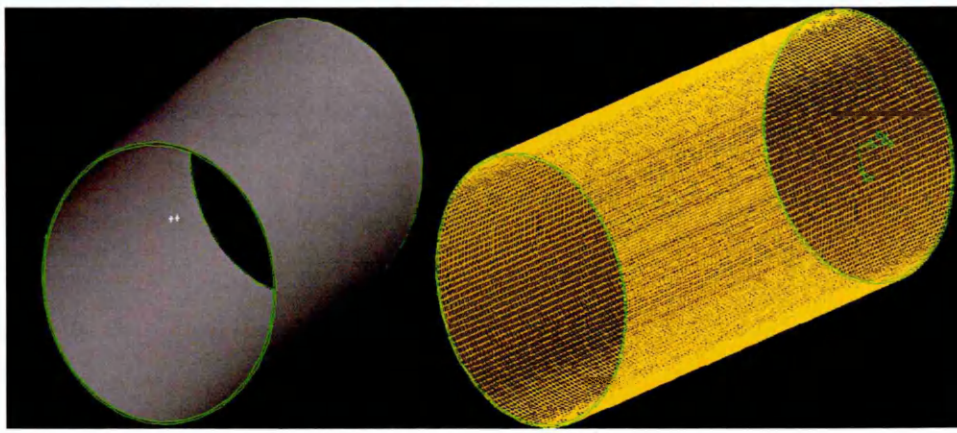
Figure 3-12 430 mm extruder - Clearance volume

4) *Die or mouth piece:* A round shaped die design was used during the initial investigation and is shown in Figure 3-13. The geometric details of the other die shapes used in this research work are available in section 3.9.4.
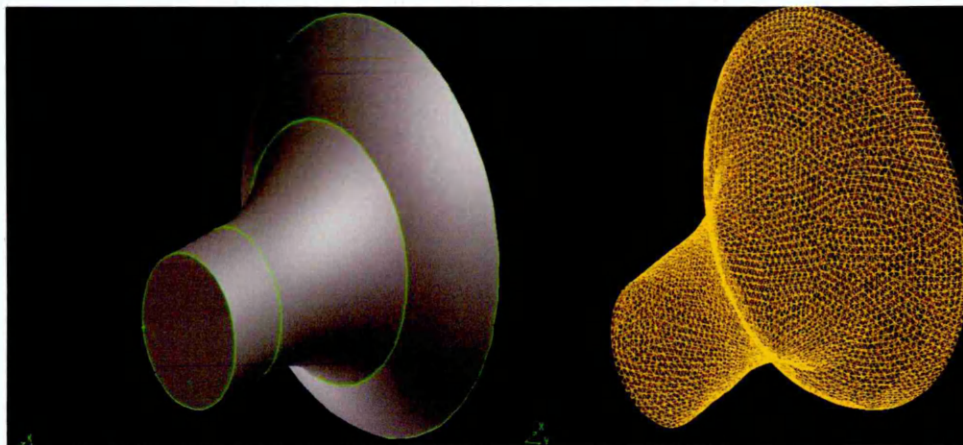
Figure 3-13 430 mm extruder - Die/ extruder mouth volume

5) *Liner volume:* The design and choice of material for liner depends on the requirement and type of clay extruded. It varies with respect to size of extruders and sometimes varies even for the same size. The factors that influence the design include the clay material, production rate and manufacturing feasibilities. The extruders modelled and investigated in this research work have different liner designs. Suitable mesh size, meshing element and meshing scheme was chosen with respect to the design. Meshed liner geometry of a 430 mm extruder used in the investigation is shown in Figure 3-14.
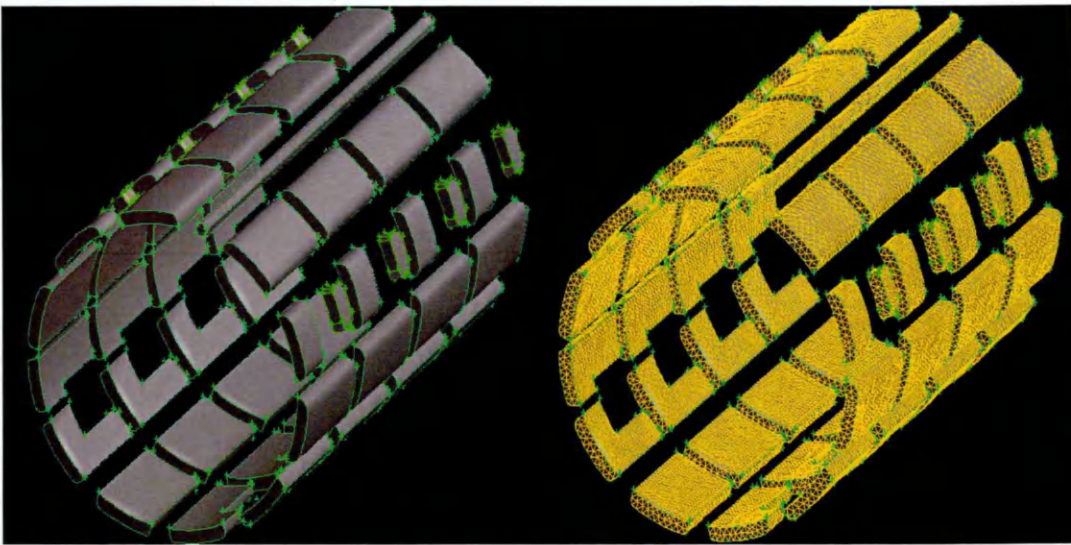
Figure 3-14 430 mm extruder- Liner volume

The final geometry of a 430 mm extruder, with assembled fluid volumes is shown Figure 3-15.
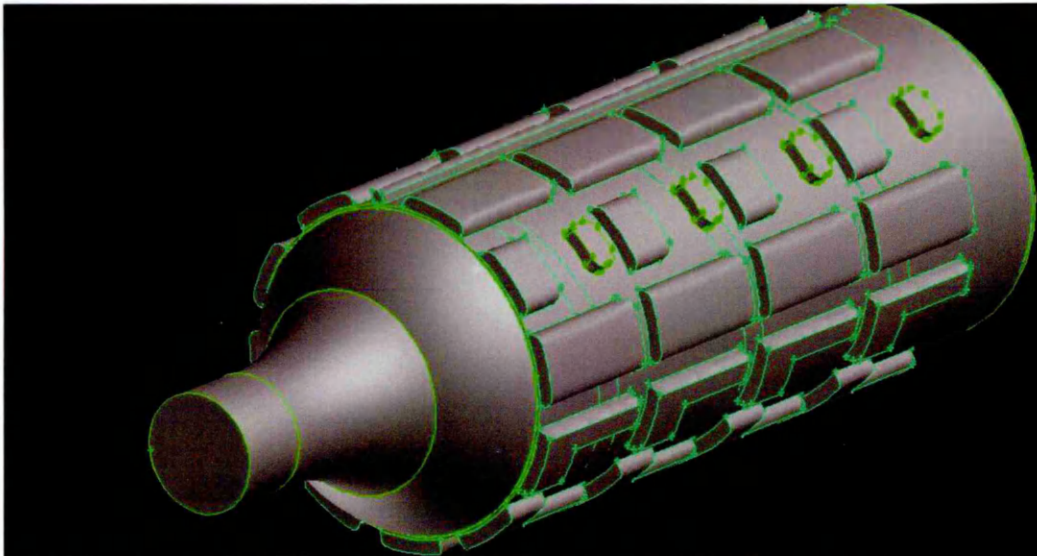
Figure 3-15 430 mm extruder components and die assembled view

The meshed geometries of 500 mm and 600 mm extruder are available in Appendix A - section I. Table 3-2 summarises the details of mesh generated for various extruders investigated in this research.

Extruder size	Auger and Liner volume mesh elements	No. of cell elements
430 mm	Tetra hedral,Tgrid-Hybrid	956,143
500 mm	Tetra hedral,Tgrid-Hybrid	1,312,961
600 mm	Tetra hedral,Tgrid-Hybrid	1,545,053

Table 3-2 Extruder mesh details

3.4.3 Boundary conditions

The choice of boundary condition for various elements of the geometry depends on the flow problem being studied and there are 22 different types of boundary conditions available in GAMBIT, suitable for various flow problems. It is recommended to choose an appropriate boundary condition such that it gives an accurate or a fair representation of the real condition. Due to the lack of availability in previous experimental data and knowledge of flow physics that occurs in an extruder, it was tedious to choose a precise boundary condition. However from the various scientific works discussed in Chapter 2, it was considered pressure inlet or velocity inlet or mass flow rate for the inlet of an extruder system and for the outlet of die either pressure outlet or outflow as an appropriate choice of boundary conditions. During the initial stage of the research, 1) pressure inlet, pressure outlet and 2) velocity inlet-pressure outlet boundary conditions were used to run the simulation. Since satisfactory results were not obtained when compared with actual scenarios, a different approach was undertaken.

It was decided to use mass flow rate for the inlet section of the extruder and outflow boundary condition for the outlet section of the die. The two main reasons behind this are,

1) The size of an extruder system is always determined by the number of bricks to be extruded per hour and the shape of the outlet section of die is based on the shape and size of the brick. Other components like liners and barrel chamber are scaled suitably to meet the extrusion rate requirement.

2) A significant amount of real time data was available for variables like extrusion rate, compacted and un-compacted clay density, for

various size of extruders investigate in this research work. These facilitated in using sensible values for the boundary condition and compare the results obtained from the CFD analysis with real time data.

Wall boundary condition was used for all the other geometrical features, where fluid volume interacts with solid volumes. Interface boundary condition was used for connecting surfaces between two fluid zones or components of extruder, through which transfer of fluid from one to other occurs. Simulations completed during the initial stage of investigation, using these boundary conditions, yielded results that were in good agreement to actual scenarios. Furthermore the solver was stable and a better convergence of residual was noted for a significant number of iterations, compared to the other boundary conditions mentioned earlier.

The extruder system is sub-dived into moving and stationary zones/components. In order to understand the actual flow process and assess the performance of the system, it was considered that representing these features in the numerical model is an essential requirement. FLUENT has different types of in-built modelling features that help to model and simulate such kind of systems. Dynamic mesh modelling is one such feature that allows users to specify moving and deforming fluid zones or stationary fluid zones that exist within a single flow domain (refer to section 3.4.4.2 for further details). In order to be able to use this feature at the solver stage, it is necessary to discretise the domain suitably and specify the features of various zones clearly at this stage of the process. In this research work, the solid volume of the auger and the fluid volume around the auger were defined as moving zones and the remaining components were defined as stationary zones, shown in Figure 3-16 and Figure 3-17.
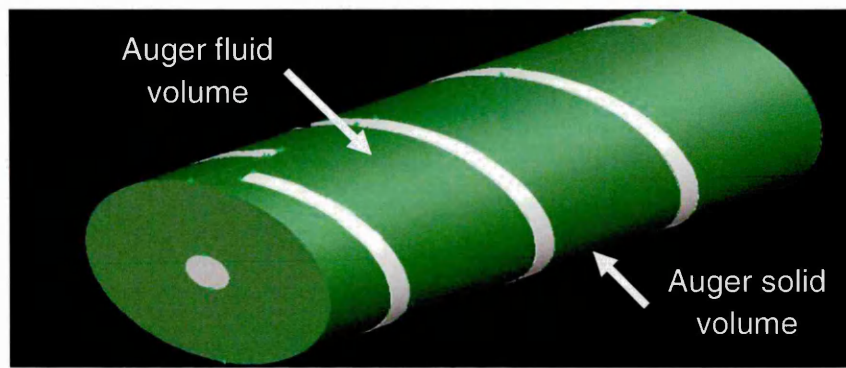
Figure 3-16 Moving volumes
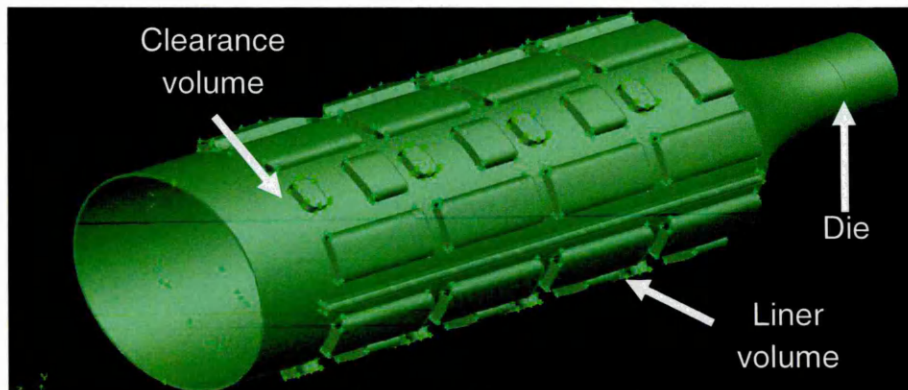
Figure 3-17 Stationary volumes

3.4.4 Solver settings

3.4.4.1 Flow modelling

Solver settings generally depend upon the flow physics that is being investigated. So it is necessary to have some preliminary understanding about the type of flow occurring in the domain of investigation, before setting up the problem in the solver.

In comparison to Newtonian fluids, there is lack of a standard method or procedure for determining the Reynolds number of non-Newtonian fluid flows. **Wilkinson (1960)** has discussed about the formula used for calculating the Reynolds number for the flow of time-dependent non-Newtonian fluids through a pipe channel, both in a laminar and turbulent flow regime. However considering the highly viscous nature of the material and speed of the auger, it was clearly understood that the material exhibits laminar flow throughout the entire length of the extruder and die sections. So an unsteady state, single phase, laminar flow model with pressure based

47

solver and coupled algorithm for pressure-velocity coupling was assigned to the model. Though the pressure based solver is predominantly used to solve incompressible flow problems, it is also recommended for solving mildly compressible flow **[Ansys 12.0-User's guide, 2009]**, as occurs in the case of clay extrusion.

The generalised form of conservation equations for mass and momentum solved by FLUENT, for both compressible and incompressible laminar flow problems are shown in Equations 3.8 and 3.9.

$$\frac{\partial \rho}{\partial t} + \nabla.(\rho \vec{v}) = S_m \quad - -3.8$$

Where, S_m= mass added to the continuous phase, ρ= density, $\vec{v}$=velocity vector.

$$\frac{\partial}{\partial t}(\rho \vec{v}) + \nabla.(\rho \vec{v}.\vec{v}) = -\nabla p + \nabla.(\overline{\overline{T}}) + \rho \vec{g} + \vec{F} \quad - -3.9$$

Where, p=static pressure, $\overline{\overline{T}}$=stress tensor, $\rho\vec{g}$=gravitational force and $\vec{F}$=external body force.

3.4.4.2 Dynamic mesh modelling

It was mentioned earlier that the extruder system comprises of both stationary and moving zones and the geometry was discretised suitably to reflect these properties. Using the moving and deforming mesh modelling feature available in FLUENT, the moving and stationery zones of an extruder system were defined in the solver.

Dynamic meshes are used in problems where boundaries move rigidly with respect to one another, may exhibit linear or rotary motion. It can also be used for deflecting and deforming boundaries (example: balloon, artificial wall) **[Fluent -6.3 user guide]**. The mesh generation will be based on the moving boundary conditions. This feature is used to model flows that involve change in domain shape with respect to time, due to moving boundaries. The mesh updates every time step based on new positions of the moving

48

boundary. The different methods by which the solver updates the mesh of moving boundaries at each time step includes,

- Smoothing method-spring based method, Laplacian method and boundary layer method.
- Dynamic layering method.
- Local remeshing.

The choice of the mesh updating method depends upon the type of problem, computation and solution requirements.

3.4.4.3 Material definition and Viscosity modelling

Assigning material properties to the discretised fluid and solid volume is the next and important step in the process of solver settings. As mentioned earlier, it was decided to use Herschel-Bulkley's model with shear rate dependent feature to model the viscosity of wet clay used in the extrusion process. Since clay is not a standard type of fluid that is commonly encountered in many flow scenarios occurring in the field of engineering, its properties are not readily available in FLUENT solver. Thus the required variables of Herschel-Bulkley's model, relevant for wet clay were added to the existing material database. Table 3-3 shows the different variable inputs required for a typical Herschel-Bulkley's model.

Variables
Consistency Index (k) (Pa.s^n)
Power law index (n)
Yield stress threshold(τ_0) (Pa)
Critical shear rate(C.S.R) ($\dot{\gamma}_c$) ((s^{-1})

Table 3-3 Variables for Herschel- Bulkley's model

The above mentioned variables vary with respect to the particle size, moisture and raw material content of clay. These variables can be related to each other as shown in Equation 3.10.

$$\tau_0 = k\dot{\gamma}_c{}^n --3.10$$

The major mineral content found in clays used for making bricks in U.K. is Kaolinite and widely used size of the clay particle is <2 mm. The uniqueness

49

in the mineral content and size of clay particles and the available mathematical model facilitated in choosing a few sets of values for Herschel-Bulkley's model variables, for representing the (kaolinite) clay with different moisture content. The values of $\tau_0, k, \dot{\gamma}_c$ and n used in this research work, for representing clays with moisture content ranging from 7-14% on wet basis (typical range for clay used in stiff extrusion process), is presented later in this chapter along with the results of various CFD simulations.

Herschel-Bulkley's model combines the effect of both Power law fluids and the Bingham plastic fluids. The viscosity at each time step during an unsteady state process is determined using the Equations 3.11 or 3.12, depending upon the $\dot{\gamma}$ value. [**Ansys-Fluent 12.0 user's guide 2010**].

For $\dot{\gamma} > \dot{\gamma}_c$,

$$\eta = \frac{\tau_0}{\dot{\gamma}} + k\left(\frac{\dot{\gamma}}{\dot{\gamma}_c}\right)^{n-1} --3.11$$

For $\dot{\gamma} < \dot{\gamma}_c$,

$$\eta = \tau_0 \frac{\left(2 - \dot{\gamma}/\dot{\gamma}_c\right)}{\dot{\gamma}_c} + k\left[(2 - n) + (n - 1)\frac{\dot{\gamma}}{\dot{\gamma}_c}\right] --3.12$$

Where, $\qquad \dot{\gamma} = \sqrt{\frac{1}{2}\overline{\overline{D}} : \overline{\overline{D}}} --5.13$

Where, $\overline{\overline{D}}$=rate of deformation tensor, η= viscosity.

3.4.4.4 Temperature dependent properties modelling

Extrusion in actual scenario is a non-Isothermal process. The heat generated during the flow of wet clay through the auger, barrel enclosure and die, because of frictional forces, is understood to attain a significant value during stiff extrusion process and also influences the quality of extruded material and the flow process. The energy equation along with viscous heat dissipation feature available in the FLUENT was used to model this phenomenon. The properties of the extruded clay column that are subjected

50

to variation with respect to change in temperature include compacted density, thermal conductivity and specific heat capacity.

The density (bulk density) of the wet clay that enters the extruder system varies significantly with respect to the clay column that leaves the extruder system. In a stiff extrusion process, the density of compacted and un-compacted wet clay typically falls in the range of 1602 kgm^{-3} to 1742 kgm^{-3} **[Walker,2012]** and the rise in temperature falls in the range of 50°C to 60°C. These values could be even higher if dies with a single or multiple core is used. Since such die designs were not considered in this research work, it is not discussed any further. This change in density along with thermal conductivity and specific heat capacity of the wet clay was expressed as a linear function with respect to the temperature rise, experienced during the extrusion process. Due to the lack of availability of proper material data and experimental works on the thermal conductivity and specific heat capacity of wet clay, suitable values were obtained from the work completed by **Robie and Hemingway (1991) and Michot et al. (2008)**.Though the values discussed by these authors do not specify the moisture content of the clay, suggested values were used as a guidance to calculate the values required for the CFD modelling work undertaken in this research.

3.5 Experimental validation of CFD modelling

The CFD modelling technique for assessing the performance of an extruder system, discussed above was validated by modelling and comparing the numerical results with experimental results of a lab scale extruder.

The experimental investigation of performance characters of a lab scale extruder are discussed in this part. A lab scale extrusion unit with an extruder of diameter 75 mm was used for the investigation and is shown in Figure 3-18.
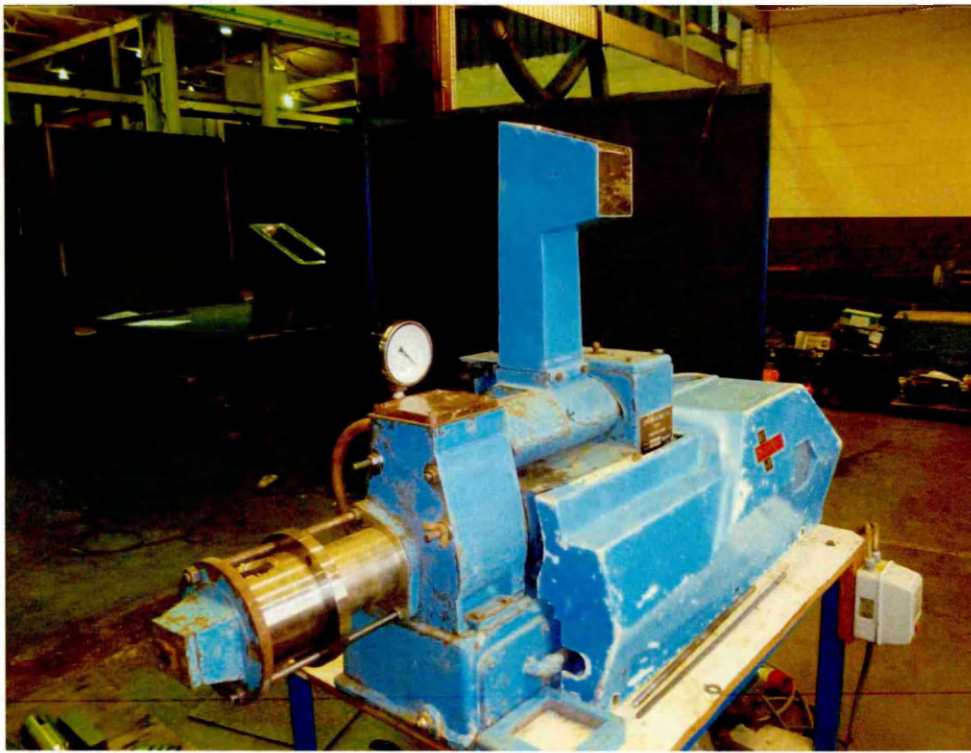
Figure 3-18 Scaled extruder

Experimental set up

The extrusion pressure was measured using a special type of pressure sensor, power consumption using an ammeter and vacuum pressure using a vacuum gauge. A schematic representation of the experimental set up used for the investigation is shown in Figure 3-19.
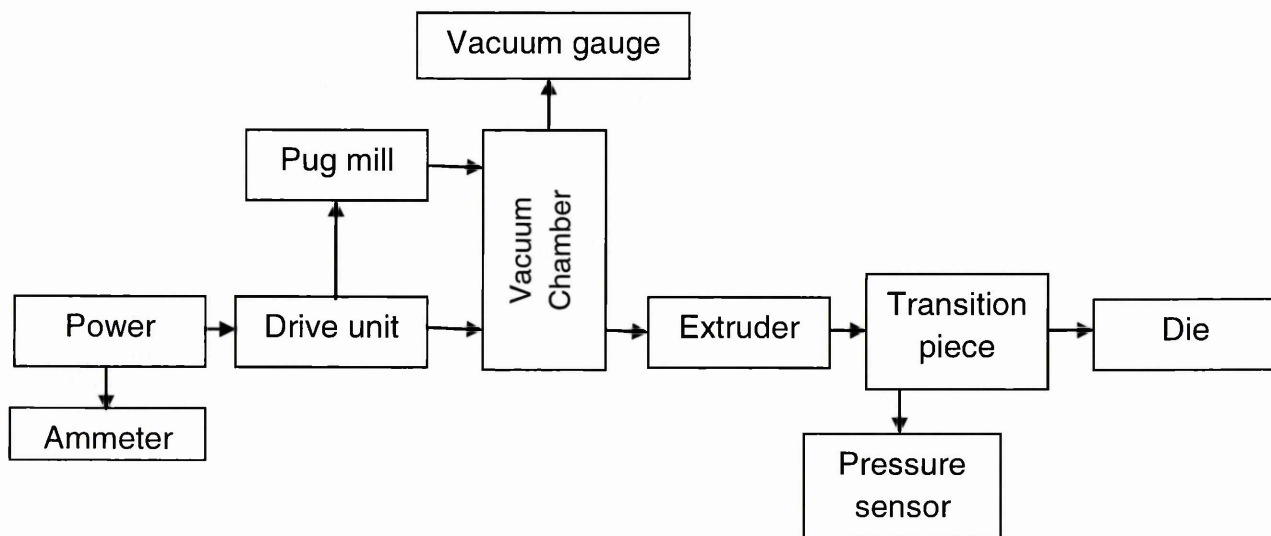
Figure 3-19 Experimental set up layout

Extrusion pressure and power consumed by the lab scale extruder was measured for two different extrusion scenarios (two different clays with different moisture content). The operating parameters used and results obtained from the experimental investigation are summarised below.

Trial: 1

In this case, clay from M/s Hanson Brick Limited, Desford, U.K. was used for the investigation. The actual moisture content of the clay obtained from the source was assessed based on dry and wet method, and then suitable amount of water was added per unit mass of clay sample to achieve a moisture content of 12-13% on dry basis (recommended moisture content level for stiff extrusion process). Suitable care was taken to prevent significant loss of moisture content during the experiment. The extrusion pressure and current consumption was recorded at a point when the extruded mass of clay reached the right amount of stiffness (2.6 in the Penetrometer scale). The power consumed was calculated using the current reading obtained during extrusion and applying the standard formula. Table 3-4 summarises the measured values.

Die used for Trail:1	
Parameters	**Measured value**
Moisture content of the clay	Wet basis-11-12%, Dry basis 12-13%
Auger speed	19 rpm
Vacuum pressure	-20 mm mercury. (-2666.6 Pa)
Penetrometer scale reading	2.6
Current readings	Before feeding clay - 2.5-2.6 Amps, During feeding and when clay reached a certain level in vacuum chamber- 3.1

	Amps to 3.5 Amps, During continuous extrusion, with right stiffness- 3.9 Amps.
Current consumption by extruder alone, during extrusion.	0.3 to 0.4 Amps
Voltage	415 Volts.
Power consumed by **extruder unit alone**, during extrusion.	124.5 Watts
Extrusion rate	0.013 to 0.015 kgs^{-1}
Extrusion pressure	13-14 bar
Temperature change in the clay	Initial temperature 296 K and final temperature of extruded clay 301K (five degree rise)
Uncompacted density of clay	1298 kgm^{-3}
Compacted density of clay	2270 kgm^{-3}

Table 3-4 Experimental analysis results-trial 1

Trial: 2

In this case, clay from river Humber U.K. was used for the investigation. Since the clay obtained from the source contained more amount of moisture content of approximately about 25-30% on wet basis, the sample was directly used for the experimental investigation, without further addition of water. The required parameters were then measured and calculated using the same procedure, as discussed above in Trial: 1. Table 3-5 summarises the measured values.

Parameters	Measured value
Die used in Trial:2	
Parameters	**Measured value**
Moisture content of the clay	Wet basis 25-30%
Auger speed	19 rpm
Vacuum pressure	-13 mm mercury. (-1733.19 Pa)
Penetrometer scale reading	2.3
Current readings	Before feeding clay - 2.8 Amps, During feeding and when clay reached a certain level in vacuum chamber- 3.2 Amps to 3.3 Amps, During continuous extrusion, with right stiffness- 3.4 Amps to 3.5 Amps.
Current consumption by extruder alone, during extrusion.	0.1 Amps
Voltage	415 Volts.
Power consumed by **extruder unit alone**, during extrusion.	57.5 Watts
Extrusion rate	0.01014 kgs^{-1}
Extrusion pressure	5.8 bar to 6.0 bar
Temperature change in the clay	Initial temperature 293 K and final temperature of extruded clay 297 K (four degree rise)
Uncompacted density of clay	1200 kgm^{-3}
Compacted density of clay	2150 kgm^{-3}

Table 3-5 Experimental analysis results-trial 2

3.6 CFD modelling of a scaled extruder

The Performance assessment of the scaled extruder using CFD modelling technique is discussed in this part of the report.

CAD modelling and discretisation of scaled extruder:-

3-D CAD model of the scaled extruder components used for the investigation is shown from Figure 3-20 to 3-22.
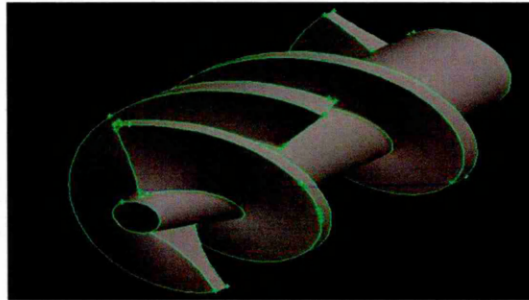
Figure 3-20 Scaled extruder-auger shaft
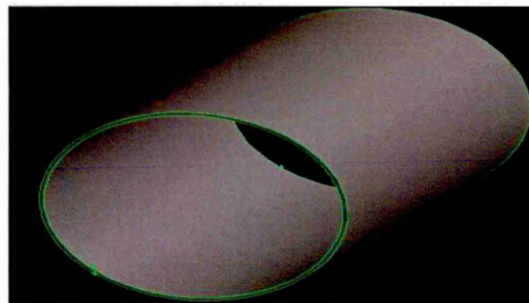
Figure 3-21 *clearance*
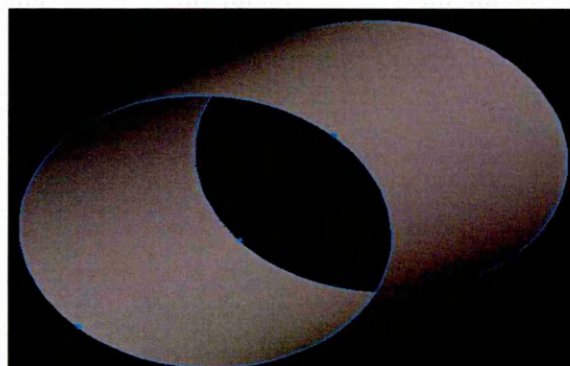
Figure 3-22 Scaled extruder-transition piece

The generated CAD model was meshed in Gambit using suitable meshing schemes for individual components. Tetrahedral / hybrid mesh elements and T-grid meshing scheme was used to mesh the fluid volume around the auger shaft and the total number of cell elements obtained was 310,552. The meshed geometry is shown in Figure 3-23.
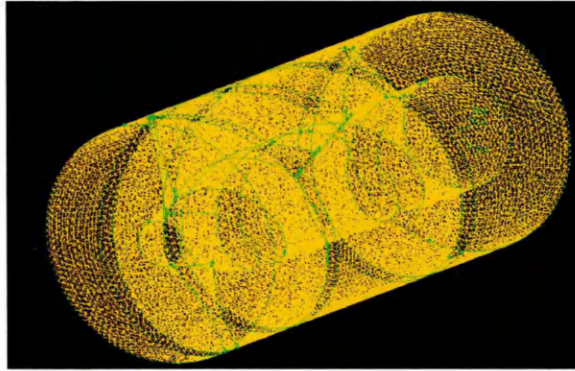
Figure 3-23 Scaled extruder-auger shaft meshed

Uniform hexagonal mesh elements with cooper scheme were used to mesh the clearance volume. The total number of cell elements obtained was 11,778 and the meshed geometry is shown in Figure 3-24.
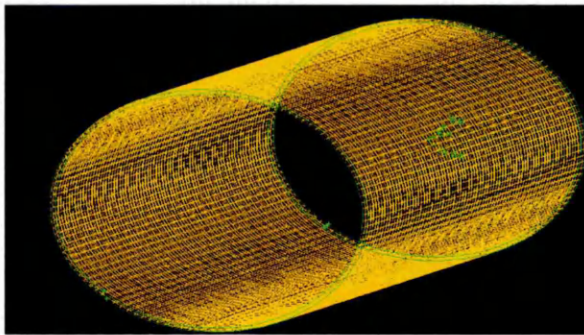
Figure 3-24 Scaled extruder-clearance meshed

Hex/wedge shaped mesh elements with cooper scheme were used to mesh the transition piece. The total number of cell elements obtained was 502,199 and the meshed geometry is shown in Figure 3-25.
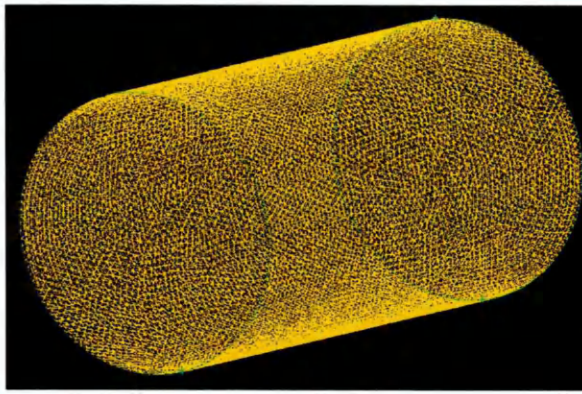
Figure 3-25 Scaled extruder- transition piece meshed

A similar boundary condition and modelling approach, used to model the full scale extruder, was used to complete the pre and post processor solver settings of scaled extruder modelling. In the earlier part of this chapter, it was discussed that the moisture content of clay determines the variable values in a Herschel-Bulkley's model and also the performance of an extruder system. Since in Trial: 1 and Trial: 2 two different clays with different moisture content was used, the values for Herschel-Bulkley's model were chosen appropriately. Table 3-6 summarises the values used for the variables of Herschel-Bulkley's model in CFD analysis.

Herschel-Bulkley's model variable	Trial:1 values	Trial:2 values
k $(Pa.s^n)$	5206.95	3200
n	0.32	0.2
τ_0 (Pa)	6500	3516
C.S.R (s^{-1})	2.1	1.6

Table 3-6 Herschel- Bulkley's model values for scaled extruder CFD analysis

The values for clay used in Trail: 2 were set to a lower value due to the soft nature of clay, and such soft clay materials are normally used in soft extrusion process. Since extruders manufactured by C.F Ltd, for the purpose of stiff extrusion are sometimes used for soft extrusion process as well, it was considered to be a useful investigation with the identified CFD methodology and compare the numerical model results with experimental results.

The results of CFD analysis for extrusion scenarios Trial: 1 and Trial: 2 are available in Appendix A- section XII & XIII. Table 3-7 shows results of the extrusion pressure and power consumption by the scaled extruder under the two extrusion scenarios, determined experimentally and using CFD analysis.

Process parameters	Experimental results	CFD results
Trial-I		
Extrusion pressure	13-14 bar	13.4 bar
Power consumption	124.5 Watts	114.06 Watts
Trial-II		
Extrusion pressure	5.8-6.0 bar	5.84 bar
Power consumption	57.5 Watts	47 watts

Table 3-7 Result comparison for scaled extruder

3.7 Experimental study of clay rheology

The most important determinant factor in selection and use of an appropriate flow model to simulate the process of clay extrusion and assess the performance of extruders numerically is the shear thinning behaviour of the clay-water system. In order to demonstrate the shear thinning behaviour of the clay and to further support the choice of flow model used in this research work, an attempt was made to study the rheological characters of wet clay by measuring the viscosity, using oscillatory test in a parallel plate viscometer (Make: Anton Parr, Model no: MCR301), shown in Figure 3.26.

Figure 3-26 Parallel plate viscometer-Anton Parr (MCR301)

The viscosity of clay sample used in Trial: 2 experimental work was measured. The accuracy of the measured results when using a parallel plate viscometer depends upon the contact established between the sample surface and measuring plate surface of the instrument (It consists of a stationary and a moving plate). A gap of 2 mm is recommended to be an optimised gap between the plates, to get sensible results **[Mezger, 2006]**. In order to satisfy this criterion, clay samples with a diameter of 50 mm, thickness between 2-3 mm and surface free from disparities was prepared. Values for G` (G-prime) and G`` (G-double prime) were measured to identify suitable frequency value for oscillatory test and then by varying the plate gap from 2 mm to 2.19 mm, values for the complex modulus, storage modulus, loss modulus and damping factor were measured and a graphical plot for Apparent viscosity vs. Strain rate was obtained for the clay sample and is shown in Figure 3-27.
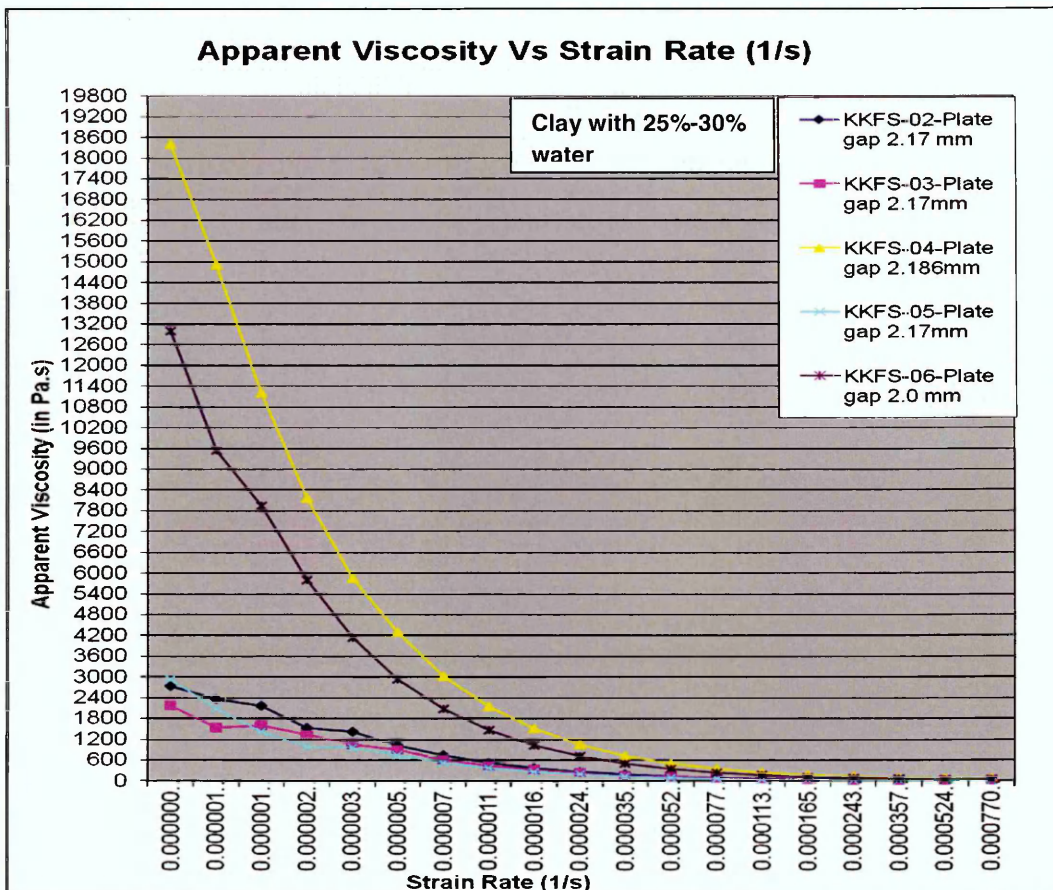
Figure 3-27 Apparent viscosity vs. Strain rate of clay- measured experimentally

The viscosity profile obtained through the viscometer experiment clearly indicates the shear thinning nature exhibited by wet clay and also demonstrates the change observed in viscosity value when it is subjected to a uniform shear. This viscosity profile determined experimentally, when compared with the CFD analysis results proves the point that, the clay exhibit shear thinning behaviour during extrusion and is well represented by the flow model and its variables used in the CFD model.

The use of the CFD modelling technique, discussed above, to assess the performance characters of full scale extruders is presented further in this chapter.

3.8 Performance assessment of extruders with different diameters

The performance of an extruder system varies significantly with respect to particle size and moisture content of clay. Extruder's diameter varies with respect to extrusion rate or number of bricks to be produced per hour and moisture content varies with respect to strength requirements and extruding ability of clay. In this part of the research work, the effect of varying the diameter of an extruder and clay moisture content on the performance parameters like extrusion pressure (static pressure) and power consumption during the process of extrusion were investigated using CFD. The variation of performance parameters was assessed for extruders of size 430 mm, 500 mm and 600 mm, using two sets of Herschel-Bulkley's model values. Operating parameters used in the CFD model are shown in Table 3-8.

Extruder Size	Feed rate (kgs^{-1})	Auger speed (rpm)	Herschel-Bulkley's model value	
			Case-I	Case-II
430 mm	15	30	$k=4908$ Pa.s^n	$k=5206.95$ Pa.s^n
500 mm	19	30	$n=0.5$ $\tau_0=8500$ Pa	$n=0.32$ $\tau_0=6500$ Pa
600 mm	11.8	22.5	C.S.R=3 s^{-1}	C.S.R=2.1 s^{-1}

Table 3-8 Data set for varying extruder diameter and moisture content analysis

61

The two data sets used for the variables in the Herschel-Bulkley's model represent uncompacted clay with different moisture content. (Value I represents harder clay and value II for softer clay). Results obtained from the CFD analysis of 430 mm extruder are summarised below, the results of 500 mm and 600 mm extruders are available in Appendix A from section II to V.

CFD Simulation results of 430 mm extruder with Herschel-Bulkley's model value-I

Extrusion pressure:

Pressure developed during the extrusion process, along the entire length of the extruder and die section, obtained from the CFD analysis is shown in Figure 3-28 and 3-29. The value varied from -605 kPa at the inlet section to a maximum of 3.4 MPa. (34 bar), observed at the tip of the auger shaft and further downstream the pressure reduced to an average value of 2.57 MPa. (25.7 bar) at the outlet.

[Note: The negative value of extrusion pressure observed at the inlet section of the extruder as discussed above and in other CFD results discussed further in this chapter is a result of the numerical evaluation on the vacuum pressure value i.e. set as the inlet boundary condition. The physical meaning of the negative pressure value is a vacuum condition exists at the inlet section.]

Contours of Static Pressure (pascal) (Time=2.0240e+00)
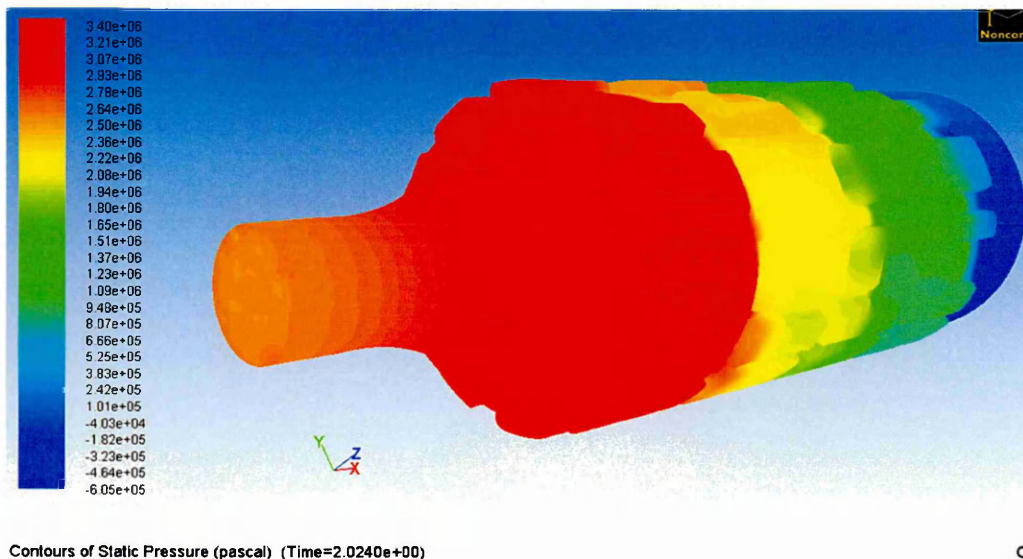
Figure 3-28 Static pressure contour (full view)-430 mm Case I

62
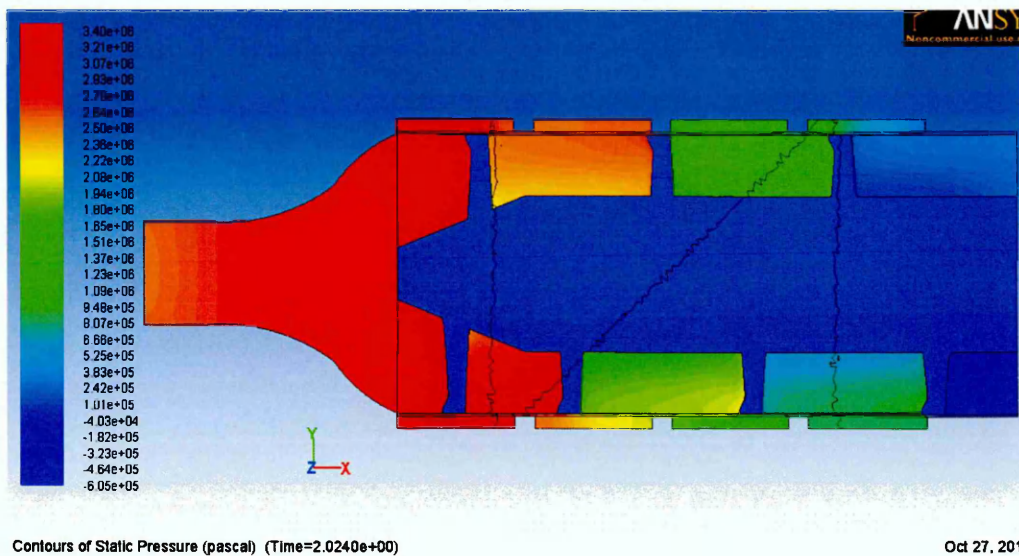
Figure 3-29 Static pressure contour (sectional view) - 430 mm Case I

Extrusion pressure values discussed above and the profile shown in Figure 3-30, clearly indicates the trend of pressure developed inside the extruder and die section during the extrusion process .This data obtained through the numerical simulation confirms the results discussed by **[Bender and Händle,1982] and [Händle,2007].**

(Note: The results of trend in pressure development during the process of extrusion, discussed in this report refer to the pressure development trend observed in the direction of extrusion.)

Static Pressure (Time=2.5050e+00)
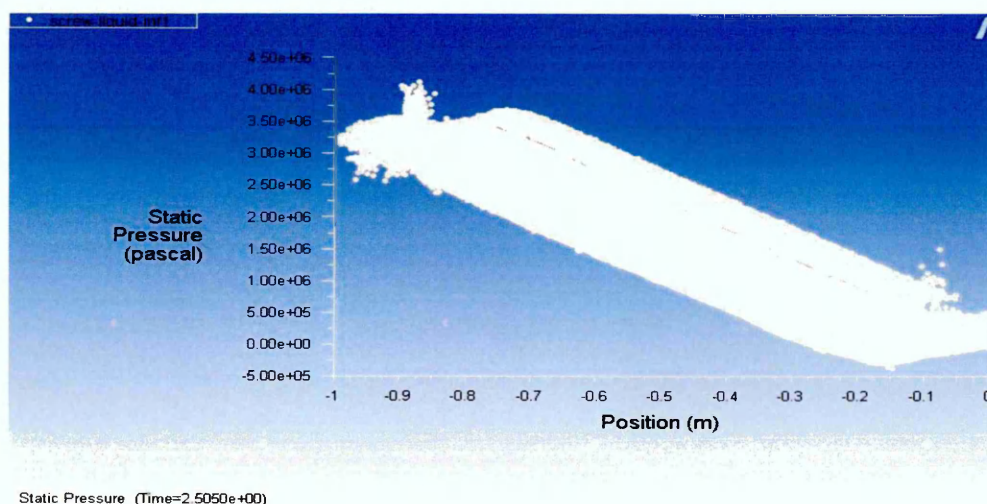
Figure 3-30 Static pressure profile-430 mm Case I

Material Flow pattern:

The flow pattern and velocity of clay during extrusion, at various sections of extruder and die, obtained from the CFD analysis is shown in Figure 3-31. In the direction of extrusion the average value observed for velocity at outlet section of die was 0.47 ms^{-1}. It is understood from the results that the material tends to deform continuously under the action of shear as it proceeds down from the inlet. It is also clear from the results that, when moving along the radial direction the material near the hub and middle of the auger gap tends to flow faster than the material near the liners. This confirms that the liners are restricting the clay from rotating along with the shaft and also it facilitates it to move in the direction of extrusion. This data obtained through numerical simulation confirms with results discussed by **Zhang et al., 2011.**

Contours of Velocity Magnitude (m/s) (Time=2.0240e+00)   Oct 27, 201ʹ
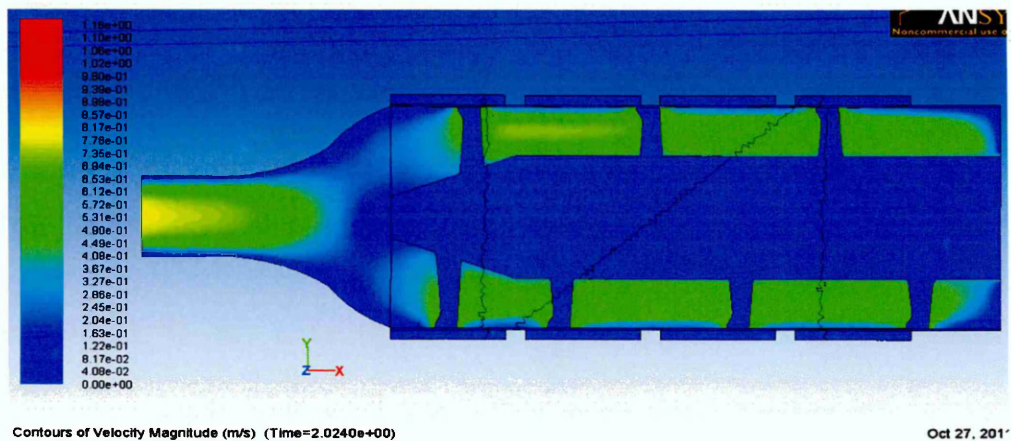
Figure 3-31 Flow velocity during extrusion (sectional view)- 430 mm Case I

Viscosity profile:

Shear thinning behaviour of clay during the process of extrusion was verified by plotting a graph with molecular viscosity against strain rate (shear rate) at different sections of extruder and die. The profile for molecular viscosity vs. strain rate at the outlet, obtained from the CFD analysis is shown in Figure 3-32.

Molecular Viscosity vs. Strain Rate (Time=2.0240e+00)
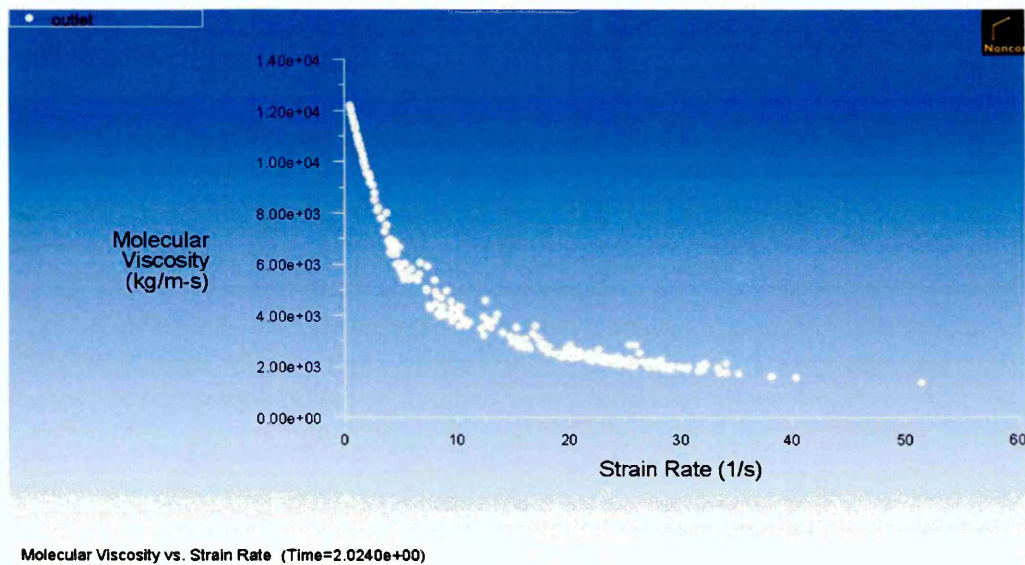
Figure 3-32 Molecular viscosity vs. Strain rate- 430 mm Case I

Convergence monitoring:

The accuracy and validity of the solution in any CFD analysis is ensured by monitoring the convergence of residuals and other problem relevant process parameters like mass flow rate, velocity components, co-efficient of drag and pressure components. In this research work it was accomplished through monitoring the convergence of residuals and mass flow rate at the outlet. It was very hard to acquire a complete converged solution and hence the iteration was stopped when the monitored residuals convergence stayed constant for a certain number of iterations and results were obtained. Figure 3-33 and 3-34 shows the results obtained in this case for convergence monitoring.

Scaled Residuals (Time=2.0240e+00)   o
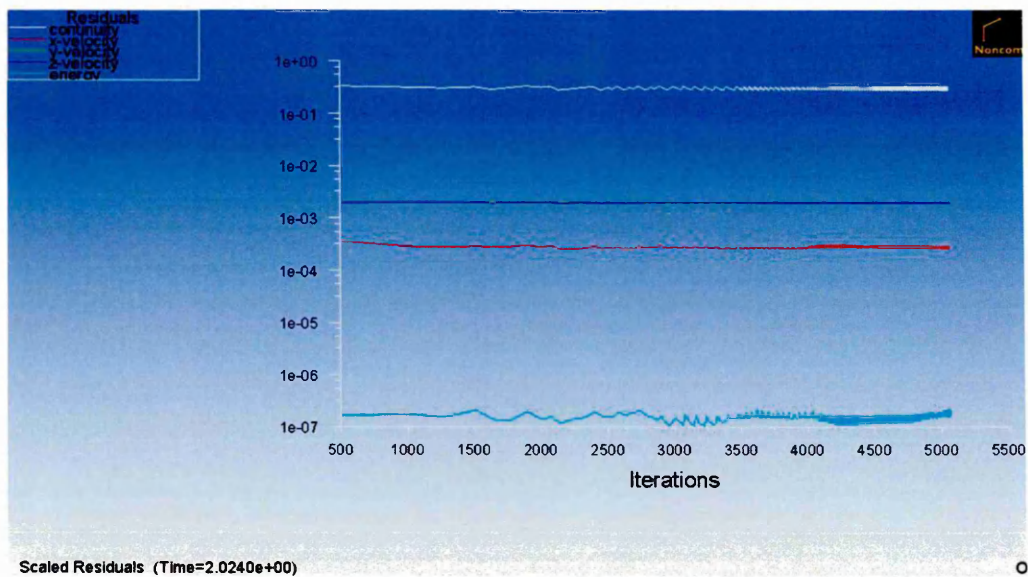
Figure 3-33 Residual convergence-430 mm Case I

Convergence history of Mass Flow Rate on outlet (Time=2.0240e+00)   Oc
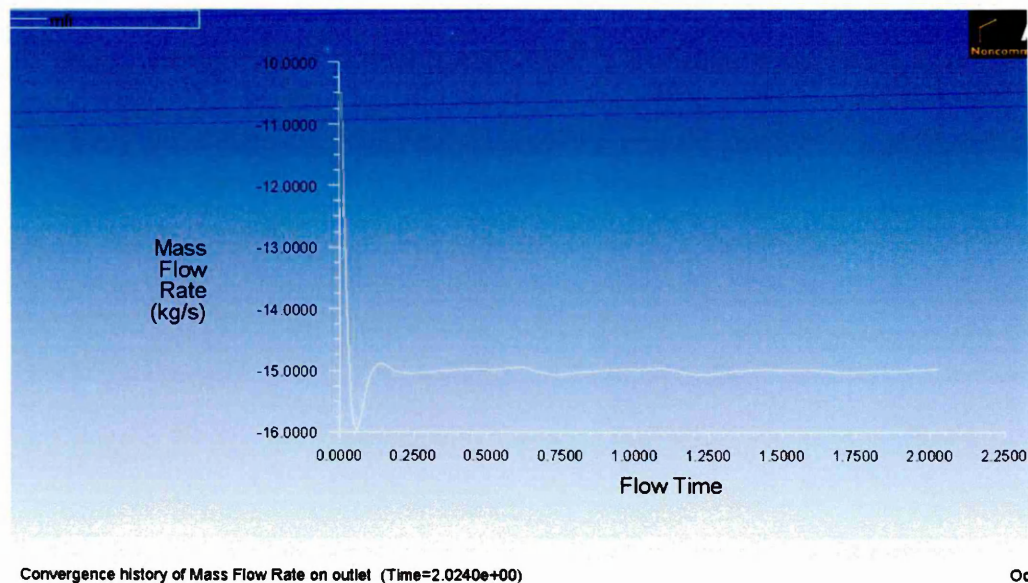
Figure 3-34 Mass flow rate convergence- 430 mm Case I

The results of convergence monitoring obtained from other CFD analysis are similar to the case presented above and hence these results were not discussed for other cases of CFD analysis presented later in this chapter.

The energy required to extrude per unit mass of clay was calculated for each case using the torque value at the auger section, obtained from the CFD analysis. A graph was plotted to analyse the trend of variation in maximum pressure and energy required during the extrusion process, with respect to change in diameter of extruder, shown in Figure 3-35.

66
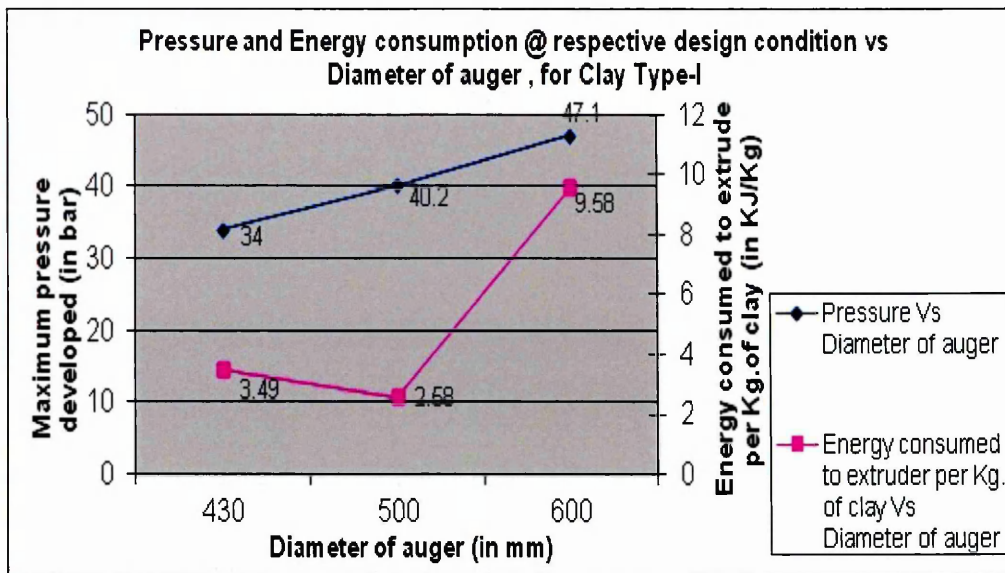
Figure 3-35 Extrusion pressure and Energy consumption vs. Diameter (Case-I)

The general trend clearly indicates that the pressure and energy consumption during extrusion varies significantly with respect to design (size) and operating parameters (speed and feed rate) of an extruder, even if the type and moisture content of clay material remains the same.

CFD Simulation results of 430 mm extruder with Herschel-Bulkley's model value-II

Extrusion pressure:

Pressure developed during extrusion in a 430 mm extruder, with respect to change in clay moisture content is shown in Figure 3-36 and 3-37.The pressure varied from a minimum value of -334 kPa at the inlet section to a maximum of 1.98 MPa (rounded off to 20 bar), observed at the tip of the auger shaft and further downstream the pressure reduced to an average value of 1.47 MPa (14.7 bar) at the outlet. In comparison to the case discussed earlier, the pressure developed during the extrusion of softer clay is lower than the pressure developed for the harder clay.
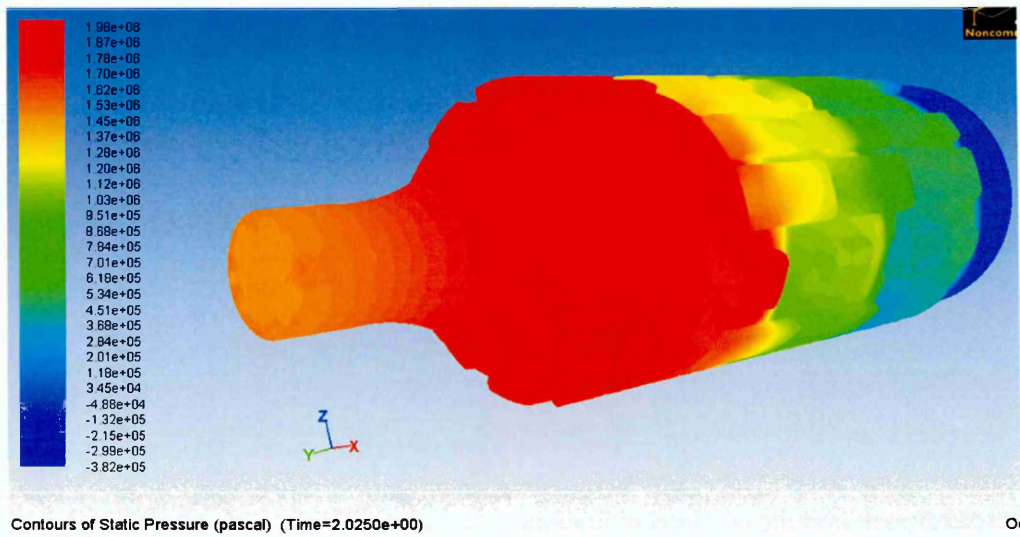
Figure 3-36 Static pressure contour (full view)-430 mm Case II
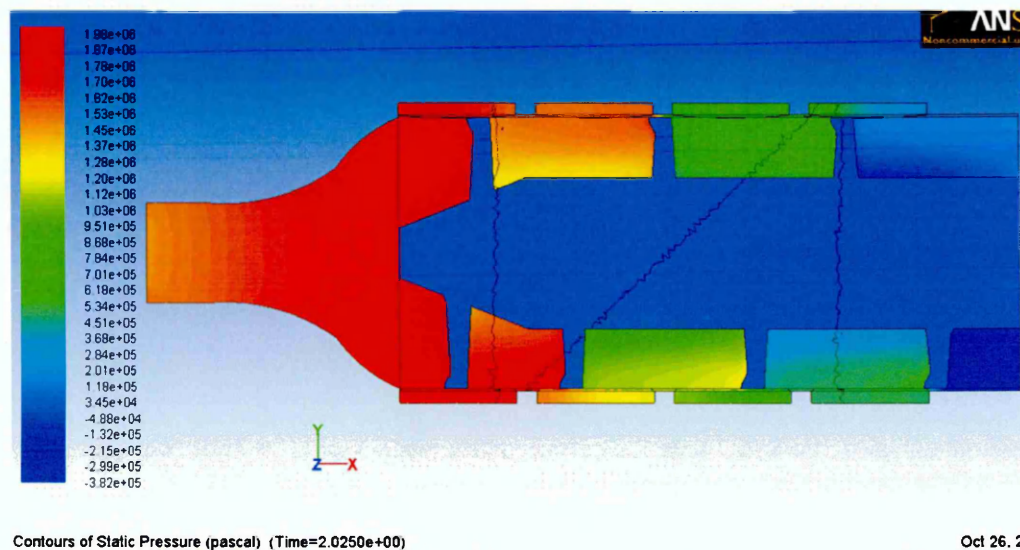
Figure 3-37 Static pressure contour (sectional view)- 430 mm Case II

The trend observed in extrusion pressure, developed during extrusion is shown in Figure 3-38. No significant variation was noted when compared with the earlier case.

68

Figure 3-38 Static pressure profile-430 mm Case II

Material Flow pattern:

The flow pattern and velocity of clay observed during extrusion is shown in Figure 3-39. In the direction of extrusion the average value observed for velocity at outlet section of die was 0.47 ms^{-1}. A significant difference in material deformation pattern and in velocity was noted within the auger and barrel section, for softer clay when compared with harder clay. It indicates that the softer clay deforms more uniformly, observed along the radial direction, compared to the harder clay, when subjected to equal shear force.
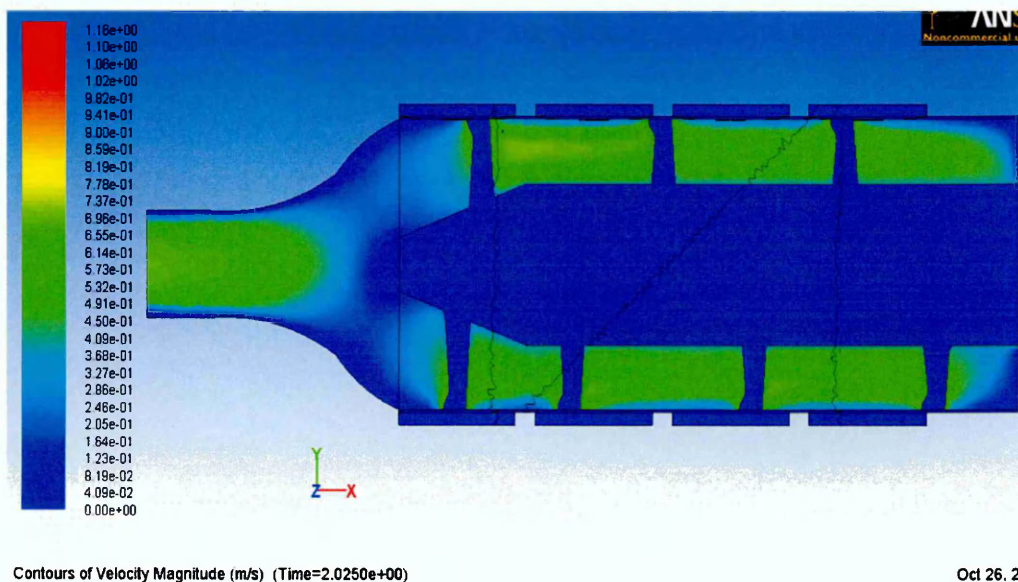
Figure 3-39 Flow velocity during extrusion (sectional view)- 430 mm Case II

The profile of shear thinning behaviour of clay at the outlet section of die is shown Figure 3-40. It also indicates that the softer clay deforms more easily than the harder clay when subjected to shear.

Molecular Viscosity vs. Strain Rate (Time=2.0250e+00)
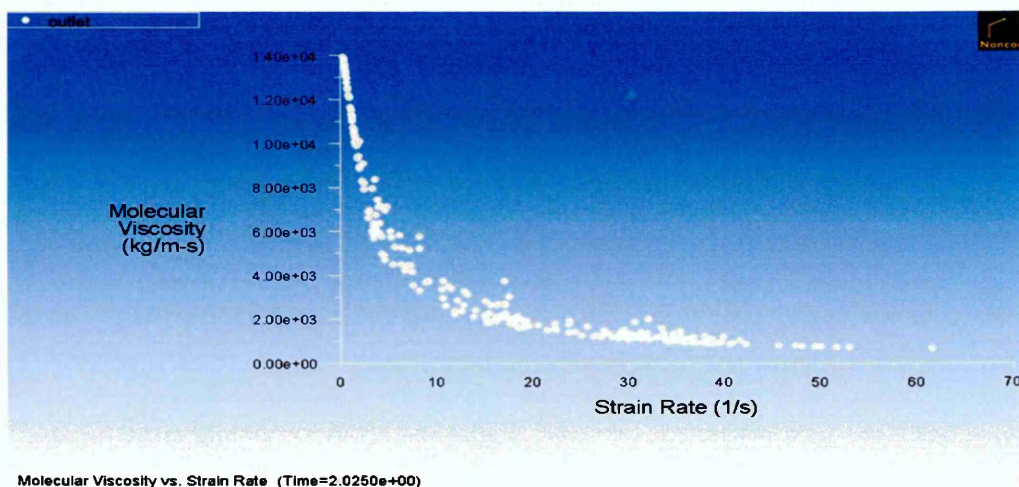
Figure 3-40 Molecular viscosity vs. Strain rate-430 mm Case II

The graph shown in Figure 3-41 indicates the trend of variation in energy required to extrude per unit mass of clay and maximum pressure developed during extrusion with respect to size of extruder, for softer clay.
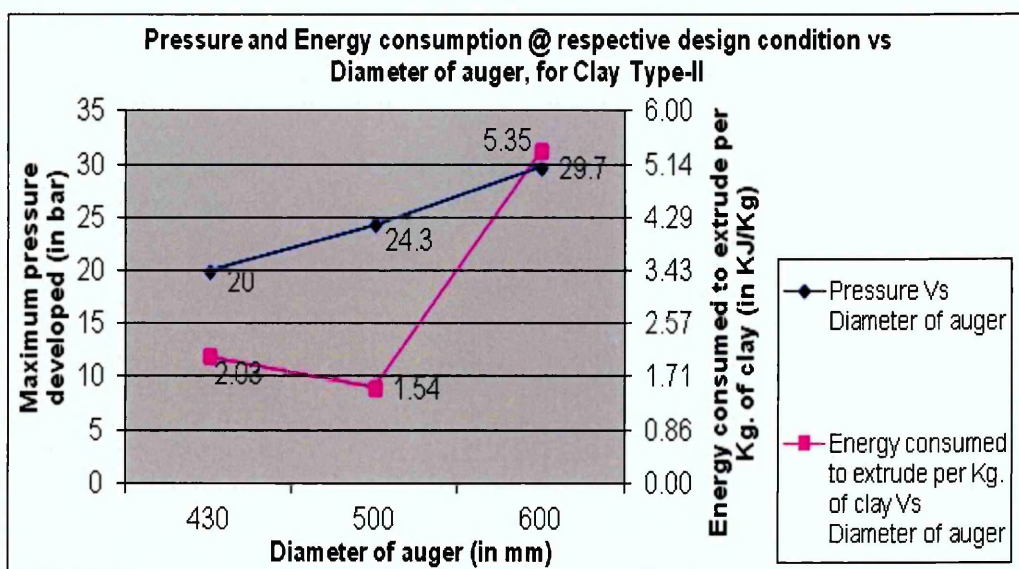
Figure 3-41 Extrusion pressure, Energy consumption vs. Diameter (Case-II)

The general trend in energy requirement and maximum pressure developed during extrusion remained the same for both hard and soft clay extrusion. It

70

is clearly understood from the graphs, that irrespective of the extruder size, the extrusion pressure and power required for extruding clays with high moisture content will be low compared with extruding harder clay. The extrusion pressure increases with respect to increase in the size of extruder even for the clay with same moisture content, but not necessarily the power required in all cases. It also clearly demonstrates the effect of changing moisture content of clay on the performance of extruder.

3.9 Performance assessment of a 500 mm extruder

The effect of varying design and operating parameters on the performance of a 500 mm extruder system was investigated in this part of the research, using CFD. The results obtained from the CFD analysis are summarised below.

3.9.1 Effect of varying feed rate on performance of extruder

The effect of changing the feed rate of uncompacted clay, on the performance of a 500 mm extruder was investigated in this part. The other parameters like the die design, extruder design, clay material, size, clay moisture content and auger speed were kept constant. Table 3-9 summarises the operational parameters and material properties used in the CFD analysis.

Extruder Size	Feed rate (kgs^{-1})	Auger speed (rpm)	Herschel-Bulkley's model value
500 mm	Varying	30	$k=5206.95$ Pa.s^n $n=0.32$ $\tau_0=6500$ Pa C.S.R$=2.1$ s^{-1}

Table 3-9 Data set for varying feed rate analysis

The performance characters were assessed for the following feed rates 10 kgs^{-1}, 15 kgs^{-1}, 19 kgs^{-1}, 25 kgs^{-1}, 30 kgs^{-1}, 40 kgs^{-1} and 50 kgs^{-1}. The results obtained from the CFD analysis are summarised below.

71

Extrusion Pressure:

Pressure developed during extrusion in a 500 mm extruder with 10 Kgs^{-1} of feed rate is shown in Figure 3-42 and 3-43. The pressure varied from a minimum value of -150 kPa at the inlet section to a maximum of 2.68-2.78 MPa (rounded off to 28 bar) observed at the end of auger shaft and reduced to an average value of 2.13 MPa (21.3 bar) at the outlet.

Contours of Static Pressure (pascal) (Time=4.4200e-01)
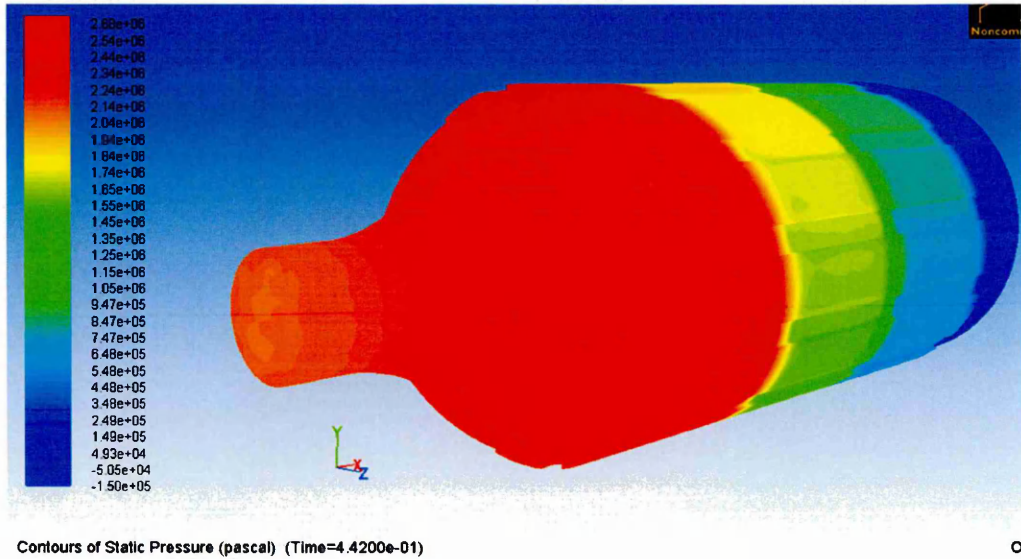
Figure 3-42 Static pressure contour (full view) - feed rate 10 kgs^{-1}

Contours of Static Pressure (pascal) (Time=4.4200e-01)   Oct 10, 2011
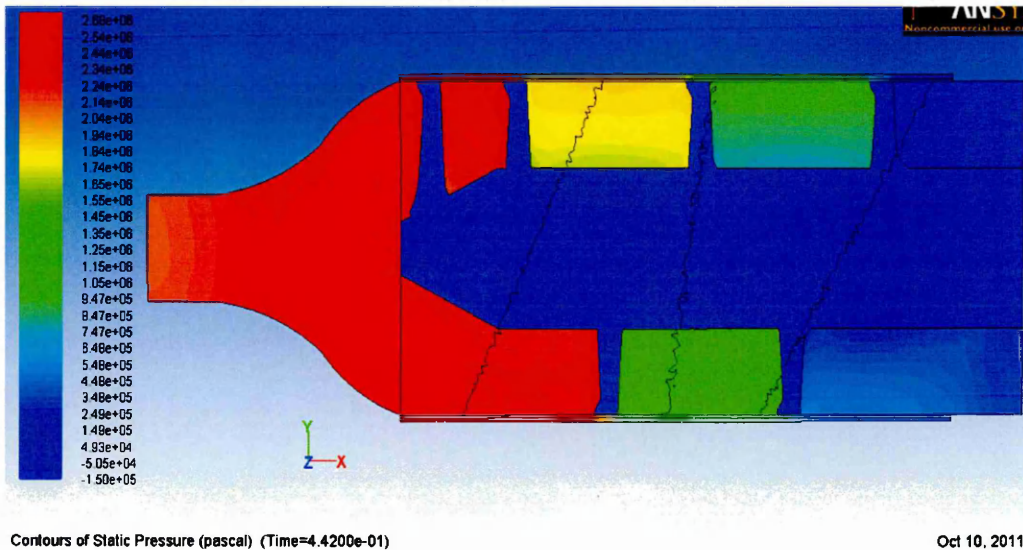
Figure 3-43 Static pressure contour (sectional view) - feed rate 10 kgs^{-1}

The trend of pressure development within the extruder section, observed during extrusion is shown in Figure 3-44.

Static Pressure (Time=4.4200e-01)

Figure 3-44 Static pressure profile- feed rate 10 kgs⁻¹

Material Flow pattern:

The flow pattern and velocity of clay observed during extrusion at various sections of extruder and die, in a 500 mm extruder with 10 kgs⁻¹ feed rate is shown in Figure 3-45. In the direction of extrusion the average value observed for velocity at outlet section of die was 0.32 ms⁻¹.

Contours of Velocity Magnitude (m/s) (Time=4.4200e-01)   Oct 10, 201

Figure 3-45 Flow velocity during extrusion (sectional view)- feed rate 10 kgs⁻¹

Viscosity Profile:

The profile of shear thinning behaviour of clay observed at the outlet section of die in a 500 mm extruder with 10 kgs⁻¹ feed rate is shown in Figure 3-46.

The viscosity value was observed to be higher at lower mass flow rate when compared with higher mass flow rate.

Molecular Viscosity vs. Strain Rate (Time=4.4200e-01)
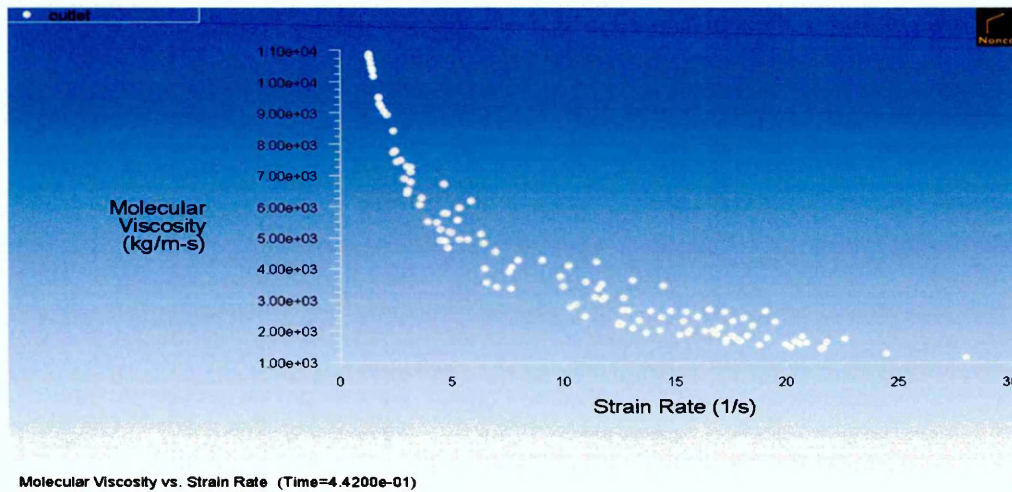
Figure 3-46 Molecular viscosity vs. Strain rate- feed rate 10 kgs⁻¹

The results of CFD analysis, for feed rates 15 kgs⁻¹, 19 kgs⁻¹, 25 kgs⁻¹, 30 kgs⁻¹, 40 kgs⁻¹ and 50 kgs⁻¹ is available in Appendix A-section VI.

The trend of variation in maximum extrusion pressure and energy required in extruding per unit mass of clay, with respect to change in feed rate of clay for a 500 mm extruder is shown in Figure 3-47.
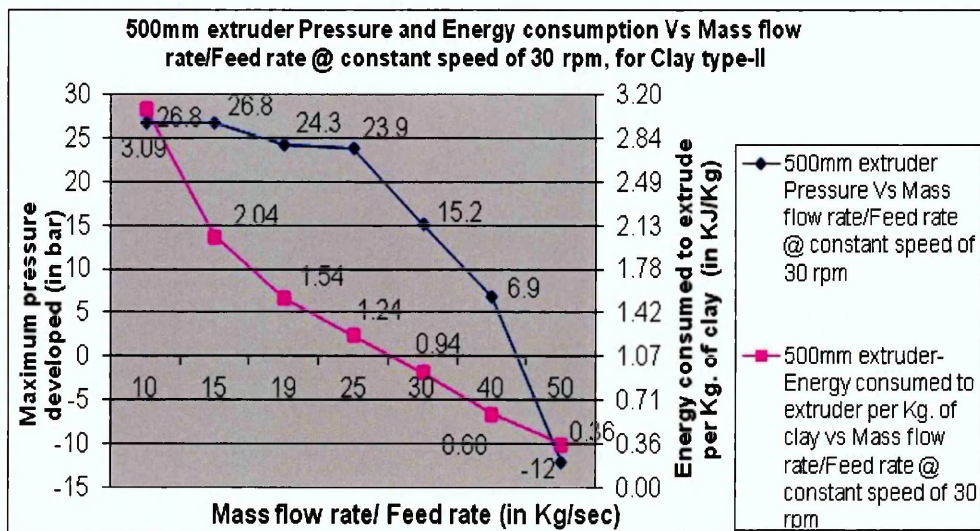
Figure 3-47 Extrusion pressure, Energy consumption vs. Feed rate

3.9.2 Effect of varying auger speed on performance of extruder

The effect of varying auger speed on the performance characters of a 500 mm extruder was investigated in this part. The other parameters like the die design, extruder design, clay material, size, clay moisture content and feed rate were kept constant. Table 3-10 summarises the operational parameters and material properties used in the CFD analysis.

Extruder Size	Feed rate (kgs^{-1})	Auger speed (rpm)	Herschel-Bulkley's model value
500 mm	19	varying	$k=5206.95$ Pa.s^n $n=0.32$ $\tau_0=6500$ Pa C.S.R$=2.1$ s^{-1}

Table 3-10 Data set for varying auger speed analysis

The performance characters were assessed for the following auger speeds- 10 rpm, 15 rpm, 20 rpm, 25 rpm, 30 rpm, 40 rpm and 50 rpm. The results obtained from the CFD analysis are summarised below.

Extrusion Pressure:

Pressure developed during extrusion in a 500 mm extruder with auger speed of 10 rpm is shown in Figure 3-48 and 3-49. Negative pressure was observed at the outlet and at the tip auger section of the extruder. The maximum pressure observed was 192 kPa (1.92 bar) at the inlet section, which indicates that the speed of the auger is not sufficient enough to induce the required shear force for the clay to deform and resulting in clay being stopped at the inlet section.

75

Contours of Static Pressure (pascal) (Time=2.6040e+00)
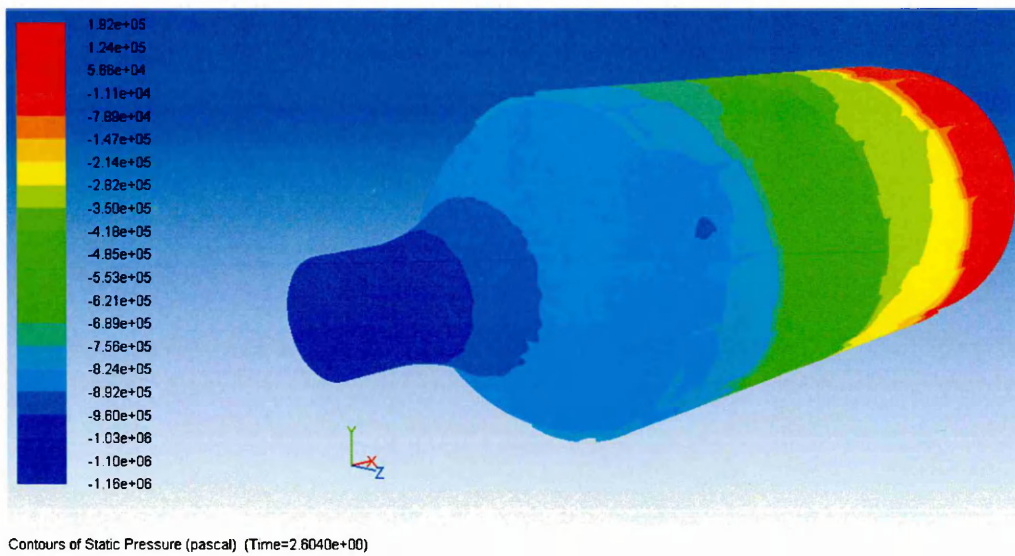
Figure 3-48 Static pressure contour (full view) - auger speed 10 rpm

Contours of Static Pressure (pascal) (Time=2.6040e+00)   Sep 28, :

Figure 3-49 Static pressure contour (sectional view) - auger speed 10 rpm

The trend of pressure development observed within the extruder section, during extrusion is shown in Figure 3-50.
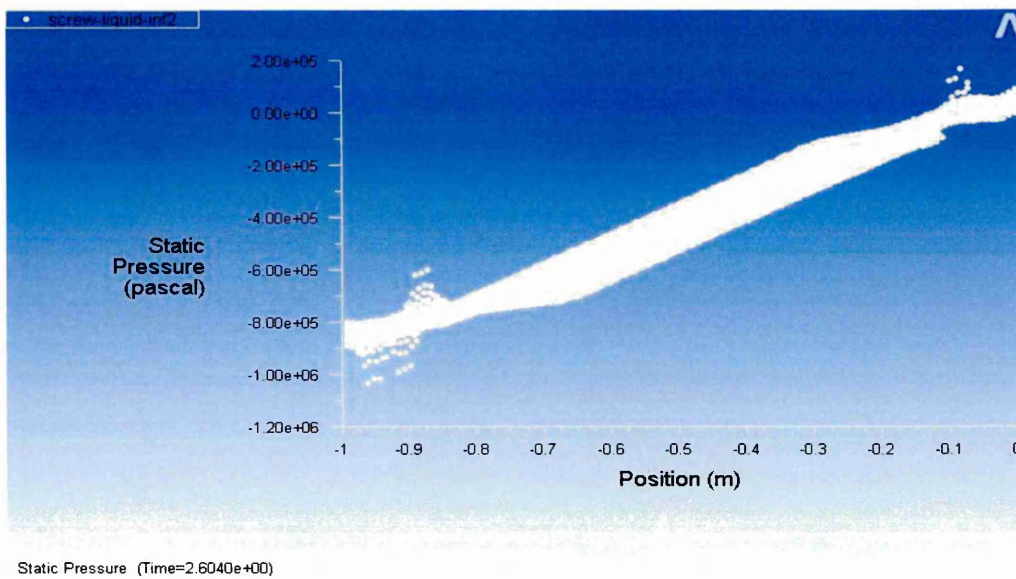
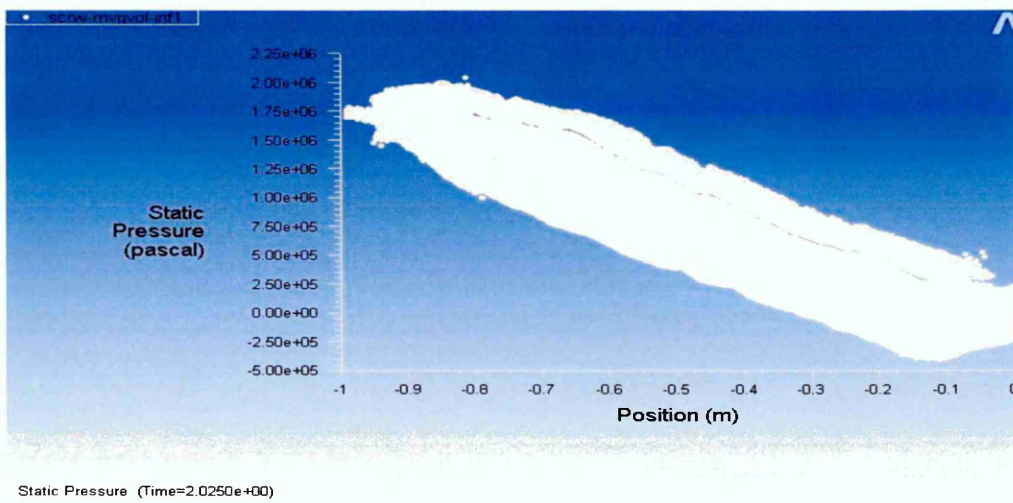*Figure 3-50 Static pressure profile-auger speed 10 rpm*

Material Flow pattern:

The flow pattern and velocity of clay observed during extrusion, at various sections of extruder and die, in a 500 mm extruder with auger speed of 10 rpm is shown in Figure 3-51.

Figure 3-51 Flow velocity during extrusion (sectional view) - auger speed 10 rpm

The profile of shear thinning behaviour of clay observed at the outlet section of die in a 500 mm extruder with auger speed of 10 rpm is shown in Figure 3-52.

Molecular Viscosity vs. Strain Rate (Time=2.6040e+00)

Figure 3-52 Molecular viscosity vs. Strain rate - auger speed 10 rpm

The results of CFD analysis, for auger speed of 15 rpm, 20 rpm, 25 rpm, 30 rpm, 40 rpm and 50 rpm are available in Appendix A-section VII.

The trend of variation in maximum extrusion pressure and energy required in extruding per unit mass of clay, with respect to change in auger speed for a 500 mm extruder is shown in Figure 3-53.
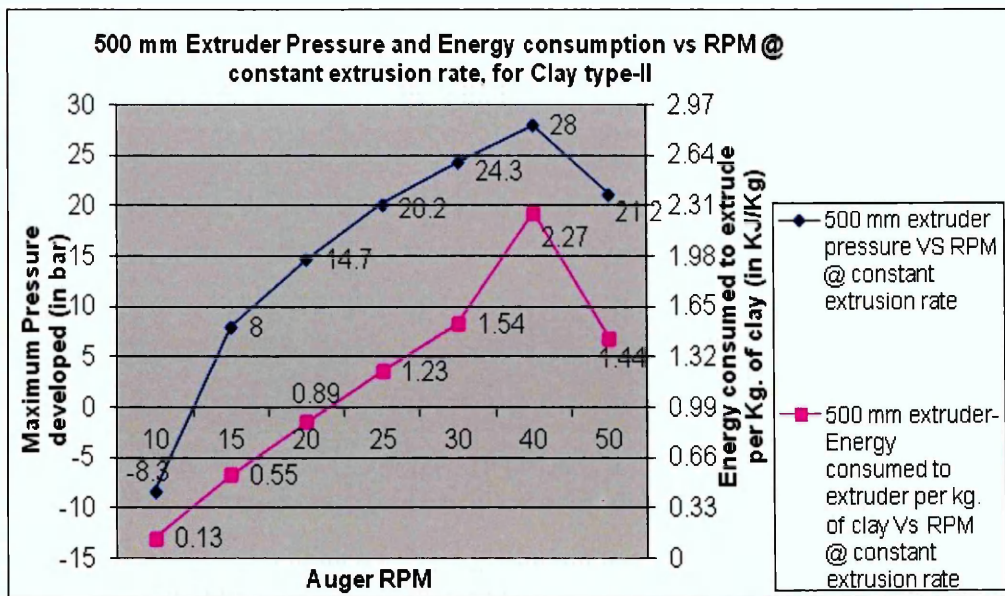
Figure 3-53 Extrusion pressure, Energy consumption vs. Auger speed

The trend clearly indicates the effect of varying auger speed on the performance of an extruder. It is also understood that, depending upon the moisture content of the clay, an optimum auger speed is necessary to induce the required amount of shear in the clay for generating sufficient extrusion pressure at specified extrusion rates.

3.9.3 Effect of varying pitch distance on performance of extruder

The effect of increasing and decreasing the pitch distance of the auger on the performance characters of a 500 mm extruder was investigated in this part. The other parameters like the die design, barrel design, auger speed, clay material, size, clay moisture content and feed rate were kept constant. Table 3-11 summarises the operational parameters and material properties used in the CFD analysis.

Extruder Size	Feed rate (kgs^{-1})	Auger speed (rpm)	Herschel-Bulkley's model value
500 mm	19	30	$k=4908$ Pa.s^n $n=0.5$ $\tau_0=8500$ Pa C.S.R=3 s^{-1}

Table 3-11 Data set for varying pitch distance analysis

79

The performance characters were assessed for augers with following pitch distances 246.13 mm, 292 mm and 338.012 mm. The results obtained from the CFD analysis are summarised below.

Extrusion Pressure:

Pressure developed during extrusion in a 500 mm extruder with 246.13 mm auger pitch distance is shown in Figure 3-54 and 3-55. The pressure varied from a minimum value of -5.2 kPa at the inlet section to a maximum of 4.02 MPa (40.2 bar) observed at the end of auger shaft and reduced to an average value of 2.92 MPa (29.2 bar) at the outlet.

Contours of Static Pressure (pascal) (Time=2.5350e+00)   Nov
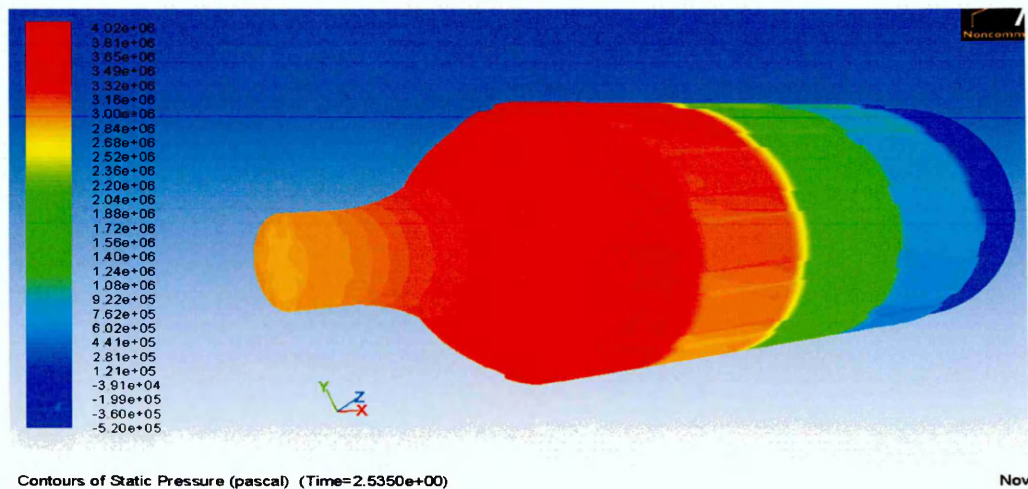
Figure 3-54 Static pressure contour (full view)-pitch dist. 246.13 mm

Contours of Static Pressure (pascal) (Time=2.5350e+00)   Nov 03, 201
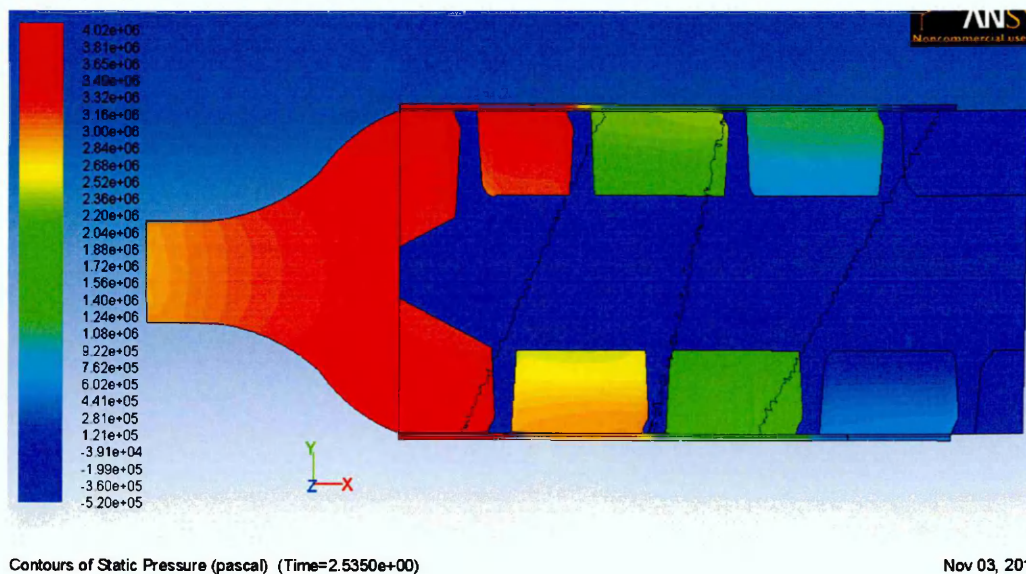
Figure 3-55 Static pressure contour (sectional view)-pitch dist. 246.13 mm

The trend of pressure development observed within the extruder section, during extrusion is shown in Figure 3-56.
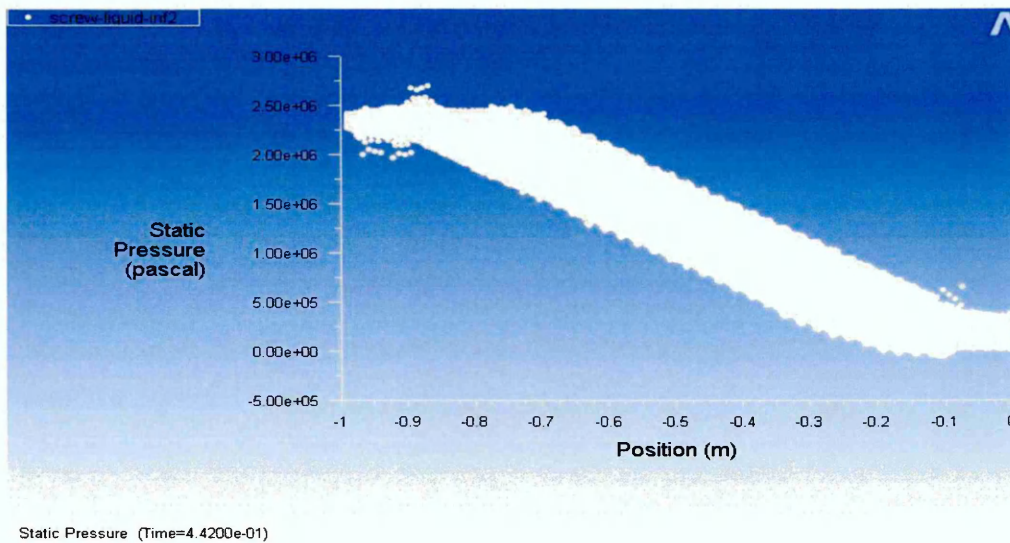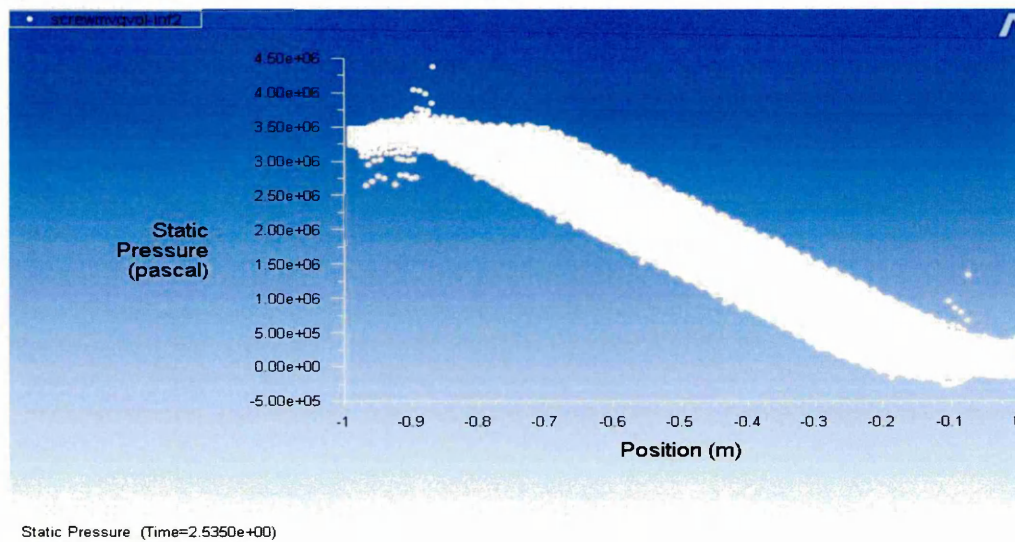

Figure 3-56 Static pressure profile-pitch dist. 246.13 mm

Material flow pattern:

The flow pattern and velocity of clay observed during extrusion at various sections of extruder and die, in a 500 mm extruder with 246.13 mm auger pitch distance is shown in Figure 3-57. In the direction of extrusion the average value observed for velocity at outlet section of die was 0.59 ms^{-1}.
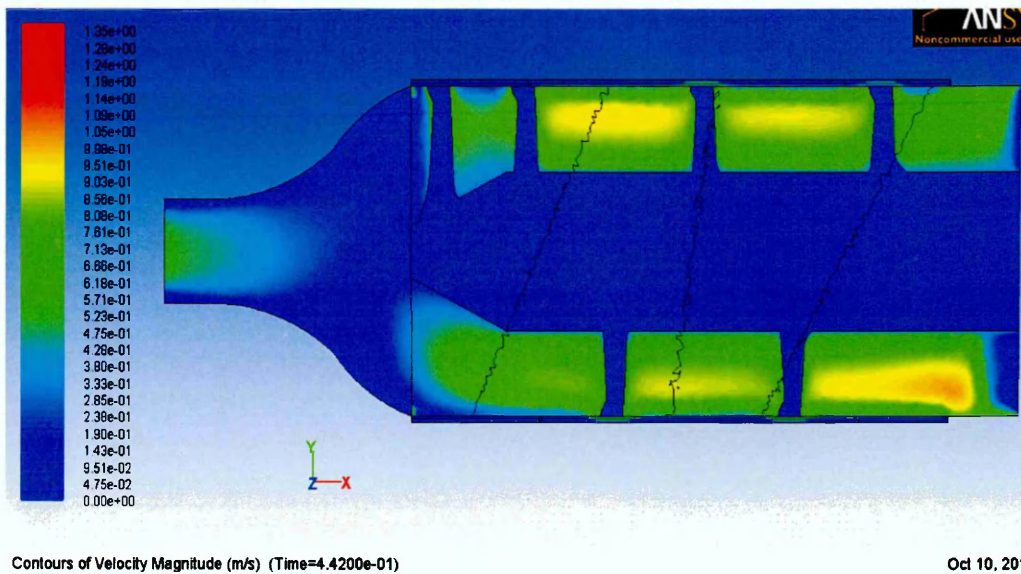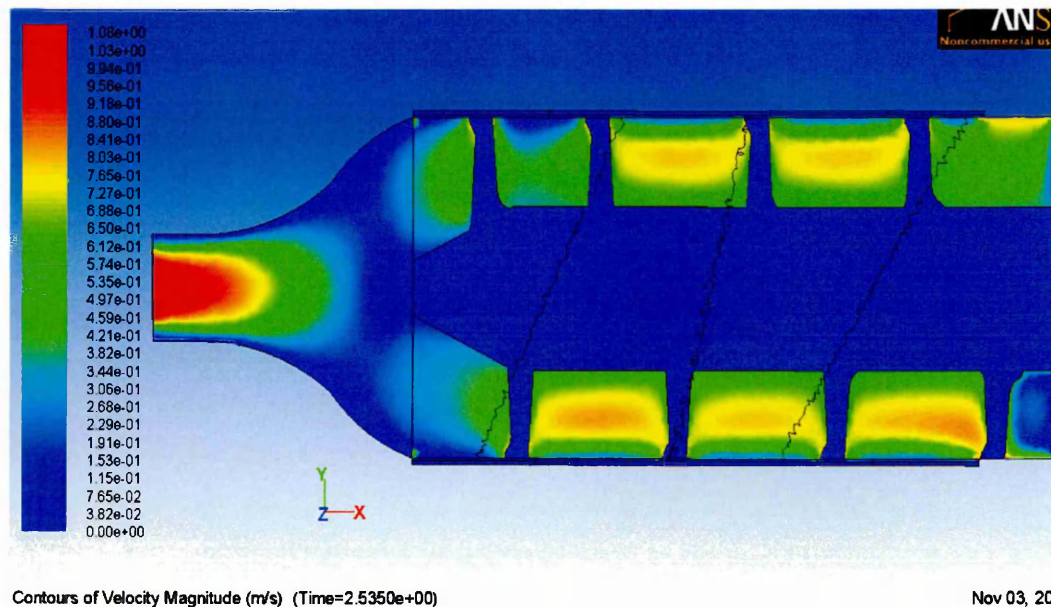

Figure 3-57 Flow velocity during extrusion (sectional view)-pitch dist. 246.13 mm

Viscosity profile:

The profile of shear thinning behaviour of clay observed at the outlet section of die in a 500 mm extruder with 246.13 mm auger pitch distance is shown in Figure 3-58.
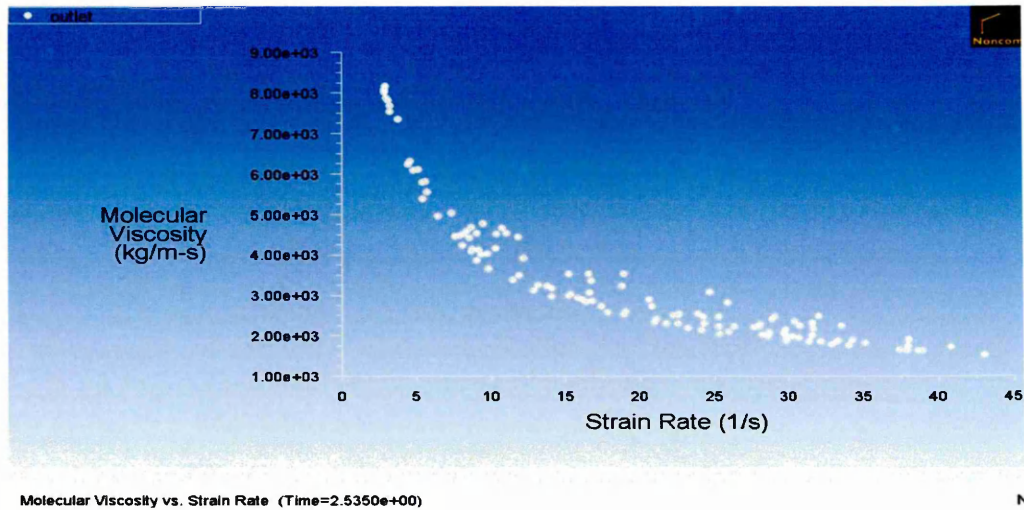
Figure 3-58 Molecular viscosity vs. Strain rate-pitch dist. 246.13 mm

The results of CFD analysis for augers with pitch distance of 292 mm are available in Appendix A- section II and for 338.012 mm distance in Appendix A- section VIII.

The trend of variation in maximum extrusion pressure and energy required in extruding per unit mass of clay, with respect to change in auger pitch distance for a 500 mm extruder is shown in Figure 3-59.
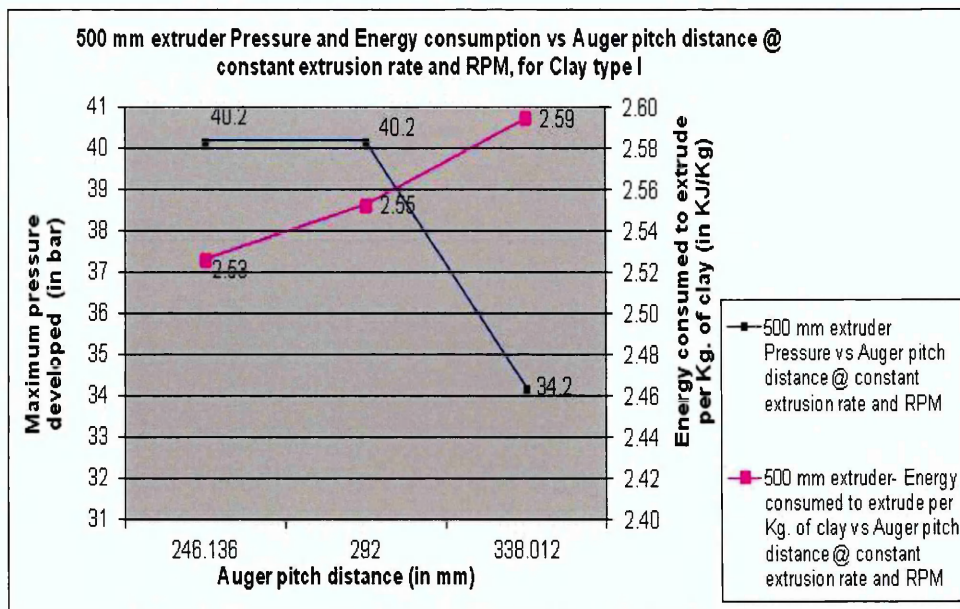
Figure 3-59 Extrusion pressure, Energy consumption vs. Auger pitch distance

The observed trend in the change of performance characters clearly indicates that reducing pitch distance does not influence the performance characters of an extruder significantly compared to increasing pitch distance.

3.9.4 Effect of varying die shapes on performance of extruder

The effect of varying the design of die outlet on the performance characters of a 500 mm extruder was investigated in this part. The other parameters like the auger design, barrel design, auger speed, clay material, size, clay moisture content and feed rate were kept constant. Table 3-12 summarises the operational parameters and material properties used in the CFD analysis.

Extruder Size	Feed rate (kgs^{-1})	Auger speed (rpm)	Herschel-Bulkley's model value
500 mm	19	30	$k=4908$ Pa.s^n $n=0.5$ $\tau_0=8500$ Pa C.S.R=3 s^{-1}

Table 3-12 Data set for varying die design analysis

The performance characters of the extruder were assessed with respect to three different types of die design, shown in Figure 3-60.

Die Type-I

Die Type-II

Die Type-III
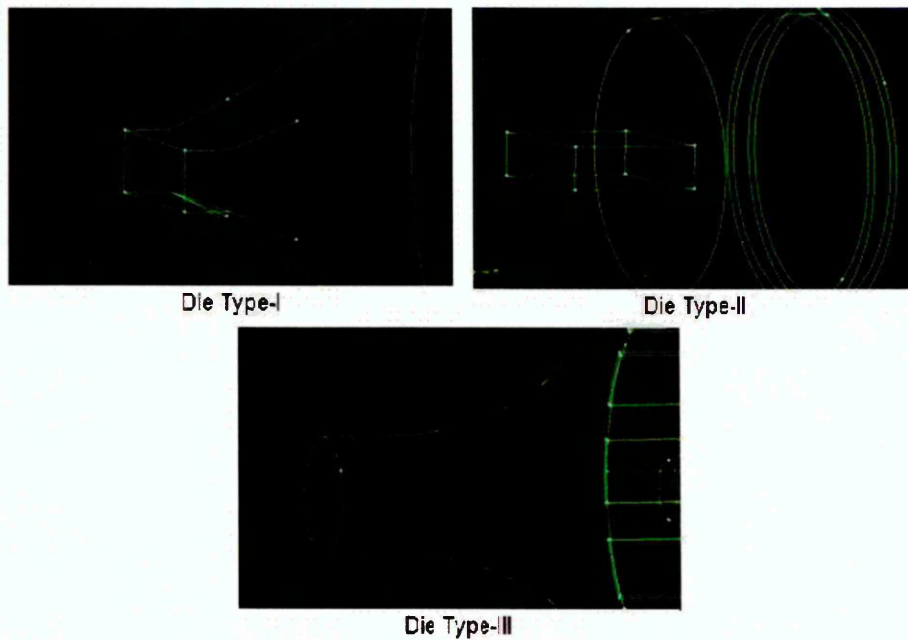
Figure 3-60 Types of die design investigated

The above shown die designs are intended to produce clay columns with different cross sections used by C.F Ltd, in different applications. The results obtained from the CFD analysis are summarised below.

Extrusion pressure:

Pressure developed during extrusion in a 500 mm extruder with die type-II is shown in Figure 3-61 and 3-62. The pressure varied from a minimum value of -616 kPa at the inlet section to a maximum of 3.54 MPa (35.4 bar) and reduced to an average value of 2.79 MPa (27.9 bar) at the outlet. The maximum extrusion pressure developed during extrusion remained constant even within the die section until the outlet, where the actual reduction occurred. In the other die designs a gradual decrease in extrusion pressure was observed along the entire length of the die section.

Contours of Static Pressure (pascal) (Time=2.4750e+00)
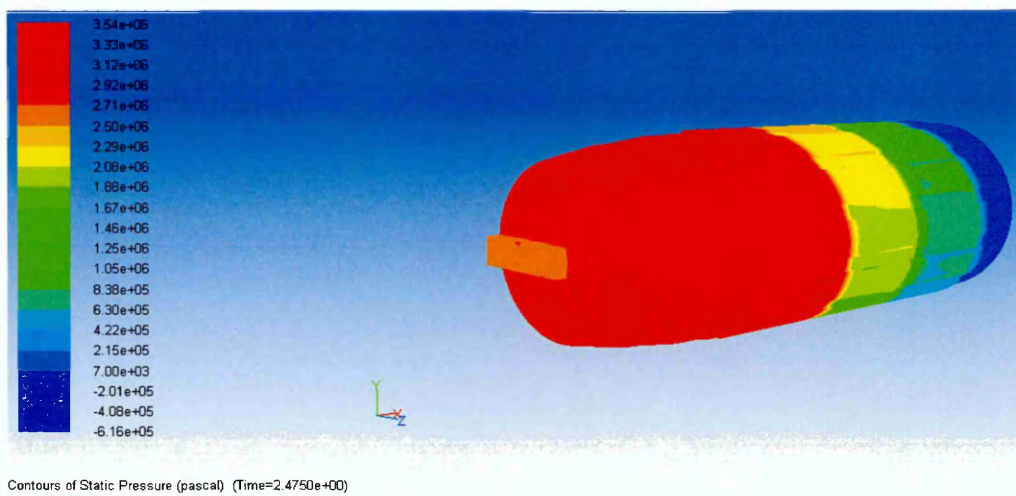
Figure 3-61 Static pressure contour (full view)-die type-II
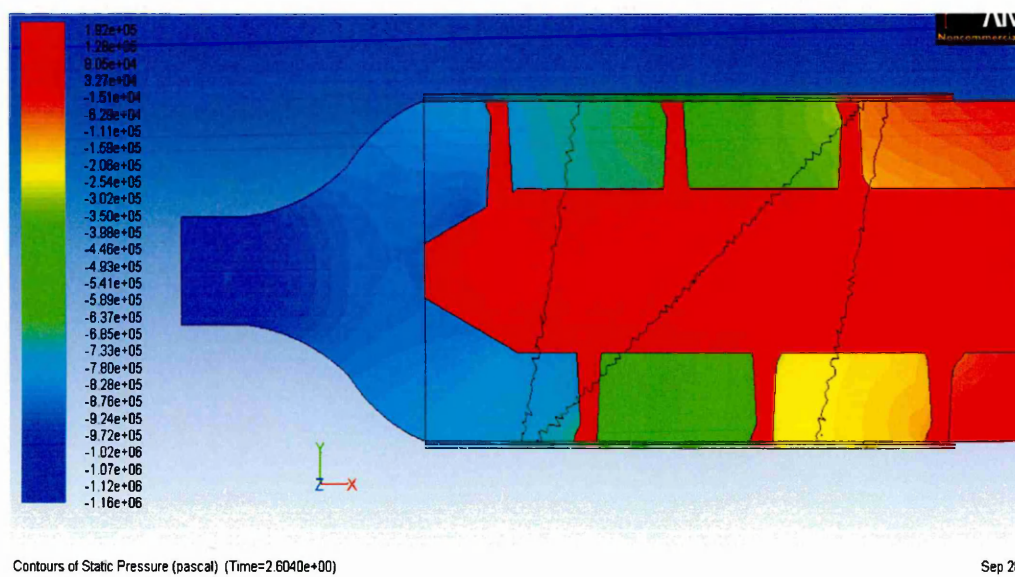

Contours of Static Pressure (pascal) (Time=2.0000e+00)
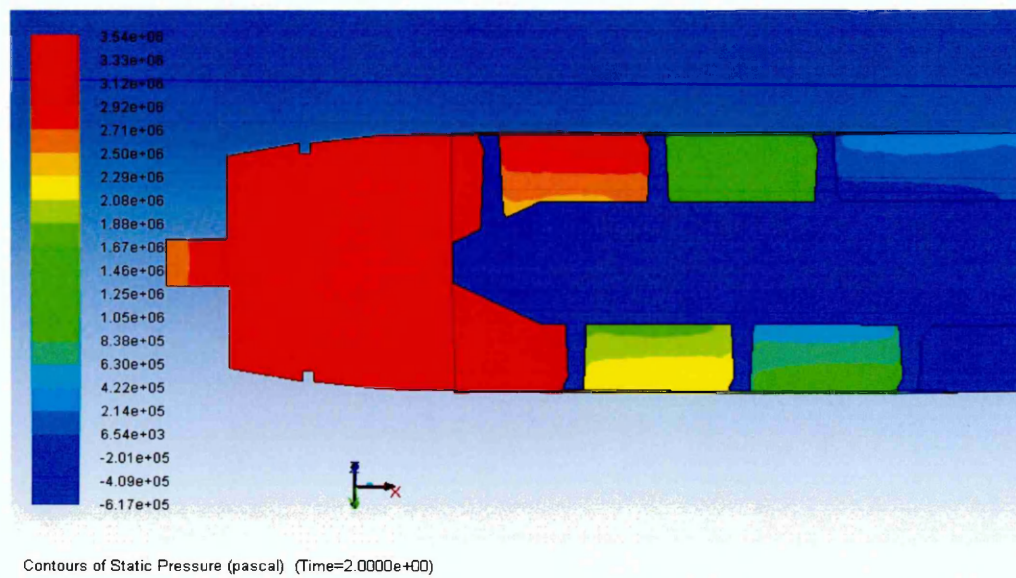
Figure 3-62 Static pressure contour (sectional view)-die type-II

The trend of pressure development observed within the extruder section, during extrusion is shown in Figure 3-63.

Static Pressure (Time=2.0000e+00)
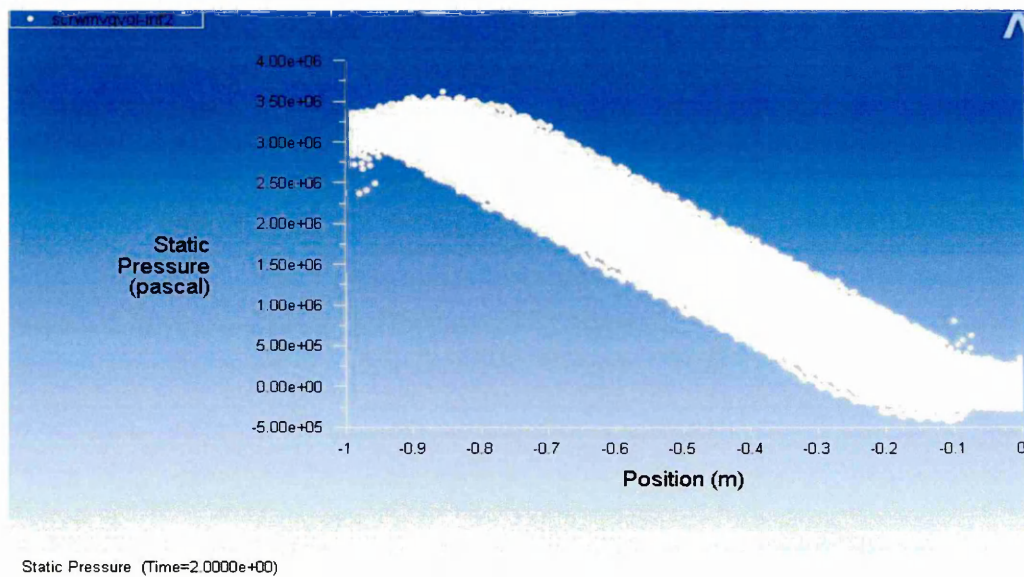
Figure 3-63 Static pressure profile-die type-II

<u>*Material flow pattern:*</u>

A significant change was observed in the flow pattern and the exit velocity values with respect to the die shape and die outlet flow area. The flow pattern and velocity of clay observed during extrusion, at various sections of extruder and die, in a 500 mm extruder with die type-II is shown in Figure 3-64. In the direction of extrusion the average value observed for velocity at outlet section of die was 0.74 ms^{-1}.
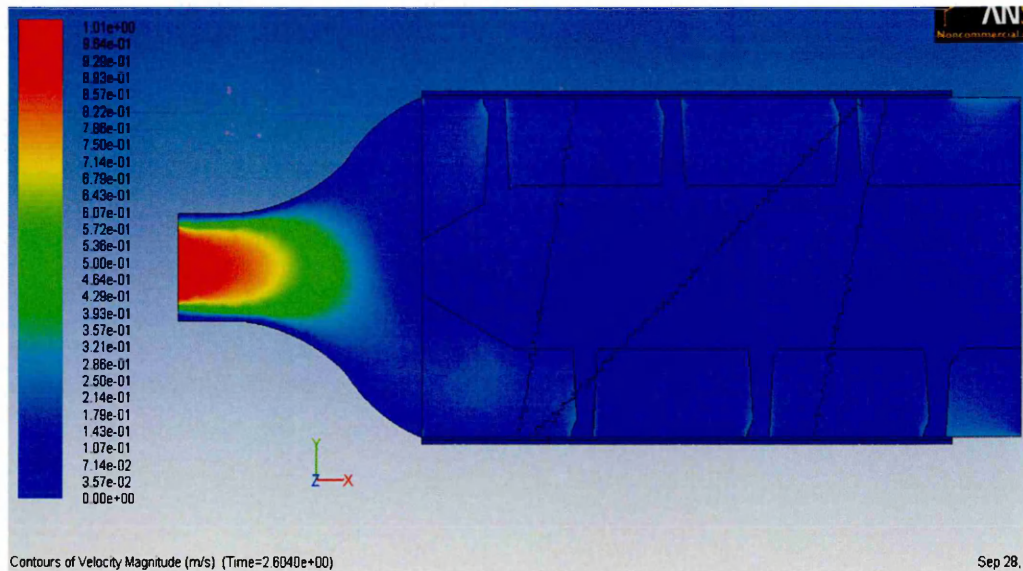

Contours of Velocity Magnitude (m/s) (Time=2.0000e+00)
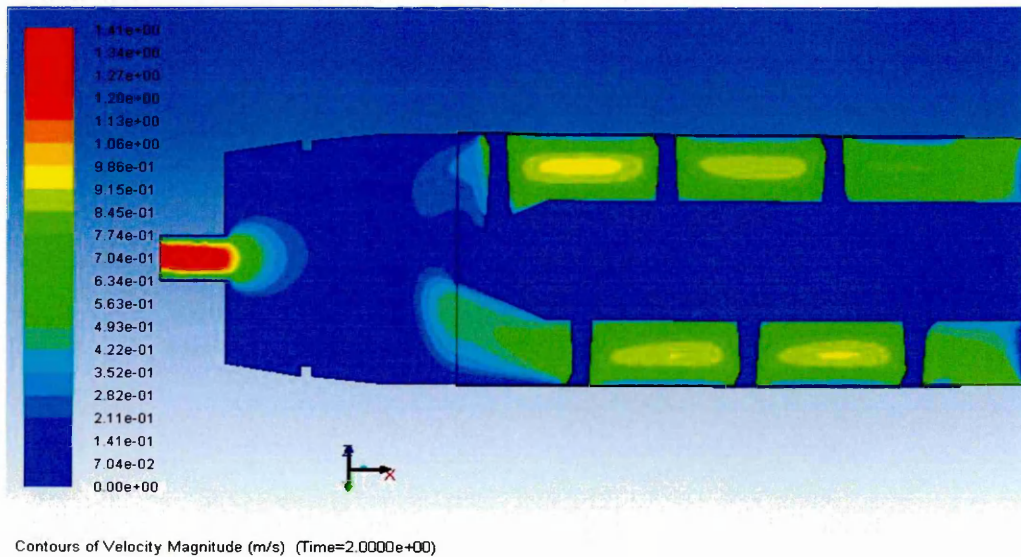
Figure 3-64 Flow velocity during extrusion (sectional view)-die type-II

Viscosity profile:

The profile of shear thinning behaviour of clay observed at the outlet section of die in a 500 mm extruder with die type-II is shown in Figure 3-65.

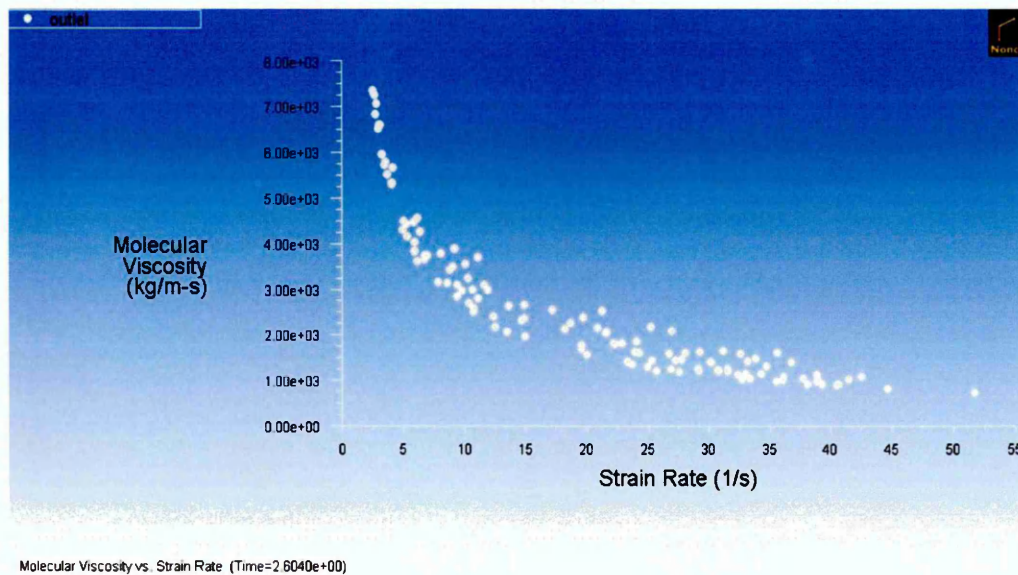Molecular Viscosity vs. Strain Rate (Time=2.0000e+00)   Ju
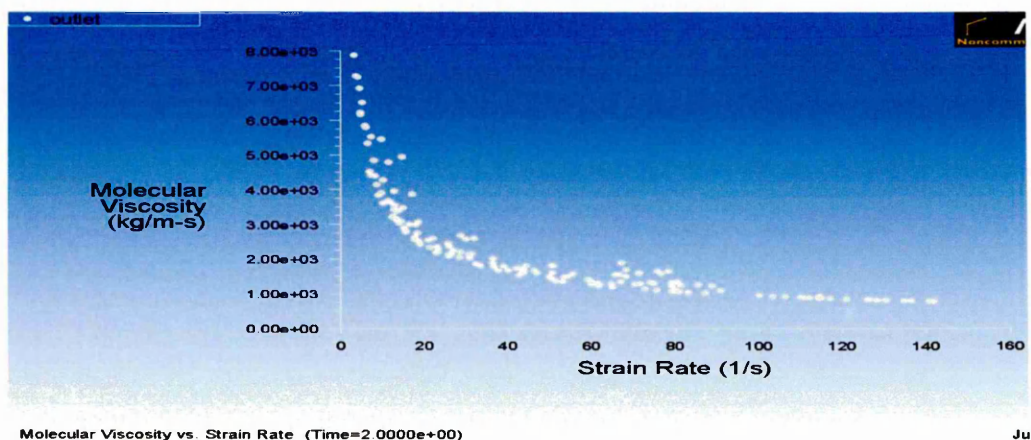
Figure 3-65 Molecular viscosity vs. Strain rate- die type-II

The results of CFD analysis, for the other types of die design are available in Appendix A - section IX.

The trend of variation in average pressure observed at the outlet section of the die and energy required in extruding per unit mass of clay, with respect to change in die design for a 500 mm extruder is shown in Figure 3-66. It is understood from the results that the cross sectional area at the outlet and the profile of a die has significant effect on the performance characters of an extruder.
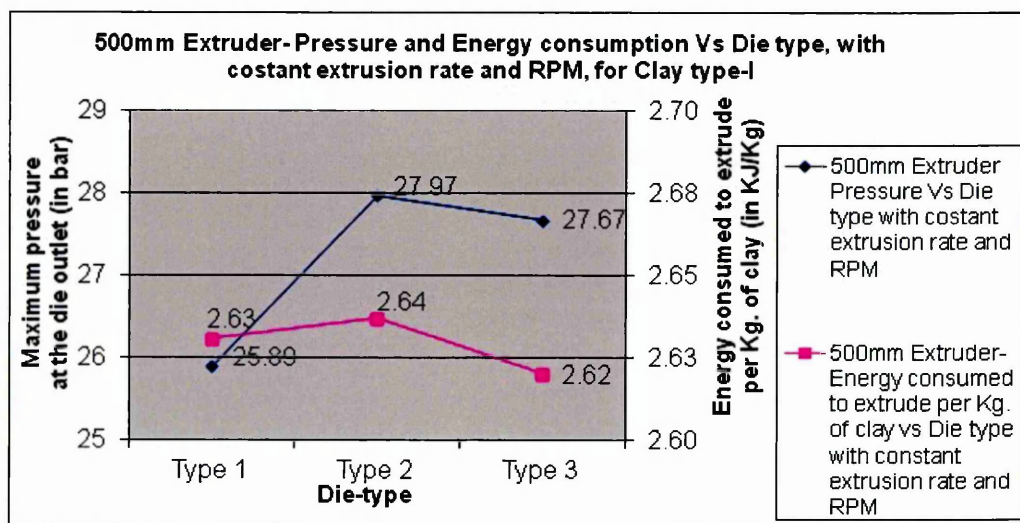
Figure 3-66 Extrusion pressure, Energy consumption vs. Die design

87

3.9.5 Effect of varying number of split worms on performance of extruder

The effect of adding split worms or half flight at downstream side of an auger shaft is understood to have significant effect on the material flow, extrusion pressure and power consumption in an extruder system **[Seanor and Schweizer, 1962]**. The effect of varying the number of split worms on the performance characters of a 500 mm extruder was investigated in this part using CFD analysis. The other parameters like the die design, auger pitch, barrel design, auger speed, clay material, size, clay moisture content and feed rate were kept constant. Table 3-13 summarises the operational parameters and material properties used in the CFD analysis.

Extruder Size	Feed rate (kgs^{-1})	Auger speed (rpm)	Herschel-Bulkley's model value
500 mm	19	30	$k=4908$ Pa.s^n $n=0.5$ $\tau_0=8500$ Pa C.S.R$=3$ s^{-1}

Table 3-13 Data set for varying split worm analysis

The performance characters of the extruder were assessed for three different cases, which includes 1) auger shaft with no split worm, 2) auger shaft with one split worm and 3) auger shaft with two split worms. The position and orientation of the worms on the auger shaft were as shown in Figure 3-67.

No split worm

One split worm
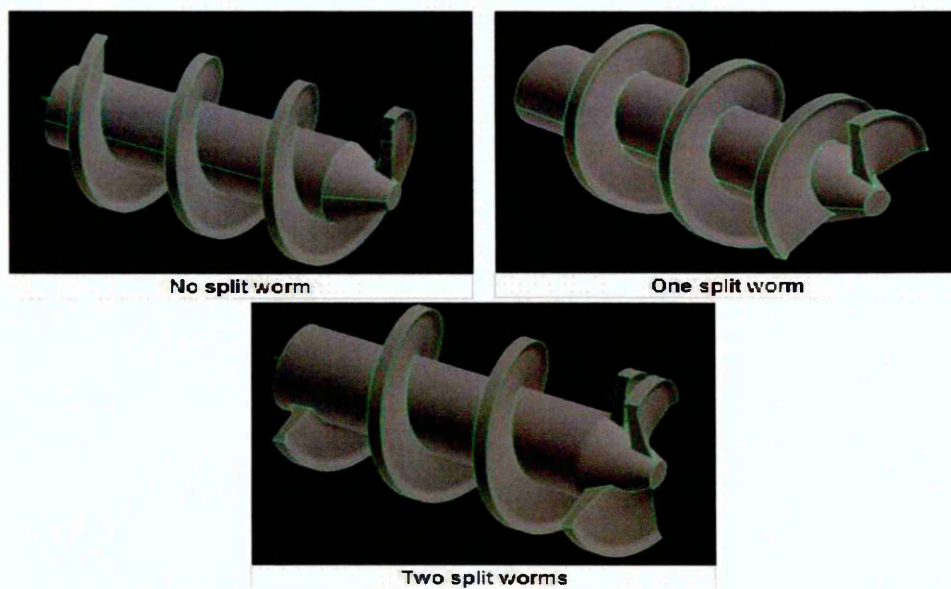
Two split worms

Figure 3-67 Types of split worm design investigated

The results obtained from the CFD analysis for auger shaft with two split worms are summarised below.

Extrusion pressure:

Pressure developed during extrusion in a 500 mm extruder with two split worms at the end of auger shaft is shown in Figure 3-68 and 3-69. The pressure varied from a minimum value of -237 kPa at the inlet section to a maximum of 3.79 MPa (rounded off to 38 bar) observed at the end of auger and reduced to an average value of 2.72 MPa (27.2 bar) at the outlet.

Contours of Static Pressure (pascal) (Time=2.5000e+00)
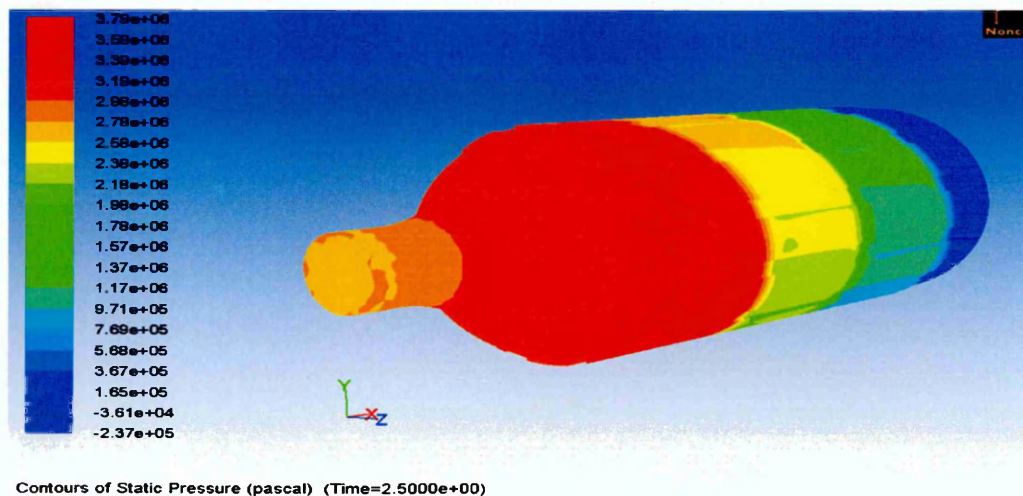
Figure 3-68 Static pressure contour (full view)-two split worms

89

Contours of Static Pressure (pascal) (Time=2.5000e+00)
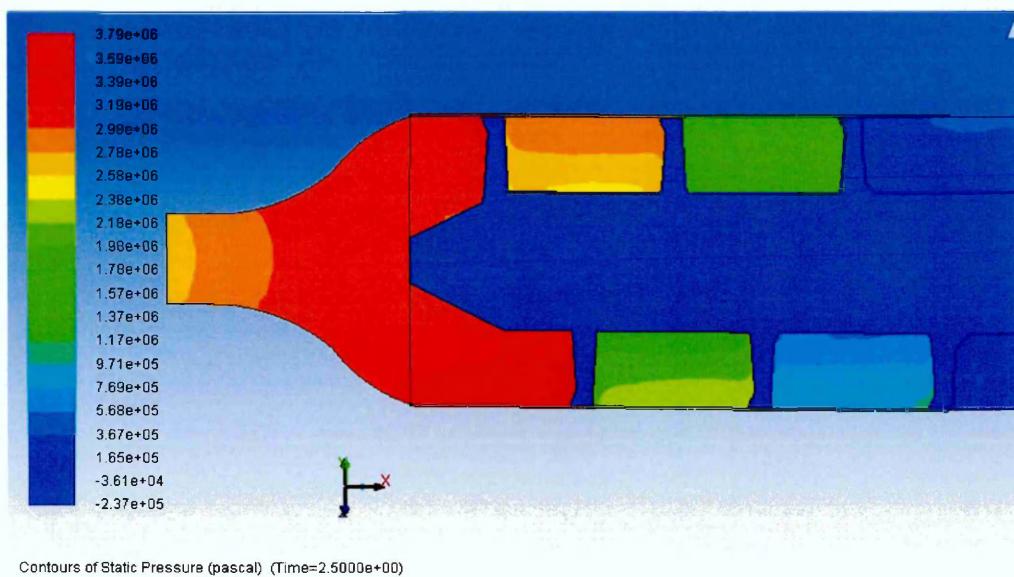
Figure 3-69 Static pressure contour (sectional view)-two split worms

The trend in the pressure developed during extrusion was linear and similar to the other cases, as shown in Figure 3-70. The pressure distribution at the exit of extruder or at the inlet section of the die was observed to be more uniform, when compared with other cases.

Static Pressure (Time=2.5000e+00)
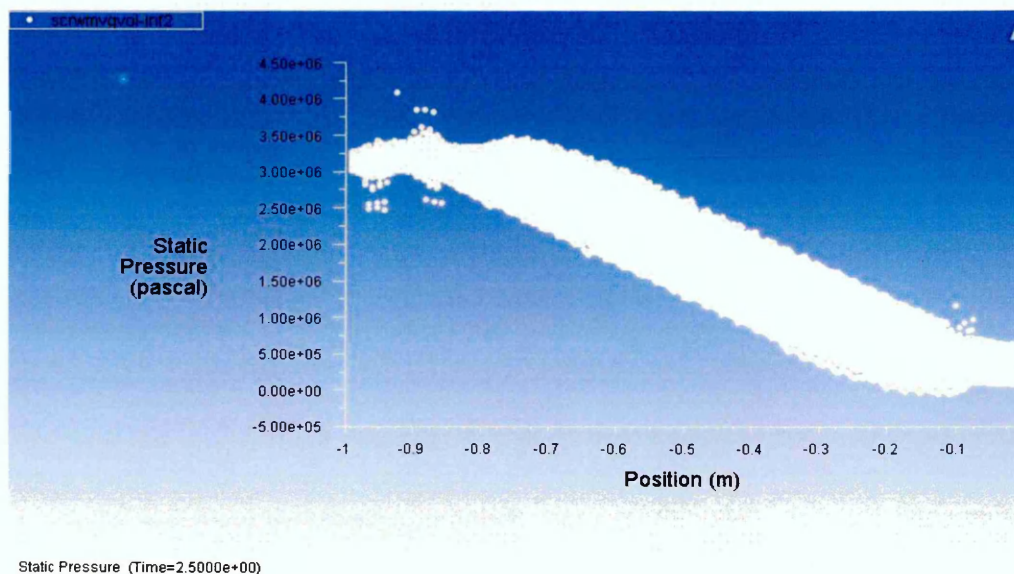
Figure 3-70 Static pressure profile-two split worms

Material flow pattern:

The flow pattern and velocity of clay observed during extrusion at various sections of extruder and die, in a 500 mm extruder with two split worms at the end of the auger shaft is shown in Figure 3-71. In the direction of

90

extrusion the average value observed for velocity at outlet section of die was 0.6 ms^{-1}.

Contours of Velocity Magnitude (m/s) (Time=2.5000e+00)
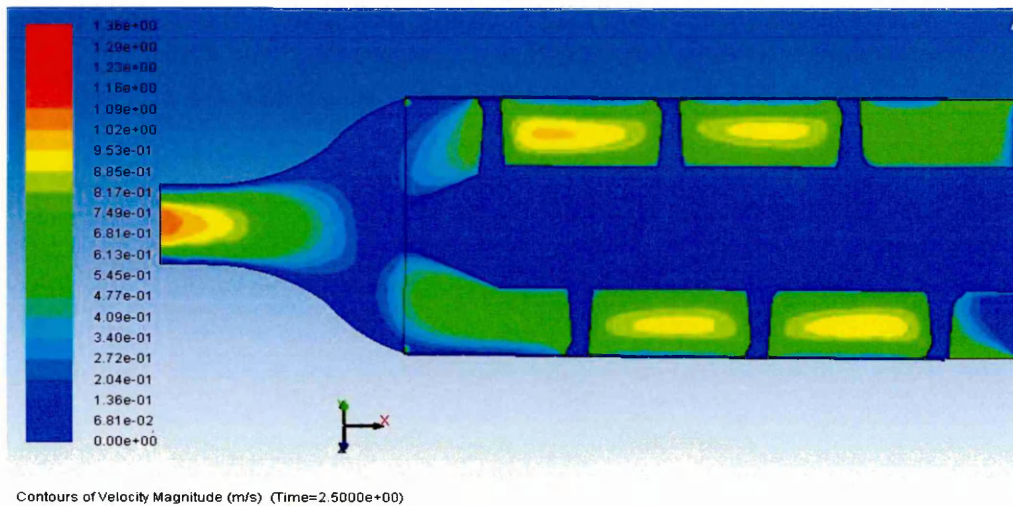
Figure 3-71 Flow velocity during extrusion (sectional view)-two split worms

The effect of split worms on the flow pattern at the exit section of extruder was also analysed and a significant change was observed. The flow pattern observed at the exit section of extruder with respect to number of split worms in the auger shaft is shown from Figure 3-72 to 3-74.

Contours of Velocity Magnitude (m/s) (Time=2.5000e+00)

Contours of Velocity Magnitude (m/s) (Time=2.5050e+00)
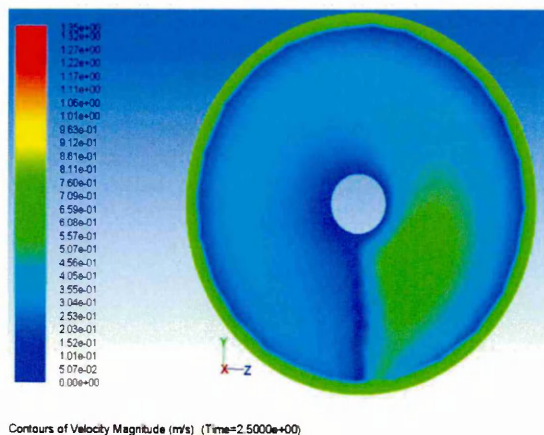
Figure 3-72 Flow pattern with no split worm
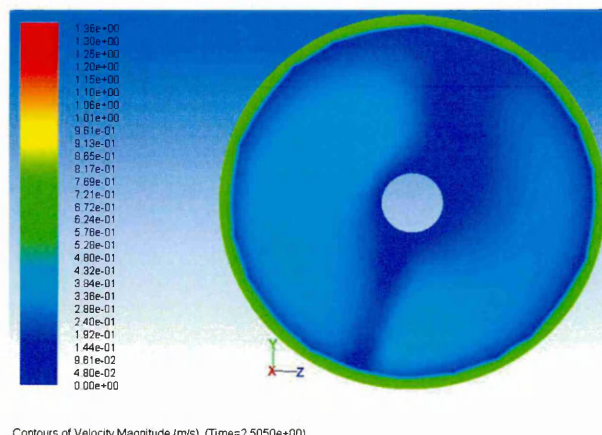
Figure 3-73 Flow pattern with one split worm

Contours of Velocity Magnitude (m/s) (Time=2.5000e+00)
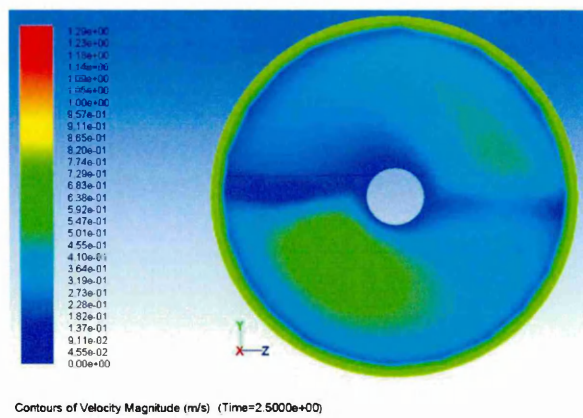
Figure 3-74 Flow pattern with two split worms

<u>*Viscosity profile:*</u>

The profile of shear thinning behaviour of clay observed at the outlet section of die in a 500 mm extruder with two split worms is shown in Figure 3-75.

Molecular Viscosity vs. Strain Rate (Time=2.5000e+00)   J

Figure 3-75 Molecular viscosity vs. Strain rate-two half flights

The results of CFD analysis for auger with no split worms are presented in Appendix A - section IX (b) and for auger with one split worm are presented in Appendix A - section II.

The trend of variation in maximum pressure developed during extrusion and energy required in extruding per unit mass of clay with respect to number of split worms in an auger shaft, for a 500 mm extruder is shown in Figure 3-76.

Figure 3-76 Extrusion pressure, Energy consumption vs. Split worms

It clearly indicates that the addition of split worm at the end of auger shaft influences the extrusion pressure but not the power consumption, confirms with the recommendations of **Seanor and Schweizer (1962)** from their work.

3.10 Performance assessment of a 600 mm extruder

The effect of varying the design and operating parameters on performance characters of a 600 mm extruder system, without varying the type of clay was investigated in this part of the research, using the CFD modelling.

3.10.1 Effect of varying feed rate on performance of extruder

The effect of increasing the feed rate of uncompacted clay, in a 600 mm extruder was investigated in this part. The other parameters like the die design, extruder design, clay material, size, clay moisture content and auger speed were kept constant. Table 3-14 summarises the operational parameters and material properties used in the CFD analysis.

Extruder Size	Feed rate (kgs^{-1})	Auger speed (rpm)	Herschel-Bulkley's model value
600 mm	Varying	22.5	$k=5206.95$ Pa.s^n $n=0.32$ $\tau_0=6500$ Pa C.S.R$=2.1$ s^{-1}

Table 3-14 Data set for varying feed rate analysis

The performance characters were assessed for the following feed rates 8.1 kgs^{-1}, 11.8 kgs^{-1} and 19 kgs^{-1}. The results obtained from the CFD analysis are summarised below.

Extrusion pressure:

Pressure developed during extrusion in a 600 mm extruder with a feed rate of 8.1 kgs^{-1} is shown in Figure 3-77 and 3-78. The pressure varied from a minimum value of -228 kPa at the inlet section to a maximum of 3.15 MPa (31.5 bar) observed at the end of the auger shaft and reduced to an average value of 2.7 MPa (27 bar) at the outlet.
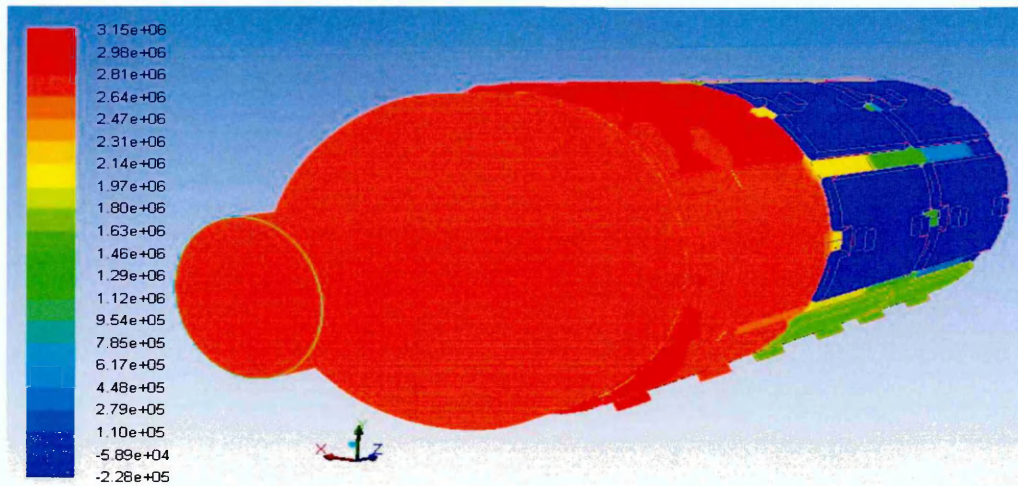
Contours of Static Pressure (pascal) (Time=2.6750e+00)

Figure 3-77 Static pressure contour (full view) - feed rate 8.1 kgs^{-1}

Contours of Static Pressure (pascal) (Time=2.6750e+00)
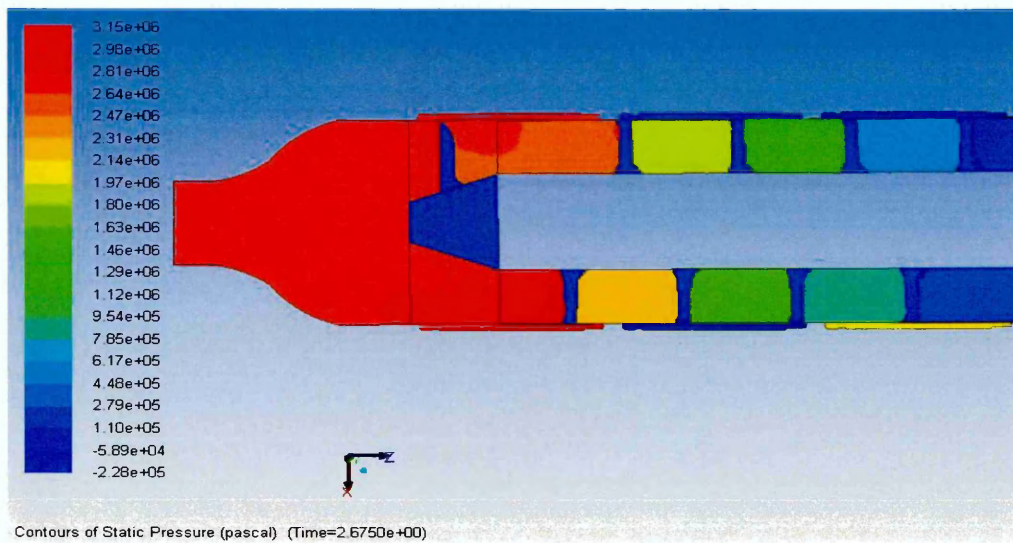
Figure 3-78 Static pressure contour (sectional view) - feed rate 8.1 kgs^{-1}

The trend of pressure development observed within the extruder section, during extrusion is shown in Figure 3-79.

Static Pressure (Time=2.6750e+00)
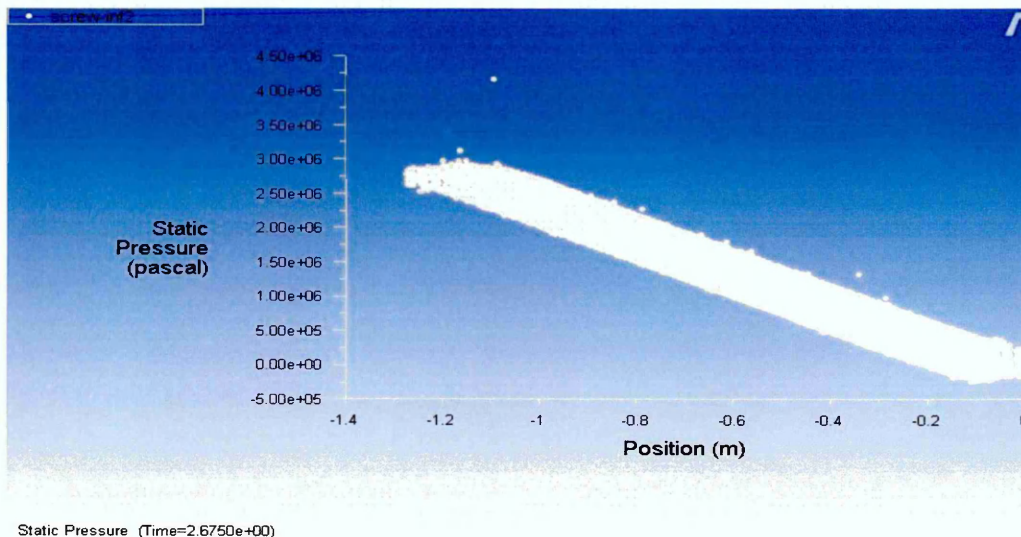
Figure 3-79 Static pressure profile- feed rate 8.1 kgs^{-1}

Material flow pattern:

The flow pattern and velocity of clay observed during extrusion at various sections of extruder and die, in a 600 mm extruder with 8.1 kgs^{-1} feed rate is shown in Figure 3-80. In the direction of extrusion the average value observed for velocity at outlet section of die was 0.07 ms^{-1}.

95

Contours of Velocity Magnitude (m/s) (Time=2.6750e+00)
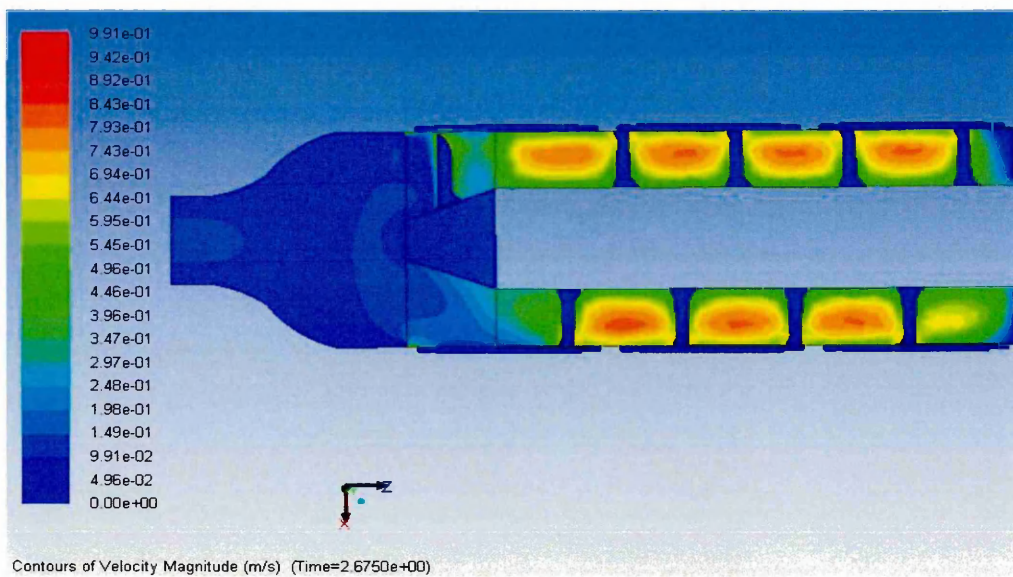
Figure 3-80 Flow velocity during extrusion (sectional view)-feed rate 8.1 kgs⁻¹

<u>Viscosity profile:</u>

The profile of shear thinning behaviour of clay observed at the outlet section of die in a 600 mm extruder with 8.1 kgs⁻¹ feed rate is shown in Figure 3-81.
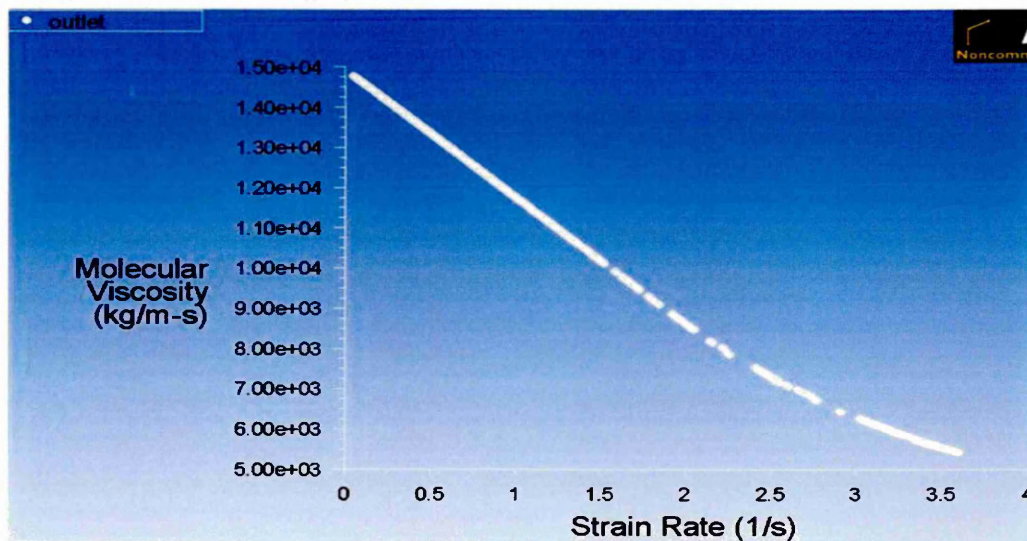
Figure 3-81 Molecular viscosity vs. Strain rate- feed rate 8.1 kgs⁻¹

The results of CFD analysis, for feed rates 11.8 kgs⁻¹ and 19 kgs⁻¹ are available in Appendix A- section X.

The trend of variation in maximum extrusion pressure and energy required in extruding per unit mass of clay, with respect to change in feed rate of clay for a 600 mm extruder is shown in Figure 3-82.

96

Sheffield Hallam University

Author: SARAVANAKUMAR KANDASAMY

Title/Thesis Number: 27440 ADVANCED APPLICATIONS

Degree PHD PHILOSOPHY OF NUMERICAL

Year: 2013

Copyright Declaration

Date	Name and Institution /Organisation (in block letters)	Signature

Figure 3-82 Extrusion pressure, Energy consumption vs. feed rate

3.10.2 Effect of varying auger speed on performance of extruder

The effect of varying auger speed on the performance characters of a 600 mm extruder was investigated in this part. The other parameters like the die design, extruder design, clay material, size, clay moisture content and feed rate were kept constant. Table 3-15 summarises the operational parameters and material properties used in the CFD analysis.

Extruder Size	Feed rate (kgs^{-1})	Auger speed (rpm)	Herschel-Bulkley's model value
600 mm	11.8	varying	k=5206.95 Pa.s^n n=0.32 τ_0=6500 Pa C.S.R=2.1 s^{-1}

Table 3-15 Data set for varying auger speed analysis

The performance characters of the extruder were assessed for the following auger speeds- 15 rpm, 22.5 rpm and 30 rpm. The results obtained from the CFD analysis are summarised below.

97

Pressure developed during extrusion in a 600 mm extruder with an auger speed of 15 rpm is shown in Figure 3-83 and 3-84. The pressure varied from a minimum value of -181 kPa at the inlet section to a maximum of 1.97 MPa (19.7 bar) observed at the end of the auger shaft and reduced to an average value of 1.54 MPa (15.4 bar) at the outlet.
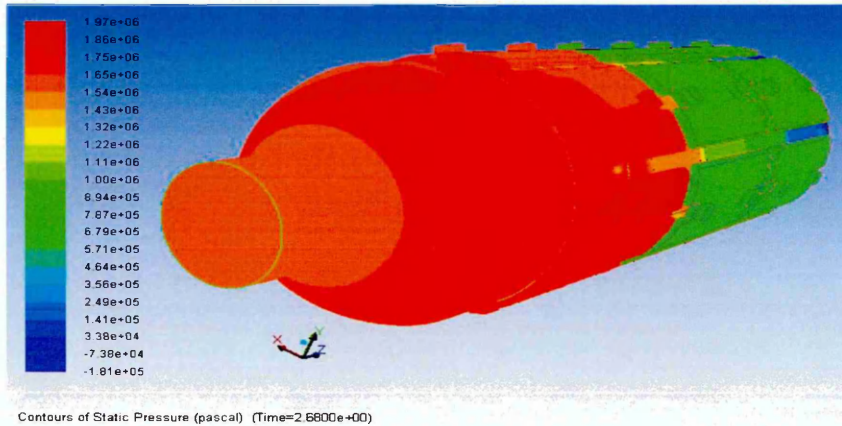
Figure 3-83 Static pressure contour (full view) - auger speed 15 rpm
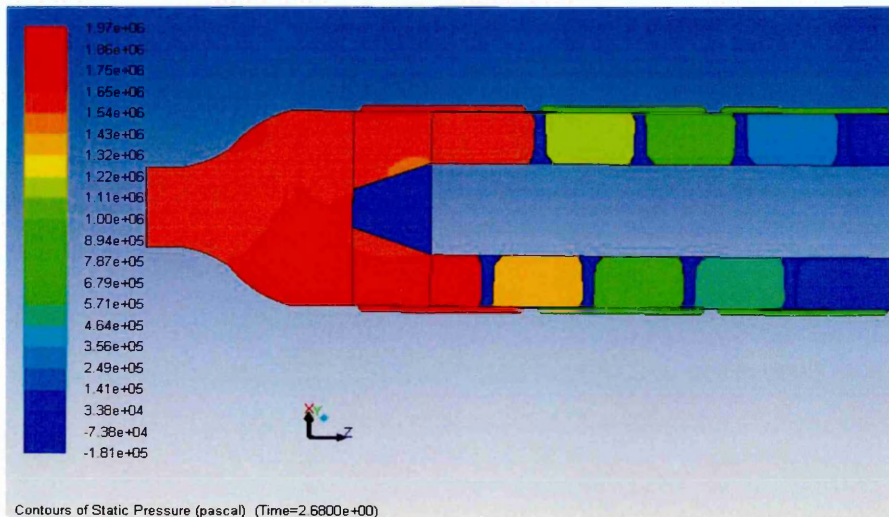
Figure 3-84 Static pressure contour (full view) - auger speed 15 rpm

The trend of pressure development observed within the extruder section, during extrusion is shown in Figure 3-85.
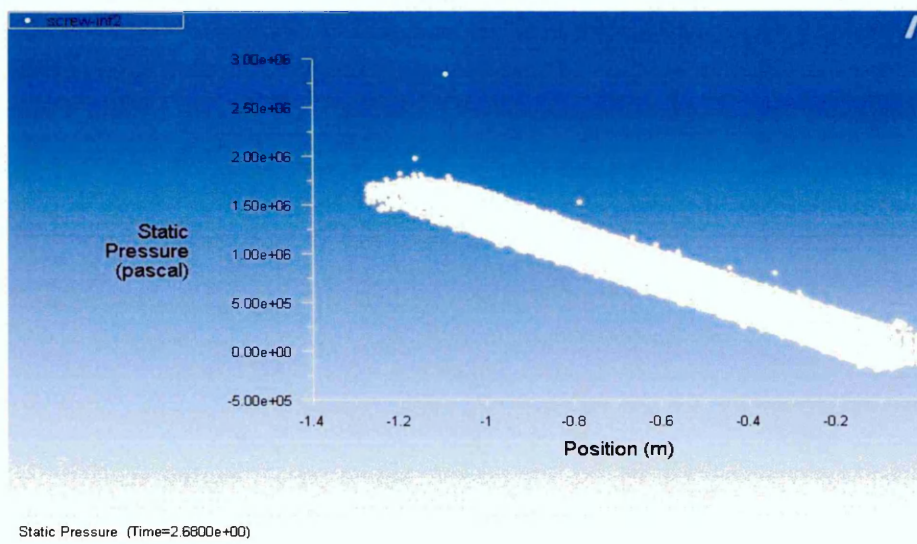
Static Pressure (Time=2.6800e+00)

Figure 3-85 Static pressure profile- auger speed 15 rpm

Material flow pattern:

The flow pattern and velocity of clay observed during extrusion at various sections of extruder and die, in a 600 mm extruder with auger speed of 15 rpm is shown in Figure 3-86. In the direction of extrusion the average value observed for velocity at outlet section of die was 0.13 ms^{-1}.

Contours of Velocity Magnitude (m/s) (Time=2.6800e+00)
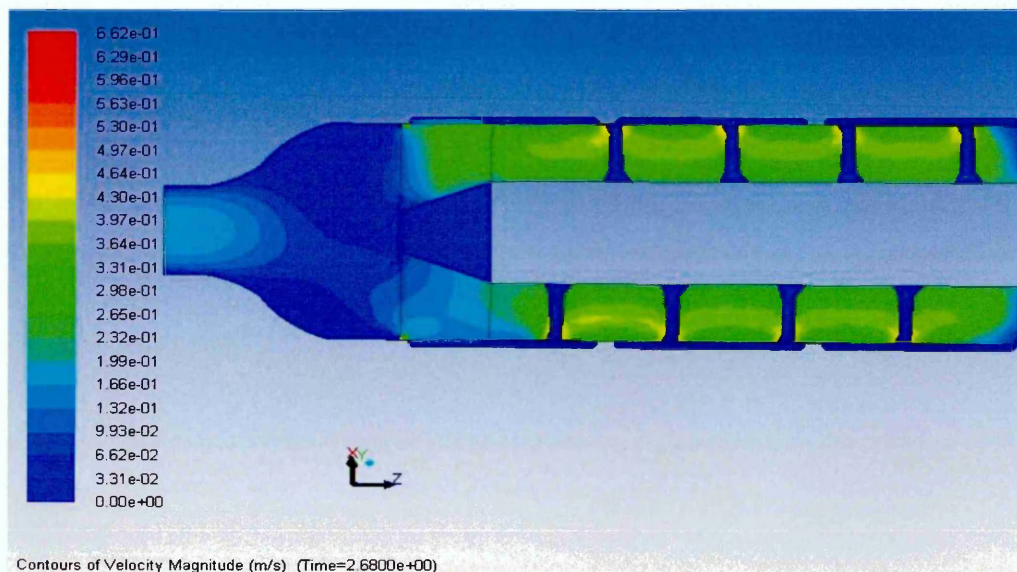
Figure 3-86 Flow velocity during extrusion (sectional view) - auger speed 15 rpm

The profile of shear thinning behaviour of clay observed at the outlet section of die in a 600 mm extruder with an auger speed of 15 rpm is shown in Figure 3-87.
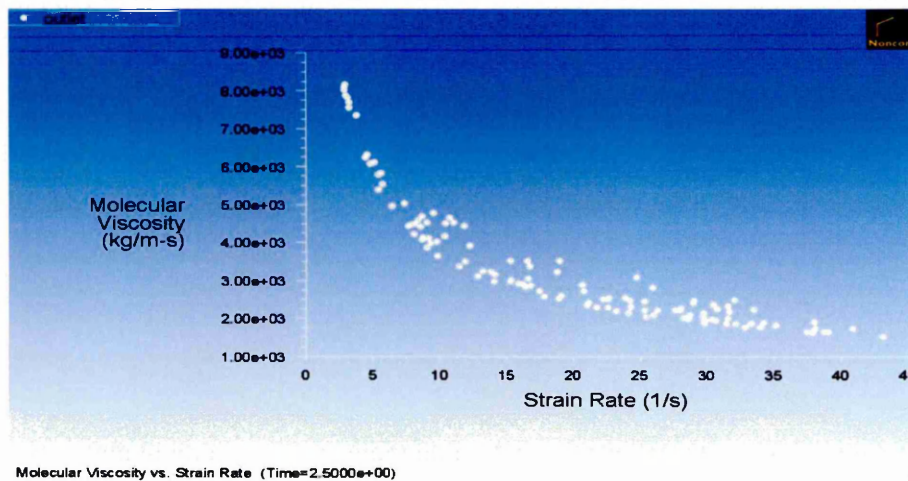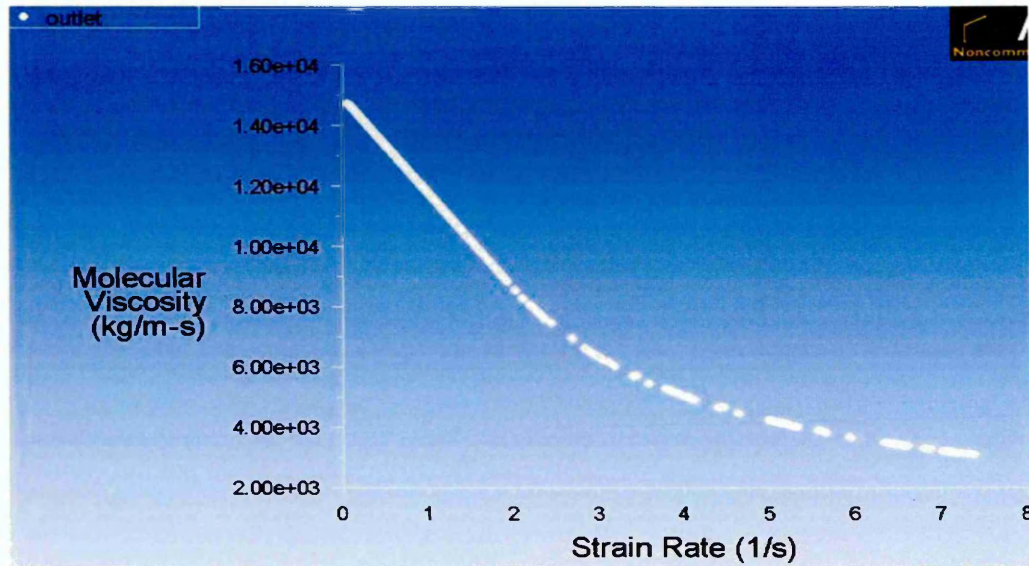

Figure 3-87 Molecular viscosity vs. Strain rate- auger speed 15 rpm

The results of CFD analysis, for auger speed of 22.5 rpm are available in Appendix A- section X (a) and 30 rpm are available in Appendix A -section XI.

The trend of variation in maximum extrusion pressure and energy required in extruding per unit mass of clay, with respect to change in auger speed for a 600 mm extruder is shown in Figure 3-88.
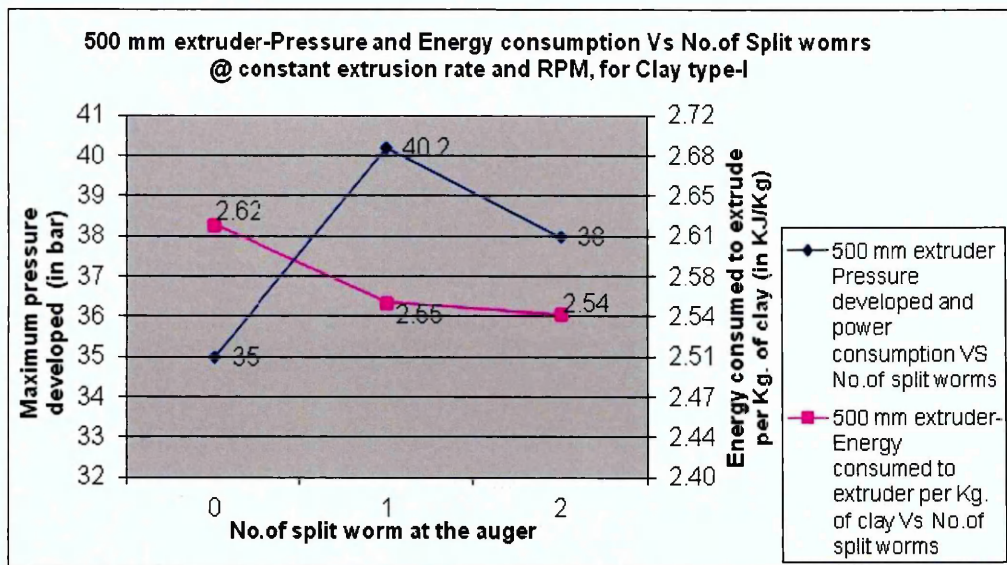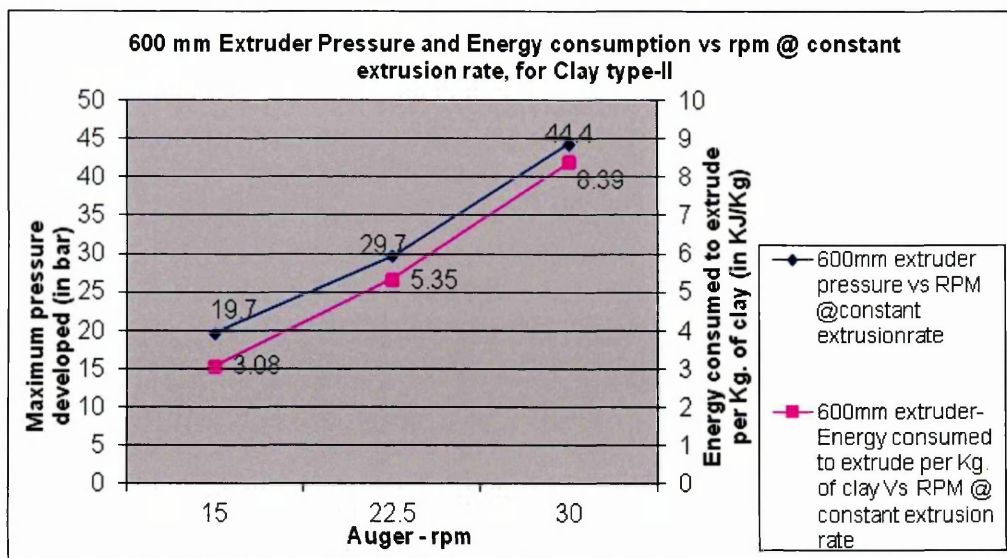
Figure 3-88 Extrusion pressure, Energy consumption vs. auger speed

Similar to the 500 mm extruder, the trend observed for variation in performance characters of a 600 mm extruder with respect to change in auger speed indicates that the increase in speed will increase the pressure and energy requirement of an extruder system to a certain extent.

3.11 Conclusion

Performance assessment of extruders using CFD technique along with experimental validation of the methodology and fluid model used was presented in this chapter. The ability to use CFD technique to design a clay extruder system and the advantages that could be gained within the heavy ceramics industries has clearly been demonstrated through the results obtained.

Chapter-4   Finite Element Analysis of clay extruder

4.1 Introduction:

In this part of the research work, mechanically induced stress and strain on the components of a 430 mm extruder were assessed using FEA technique. Components investigated include barrel, liner, distance piece and auger. Based upon the maximum extrusion pressure expected under actual working conditions, the component were assessed for two different load conditions 1) 1.8 MPa and 2) 2.6 MPa.

Stress and deformation induced with respect to applied load were investigated for three different materials, which include A) Structural steel (Grade BS EN 10025 Fe 430A), B) Grey Cast Iron (GCI) (Grade: EN-GJL-250) and C) Austempered Ductile Iron (ADI) (Grade GJS-1400-1). Structural steel is the most commonly used material by C.F Ltd to manufacture the majority of extruder components. GCI and ADI are alternate material chosen to be investigated through this research work, to identify their technical and commercial suitability for manufacturing extruder components. In recent years ADI has been proven to be a highly useful material for heavy clay industrial applications **[Da and Jincheng, 2000], [Chowdhury et al., 2010] [Ductile Iron Society, 2012]**, due to its excellent wear resistant properties and light weight. The technical suitability of these alternate materials was analysed using FEA results for stress and deformation induced due to extrusion pressure and the commercial feasibility was analysed by comparing the cost to manufacture with existing and alternate materials. The finding are summarised below.

4.2 FEA of clay extruder components

4.2.1 Barrel

The stress and deformation induced by the pressure developed during extrusion, on the barrel was assessed in this part.

Geometry:

The Barrel geometry used for investigation is shown in Figure 4-1.

103

Figure 4-1 430 mm extruder barrel geometry

Load and boundary condition:

The geometry was suitably meshed using tetrahedral mesh and investigated for two different load conditions, 1) 2.6 MPa and 2) 1.8 MPa. Pressure load was applied on all the inner surfaces of the barrel and fixed support condition on the appropriate surfaces, as highlighted in the Figure 4-2.

Figure 4-2 430 mm extruder barrel- load applied

Stress and deformation results:

Values of equivalent stress, obtained for different materials from the analysis, with respect to applied load conditions are summarised in Table 4-1.

Material	Max. Von-Misses stress value, load-2.6 MPa	Max. Von-Misses stress value, load-1.8 MPa
Structural steel	59.03 MPa	40.87 MPa
GCI	59.938 MPa	41.496 MPa
ADI	60.164 MPa	41.652 MPa

Table 4-1 Stress results-barrel

There was no significant change observed in stress distribution pattern across the component with respect to applied load conditions. The results of FEA for applied load of 2.6 MPa is shown in Figure 4-3. The results of FEA for the applied load of 1.8 MPa is available in Appendix B- section I.
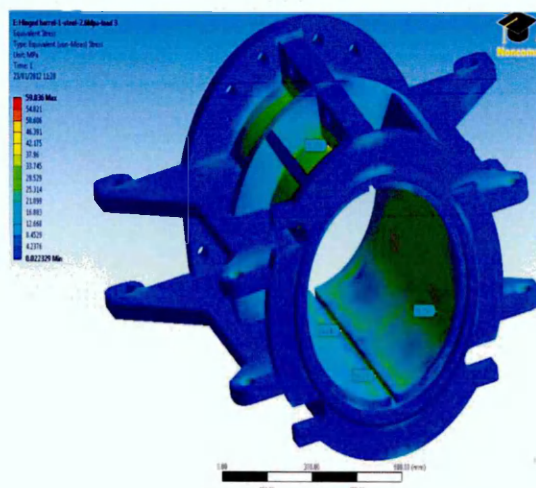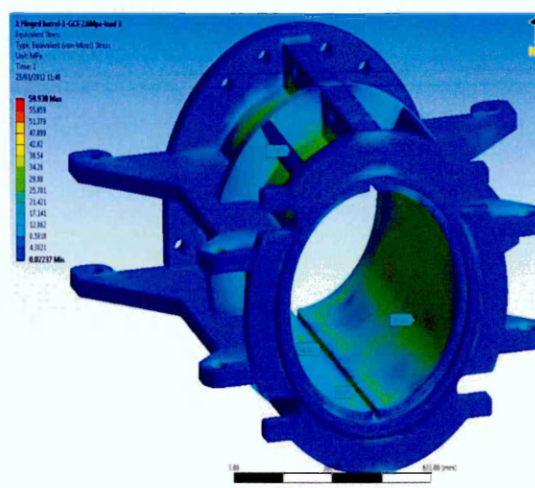
a) Structural steel   **b) GCI**
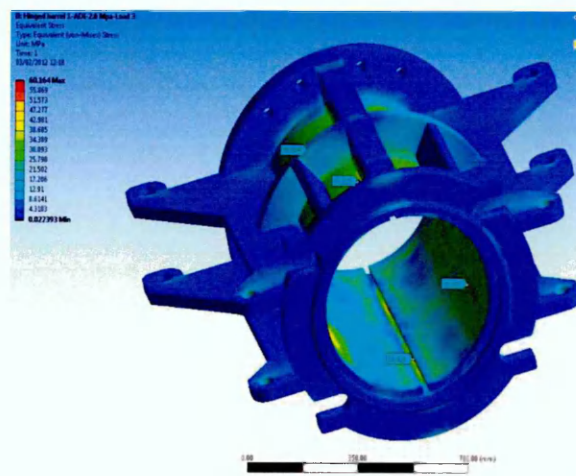
c) ADI

Figure 4-3 Stress induced in barrel @ 2.6 MPa load

105

The strain induced in the barrel was investigated by analysing the deformation pattern in the direction of extrusion. The results obtained are summarised in Table 4-2.

Material	Max. deformation, load-2.6 MPa	Max. deformation, load-1.8 MPa
Structural steel	0.071 mm	0.049 mm
GCI	0.129 mm	0.089 mm
ADI	0.088 mm	0.061 mm

Table 4-2 Deformation results- barrel

There was no significant difference noted in the deformation pattern, for both the load conditions. The deformation pattern observed in barrel for applied load of 2.6 MPa is shown in Figure 4-4 and the results for applied load of 1.8 MPa is available in Appendix B- section II.

a) Structural steel   **b) GCI**

c) ADI

Figure 4-4 Deformation in barrel @ 2.6 MPa load

The stress and deformation results obtained from the FEA clearly indicates that, barrel made up of any of the following materials Structural Steel, GCI or ADI, will be able to withstand the stress induced during extrusion, without breaking during operation. The material currently used by C.F Ltd is Structural Steel and its cost of manufacturing was compared with the cost of alternate materials used in FEA and is summarised in Table 4-3.

Material	Cost per piece (in £'s)
Structural steel	6475.00
GCI	3886.00
ADI (cost with pattern)	6680.00
ADI (cost without pattern)	4380.00

Table 4-3 Manufacturing cost comparison for extruder barrel

It is understood from the preliminary investigations that ADI could be used as an alternate material of construction for extruder barrels. GCI is not recommended, even though it is cheaper than the other materials, due to its limitations in manufacturing certain geometrical features.

4.2.2 Distance piece

Distance piece is an intermediate component used to connect the extruder with the die. The stress and deformation induced by the pressure developed during extrusion, on distance piece was assessed in this part.

Geometry:

Distance piece geometry used for the investigation is shown in Figure 4-5.

Figure 4-5 430 mm extruder distance piece geometry

Load and boundary condition:

The geometry was suitably meshed using tetrahedral mesh and investigated for two different load conditions, applied to the inner surfaces. Pressure load was applied to appropriate inner surfaces and fixed constraints on the required external surfaces as shown in Figure 4-6.
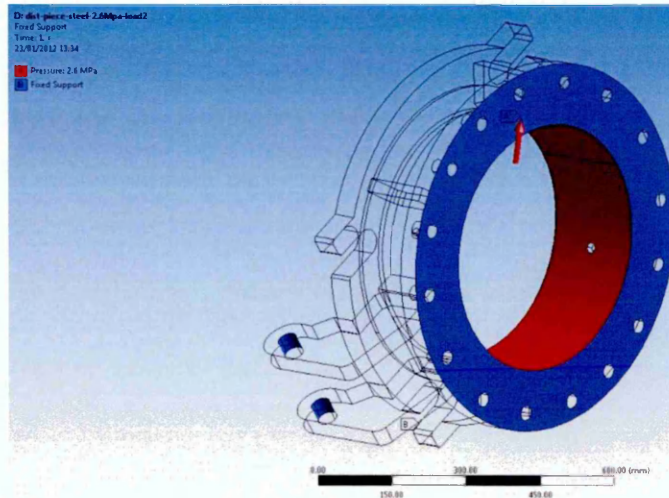
Figure 4-6 430 mm extruder distance piece- load applied

Stress results:

Values of equivalent stress, obtained for different materials from the analysis, with respect to applied load conditions are summarised in Table 4-4.

Material	Max. Von-Misses stress value, load- 2.6 MPa	Max. Von-Misses stress value, load- 1.8 MPa
Structural steel	52.749 MPa	36.519 MPa
GCI	52.403 MPa	36.279 MPa
ADI	52.314 MPa	36.217 MPa

Table 4-4 Stress results-distance piece

There was no significant change observed in the stress distribution pattern across the component with respect to applied load conditions. The stress distribution pattern on the distance piece, for applied load of 2.6 MPa is shown in Figure 4-7 and the results for the applied load of 1.8 MPa is available in Appendix B- section III'

108
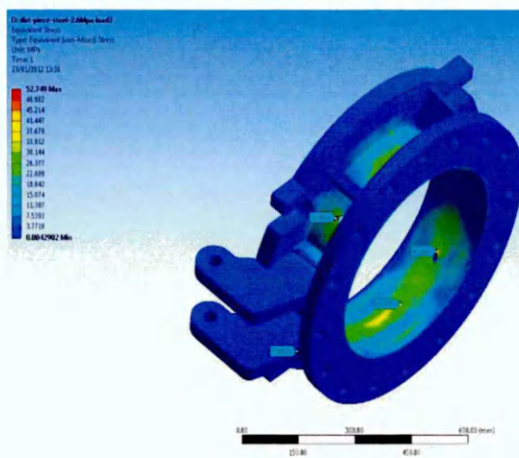
a) Structural steel
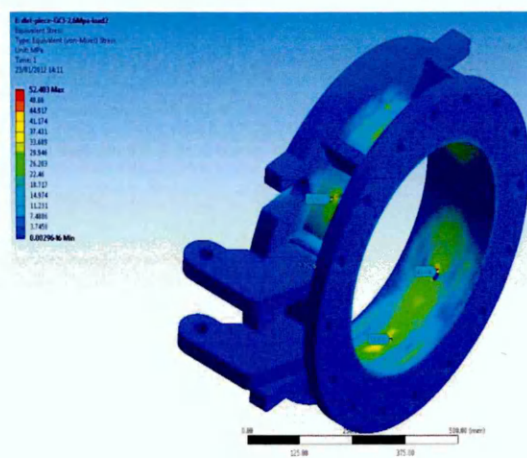
b) GCI
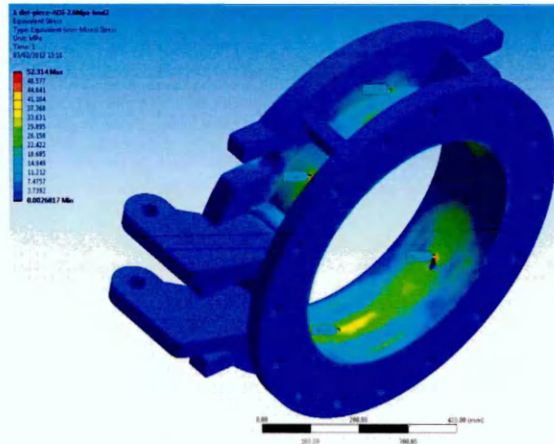
c) ADI

Figure 4-7 Stress induced in distance piece @ 2.6 MPa load

The strain induced in the distance piece was investigated by analysing the deformation pattern in the direction of extrusion. The results obtained are summarised in Table 4-5.

Material	Max. deformation, load-2.6 MPa	Max. deformation, load-1.8 MPa
Structural steel	0.0317 mm	0.0219 mm
GCI	0.0579 mm	0.0401 mm
ADI	0.0394 mm	0.0273 mm

Table 4-5 Deformation results- distance piece

There was no significant difference noted in the deformation pattern, for both the load conditions. The deformation pattern observed in liner for applied

load of 2.6 MPa is shown in Figure 4-8 and the results for applied load of 1.8 MPa is available in Appendix B- section IV.

a) Structural steel

b) Grey cast iron

c) ADI

Figure 4-8 Deformation in distance piece @ 2.6 MPa load

The material currently used by C.F Ltd is Structural Steel and its cost of manufacturing was compared with the cost of alternate materials used in FEA and is summarised in Table 4-6.

Material	Cost per piece (in £'s)
Structural steel	2445.00
GCI	1680.00
ADI	2170.00

Table 4-6 Manufacturing cost comparison for distance piece

It is clearly understood form the preliminary investigation that both ADI and GCI have design and cost benefits and can be used as an alternate material for manufacturing extruder distance piece.

4.2.3 Liner

The stress and deformation induced by the pressure developed during extrusion, on liners was assessed in this part.

Geometry:

Liner geometry used for the investigation is shown in Figure 4-9.
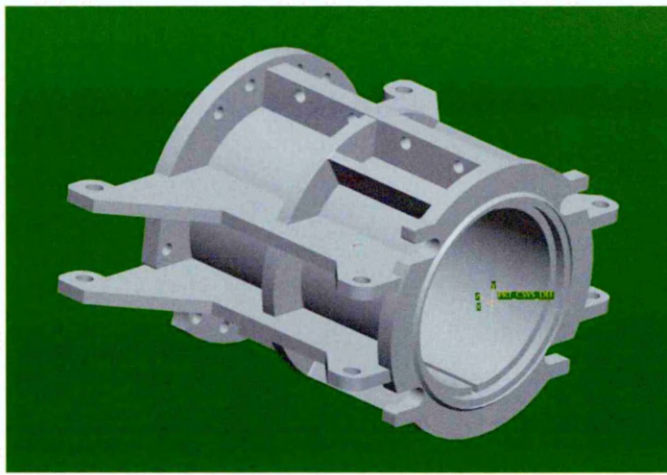

Figure 4-9 430 mm extruder liner geometry

Load and boundary condition:

The geometry was suitably meshed using tetrahedral mesh and investigated for two different load conditions, applied to the inner surfaces. Pressure load was applied to appropriate inner surfaces and fixed constraints on external surfaces as shown in Figure 4-10.
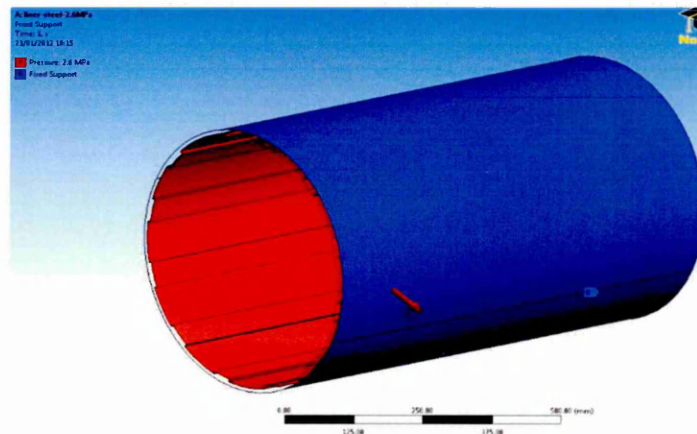
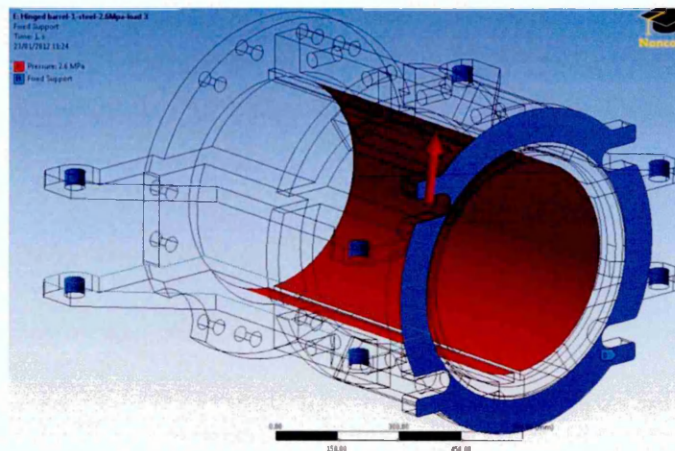*Figure 4-10 430 mm extruder liner - load applied*

Stress results:

Values of equivalent stress, obtained for different materials from the analysis, with respect to applied load conditions are summarised in Table 4-7.

Material	Max. Von-Misses stress value, load-2.6 MPa	Max. Von-Misses stress value, load-1.8 MPa
Structural steel	3.363 MPa	2.328 MPa
GCI	3.431 MPa	2.375 MPa
ADI	3.441 MPa	2.387 MPa

Table 4-7 Stress results-liner

The stress distribution pattern on the liner, for the applied load of 2.6 MPa is shown in Figure 4-11 and the results for the applied load of 1.8 MPa is available in Appendix B- section V·

a) Structural steel   **b) GCI**

c) ADI
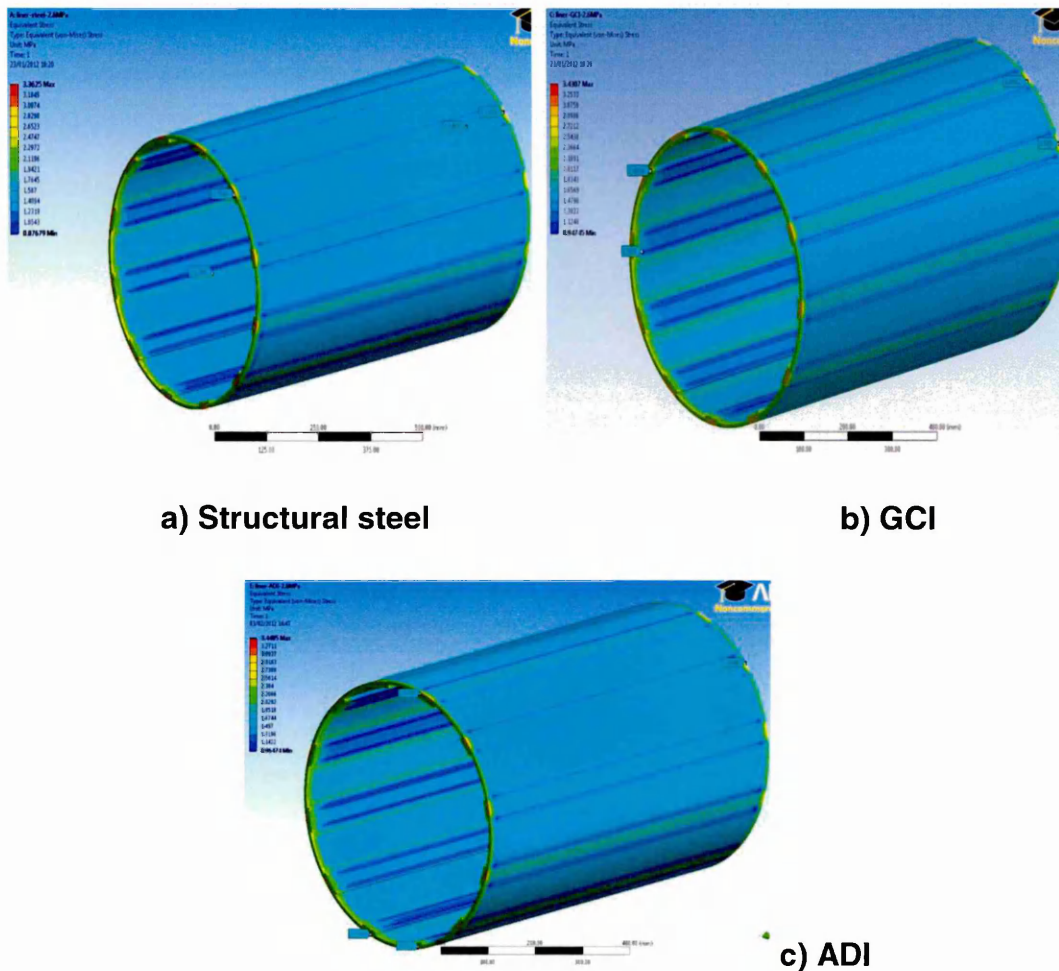
Figure 4-11 Stress induced in liner @ 2.6 MPa load

112

The strain induced in the liner was investigated by analysing the deformation pattern in the direction of extrusion. The results obtained are summarised in Table 4-8.

Material	Max. deformation, load-2.6 MPa	Max. deformation, load-1.8 MPa
Structural steel	0.0002 mm	0.0001 mm
GCI	0.0004 mm	0.0003 mm
ADI	0.0002 mm	0.0002 mm

Table 4-8 Deformation results-liner

The deformation pattern observed in liner for applied load of 2.6 MPa is shown in Figure 4-12 and the results for applied load of 1.8 MPa is available in Appendix B- section VI.
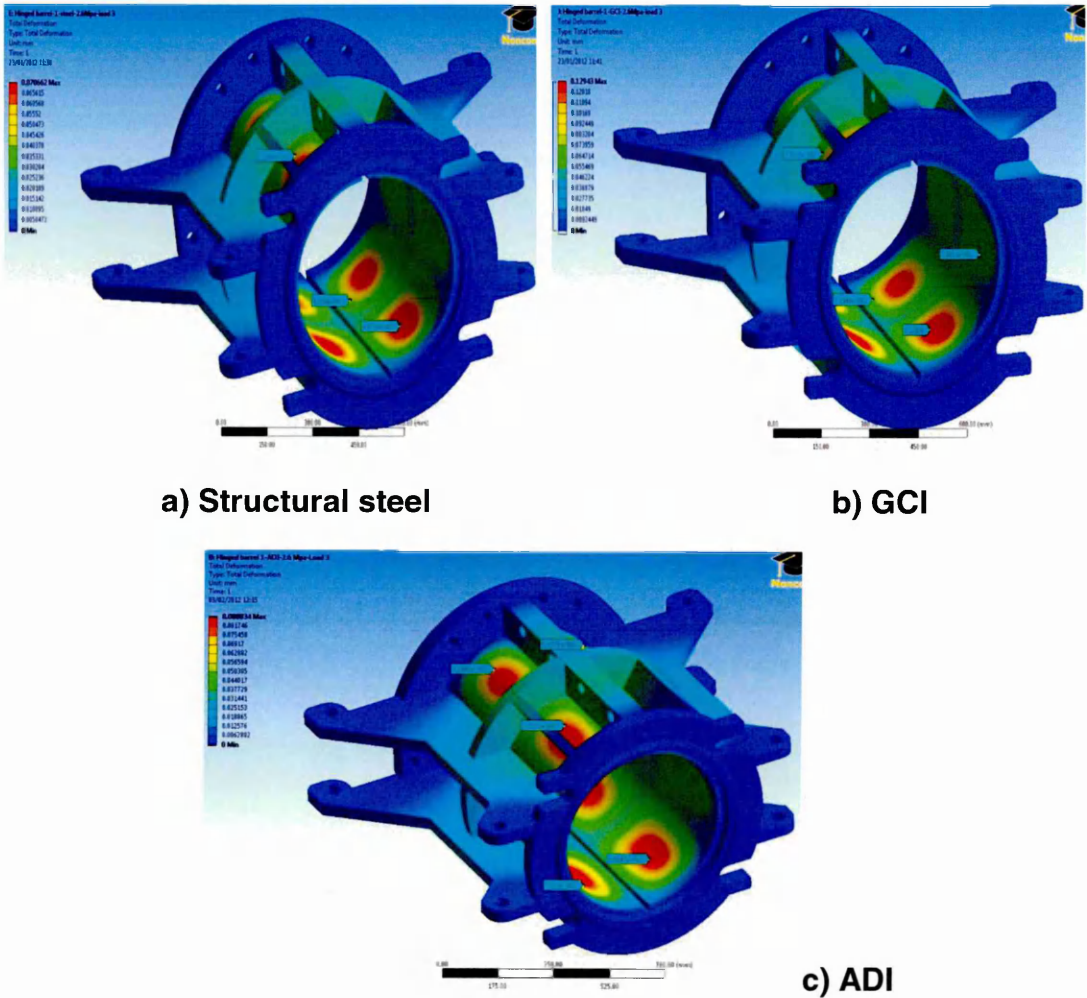

a) Structural steel   **b) GCI**

c) ADI
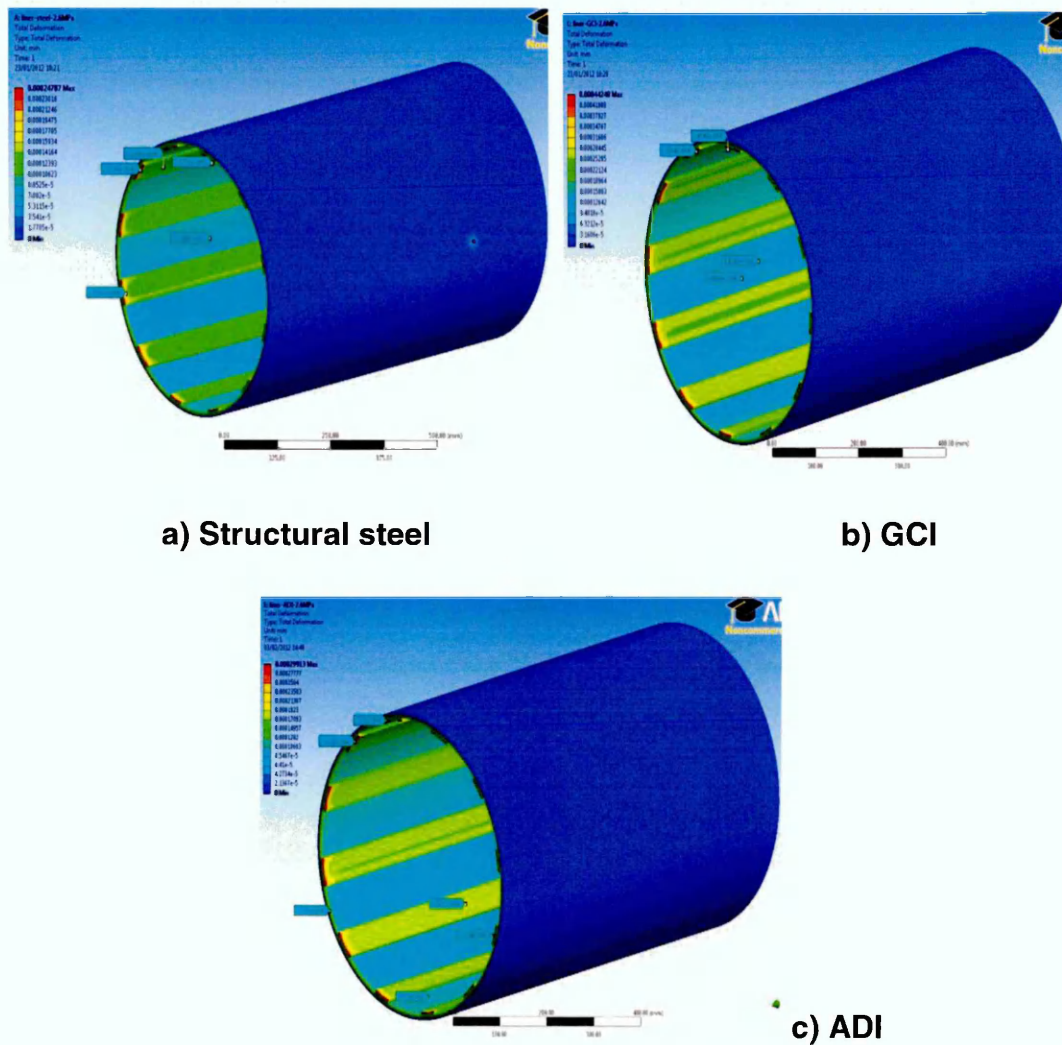
Figure 4-12 Deformation in liner @ 2.6 MPa load

113

4.2.4 Auger

The stress and deformation induced by the pressure developed during extrusion, on the auger shaft was assessed in this part.

Geometry:

Auger geometry used for the investigation is shown in Figure 4-13.
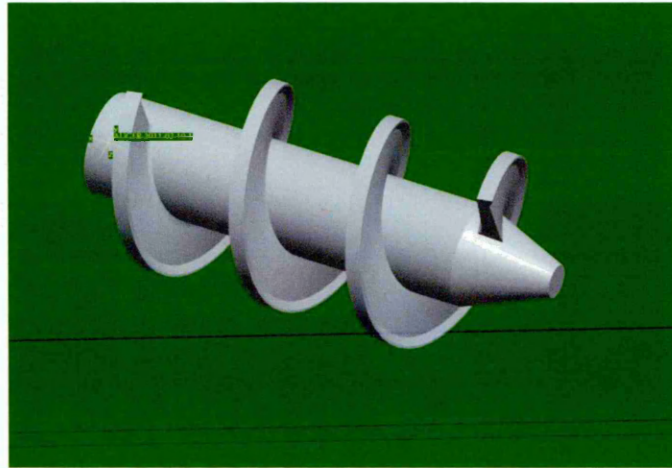
Figure 4-13 430 mm extruder auger shaft geometry

Load and boundary condition:

The geometry was suitably meshed using tetrahedral mesh and investigated for two different load conditions. Pressure load was applied on the all the faces of worm and auger shaft and fixed constraint at one end of the shaft as shown in Figure 4-14.
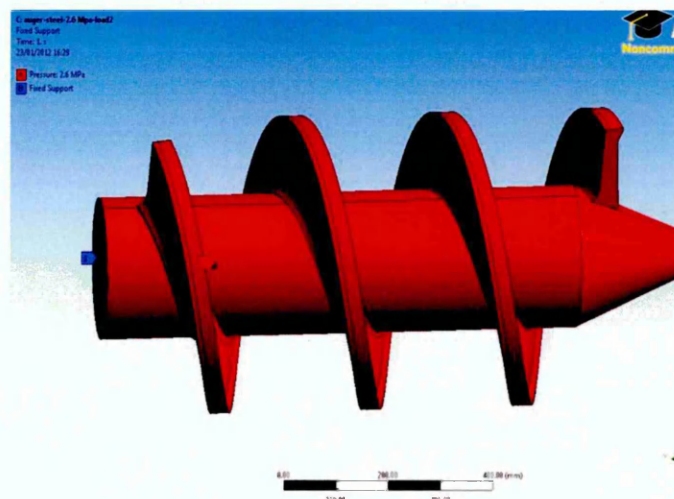
Figure 4-14 430 mm extruder auger shaft - load applied

114

Stress results:

Values of equivalent stress, obtained for different materials from the analysis, with respect to applied load conditions are summarised in Table 4-9.

Material	Max. Von-Misses stress value, load- 2.6 MPa	Max. Von-Misses stress value, load- 1.8 MPa
Structural steel	3.835 MPa	2.655 MPa
GCI	4.131 MPa	2.860 MPa
ADI	13.345 MPa	9.238 MPa

Table 4-9 Stress results-auger shaft

The stress distribution pattern on auger shaft, for applied load of 2.6 MPa is shown in Figure 4-15 and the results for applied load of 1.8 MPa is available in Appendix B- section VII⋅

a) Structural steel   **b) GCI**

c) ADI
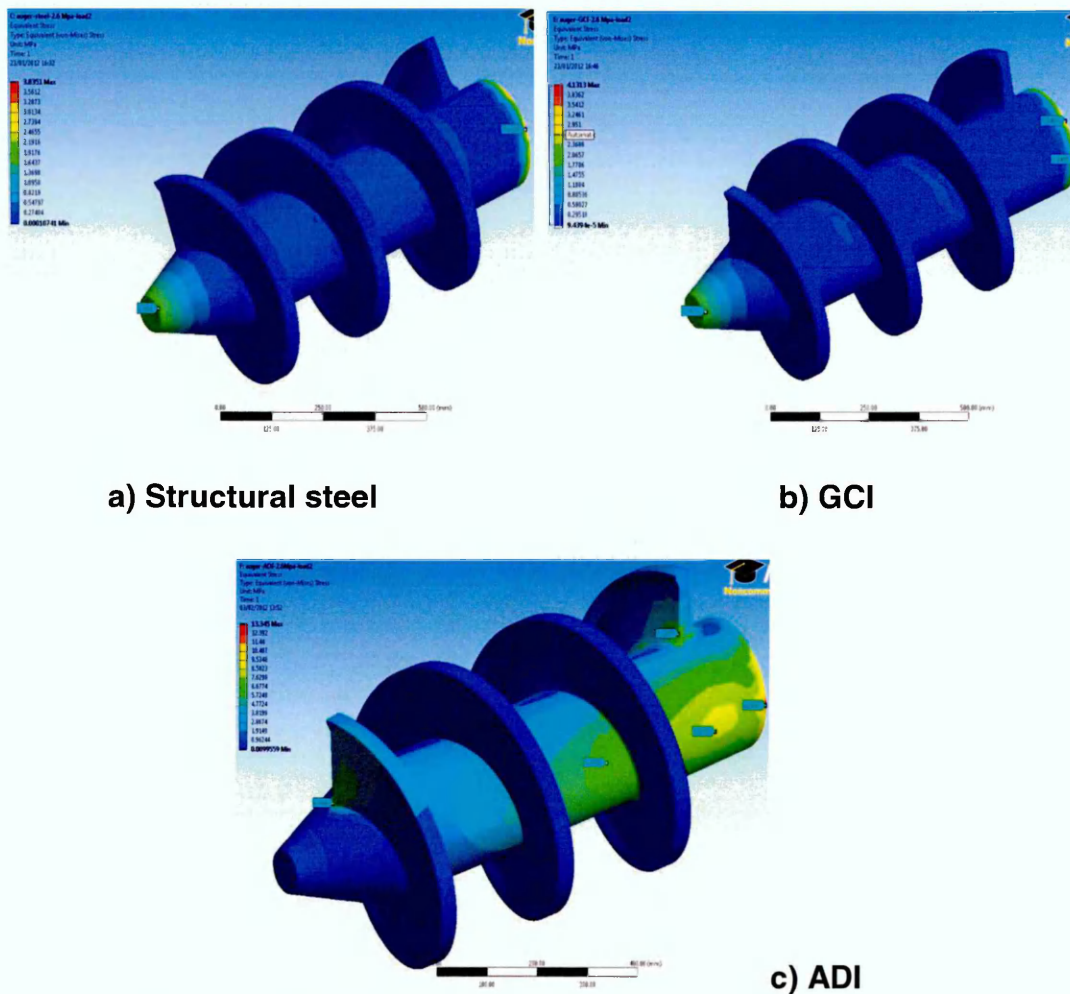
Figure 4-15 Stress induced in auger shaft @ 2.6 MPa load

The strain induced in the auger shaft was investigated by analysing the deformation pattern in the direction of extrusion. The results obtained are summarised in Table 4-10.

Material	Max. deformation, load-2.6 MPa	Max. deformation, load-1.8 MPa
Structural steel	0.004 mm	0.003 mm
GCI	0.009 mm	0.006 mm
ADI	0.198 mm	0.137 mm

Table 4-10 Deformation results-auger shaft

The deformation pattern observed in auger shaft for applied load of 2.6 MPa is shown in Figure 4-16 and the results for applied load of 1.8MPa are available in Appendix B- section VIII.

a) Structural steel   **b) GCI**

c) ADI
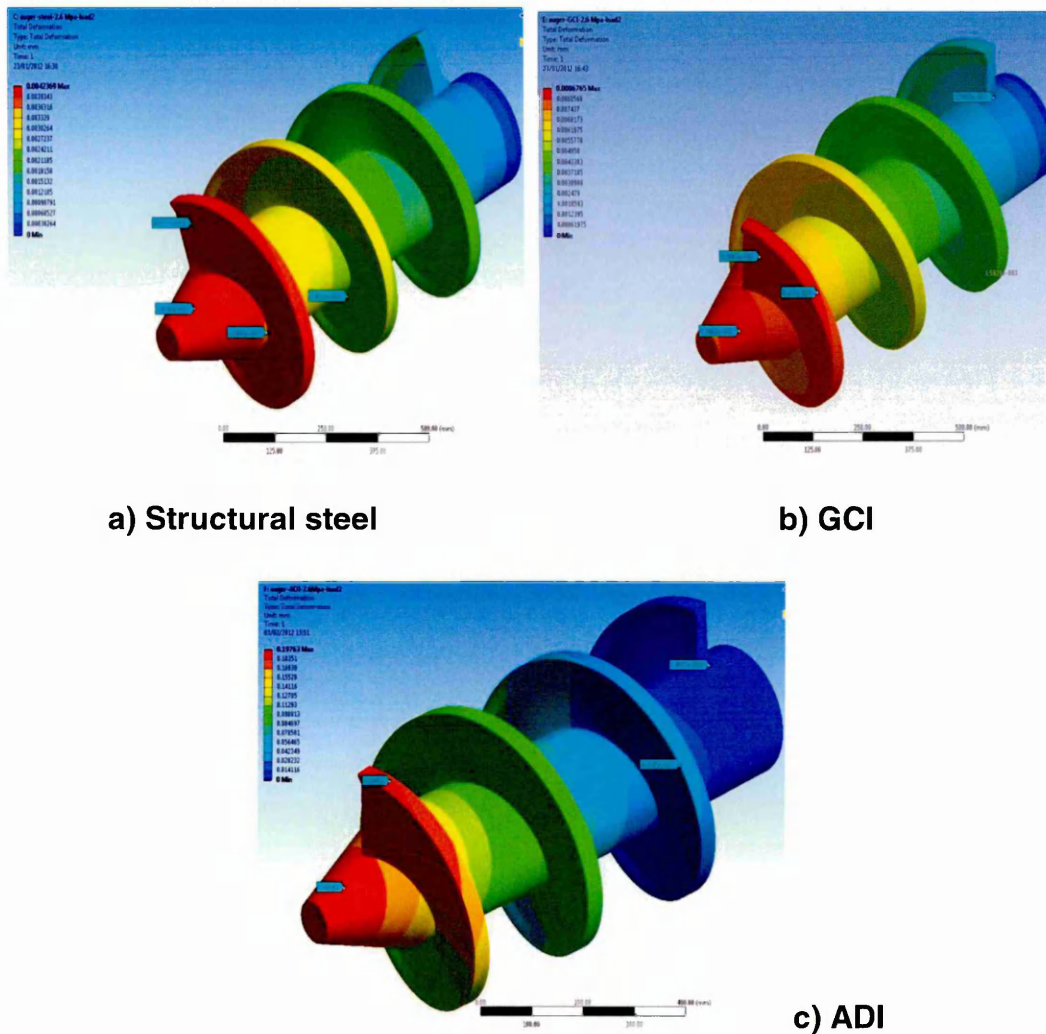
Figure 4-16 Deformation in auger shaft @ 2.6 MPa load

116

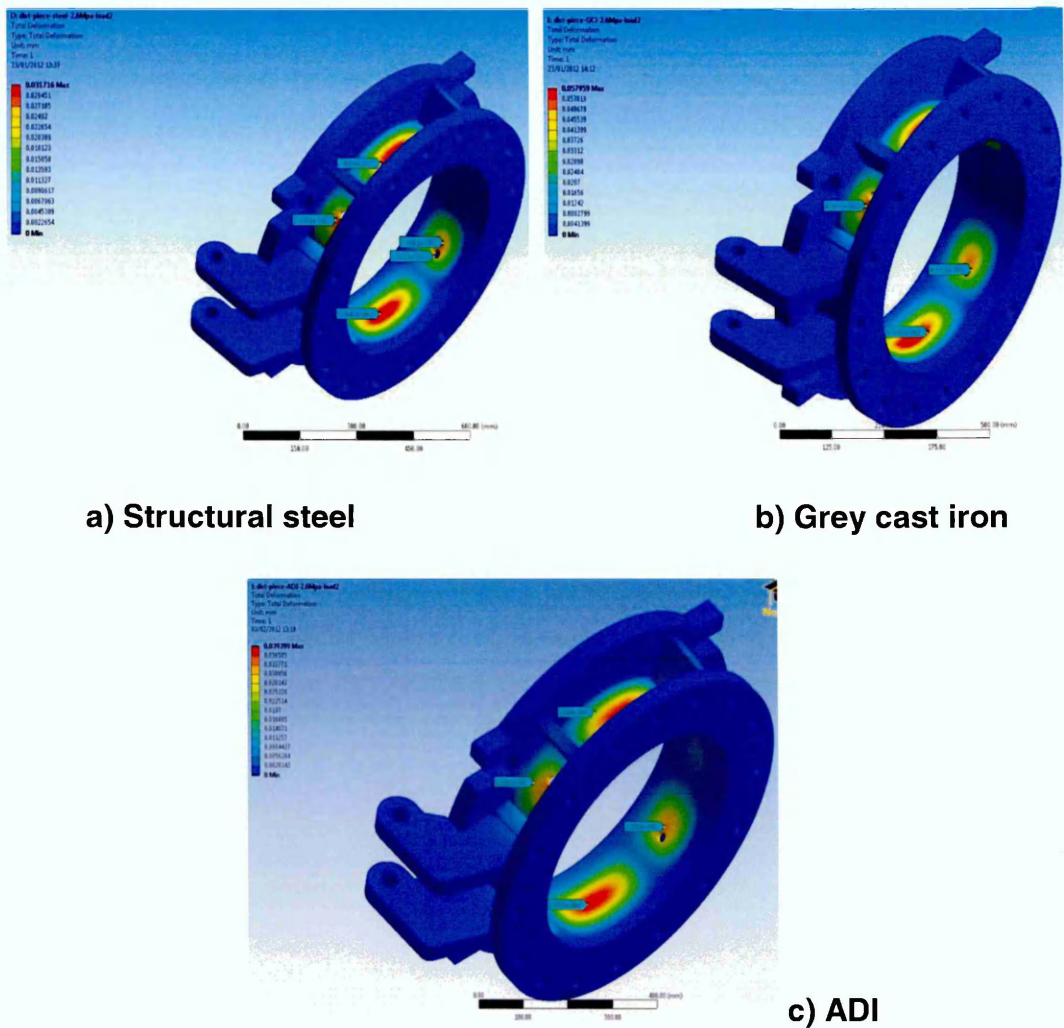The material currently used by C.F Ltd for manufacturing auger is a special type of alloy material developed in house, designated as CF-28. Material with equivalent mechanical property was used in FEA. In actual scenario, during the process of manufacturing, the casted auger has to be heat treated in order to attain the recommended hardness value of ≈60 HRC. Hence in order to have a fair comparison of manufacturing cost, the heat treatment cost for alternate materials was required. Due to amount of time and cost involved in obtaining this cost, it was decided to make a comparison without heat treatment cost and it is summarised in Table 4-11.

Material	Cost per piece (in £'s)
Chrome steel	311.00
GCI	200.00-223.00
ADI	227.00-266.00

Table 4-11 Manufacturing cost comparison for auger

It is evident from the above discussion that the alternate materials considered for manufacturing of augers, possess both design and commercial advantages.

Clay being a very abrasive substance, the hardness value of the auger is considered to be very critical to withstand the wear caused by the clay and also increase the life of auger, in order to make the system to be cost effective.GCI is not recommended by the users and design engineers, due to its brittle nature at the early stages of installation. ADI alloy is lighter and cheaper than the steel alloy which is currently used and also proven to be useful in such applications. ADI, though, has better mechanical characteristics and costs less than the existing material, the only limitation is the maximum hardness value that could be achieved through heat treatment process. As mentioned earlier it is recommended that certain areas of the auger should have a hardness value of ≈60 HRC. The maximum attainable hardness value in an ADI alloy, with the available methods of heat treatment is 55 HRC, and this increase in hardness is achievable only to a certain micron depth. However all the augers that are mounted on the shaft are not subjected to equal pressure and wear. The field data obtained on the wear

life of augers indicates that the auger located at the far end of the extruder or in other words the augers at the end of the barrel chamber is subjected to excessive wear. Whereas the augers inside the vacuum chamber are subjected to less wear. This difference in the pattern of wear characters of auger provides an opportunity for the use of alternate materials for making augers which are subjected to less pressure and wear. It is evident from the above discussion that using ADI as an alternate material for making augers is not only a cost effective option but also could yield other benefits like less power consumption at the extruder unit and increases the life of augers.

4.3 Conclusion

Thus the technical and commercial advantage of using alternate light materials was presented in this chapter. This clearly demonstrates the ability and advantages of using FEA techniques to improve the design of clay extruders within heavy ceramic industries.

Chapter-5 Conclusion and future directions

5.1 Conclusion

The main aim of this research work was to use CFD and FEA techniques to assess and improve the design of extruders. The key objectives include identifying suitable CFD methodology to simulate the clay extrusion process, assessing the performance character of extruders with respect to various design and operating parameters and investigate alternate materials for extruder components that could make the extruder more efficient and cost effective.

The first part of this research work was dedicated to identifying a suitable flow model and CFD modelling technique, for assessing the performance characters of a vacuum type de-airing extruder. The extrusion pressure developed and power consumed by full scale extruders during the extrusion was predicted using Herschel-Bulkley's fluid flow based 3-D CFD model. The extrusion pressure, power consumption and the pressure development trend were then predicted for different designs of extruder under different operating conditions, using the 3-D CFD model. The results obtained for extrusion pressure, flow pattern and velocity of clay during extrusion were in good agreement with the values suggested in the literature and occurring in actual scenarios. The results obtained from the model for properties like temperature and density variation were not very satisfactory and need further investigation.

The results for shear thinning behaviour exhibited by clay during extrusion was predicted from the CFD model and compared with the experimental results obtained from various scientific works. The similarity in the viscosity profile obtained from the model and the literature indicates that Herschel-Bulkley's flow model used in the CFD analysis is well representing the shear thinning behaviour of clay exhibited during the process of stiff extrusion.

The second part of this research work was focused in validating the CFD methodology used in the first stage. The extrusion pressure and power consumed by the lab-scale extruder was measured experimentally and compared with the results obtained from CFD analysis. The closeness in the measured values for extrusion pressure and power consumption clearly

demonstrates the suitability of using the identified CFD methodology to model and assess the performance of full-scale extruders.

The third stage of this research work was dedicated to using the FEA technique to investigate the technical suitability of alternate light weight materials and the compare the costs of extruders. The FEA results and the cost of alternate light weight materials indicate that the use of Austempered Ductile Iron to manufacture extruder components could result in both technical and commercial benefits. A careful consideration is required at the design stage in order to identify a proper area for use of this material.

The results obtained from this research work clearly demonstrate that using CFD and FEA techniques within the process of clay extruder design could be cost effective and time saving. It helps in reducing the resource and time required for developing new extruder components, compared with lab-based development processes.

5.2 Future directions

- Performing more trials in the scaled extruder with an improved experimental set up could help in obtaining further validation of the CFD methodology used.

- A further investigation in improving the quality of mesh and further mesh refinement could be beneficial in obtaining a converged solution and might improve the results in critical areas of extruder sections.

- Experimental works in a controlled environment that focus in determining the variables used for Herschel-Bulkley's model, for clays with different moisture content could be undertaken. This will enhance the accuracy of flow parameters predicted by the current CFD methodology and also reduce time and computing cost.

- A further investigation of suitable CFD based modelling methods that can predict temperature dependant properties of clay during extrusion could be helpful in predicting additional flow parameters, involved during extrusion. It might also open up new areas for investigation.

- Measuring the viscosity of clay with advanced instruments like Ball measuring system and Building Material cell, could help in obtaining

121

better results and further understanding in the flow characters of clay when subjected to shear. This could help in making a fair comparison with the results predicted from the CFD model and make suitable design changes to enhance the flow of clay in extruders during extrusion.

References

1. Administrative Centre for China's Agenda (2000), "Centre for Environmentally Sound technology Transfer (CESTT) - China, Sector Profile and Factory Report on Energy and Environmental Audits for China's Brick Sector".

2. Al-Zahrani, S.M., "A generalized rheological model for shear thinning fluids", Journal of Petroleum Science and Engineering, 1997, Volume-17, 211-215.

3. AMA research limited (2011), "Market Research-Brick and Blocks market-U.K 2011-2015".

4. Amin, S.H.K.; El-Khatib, K. & Abadir, M.F., "Rheological characteristics of clay sewer paste", Journal of Industrial Ceramics, 2009, Volume 29, 149-155.

5. Andrade, F.A.; Al-Qureshi, H.A. & Hotza,D., "Measuring and Modeling the Plasticity of Clays", Brazilian Scientific Journals, Material research, 2010, Volume 13(3), 395-399.

6. Ansys-12.0 User's guide -2009-01-29, Ansys Inc, USA.

7. Bender, W. & Händle, F., "BRICK AND TILE MAKING-Procedures and Operating Practice in the Heavy Clay Industries", 1982, Wiesbaden und Berlin, Bauverlag GMBH. ISBN 3-7625-1485-2.

8. Bouzakis, K.D.; Efstathiou, K.; Paradisiadis, G. & Tsouknidas, A., "Experimental and FEM-Supported Investigation of Wet Ceramic Clay Extrusion for the Determination of Stress Distributions on the Applied Tools' Surfaces", Proceedings of the 3rd International Conference on Manufacturing Engineering (ICMEN), 2008, Greece, 229-243.

9. Brick Development Association (BDA) (2011), "A Sustainability Strategy for Brick Industry ". (Also available at www.brick.org.uk)

10. Brookfield Engineering (2012). [Online]. Last accessed October 2011, at http://www.brookfieldengineering.com.

11. Building something great, Boral Gypsum Asia Limited (2002). [Online]. Last accessed December-2012 at http://www.boral.com.au.

12. Carl, Frahme, E., "World Cyber University, Lesson-CP4: Forming Technology", [Online]. Last accessed December-2012 at http://www.worldcyberu.com.

13. Ceramtechno Pte Limited (2010). [Online]. Last accessed December 2012, at http://www.ceramtechno.com.

14. Chowdhury, A.K. et al., "Development of Wear-Resistant Austempered Ductile Iron Hammers for Ore Crushing Application-A Case Study", Indian Foundry Journal, 2010, Volume 56.No.6, 39-42.

15. Craven Fawcett Limited (2009). [Online]. Last accessed December-2012 at http://www.cravenfawcett.com.

16. Da, S. & Jincheng, L., "Cast Irons Containing Rare Earths",-2000, Tsinghua University Press, ISBN-7-302-03918-6.

17. Department of Energy and Climate Change (July-2011), "Energy Consumption in the U.K.:2011".

18. Doltsinis.I. & Schimmler.M., "Modelling and Simulation of the Extrusion of Ceramic Bodies", The International Center for Numerical Methods in Engineering-Computational Mechanics New Trends and Applications, 1998, 1-5.

19. Energy Efficiency improvements in the Indian Brick Industry (2011). [Online]. Last accessed December-2012 at http://www.resourceefficientbricks.org.

20. Fluent 6.3 User's Guide.

21. Gambit-2 Modelling Guide-Volume 1, 2001.

22. Händle, F., " Extrusion In Ceramics", 2007, Springer-Verlag Berlin Heidelberg. ISBN-1619-0181.

23. Hedley,J., "MSc-Dissertation in Advanced Engineering"-Faculty of Arts, Computing, Engineering and Sciences, Sheffield Hallam University, U.K. (2009)

24. Johnson, W.J., "Evaluation of NCPRC Research Auger in Sewer Pipe Production", Journal of the American Ceramic Society-Ceramic Bulletin, 1962, Volume 41, No.9, 550-552.

25. Keough, J.R., Ductile Iron Society (2012). [Online]. Last accessed February-2012 at http://www.ductile.org/didata.htm.

26. Kocserha, I. & Kristàly, F., "Effects of Extruder Head's Geometry on the Properties of Extruded Ceramic Products", Materials Science Forum, 2010, Volume.659, 499-504 .

27. Lower Quartile Solutions. [Online].Last accessed January-2013 at http://www.lqsgroup.com.

28. Lund, H.H.; Bortz, S.A. & Reed, A.J., "Auger Design for Clay Extrusion", Journal of the American Ceramic Society-Ceramic Bulletin, 1962, Volume 41, No.9, 555-559.

29. Maciel, G.F.; Santos, H.K. & Ferreira, F.O., "Rheological analysis of water clay compositions in order to investigate mudflows developing in canals", Journal of Brazilian Society of Mechanical Sciences and Engineering, 2009, Volume.31, no.1, ISSN 1678-5878.

30. Mahajan, S.P. & Budhu, M., "Shear Viscosity of Clays to Compute Viscous Resistance", International Association for Computer Methods and Advances in Geomechanics- 12th International conference, 2008, 1516, 1523.

31. Mezger, T.G., "The Rheology Handbook"-2006, 2nd Edition, Vincentz Network GMBH &Co. ISBN-3-87870-174-8.

32. Michot, A.; Smith, S.D.; Degot, S. & Gault, C., ""Thermal conductivity and specific heat of kaolinite: Evolution with thermal treatment", Journal of European Ceramic Society, 2008, Volume28, 2639-2644.

33. Millberg, L.C., How Products Are Made-vol.1 (2010), [Online]. Last accessed December-2012 at http:// www.madehow.com.

34. Nelson, J.A. & Andrews, A.I., "Rheological Properties of the Clay-Water System Under Pressure", Journal of the American Ceramic Society-Ceramic Bulletin, 1959, Volume 38, No.9, 447-455.

35. Norton, F.H., "Flow Properties of the Kaolinite-Water System", The Clay Minerals Society- Clay and Clay Minerals, 1954, Volume 3, 549-556.

36. Ormsby, W.C. & Marcus, J.H., "Rheological Properties of Kaolins of Varying Degrees of Crystallinity", The Clay Minerals Society- Clay and Clay Minerals, 1963, Volume 12, 207-208.

37. Parks, J.R. & Hill, M.J., "Design of Extrusion Augers and the Characteristic Equation of Ceramic Extrusion Machines", Journal of

the American Ceramic Society-Ceramic Bulletin, 1959, Volume 42, No.1, 1-6.

38. Petavratzi, E. & Barton, J., "Industrial sector study on the utilisation of alternative minerals in the manufacture of mineral wool insulation"- DEFRA Project code WRT_177, 2007, School of Civil Engineering- University of Leeds, U.K.

39. Poyser, A., "Computational Fluid Dynamic Modeling of a Clay Extruder with Experimental Validation" - MSc.dissertation, Faculty of Arts, Computing, Engineering and Sciences, Sheffield Hallam University, U.K., (2011).

40. Punmia, B.C.; Jain, A. & Jain, A.K., "Comprehensive Basic Civil Engineering"- 2005, Laxmi Publications.

41. Renewable Energy Resources Information Centre (RERIC) Asian Institute of Technology, "Small and Medium Scale Industries in Asia: Energy and Environment Brick and Ceramic Sectors", 2003, ISBN 974-8209-03-2.

42. Robie, R.A. & Hemingway, B.S., "Heat capacities of Kaolinite From 7 to 380 K and of DMSO-Intercalated Kaolinite From 20 to 310K.The Entropy Of Kaolinite $Al_2 Si_2O_5(OH)_4$", The Clay Minerals Society- Clay and Clay Minerals, 1991, Volume 39,No:4, 362-368.

43. Seanor, J.G. & Schweizer, W.P., "Basic Theoretical Factors in Extrusion Augers", Journal of the American Ceramic Society-Ceramic Bulletin, 1962, Volume 41, No.9, 561-563.

44. Shinagawa Refectories Australia Pty Limited (2005). [Online]. Last accessed December-2012 at: http://www.shinagawa.biz.

45. The Brick Industry Association (2012). [Online]. Last accessed December 2012 at: http//www.gobrick.com.

46. The European Ceramic Industry Association-Ceramic Industry Key Facts (2010). [Online]. Last accessed December-2012, at http:www.cerameunie.eu/en/ceramic-industry/key-facts.

47. Tu, J.; Yeoh, G. & Liu, C., Computational Fluid Dynamics: A Practical Approach", 2013, Second Edition, U.K, Butterworth-Heinemann, ISBN: 978-0-08-098243-4.

48. Versteeg, H.K. & Malalasekera, W., "An Introduction to computational fluid dynamics-The Finite Volume Method", 1995, Edinburg Gate, Pearson Education Limited, ISBN-0-582-21884-5.

49. Walker, R. (2012). [Online].Last accessed March-2012 at http://www.simetric.co.uk/si_materials.htm.

50. West Lothian Archaeology Group, Brickmaking in Armadale. [Online]. Last accessed at: http// www.armadale.org.uk/brickworks.htm.

51. Wilkinson, W.L., "Non-Newtonian Fluids-Fluid Mechanics, Mixing And Heat Transfer", International Series of Monographs on Chemical Engineering, 1960, Volume-1,-Oxford Press, U.K.

52. Zhang, B.; Zhao, X.; He, J. & Tang, G., "Clay material extrusion process resulting field simulation and analysis", Advanced Materials Research, 2011, Volume 236-238, 1581-1586.

Word Count	
Pages	242
Words	35,208
Characters (no spaces)	188,562
Characters (with spaces)	222,469
Paragraphs	2,078
Lines	5,160
The count includes textboxes, footnotes & endnotes	

I. Extruder geometry

a. 500 mm extruder
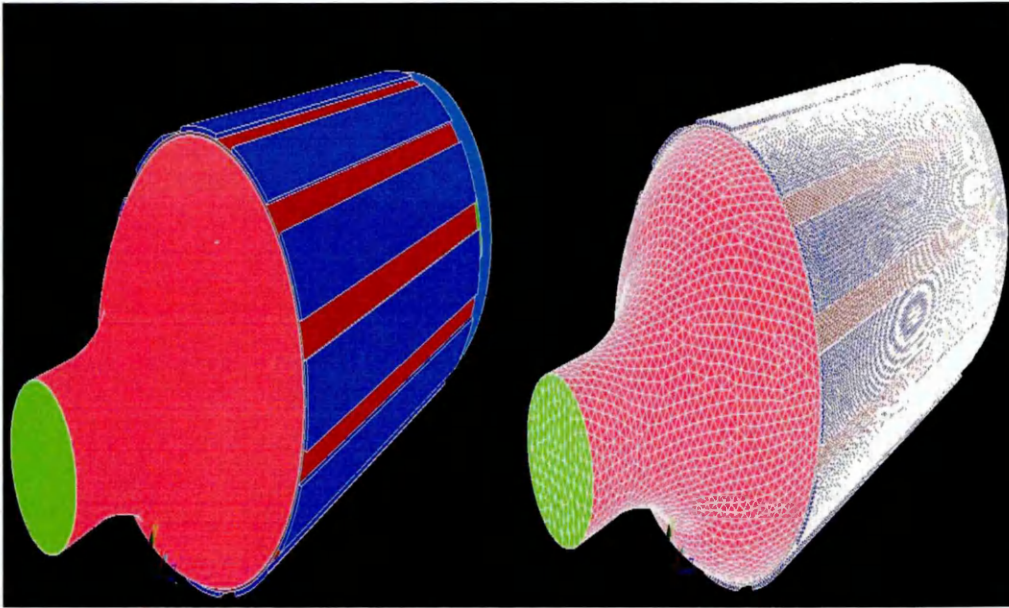
Figure A-A- 1 500 mm extruder volumes and mesh generated

b. 600 mm extruder
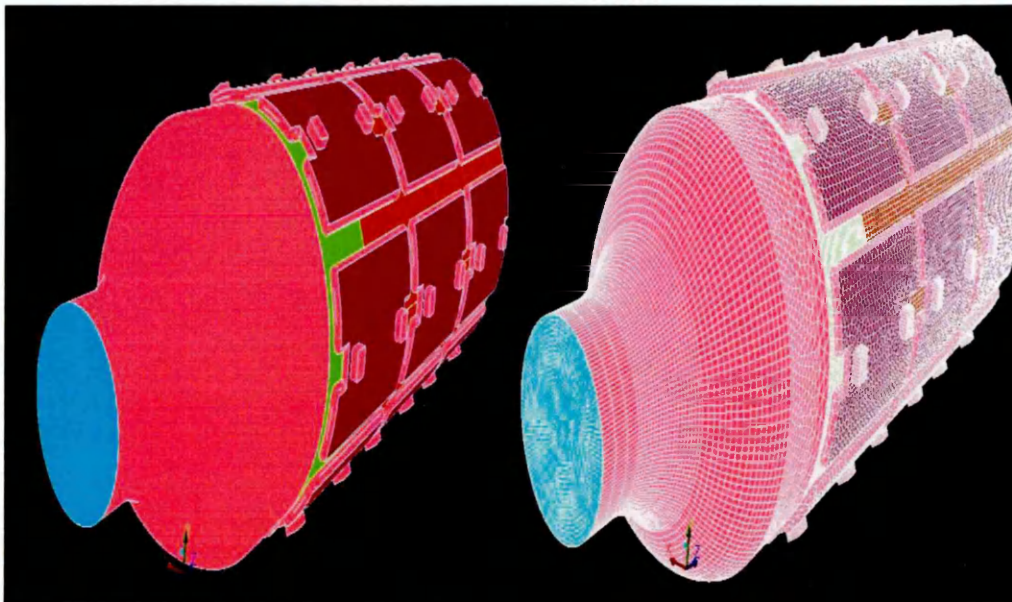
Figure A-A-2 600 mm extruder volumes and mesh generated

130

II. CFD Simulation results of 500 mm extruder with Herschel-Bulkley's model value-I

Extrusion pressure:
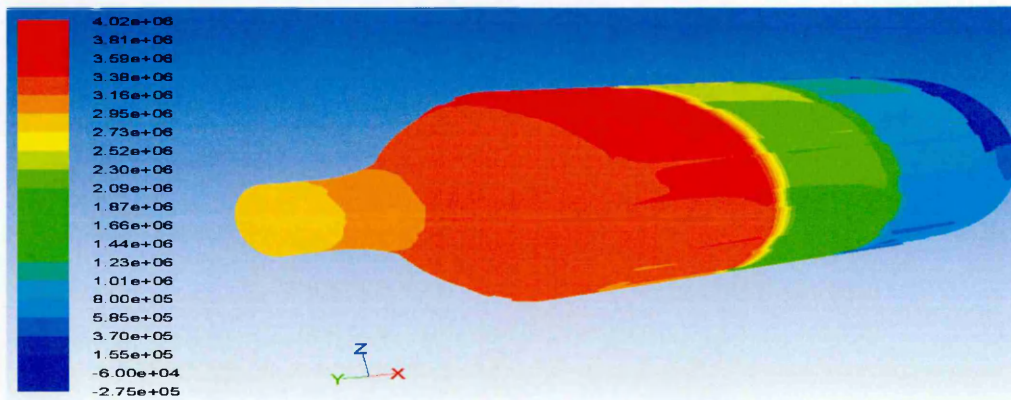
Contours of Static Pressure (pascal) (Time=2.5050e+00)

Figure A-A-3 Static pressure contour (full view)-500 mm Case I

Contours of Static Pressure (pascal) (Time=2.5050e+00)

Figure A-A-4 Static pressure contour (sectional view)-500 mm Case I

Static Pressure (Time=2.5050e+00)

Figure A-A-5 Static pressure profile -500 mm Case I

Material flow pattern:

Contours of Velocity Magnitude (m/s) (Time=2.5050e+00)

Figure A-A-6 Flow velocity during extrusion (sectional view)-500 mm Case I

Viscosity profile:
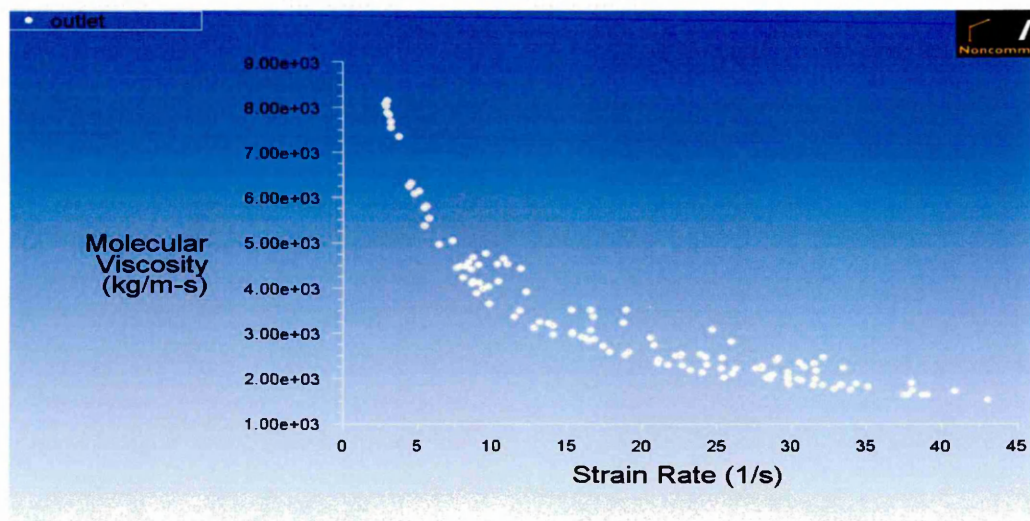
Molecular Viscosity vs. Strain Rate (Time=2.5050e+00)   Ap

Figure A-A-7 Molecular viscosity vs. Strain rate-500 mm Case I

132

Extrusion pressure:
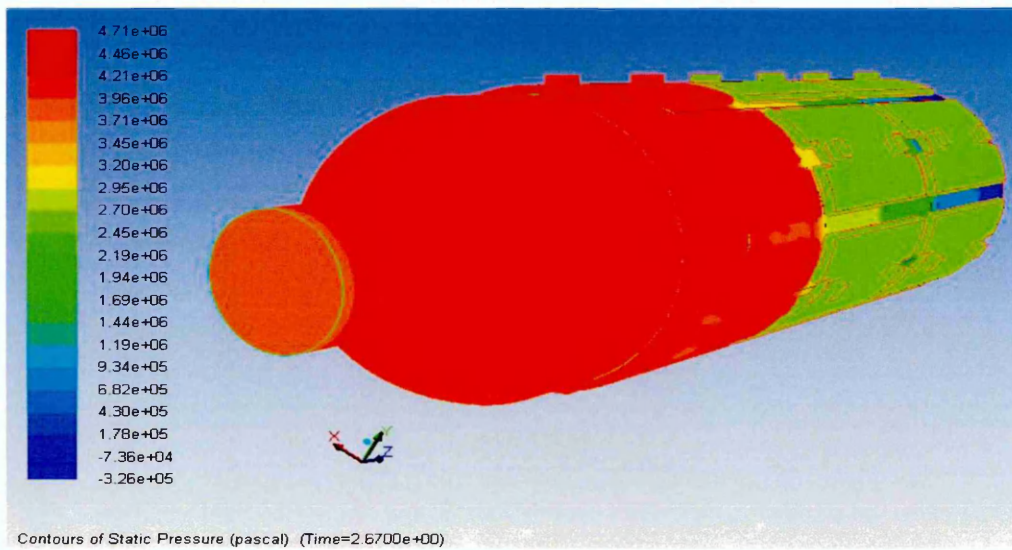
Figure A-A-8 Static pressure contour (full view)-600 mm Case I
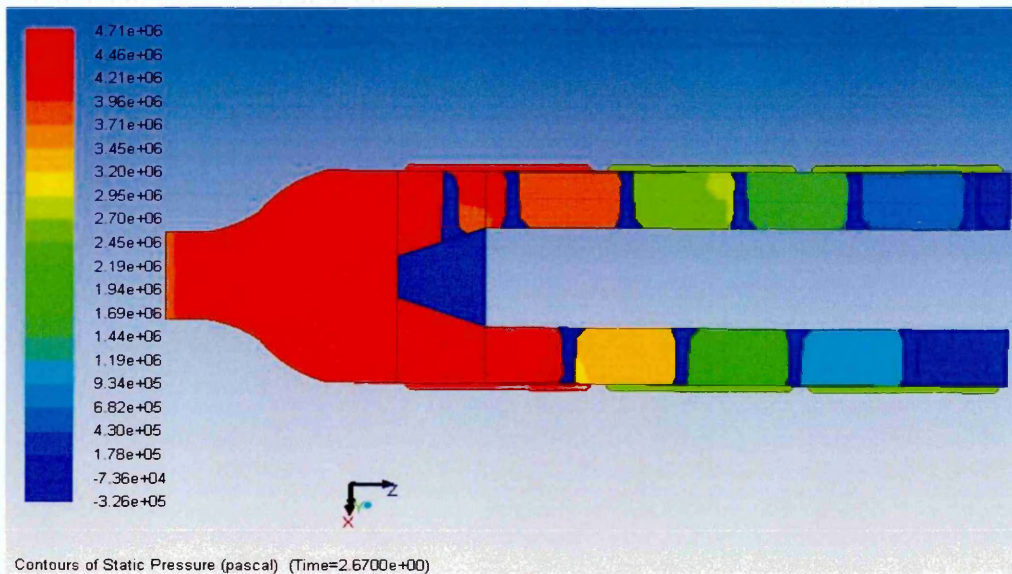
Figure A-A-9 Static pressure contour (sectional view)-600 mm Case I
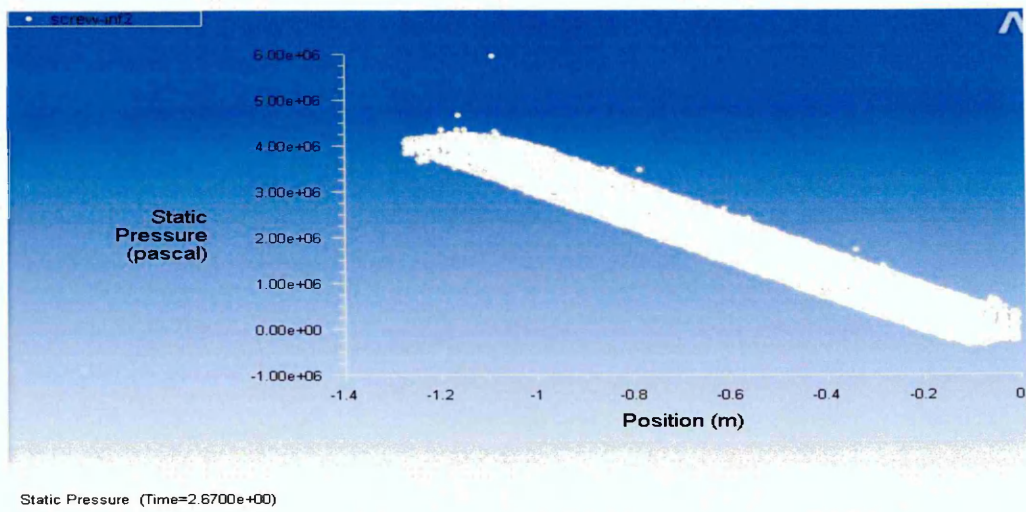
Figure A-A-10 Static pressure profile -600 mm Case I

Material flow pattern:
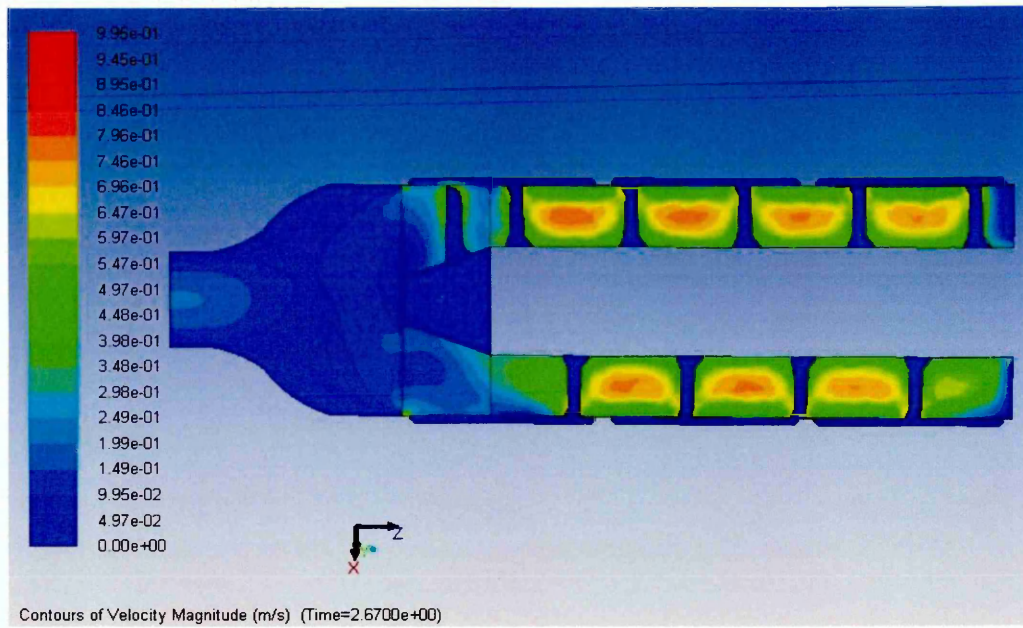
Figure A-A-11 Flow velocity during extrusion (sectional view)-600 mm Case I

134
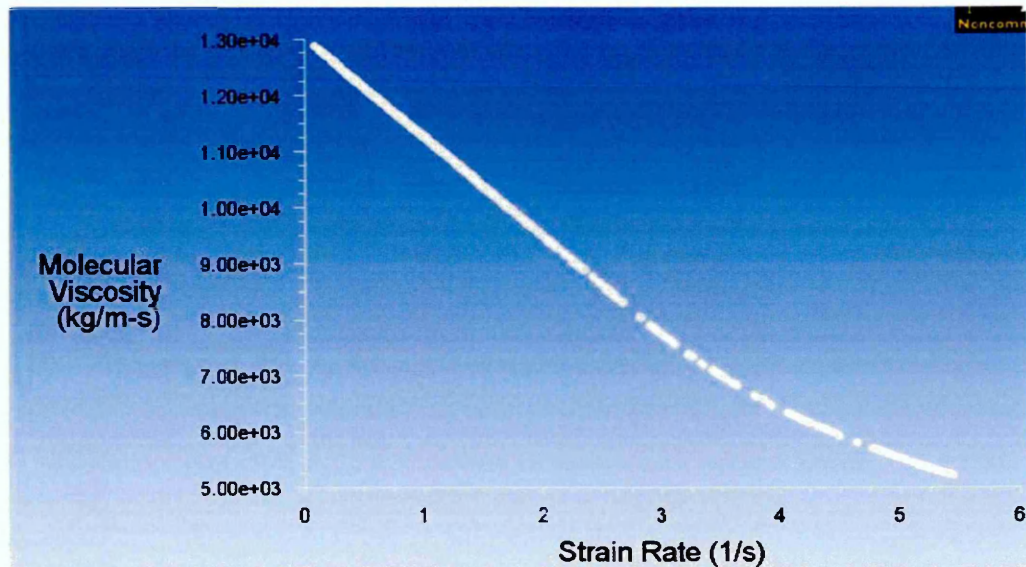
Figure A-A-12 Molecular viscosity vs. Strain rate-600 mm Case I

IV. CFD Simulation results of 500 mm extruder with Herschel-Bulkley's model value-II

Extrusion pressure:

Contours of Static Pressure (pascal) (Time=2.5000e+00)
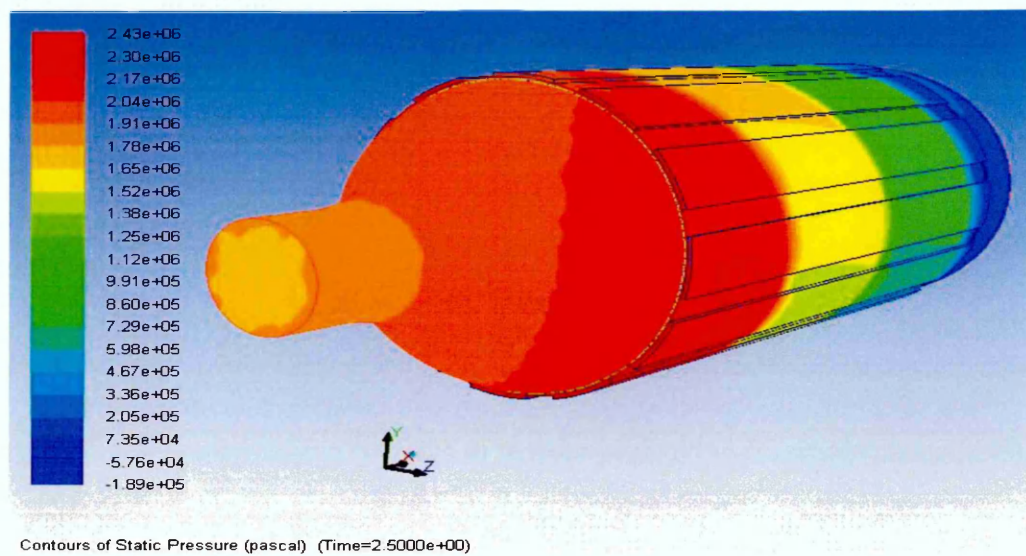
Figure A-A-13 Static pressure contour (full view)-500 mm Case II
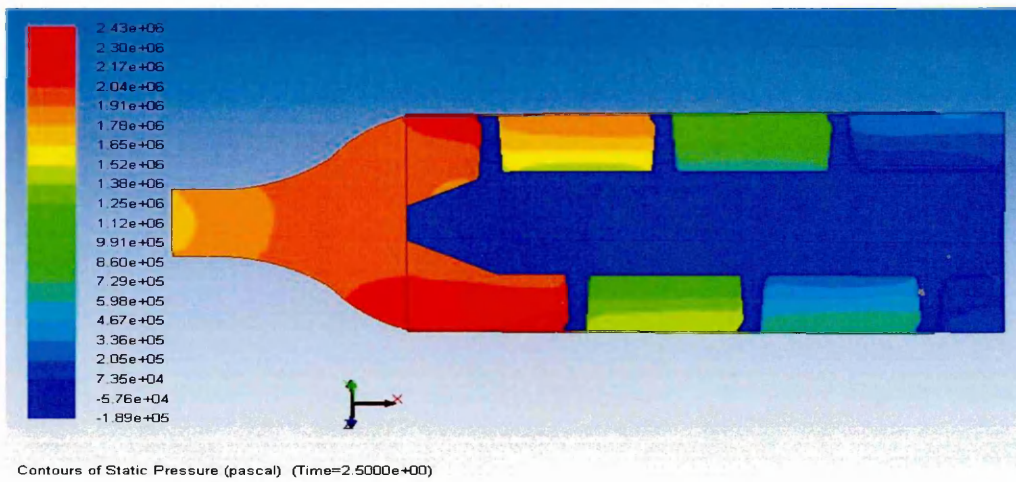
Figure A-A-14 Static pressure contour (sectional view)-500 mm Case II
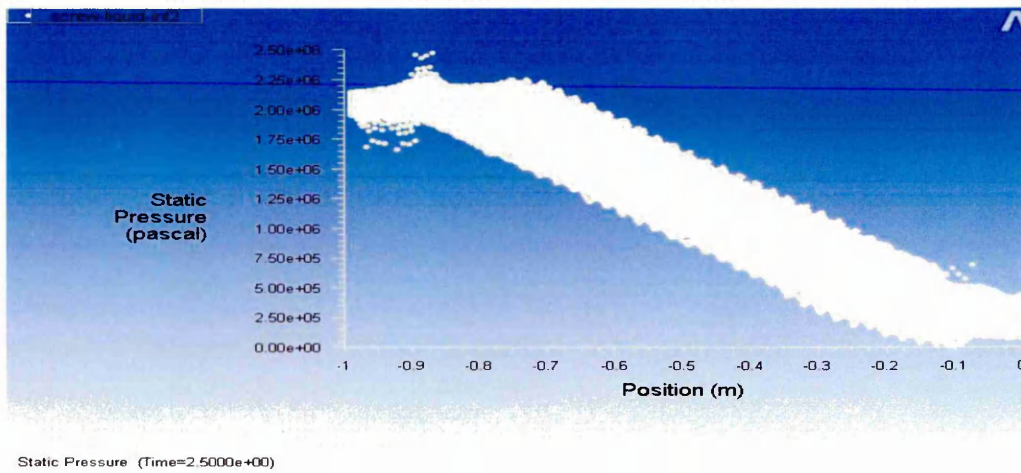
Figure A-A-15 Static pressure profile -500 mm Case II

Material flow pattern:
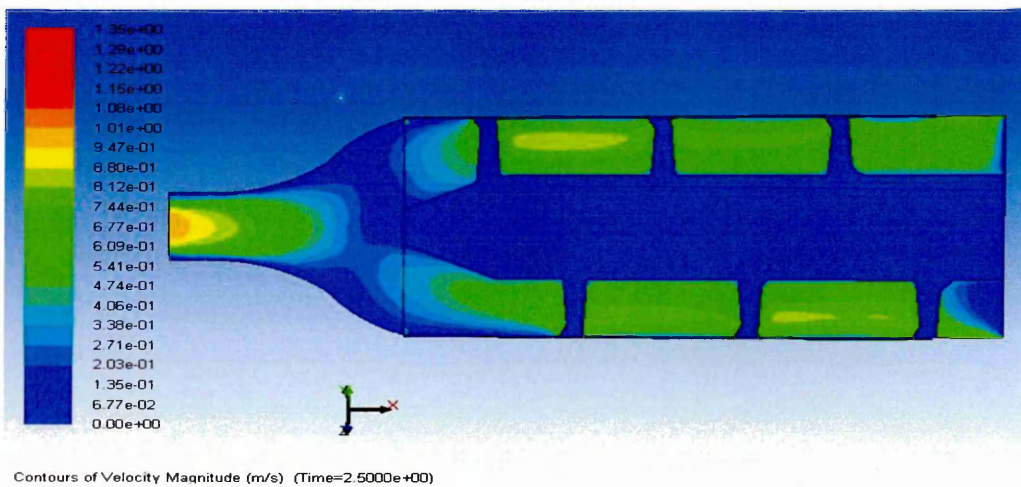
Figure A-A-16 Flow velocity during extrusion (sectional view)-500 mm Case
II

Viscosity profile:
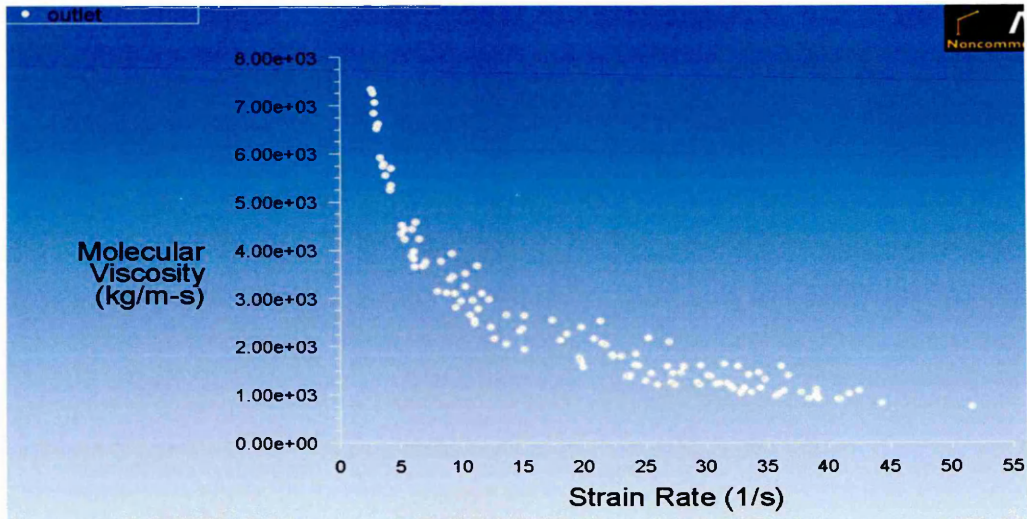
Molecular Viscosity vs. Strain Rate (Time=2.5000e+00)   Apr

Figure A-A-17 Molecular viscosity vs. Strain rate-500 mm Case II
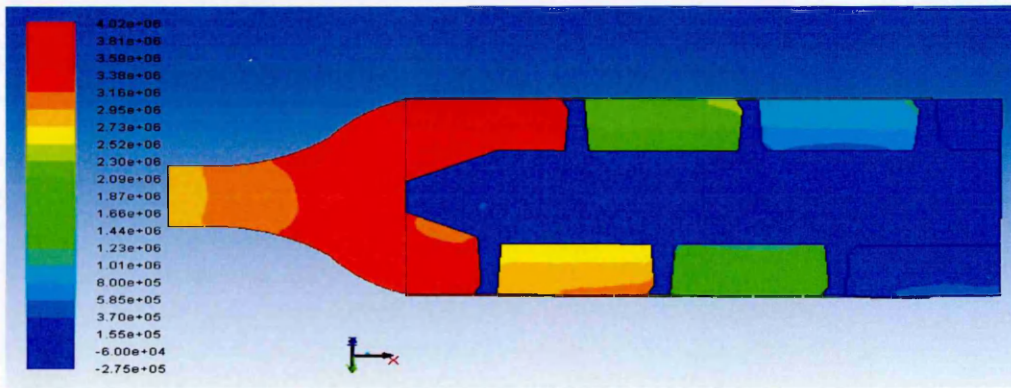
V.   CFD Simulation results of 600 mm extruder with Herschel-Bulkley's model value-II:
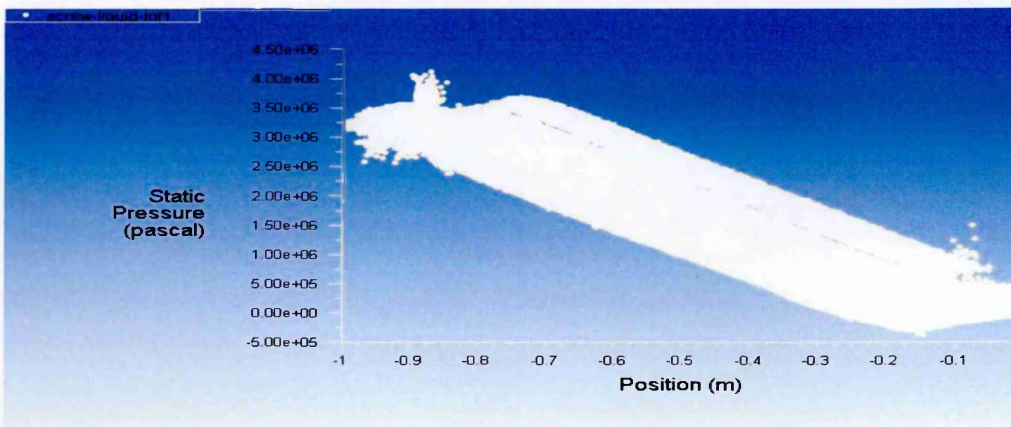
Extrusion pressure:
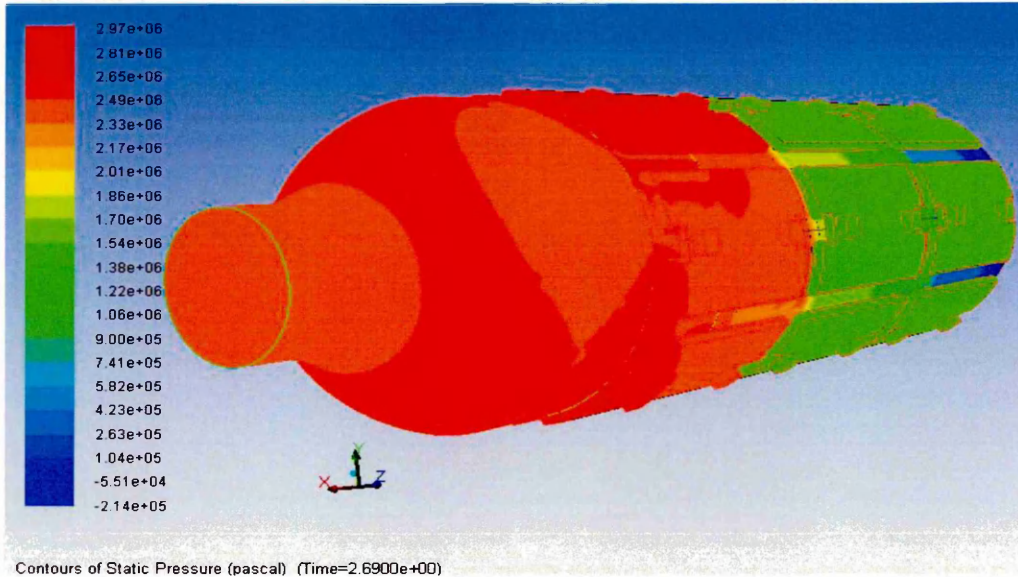
Contours of Static Pressure (pascal) (Time=2.6900e+00)

Figure A-A-18 Static pressure contour (full view)-600 mm Case II

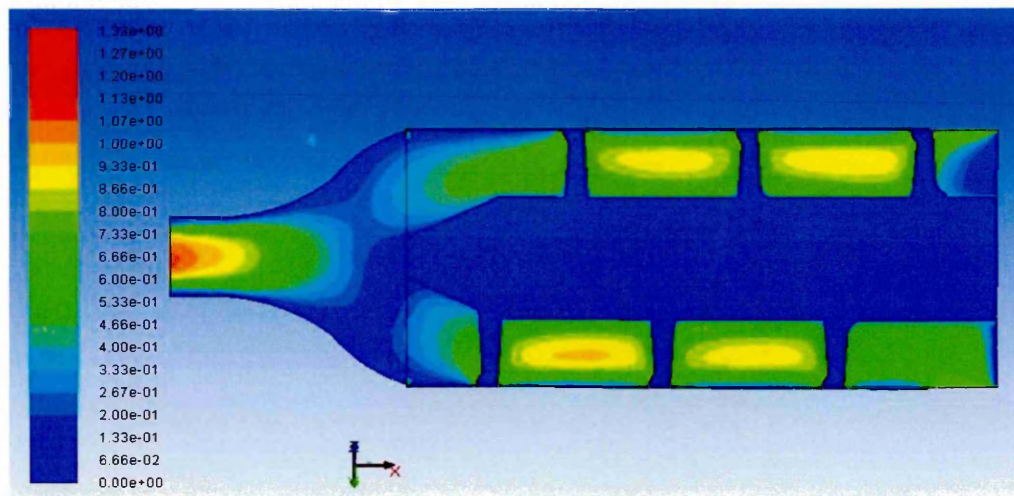Contours of Static Pressure (pascal) (Time=2.6900e+00)
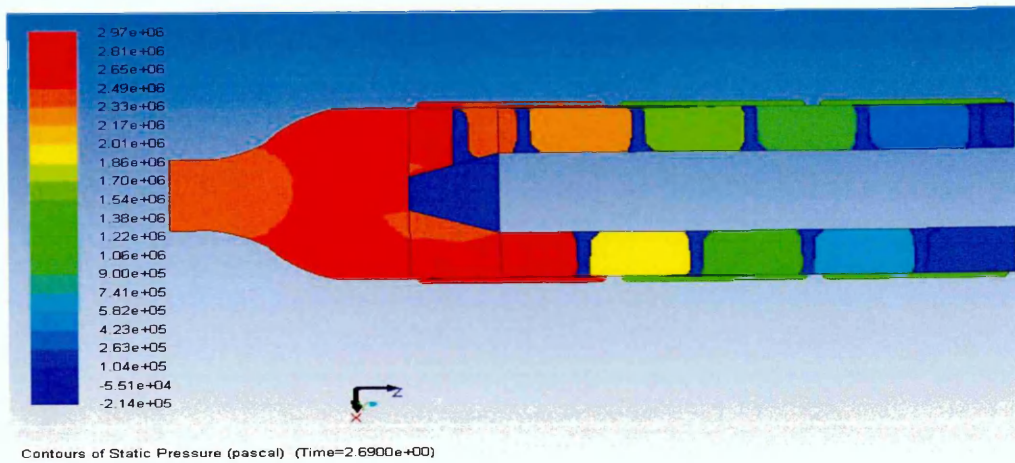
Figure A-A-19 Static pressure contour (sectional view)-600 mm Case II

Static Pressure (Time=2.6900e+00)
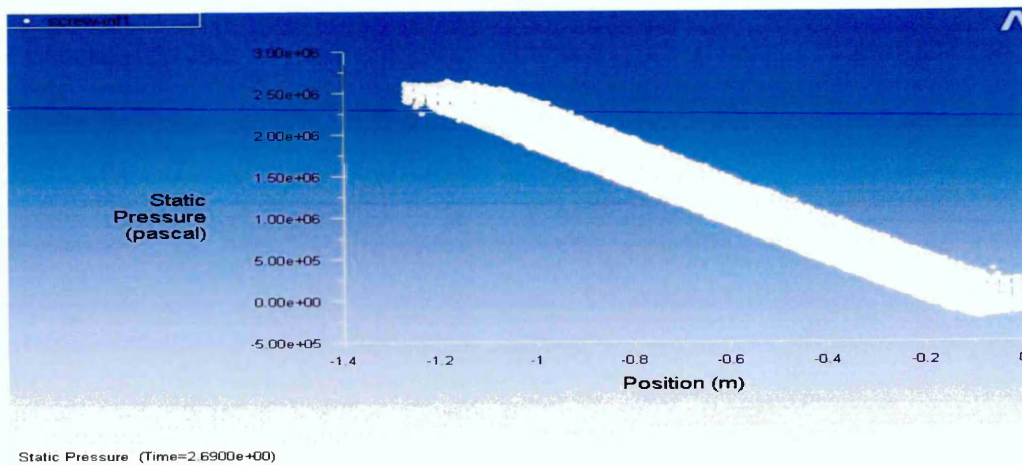
Figure A-A-20 Static pressure profile -600 mm Case II

Material flow pattern:

Contours of Velocity Magnitude (m/s) (Time=2.6900e+00)
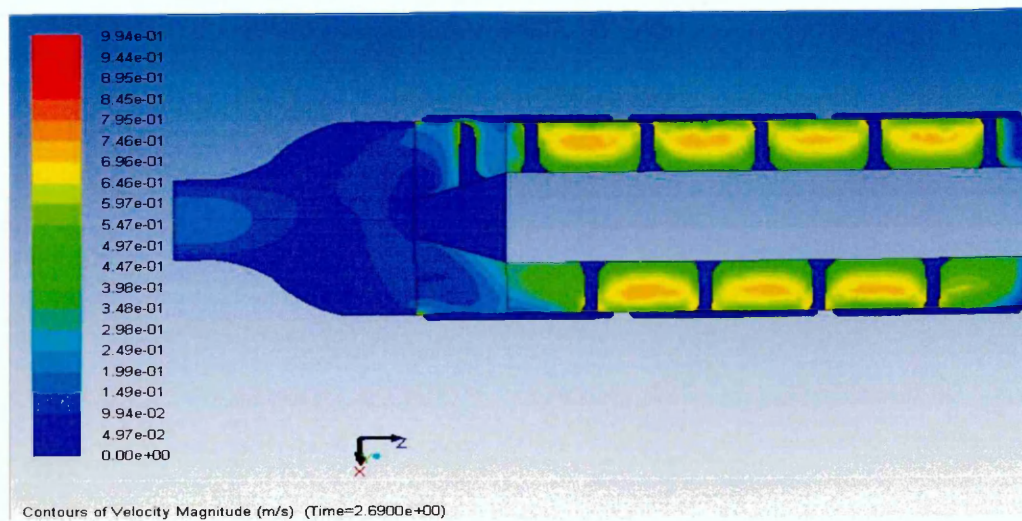
Figure A-A-21 Flow velocity during extrusion (sectional view)-600 mm Case II

138

Figure A-A-22 Molecular viscosity vs. Strain rate-600 mm Case II

VI. CFD Simulation results of 500 mm extruder with varying feed rate:-

a. Feed rate:-15 kgs⁻¹

Extrusion pressure:
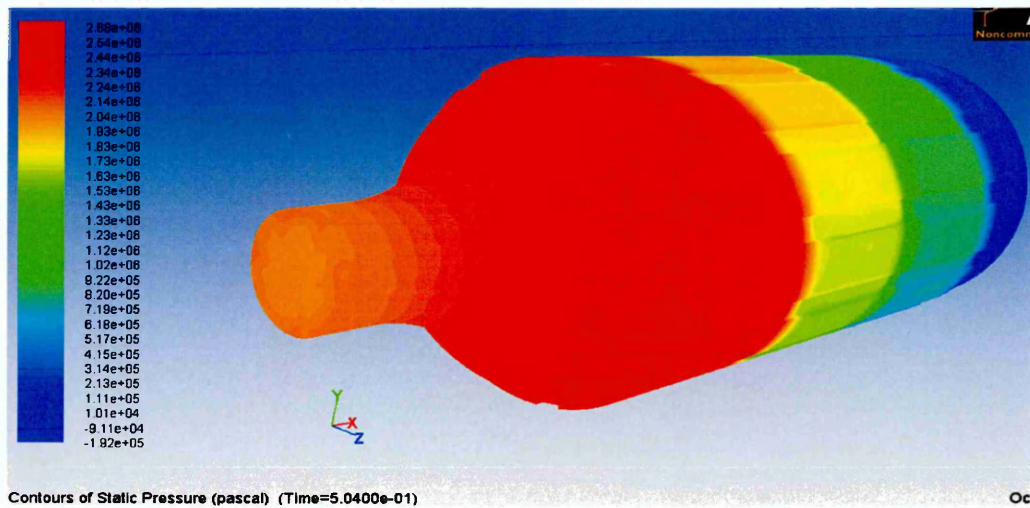
Figure A-A-23 Static pressure contour (full view) - feed rate 15 kgs⁻¹

Contours of Static Pressure (pascal) (Time=5.0400e-01)   Oct 11, 201
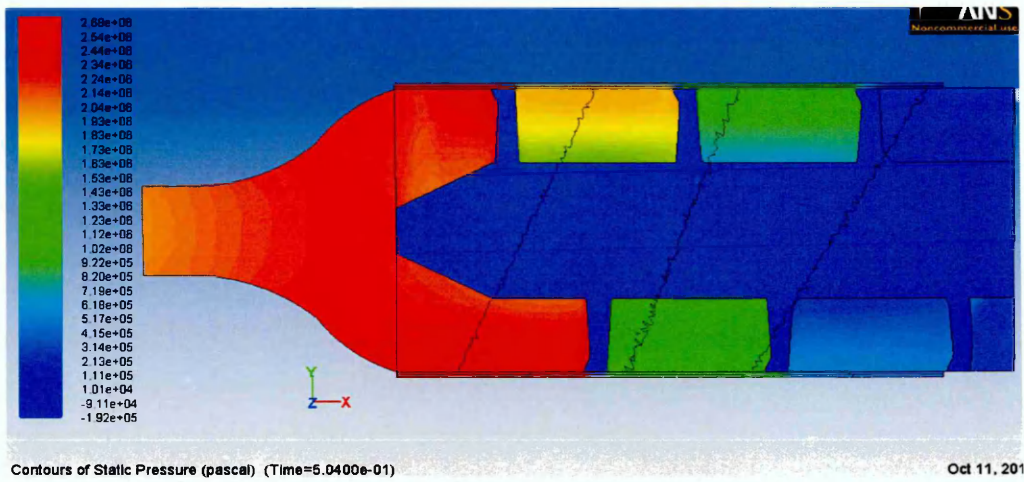
Figure A-A-24 Static pressure contour (sectional view) - feed rate 15 kgs^{-1}

Static Pressure (Time=5.0400e-01)
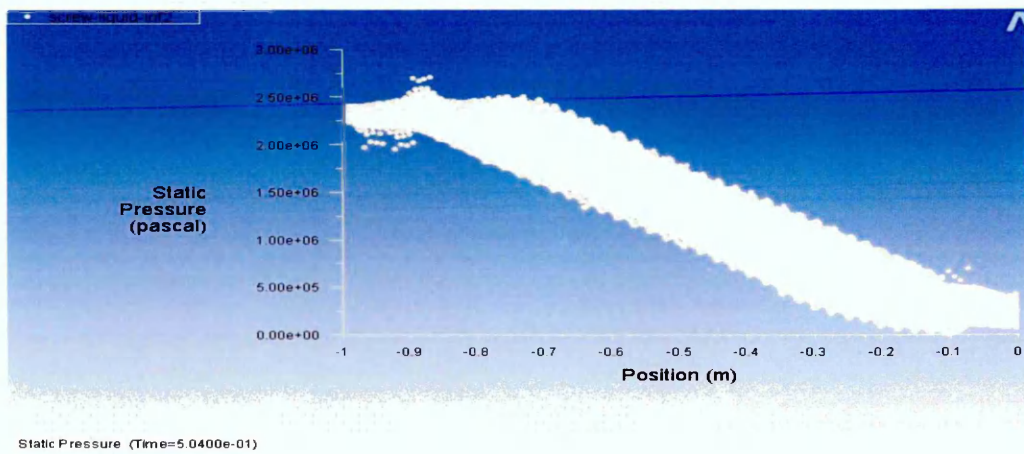
Figure A-A-25 Static pressure profile- feed rate 15 kgs^{-1}

<u>Material flow pattern:</u>

Contours of Velocity Magnitude (m/s) (Time=5.0400e-01)   Oct 11, 201
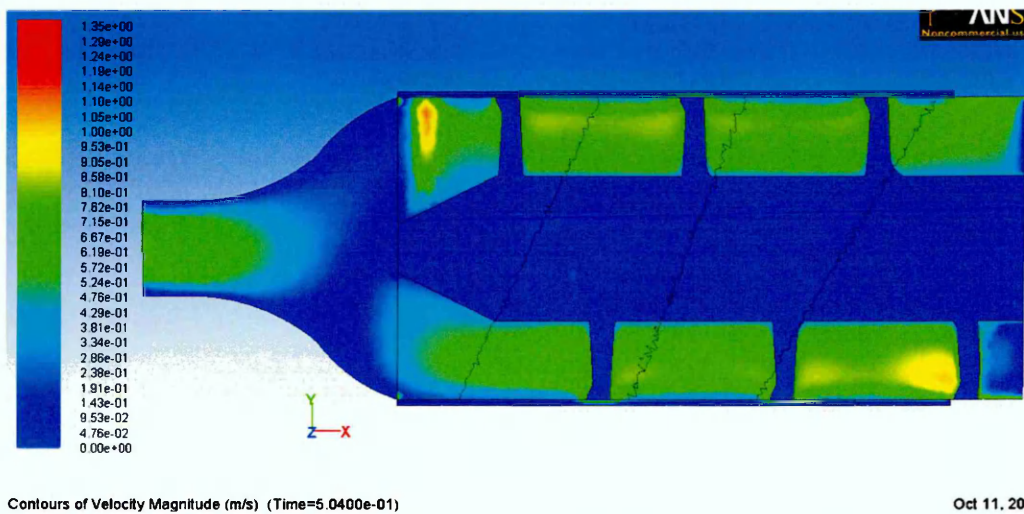
Figure A-A-26 Flow velocity during extrusion(sectional view)-feed rate 15 kgs^{-1}

140

Viscosity profile:
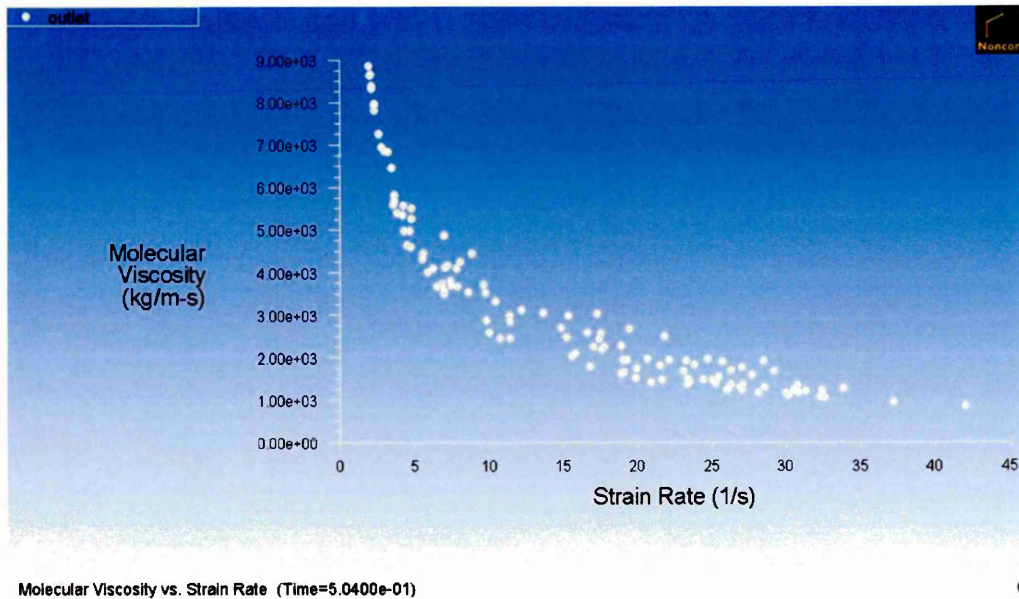
Figure A-A-27 Molecular viscosity vs. Strain rate- feed rate15 kgs⁻¹

- Results of CFD analysis for feed rate of 19 kgs⁻¹ are available in Appendix A under Section IV.

a. *Feed rate:-25 kgs⁻¹*

Extrusion pressure:

Contours of Static Pressure (pascal) (Time=4.2400e-01)

Figure A-A-28 Static pressure contour (full view) - feed rate 25 kgs⁻¹

Figure A-A-29 Static pressure contour (sectional view) - feed rate 25 kgs^{-1}

Figure A-A-30 Static pressure profile- feed rate 25 kgs^{-1}

<u>Material flow pattern:</u>
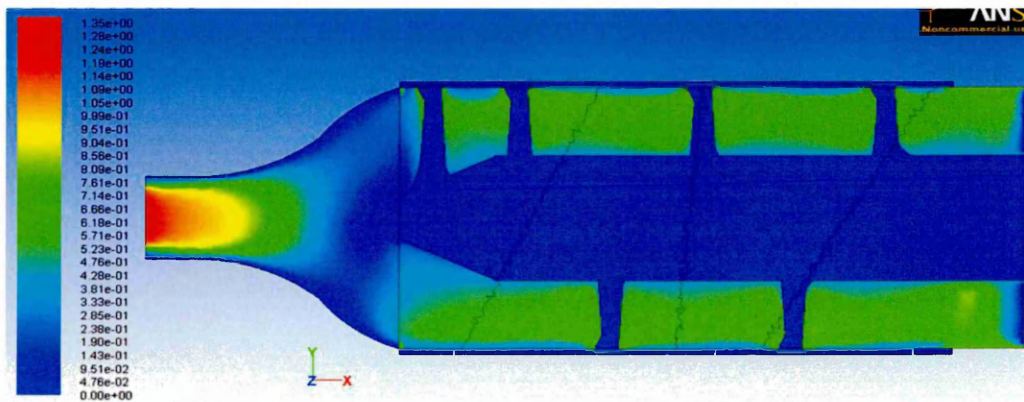
Figure A-A-31 Flow velocity during extrusion(sectional view)-feed rate 25 kgs^{-1}

Molecular Viscosity vs. Strain Rate (Time=4.2400e-01)   C
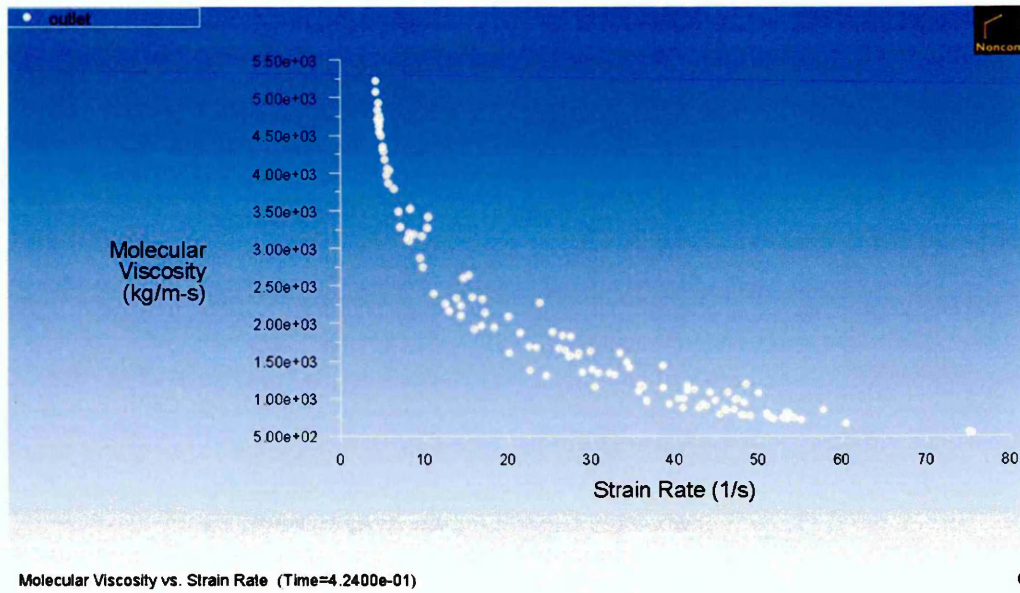
Figure A-A-32 Molecular viscosity vs. Strain rate- feed rate 25 kgs^{-1}

b. **Feed rate:-30 Kgs^{-1}**

Extrusion pressure:

Contours of Static Pressure (pascal) (Time=5.0400e-01)   Oct 17,
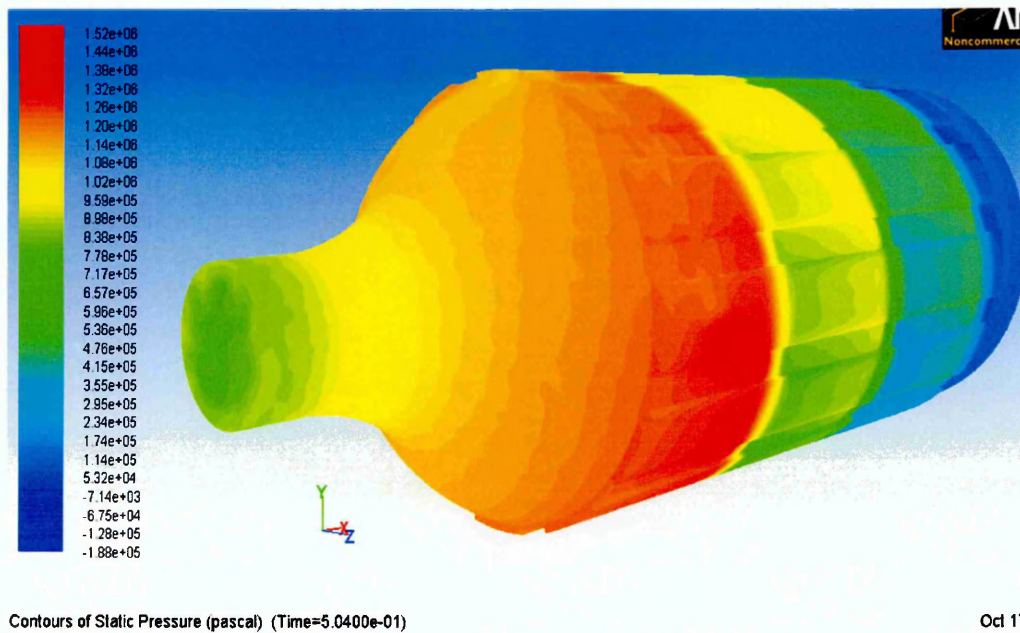
Figure A-A-33 Static pressure contour (full view) - feed rate 30 kgs^{-1}
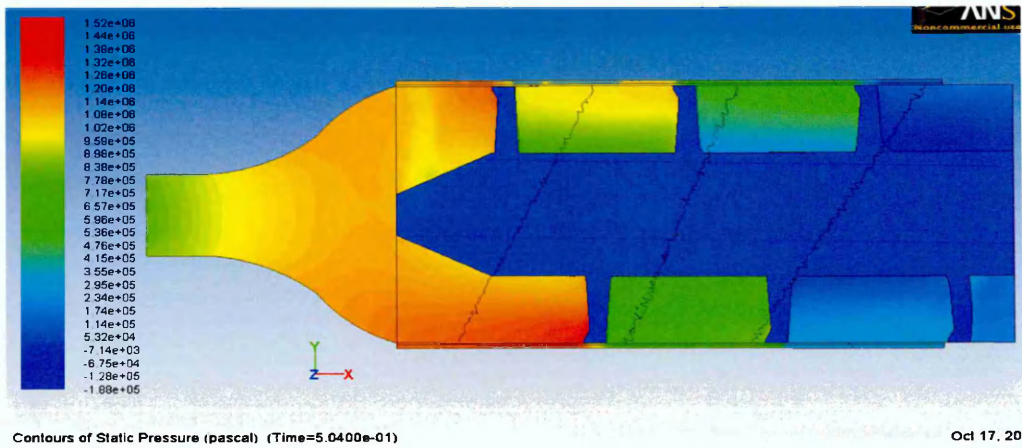
Figure A-A-34 Static pressure contour (sectional view) - feed rate 30 kgs^{-1}
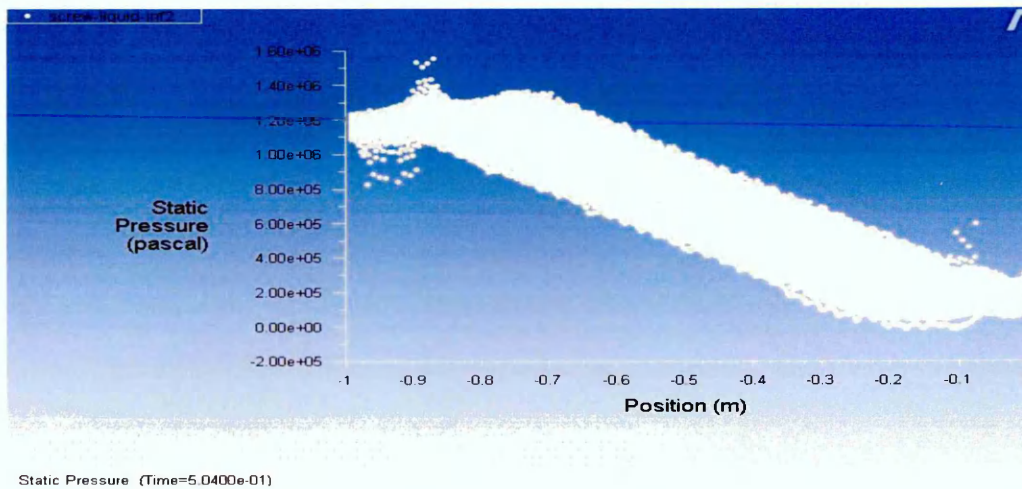
Figure A-A-35 Static pressure profile- feed rate 30 kgs^{-1}

Material flow pattern:
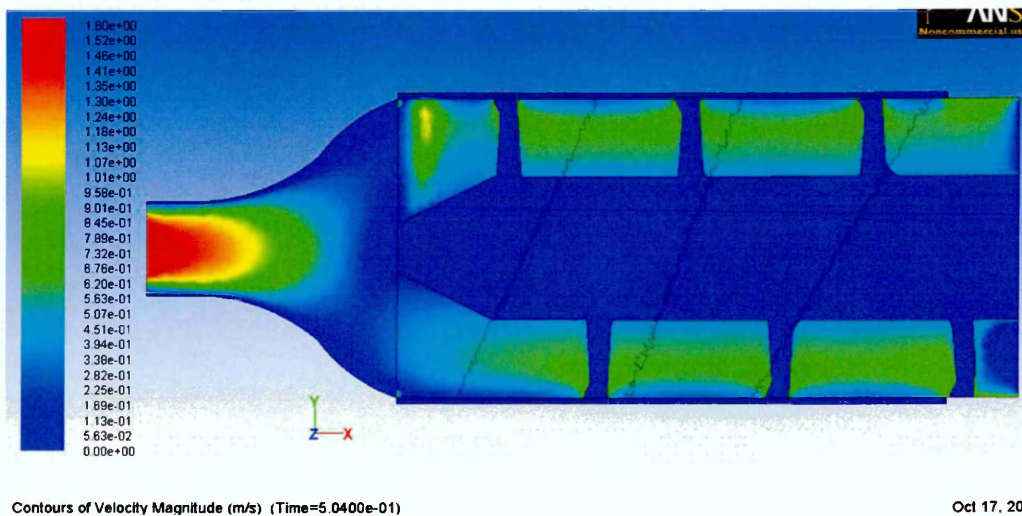
Figure A-A-36 Flow velocity during extrusion(sectional view)-feed rate 30 kgs^{-1}

144
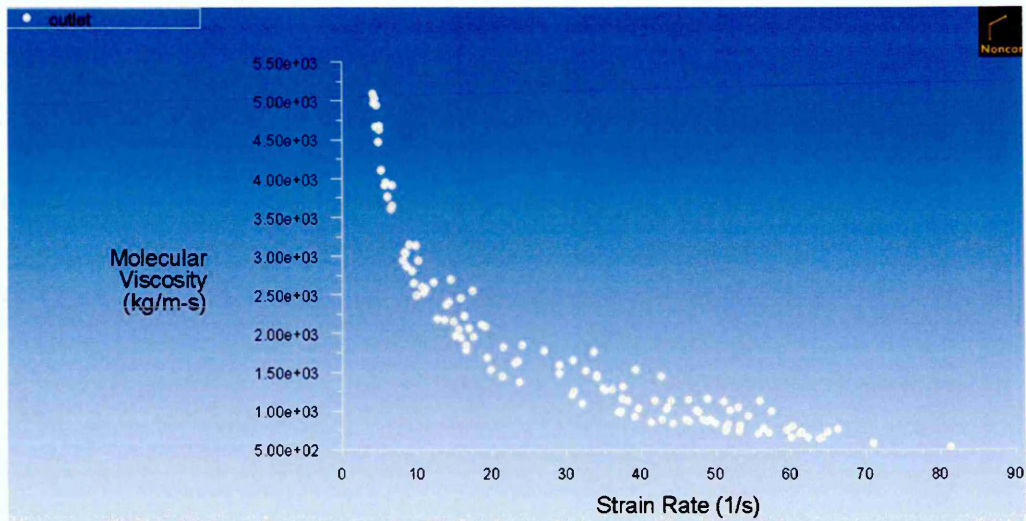
Molecular Viscosity vs. Strain Rate (Time=5.0400e-01)

Figure A-A-37 Molecular viscosity vs. Strain rate- feed rate 30 kgs^{-1}

c.   *Feed rate:-40 Kgs^{-1}*

Extrusion pressure:
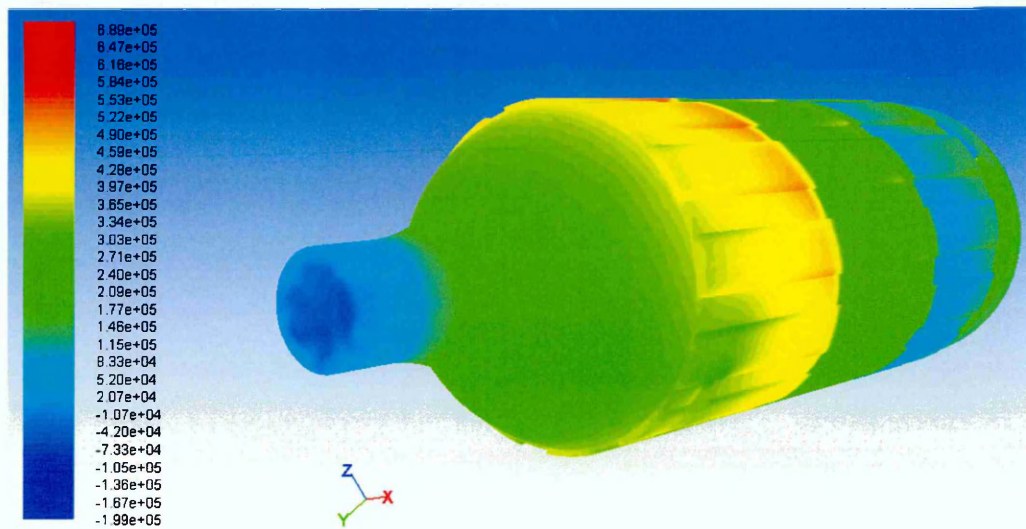
Contours of Static Pressure (pascal) (Time=5.0400e-01)

Figure A-A-38 Static pressure contour (full view) - feed rate 40 kgs^{-1}

Contours of Static Pressure (pascal) (Time=5.0400e-01)

Oct 17, 2011

Figure A-A-39 Static pressure contour (sectional view) - feed rate 40 kgs^{-1}

Static Pressure (Time=5.0400e-01)
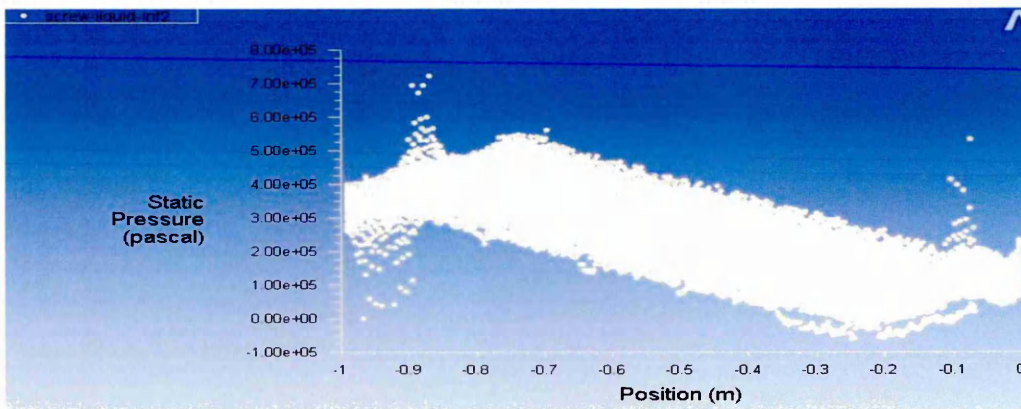
Figure A-A-40 Static pressure profile- feed rate 40 kgs^{-1}

Material flow pattern:

Contours of Velocity Magnitude (m/s) (Time=5.0400e-01)
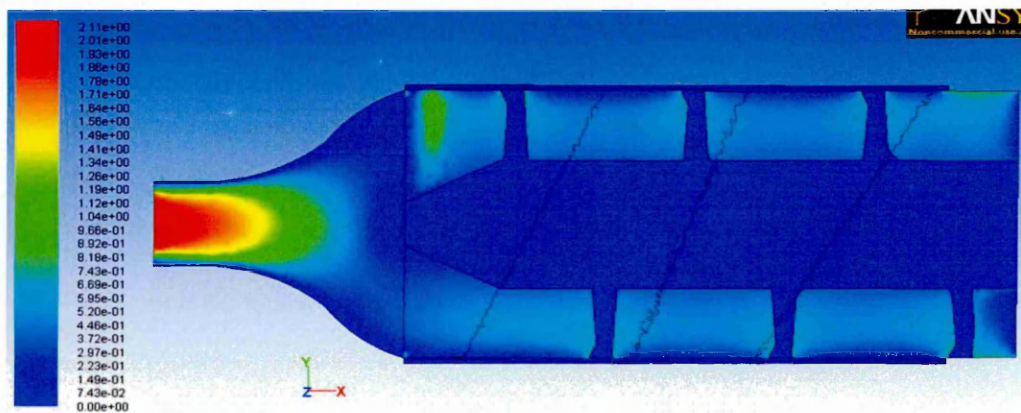
Oct 17, 2011

Figure A-A-41 Flow velocity during extrusion (sectional view)-feed rate 40 kgs^{-1}

146

Molecular Viscosity vs. Strain Rate (Time=5.0400e-01)
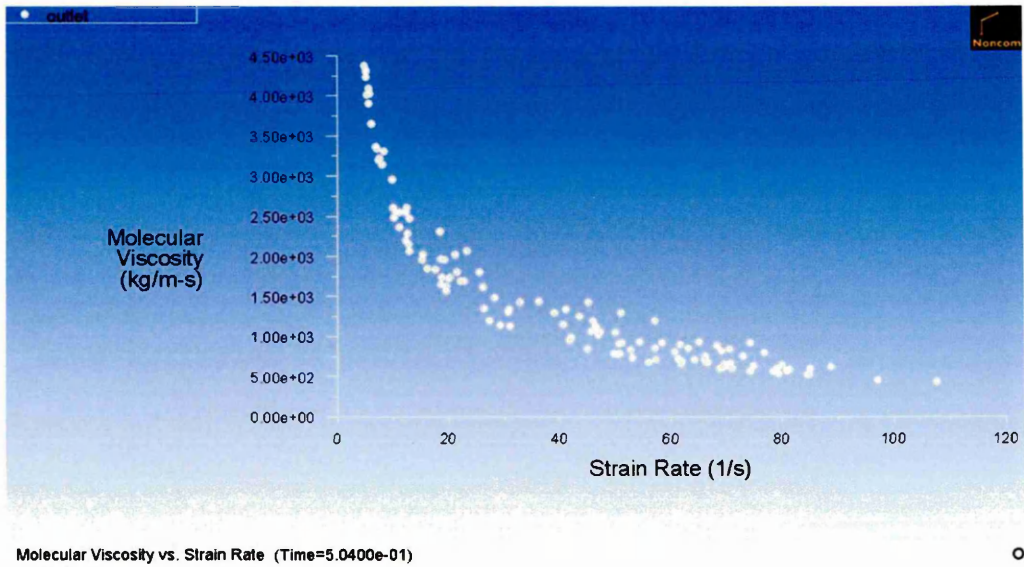
Figure A-A-42 Molecular viscosity vs. Strain rate- feed rate 40 kgs^{-1}

d. *Feed rate:-50 Kgs^{-1}*

Extrusion pressure:

Contours of Static Pressure (pascal) (Time=4.8400e-01)   Oct

Figure A-A-43 Static pressure contour (full view) - feed rate 50 kgs^{-1}

Contours of Static Pressure (pascal) (Time=4.8400e-01)   Oct 18, 2011
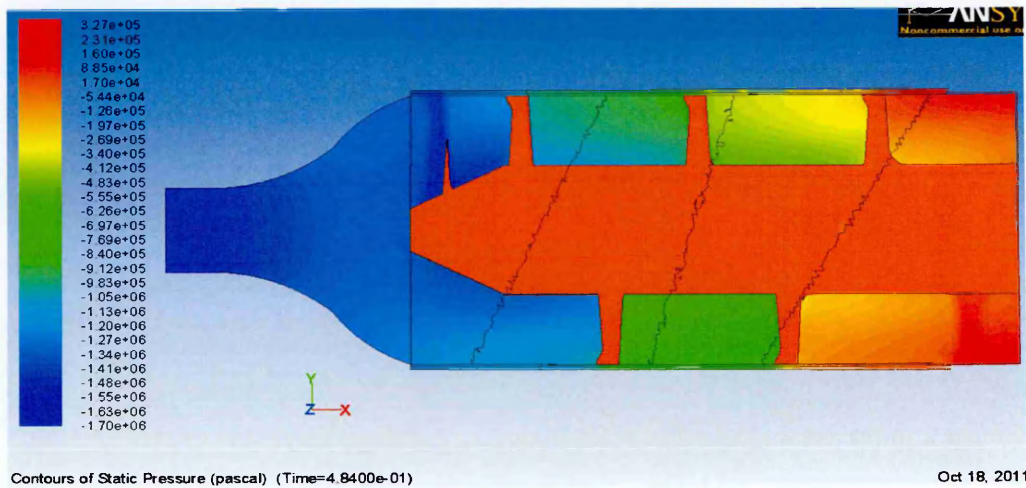
Figure A-A-44 Static pressure contour (sectional view) - feed rate 50 kgs^{-1}

Static Pressure (Time=4.8400e-01)
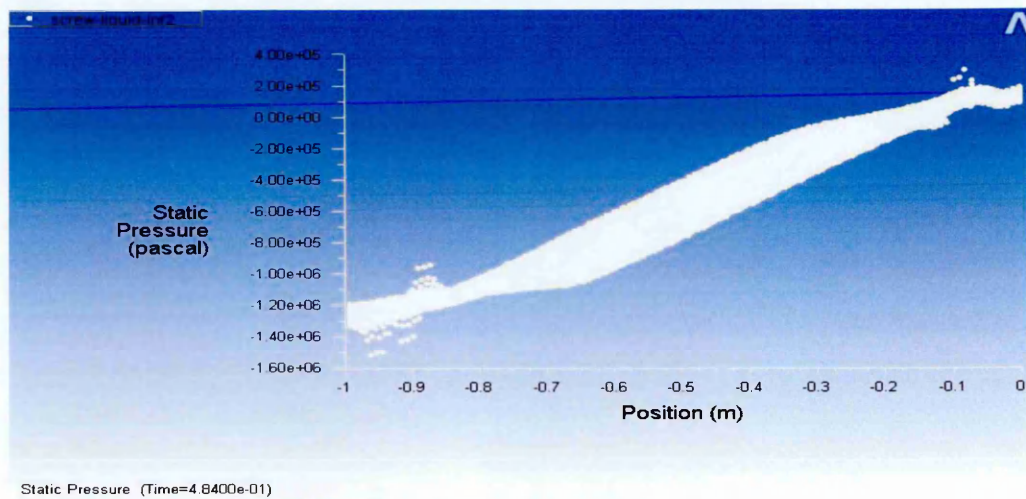
Figure A-A-45 Static pressure profile- feed rate 50 kgs^{-1}

Material flow pattern:

Contours of Velocity Magnitude (m/s) (Time=4.8400e-01)   Oct 18, 201

Figure A-A-46 Flow velocity during extrusion (sectional view)-feed rate 50 kgs^{-1}

148

Viscosity profile:

Molecular Viscosity vs. Strain Rate (Time=4.8400e-01)
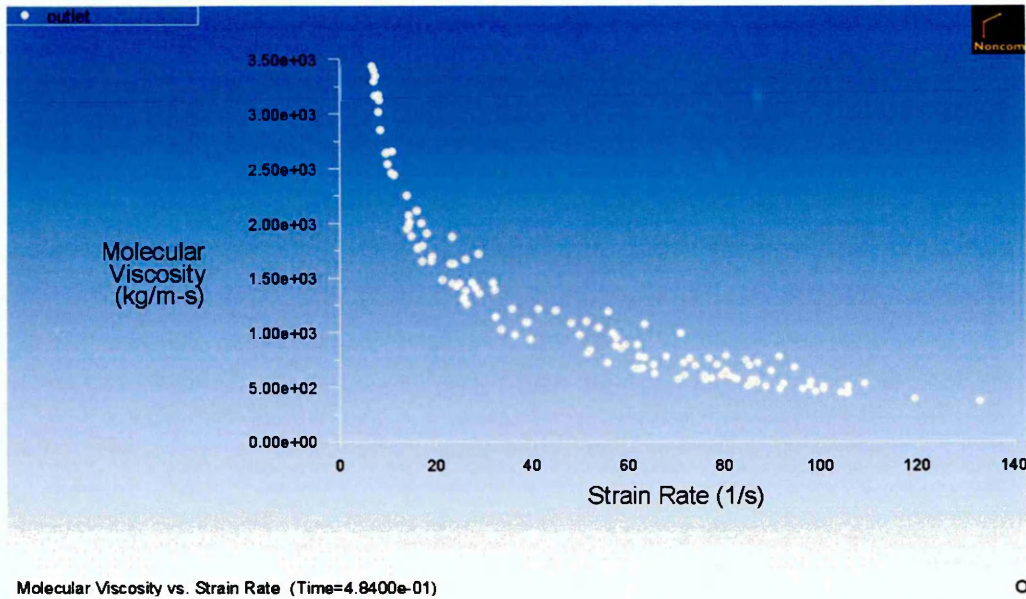
Figure A-A-47 Molecular viscosity vs. Strain rate- feed rate 50 kgs^{-1}

VII. **CFD Simulation results of 500 mm extruder with varying auger speed:-**

a. **_Auger speed:-15 rpm_**

Extrusion pressure:

Contours of Static Pressure (pascal) (Time=3.2460e+00)   Sep 29
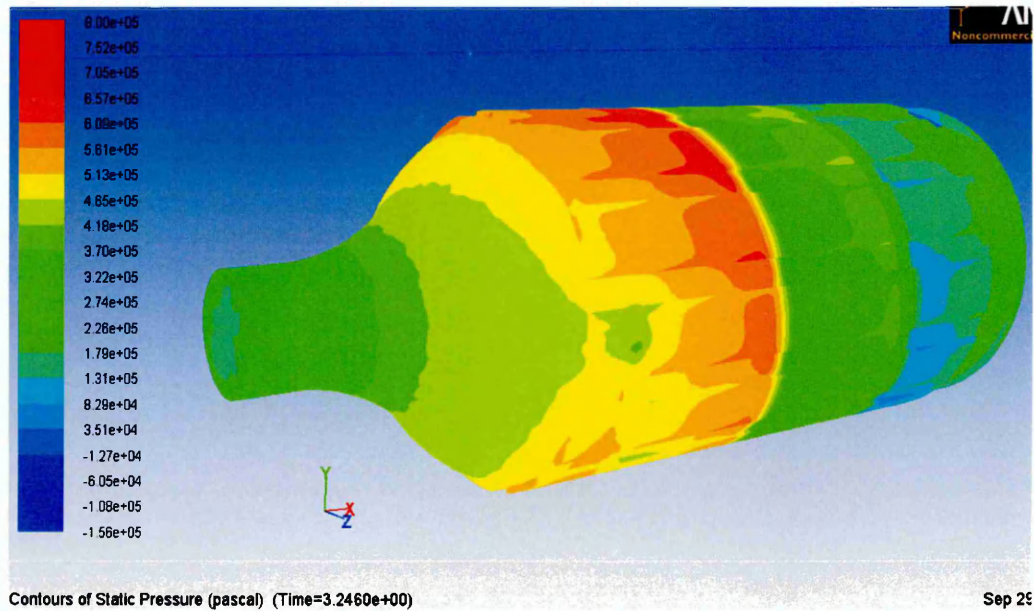
Figure A-A-48 Static pressure contour (full view) - auger speed 15 rpm

Contours of Static Pressure (pascal) (Time=3.2460e+00)   Sep 29, 2011
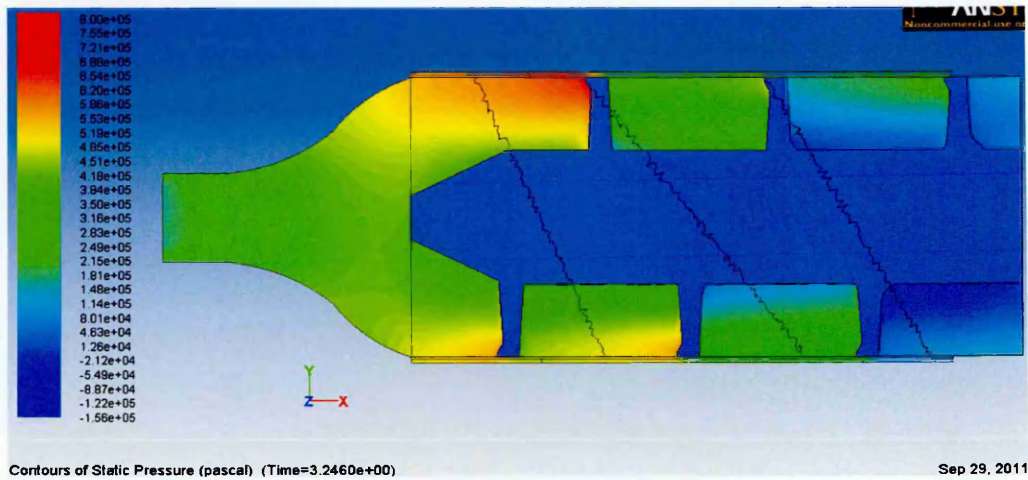
Figure A-A-49 Static pressure contour (sectional view) - auger speed 15 rpm

Static Pressure (Time=3.2460e+00)
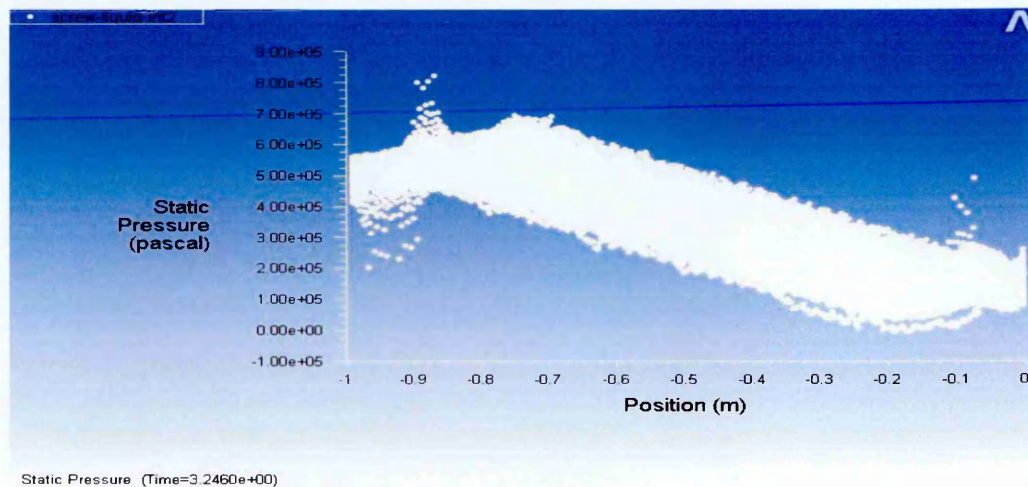
Figure A-A-50 Static pressure profile- auger speed 15 rpm

Material flow pattern:

Contours of Velocity Magnitude (m/s) (Time=3.2460e+00)   Sep 29, 2011
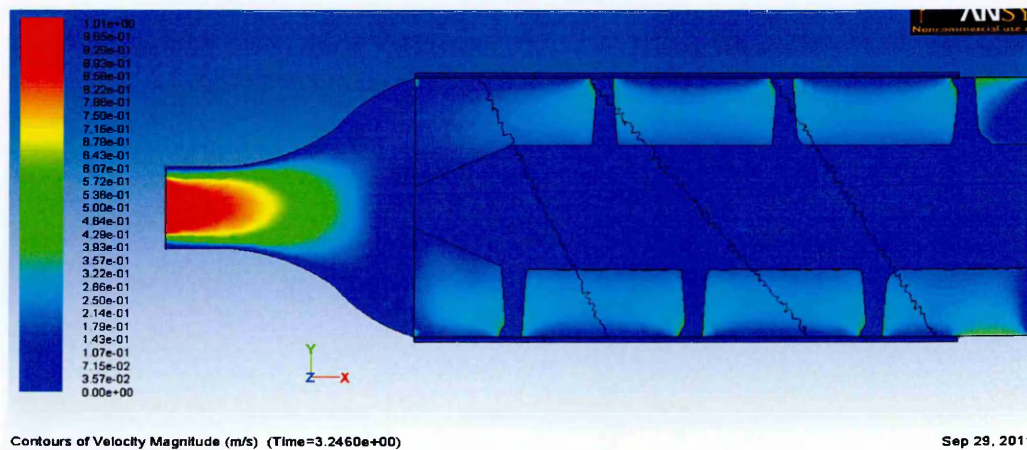
Figure A-A-51 Flow velocity during extrusion(sectional view)-auger speed 15 rpm

150
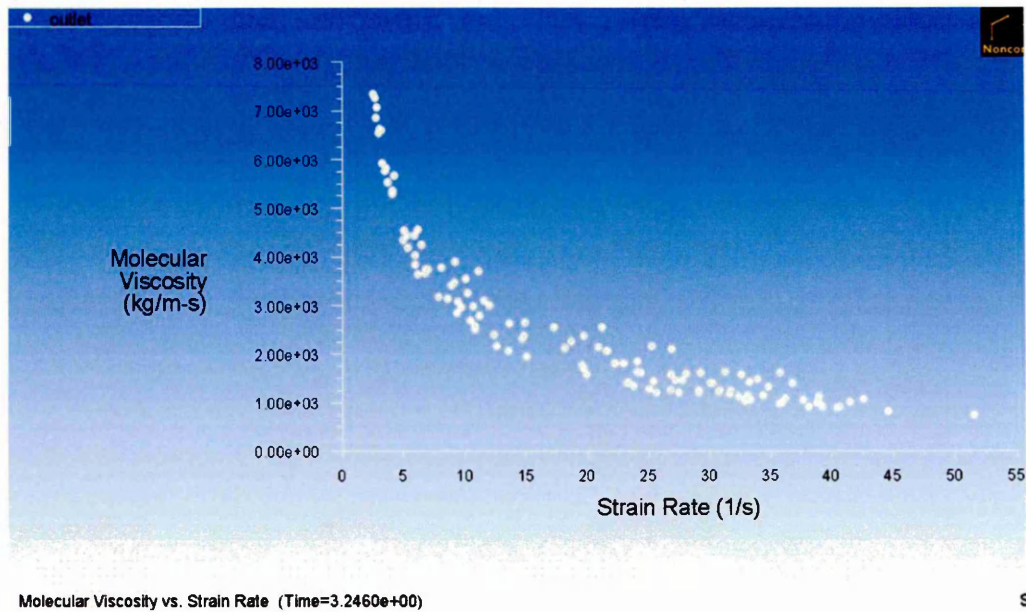
Figure A-A-52 Molecular viscosity vs. Strain rate - auger speed 15 rpm

b. **Auger speed:-20 rpm**

Extrusion pressure:
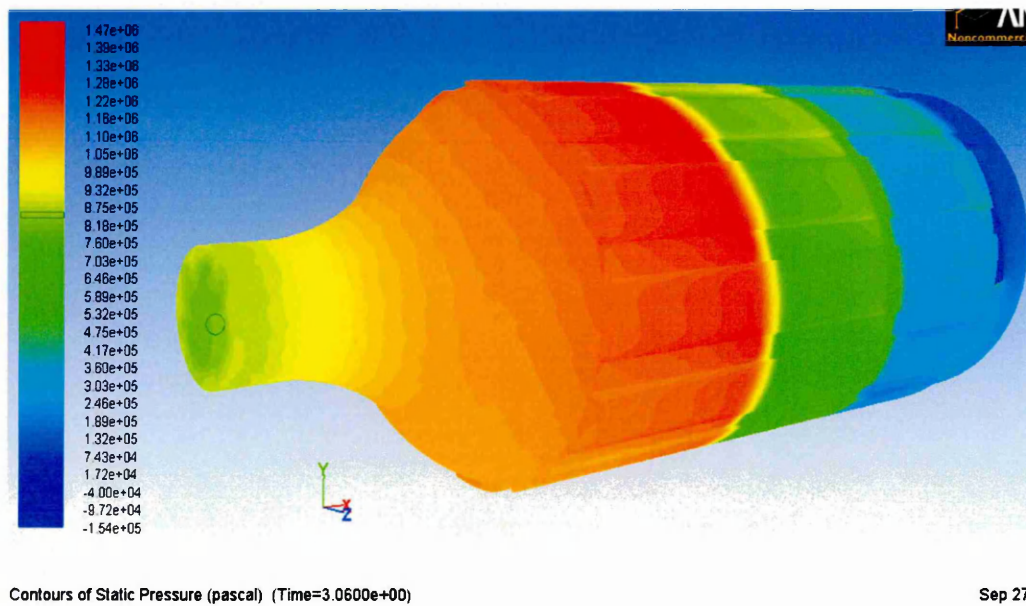
Figure A-A-53 Static pressure contour (full view) - auger speed 20 rpm

151
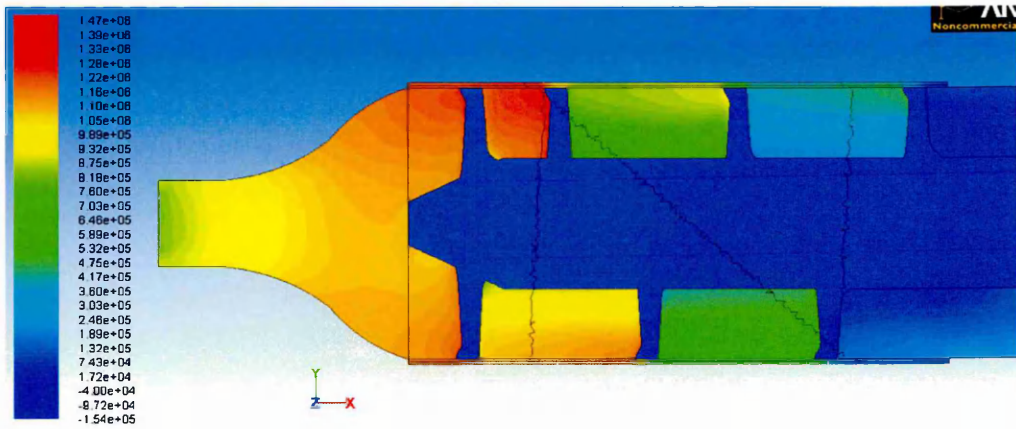
Contours of Static Pressure (pascal) (Time=3.0600e+00)   Sep 27.

Figure A-A-54 Static pressure contour (sectional view) - auger speed 20 rpm
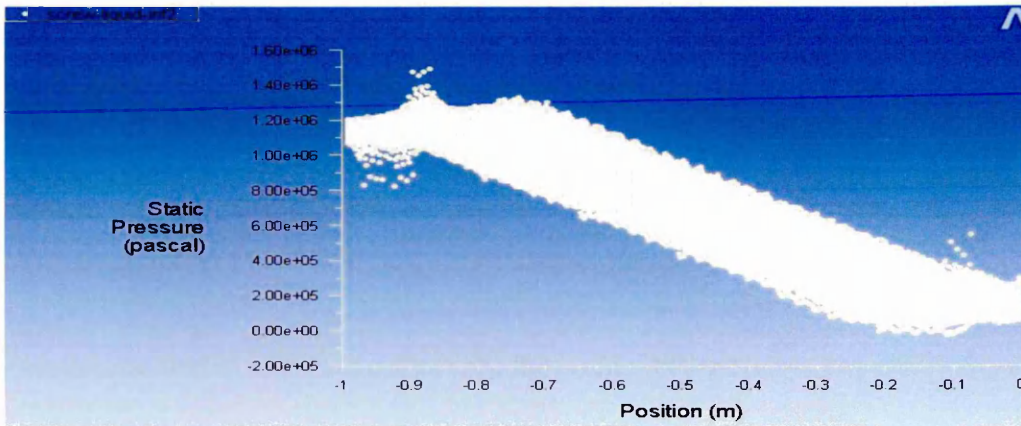
Static Pressure (Time=3.0600e+00)

Figure A-A-55 Static pressure profile- auger speed 20 rpm

<u>Material flow pattern:</u>
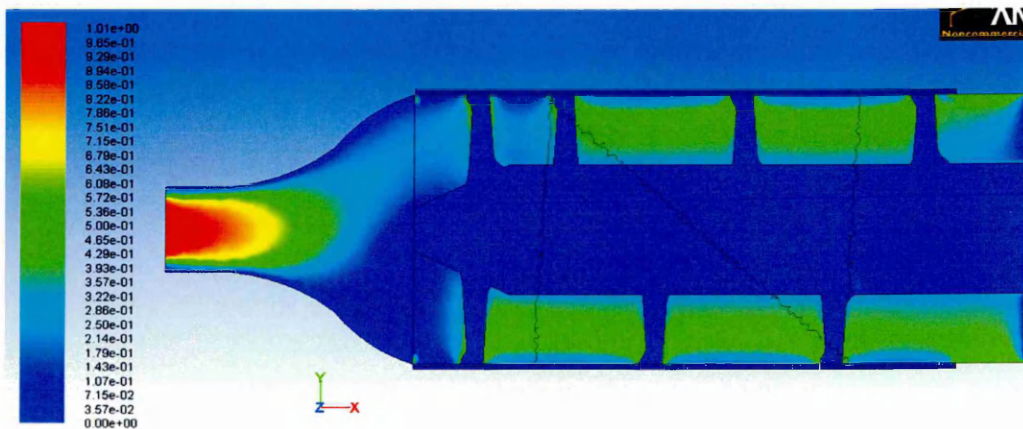
Contours of Velocity Magnitude (m/s) (Time=3.0600e+00)   Sep 27.

Figure A-A-56 Flow velocity during extrusion (sectional view)-auger speed 20 rpm
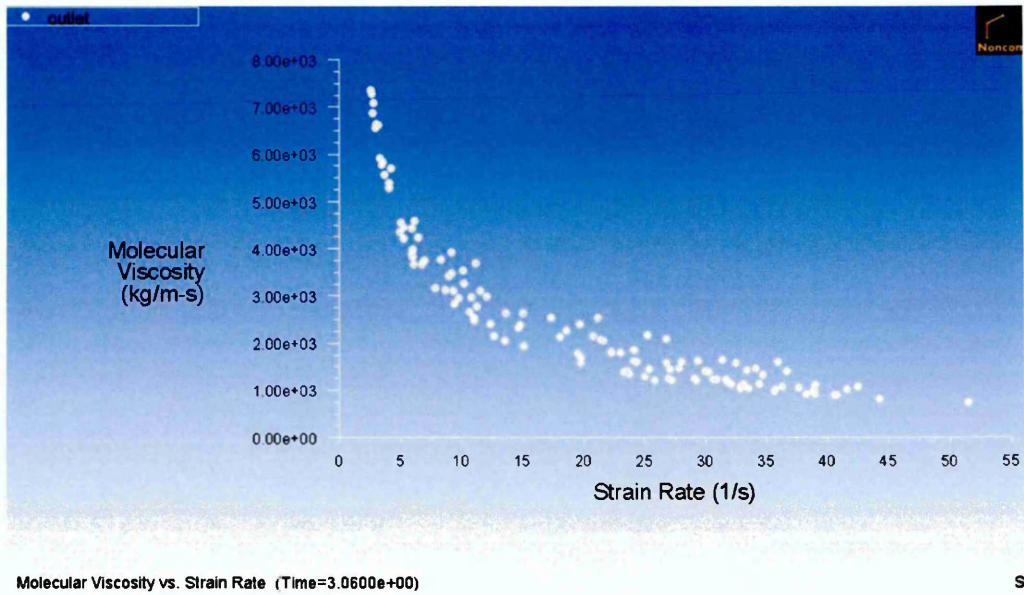
Figure A-A-57 Molecular viscosity vs. Strain rate - auger speed 20 rpm

c. **Auger speed:-25 rpm**
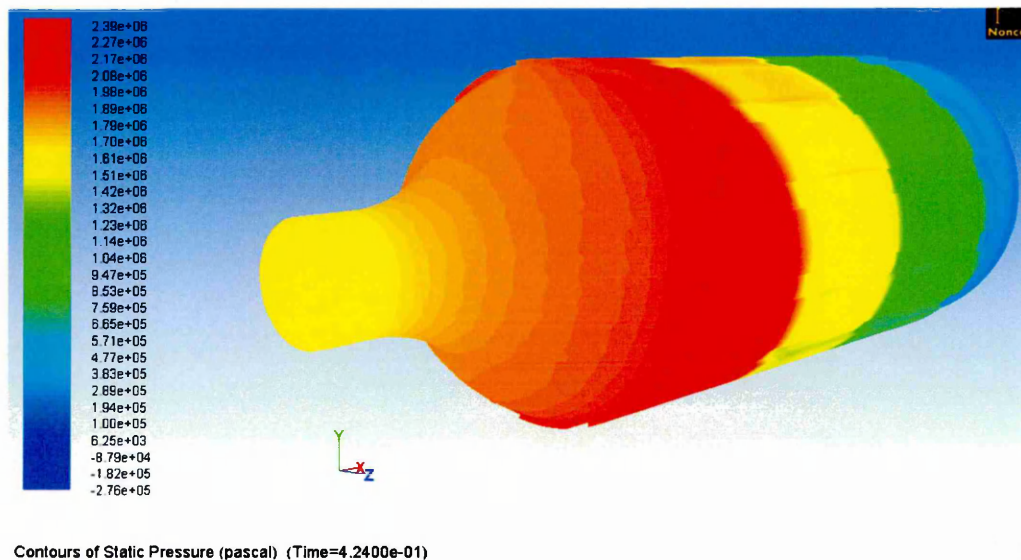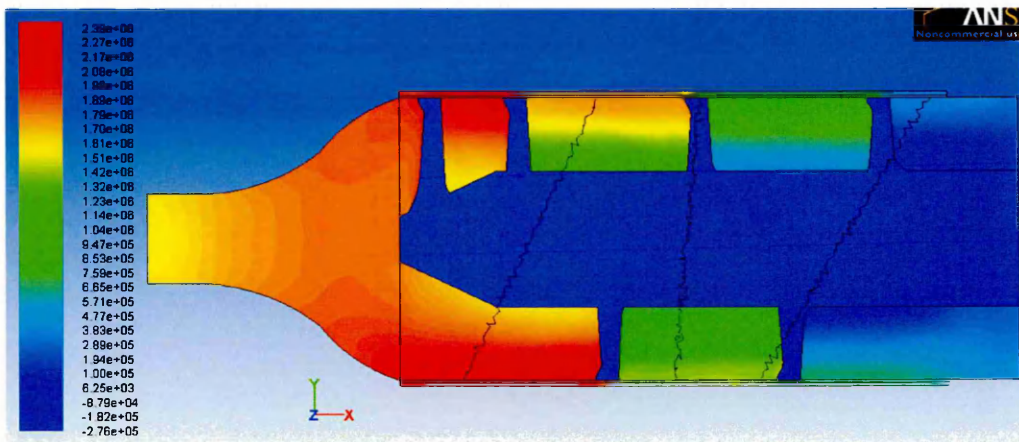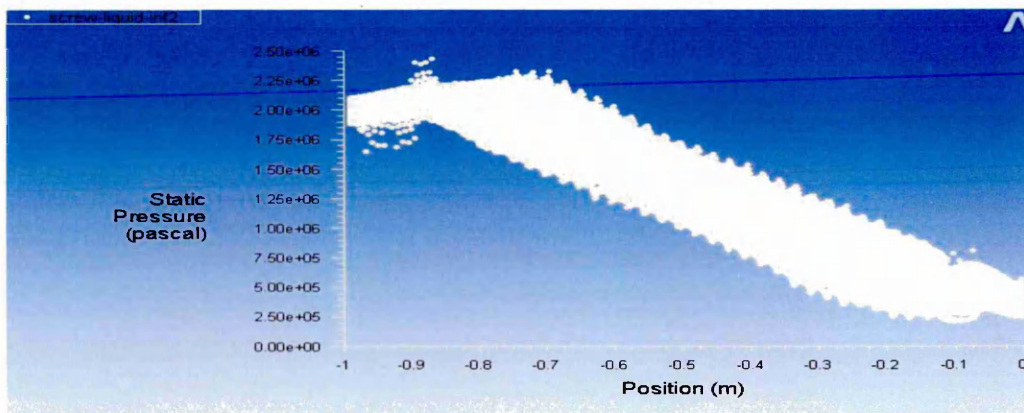
Extrusion pressure:

Figure A-A-58 Static pressure contour (full view) - auger speed 25 rpm

Contours of Static Pressure (pascal) (Time=9.6799e-01)

Oct 07, 20

*Figure A-A-59 Static pressure contour (sectional view) - auger speed 25 rpm*

Static Pressure (Time=9.6799e-01)

Figure A-A-60 Static pressure profile- auger speed 25 rpm

<u>*Material flow pattern:*</u>
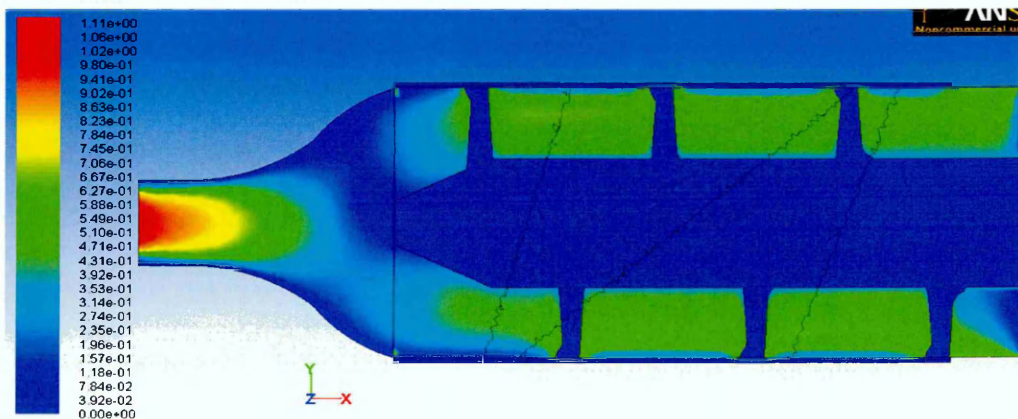
Contours of Velocity Magnitude (m/s) (Time=9.6799e-01)

Oct 07, 20

Figure A-A-61 Flow velocity during extrusion(sectional view)-auger speed 25 rpm

154

Viscosity profile:
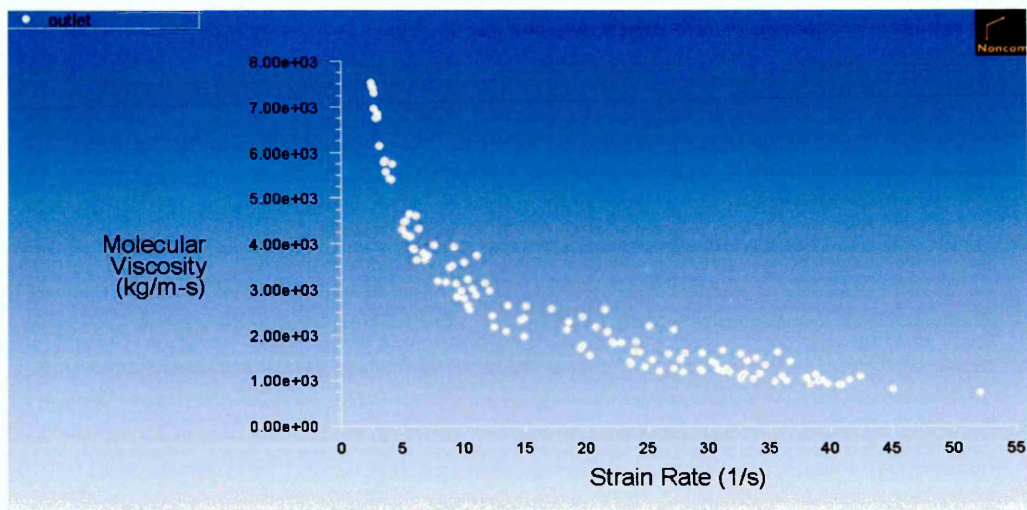
Molecular Viscosity vs. Strain Rate (Time=9.6799e-01)

Figure A-A-62 Molecular viscosity vs. Strain rate - auger speed 25 rpm

- Results of CFD analysis for auger speed of 30 rpm auger are available in Appendix A under Section IV.

d. _Auger speed:-40 rpm_

Extrusion pressure:
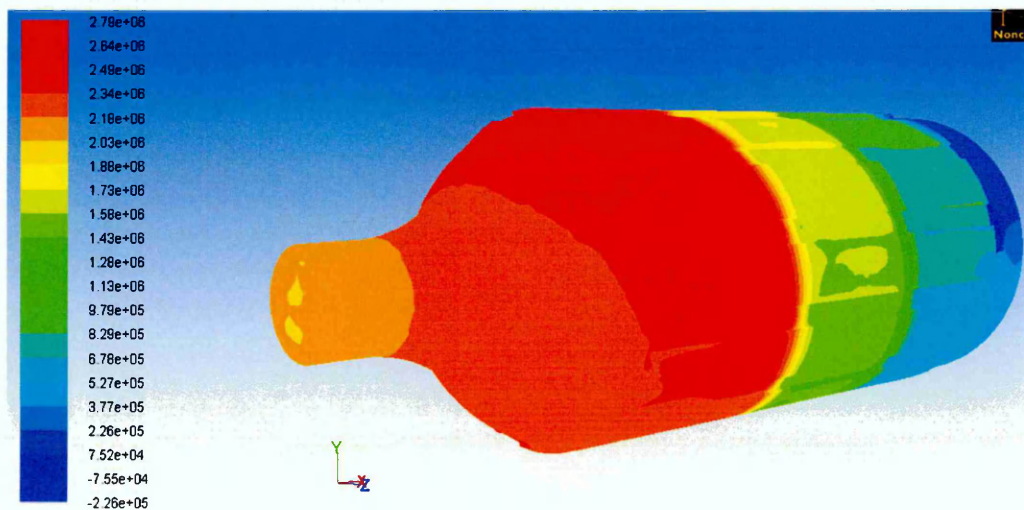
Contours of Static Pressure (pascal) (Time=1.5020e+00)

Figure A-A-63 Static pressure contour (full view) - auger speed 40 rpm

155

Contours of Static Pressure (pascal) (Time=1.5020e+00)   Oct 03, 20

Figure A-A-64 Static pressure contour (sectional view) - auger speed 40 rpm

Static Pressure (Time=1.5020e+00)

Figure A-A-65 Static pressure profile- auger speed 40 rpm

<u>Material flow pattern:</u>

Contours of Velocity Magnitude (m/s) (Time=1.5020e+00)   Oct 03, 20

Figure A-A-66 Flow velocity during extrusion(sectional view)-auger speed 40 rpm

156

Molecular Viscosity vs. Strain Rate (Time=1.5020e+00)
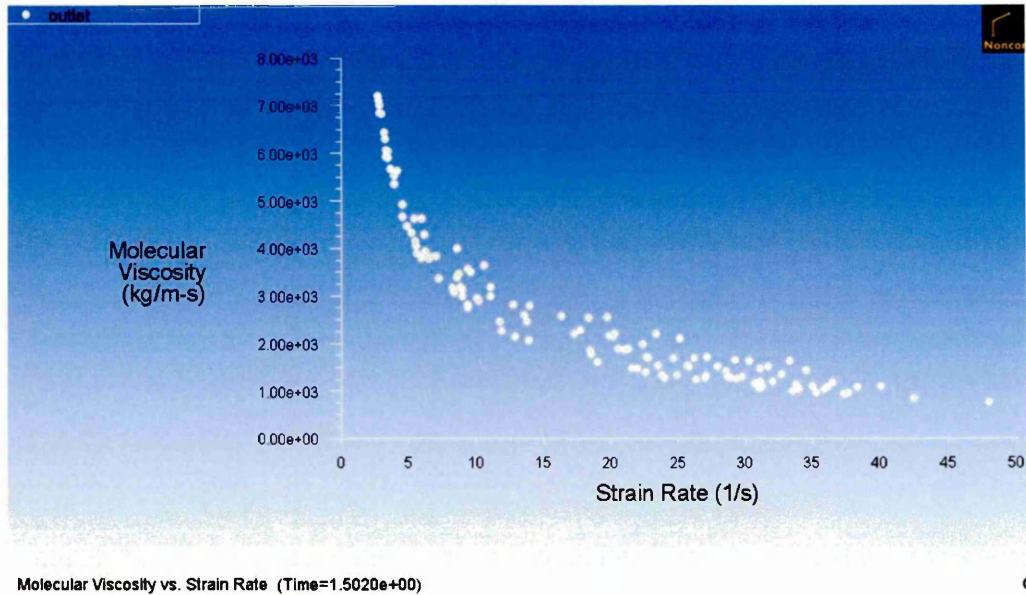
Figure A-A-67 Molecular viscosity vs. Strain rate - auger speed 40 rpm

e. Auger speed:-50 rpm

Extrusion pressure:

Contours of Static Pressure (pascal) (Time=2.6790e-01)
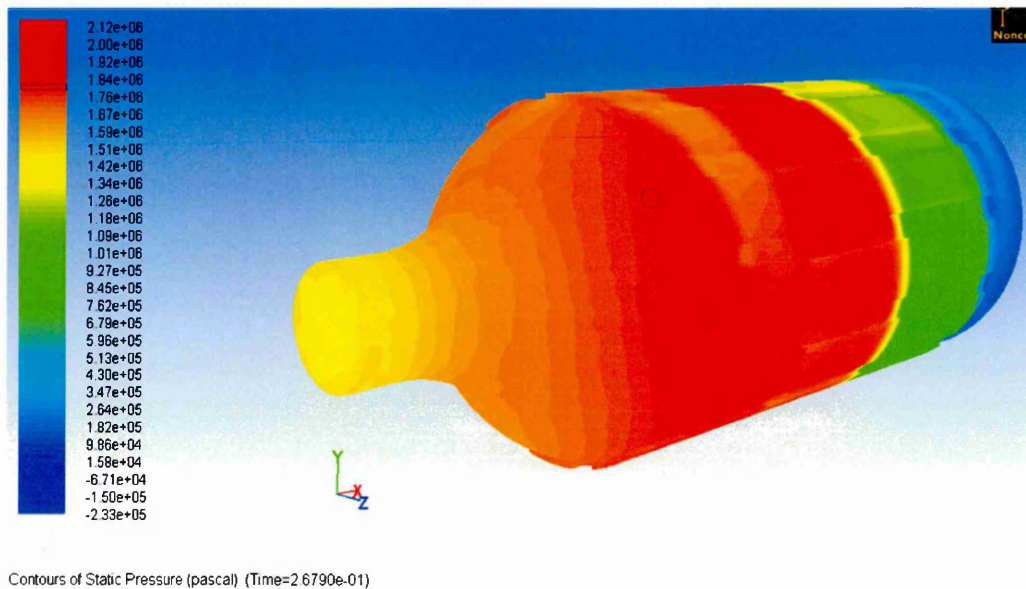
Figure A-A-68 Static pressure contour (full view) - auger speed 50 rpm
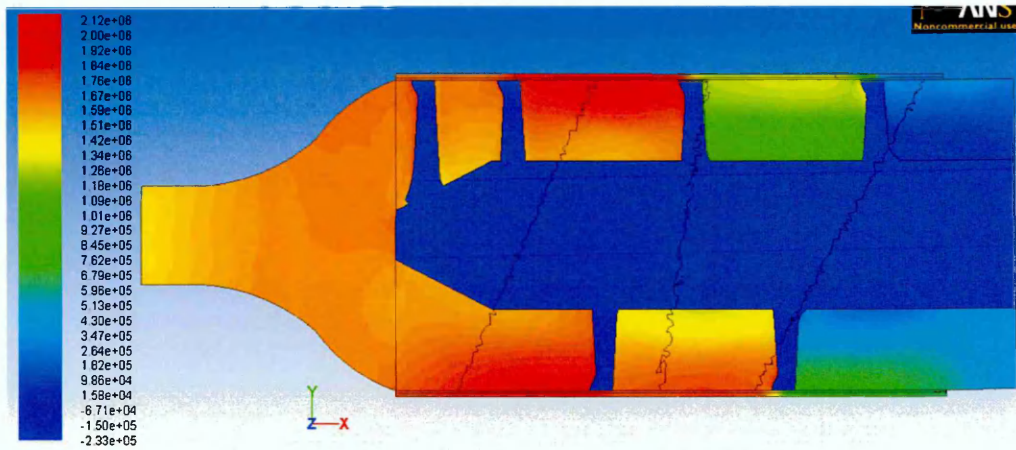
Figure A-A-69 Static pressure contour (sectional view) - auger speed 50 rpm
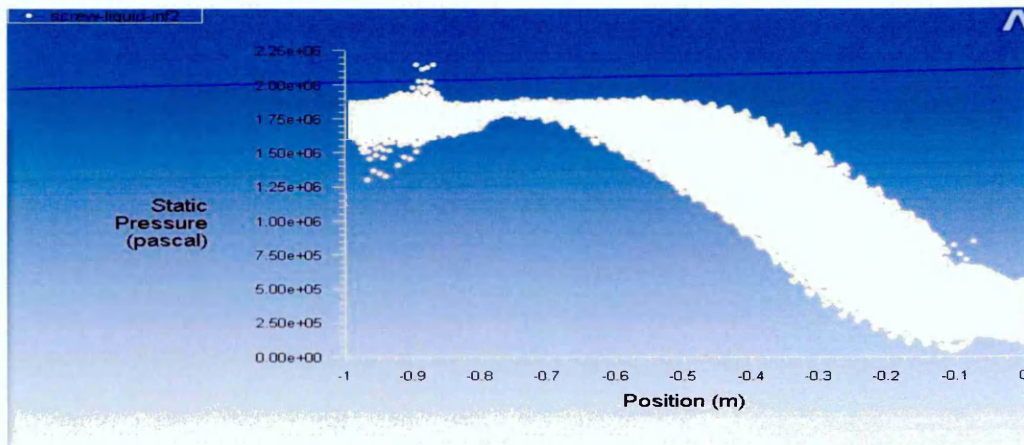
Figure A-A-70 Static pressure profile- auger speed 50 rpm

Material flow pattern:
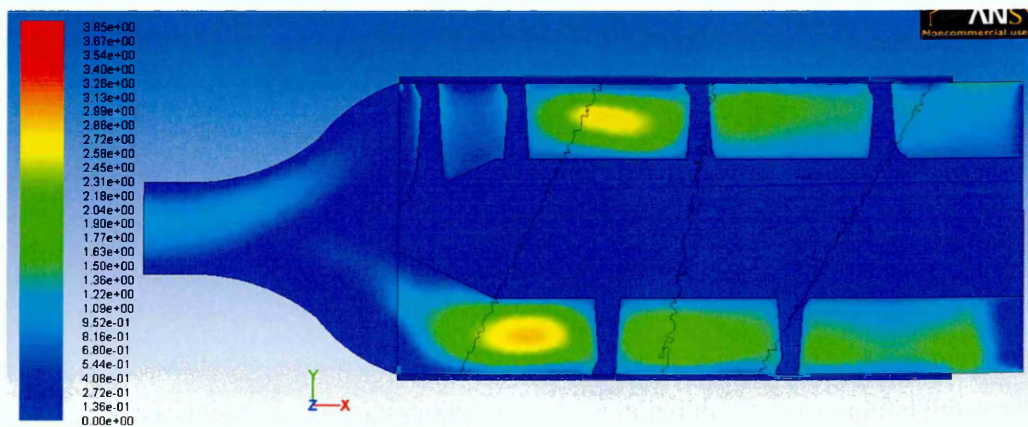
Figure A-A-71 Flow velocity during extrusion(sectional view)-auger speed 50 rpm

158

Molecular Viscosity vs. Strain Rate (Time=2.6790e-01)
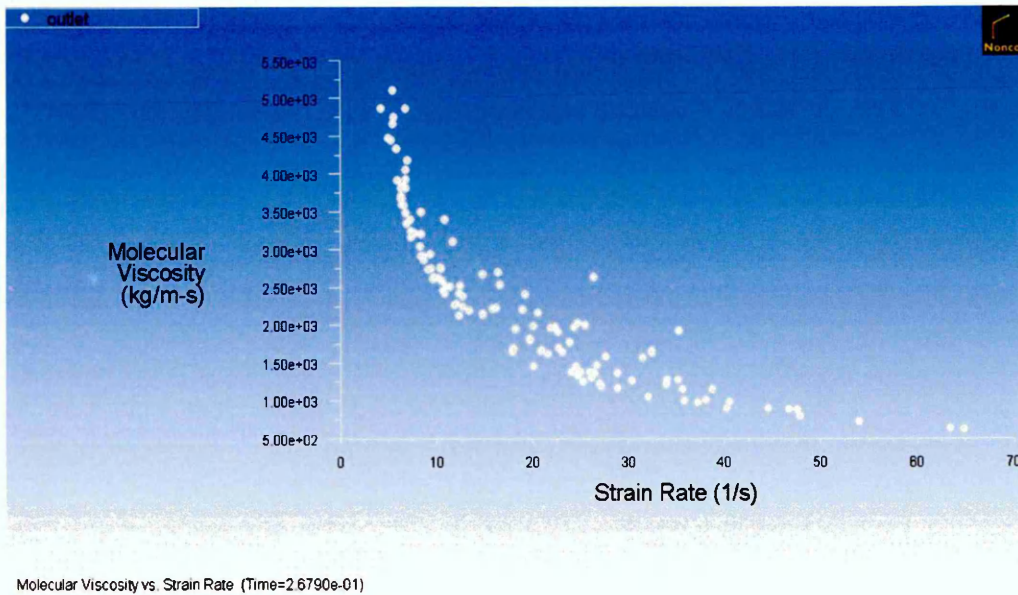
Figure A-A-72 Molecular viscosity vs. Strain rate - auger speed 50 rpm

VIII.   CFD Simulation results of 500 mm extruder with varying auger pitch distance:-

a.   Pitch distance 338.012 mm

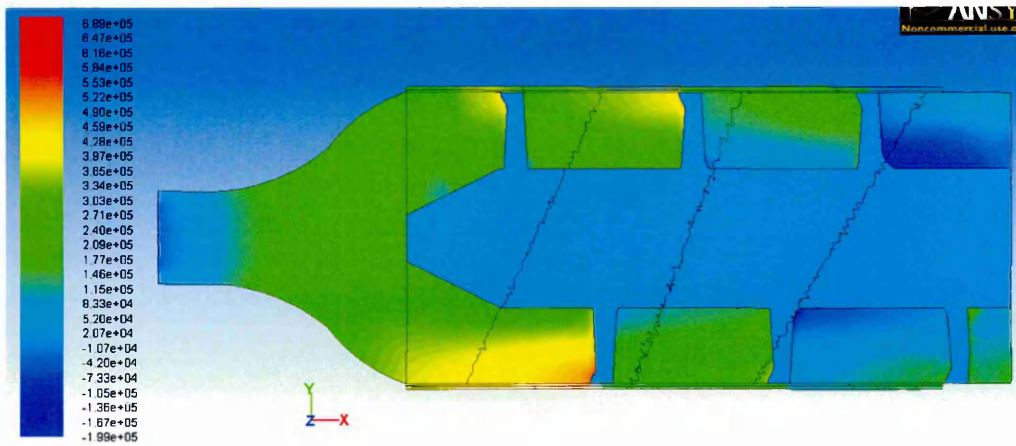*Extrusion pressure:*

Contours of Static Pressure (pascal) (Time=2.5050e+00)
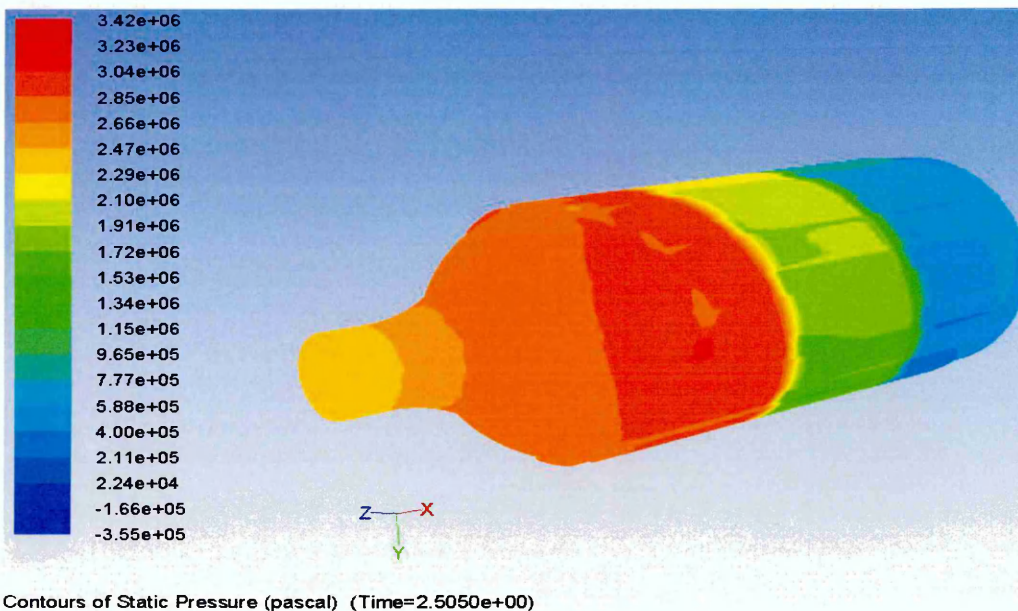
Figure A-A-73 Static pressure contour (full view)-pitch 338.012 mm

159

Contours of Static Pressure (pascal) (Time=2.5050e+00)
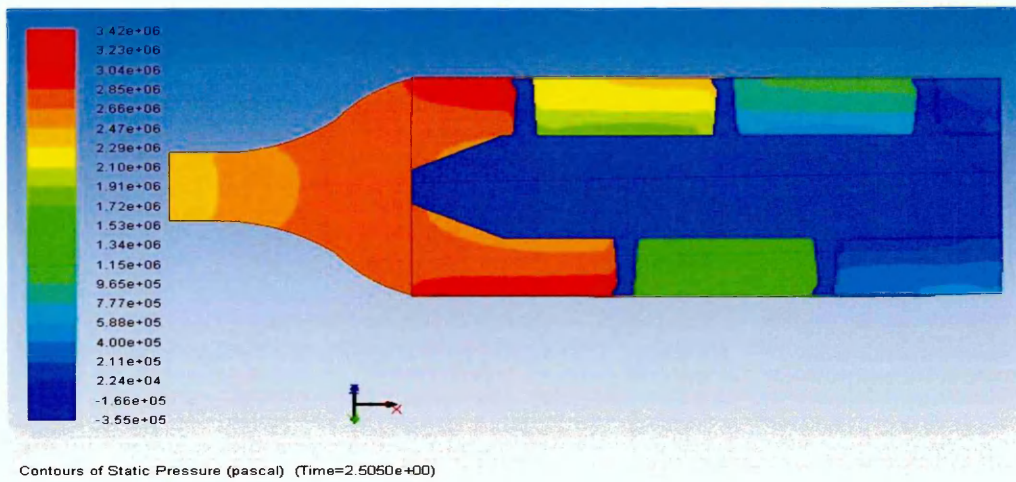
Figure A-A-74 Static pressure contour (sectional view)-pitch 338.012 mm

Static Pressure (Time=2.5050e+00)
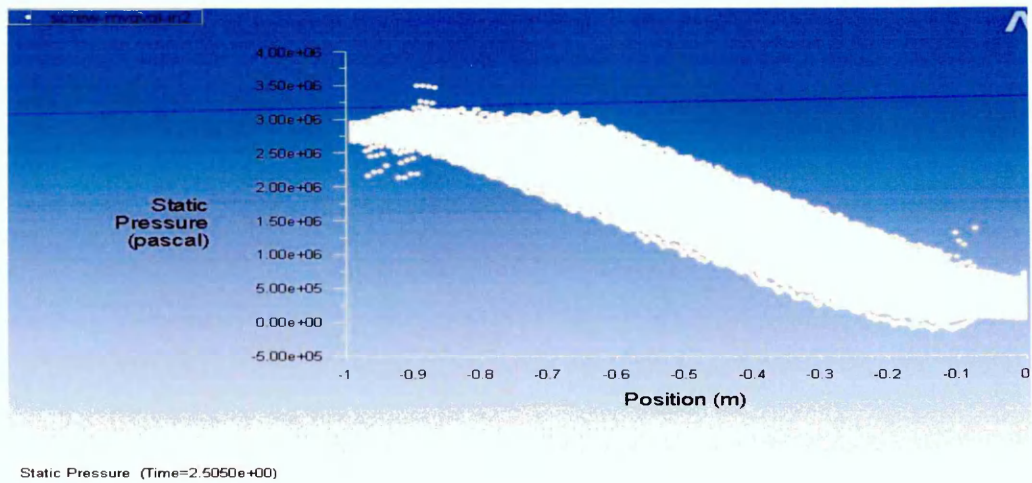
Figure A-A-75 Static pressure profile-pitch 338.012 mm

Material flow pattern:

Contours of Velocity Magnitude (m/s) (Time=2.5050e+00)
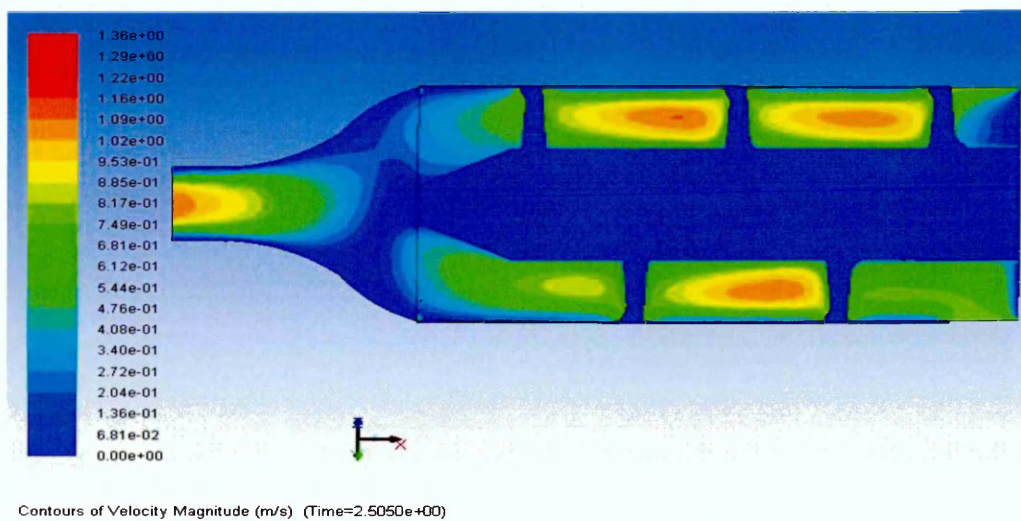
Figure A-A-76 Flow velocity during extrusion(sectional view)-pitch 338.012 mm

160

Molecular Viscosity vs. Strain Rate (Time=2.5050e+00)   J
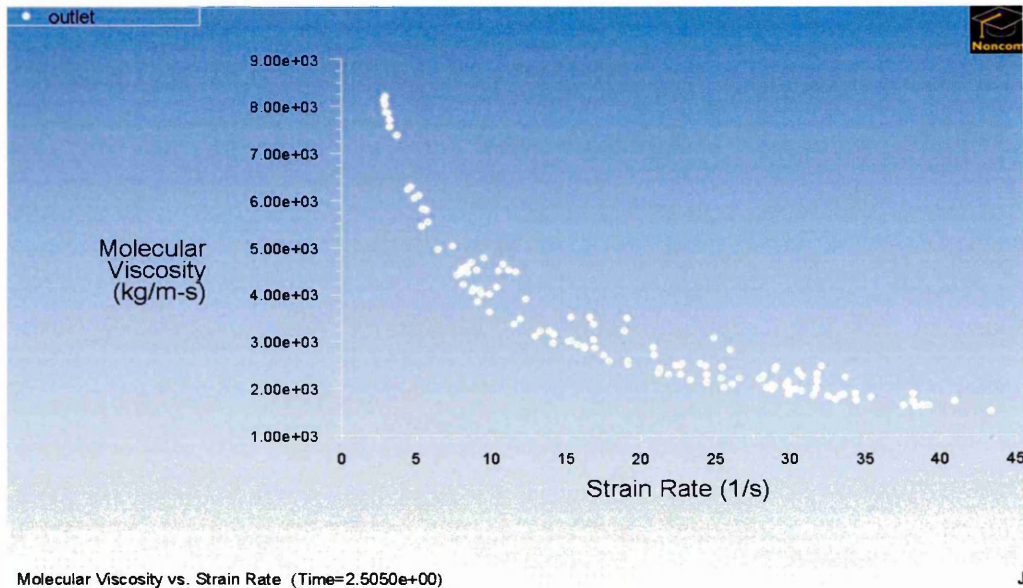
Figure A-A-77 Molecular viscosity vs. Strain rate-pitch 338.012 mm

• The results of CFD analysis with auger pitch distance 292 mm are presented in Appendix A- section II.

IX. CFD Simulation results of 500 mm extruder with varying die design:-

a. Die type-I

Extrusion pressure:

Contours of Static Pressure (pascal) (Time=2.5000e+00)
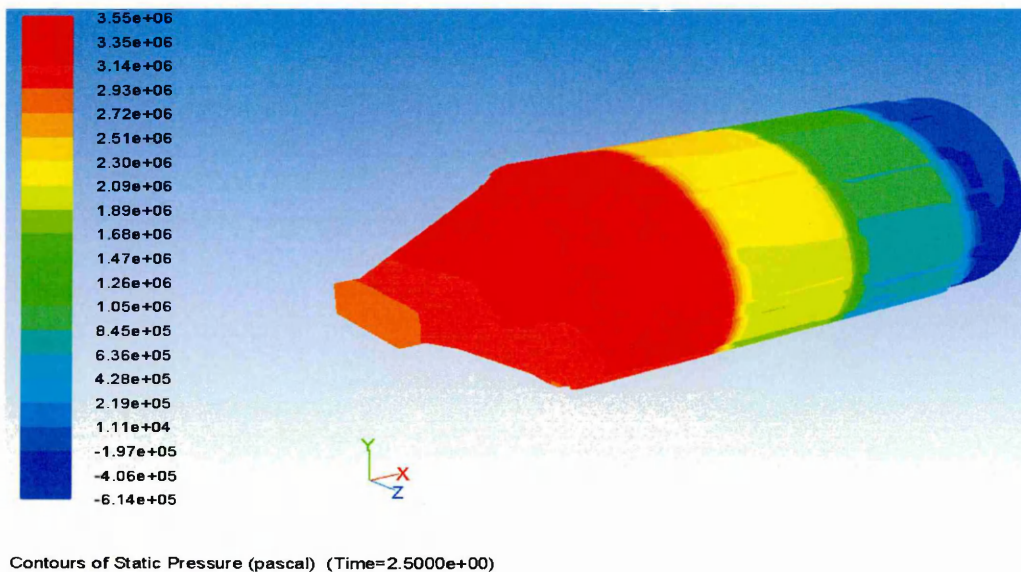
Figure A-A-78 Static pressure contour (full view)-die type-I

161
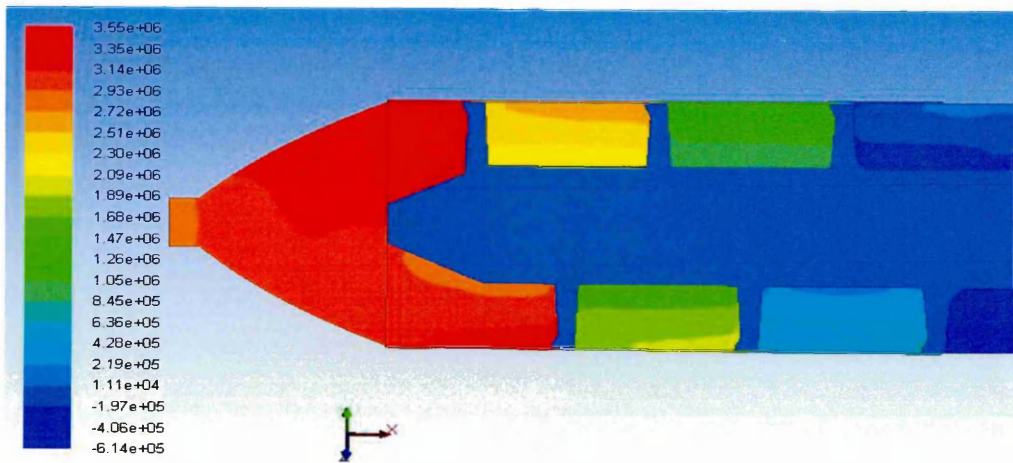
Contours of Static Pressure (pascal) (Time=2.5000e+00)

Figure A-A-79 Static pressure contour (sectional view)-die type-I
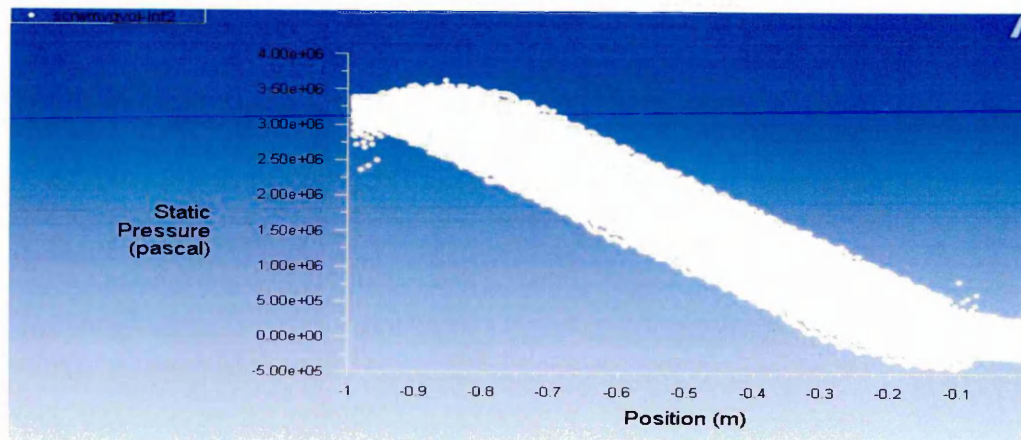
Static Pressure (Time=2.5000e+00)

Figure A-A-80 Static pressure profile-die type-I

<u>Material flow pattern:</u>
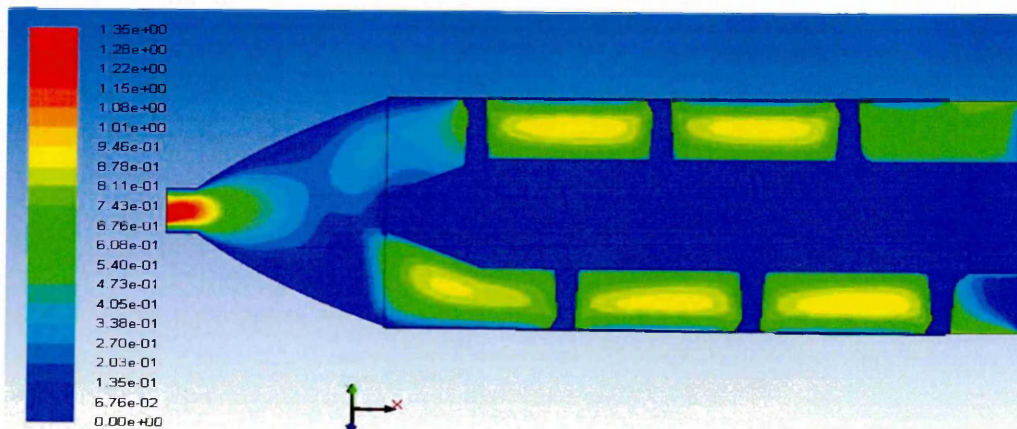
Contours of Velocity Magnitude (m/s) (Time=2.5000e+00)

Figure A-A-81 Flow velocity during extrusion (sectional view)-die type-I
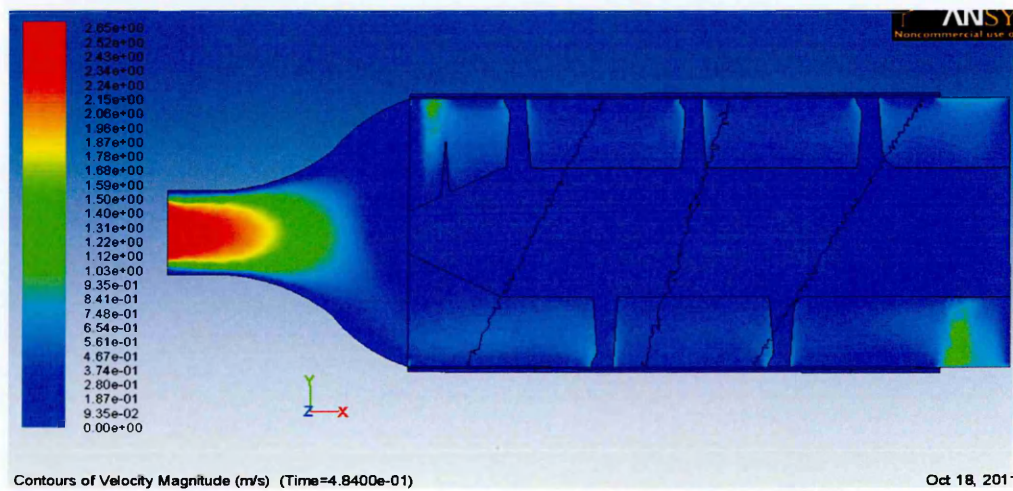
<u>Viscosity profile:</u>

162
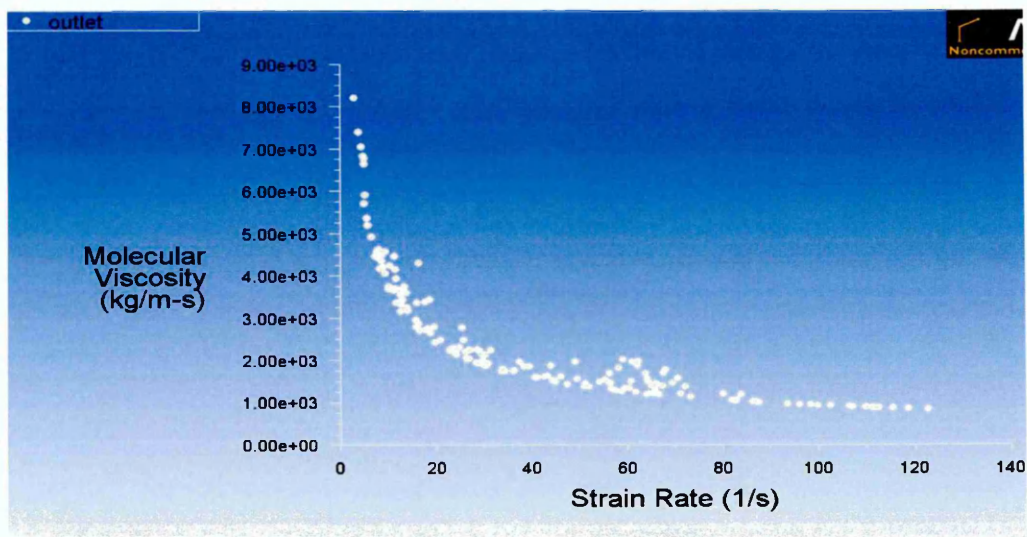
Molecular Viscosity vs. Strain Rate (Time=2.5000e+00)   Jul

Figure A-A-82 Molecular viscosity vs. Strain rate- die type-I

b. __Die type-III__

Extrusion pressure:
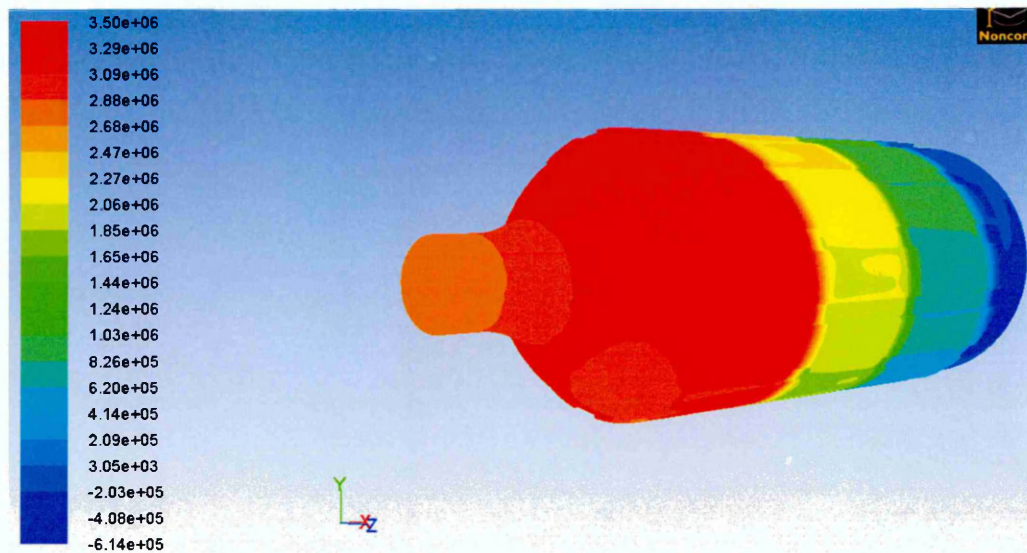
Contours of Static Pressure (pascal) (Time=2.5000e+00)

Figure A-A-83 Static pressure contour (full view)-die type-III

Contours of Static Pressure (pascal) (Time=2.5000e+00)
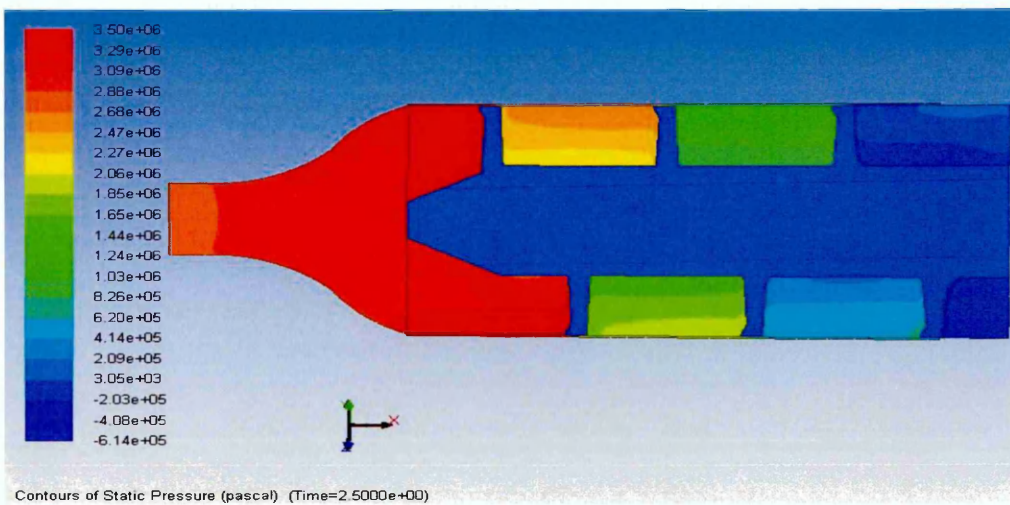
Figure A-A-84 Static pressure contour (sectional view)-die type-III

Static Pressure (Time=2.5000e+00)
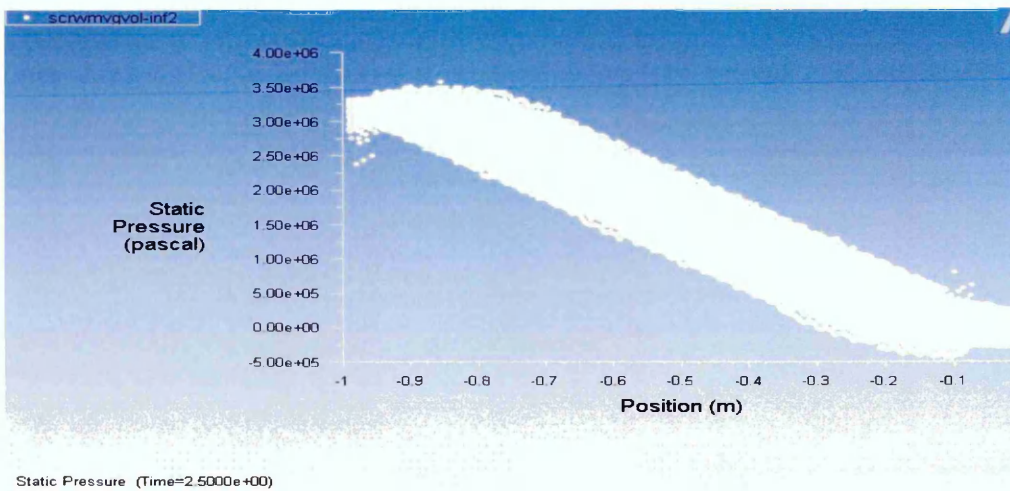
Figure A-A-85 Static pressure profile-die type-III

<u>Material flow pattern:</u>

Contours of Velocity Magnitude (m/s) (Time=2.5000e+00)
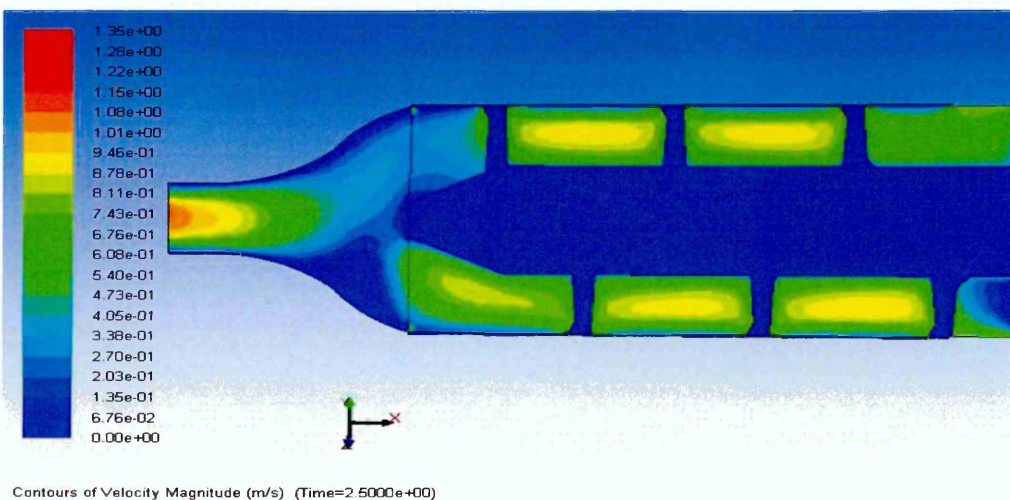
Figure A-A-86 Flow velocity during extrusion (sectional view)-die type-III

164
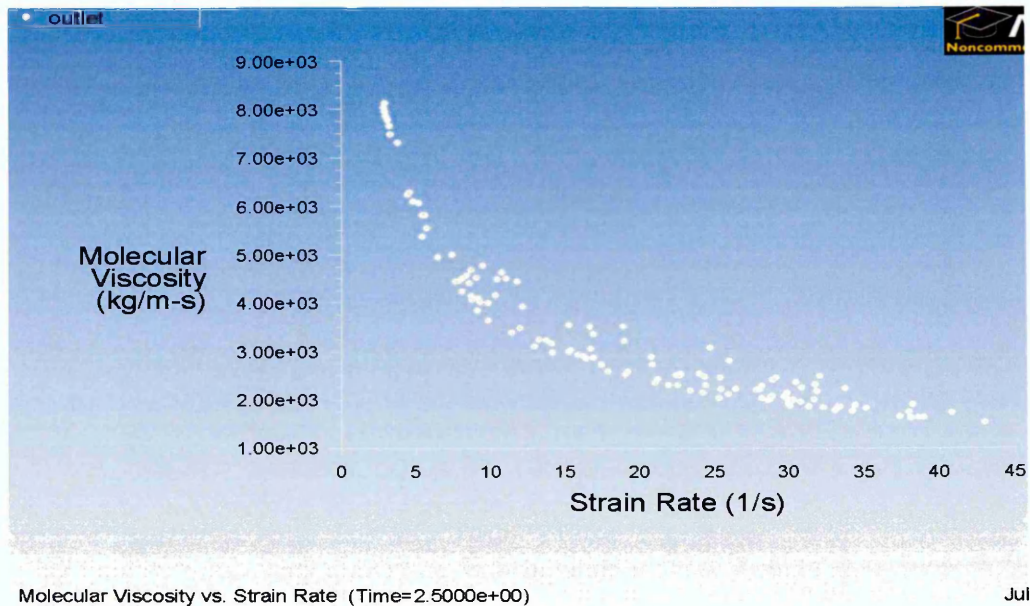
Figure A-A-87 Molecular viscosity vs. Strain rate- die type-III

X. CFD Simulation results of 600 mm extruder with varying feed rate:-

a. Feed rate:-11.8 kgs⁻¹

Extrusion pressure:
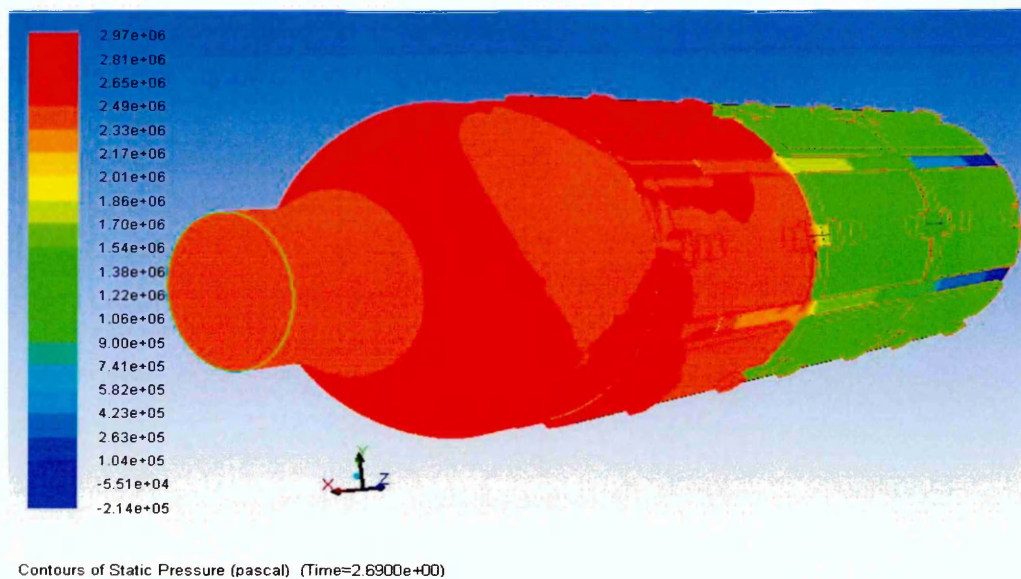
Figure A-A-88 Static pressure contour (full view) - feed rate 11.8 kgs⁻¹

Contours of Static Pressure (pascal) (Time=2.6900e+00)

Figure A-A-89 Static pressure contour (sectional view) - feed rate 11.8 kgs⁻¹

Static Pressure (Time=2.6900e+00)

Figure A-A-90 Static pressure profile- feed rate 11.8 kgs⁻¹

<u>Material flow pattern:</u>

Contours of Velocity Magnitude (m/s) (Time=2.6900e+00)

Figure A-A-91 Flow velocity during extrusion(sectional view)-feed rate 11.8 kgs⁻¹

166

Contours of Static Pressure (pascal) (Time=2.6900e+00)

Figure A-A-89 Static pressure contour (sectional view) - feed rate 11.8 kgs^{-1}

Static Pressure (Time=2.6900e+00)

Figure A-A-90 Static pressure profile- feed rate 11.8 kgs^{-1}

<u>Material flow pattern:</u>

Contours of Velocity Magnitude (m/s) (Time=2.6900e+00)

Figure A-A-91 Flow velocity during extrusion(sectional view)-feed rate 11.8 kgs^{-1}
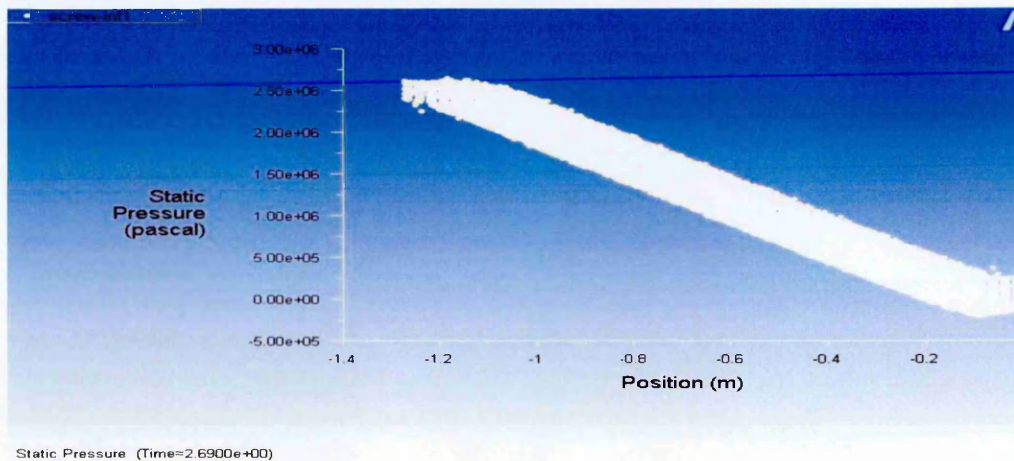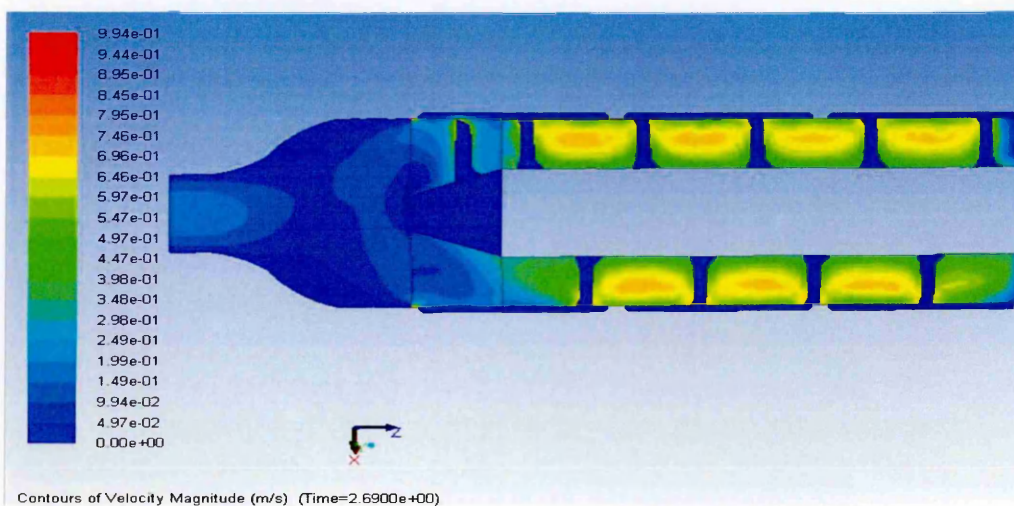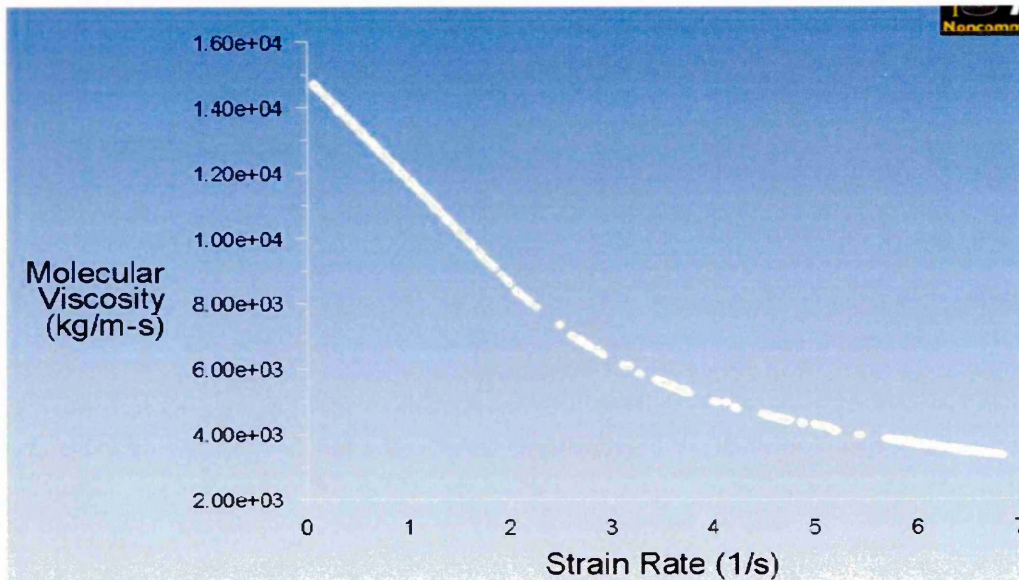
Figure A-A-92 Molecular viscosity vs. Strain rate- feed rate 11.8 kgs^{-1}

b. Feed rate:-19 kgs^{-1}

Extrusion pressure:
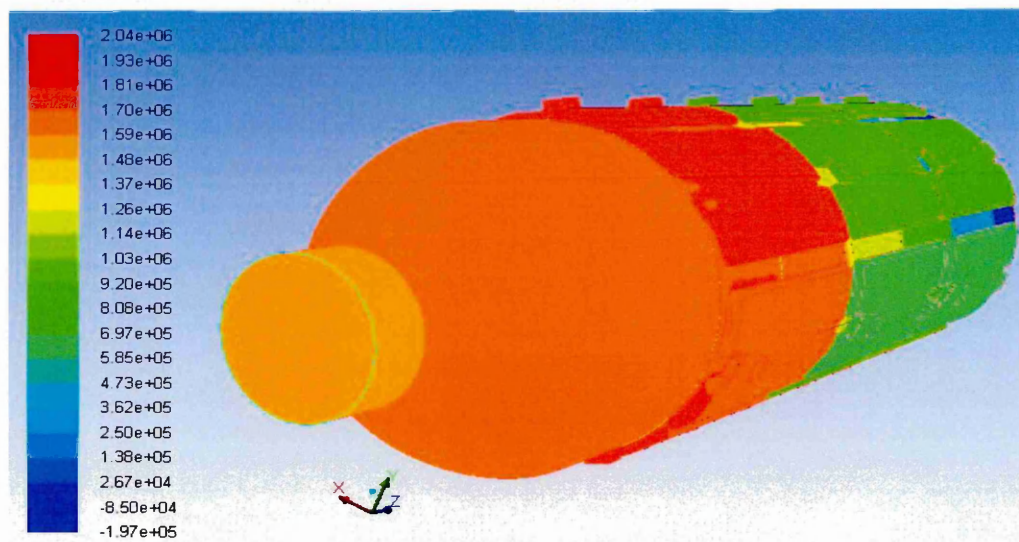
Contours of Static Pressure (pascal) (Time=2.6750e+00)

Figure A-A-93 Static pressure contour (full view) - feed rate 19 kgs^{-1}

Contours of Static Pressure (pascal) (Time=2.6750e+00)
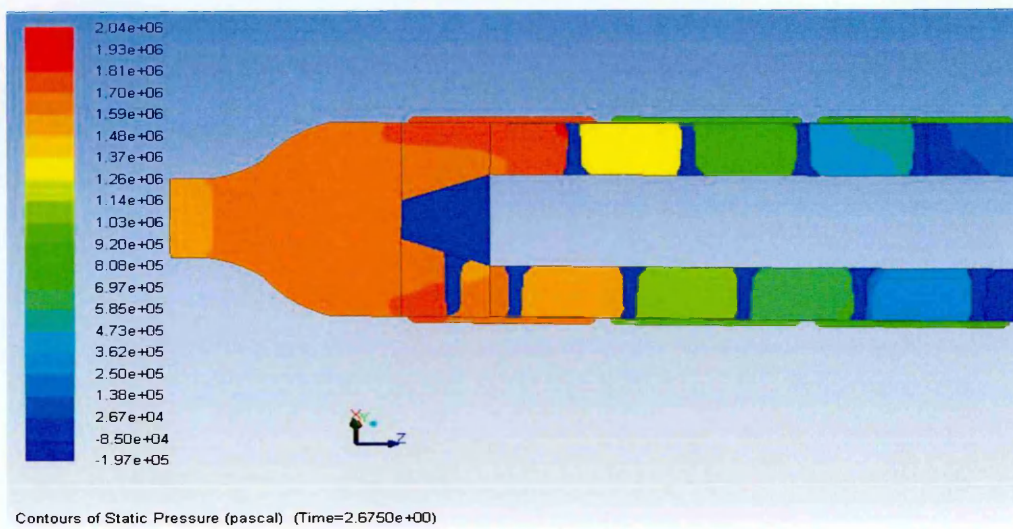
Figure A-A-94 Static pressure contour (sectional view) - feed rate 19 kgs^{-1}

Static Pressure (Time=2.6750e+00)
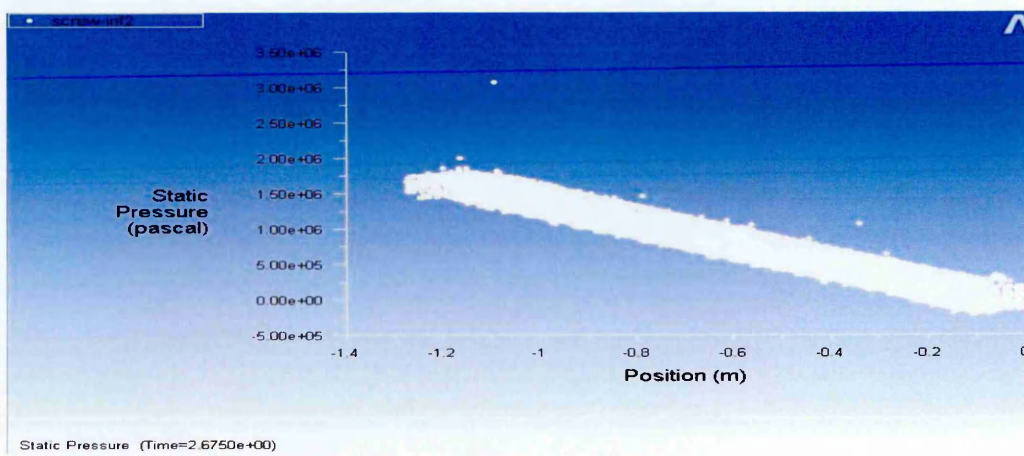
Figure A-A-95 Static pressure profile- feed rate 19 kgs^{-1}

<u>Material flow pattern:</u>

Contours of Velocity Magnitude (m/s) (Time=2.6750e+00)
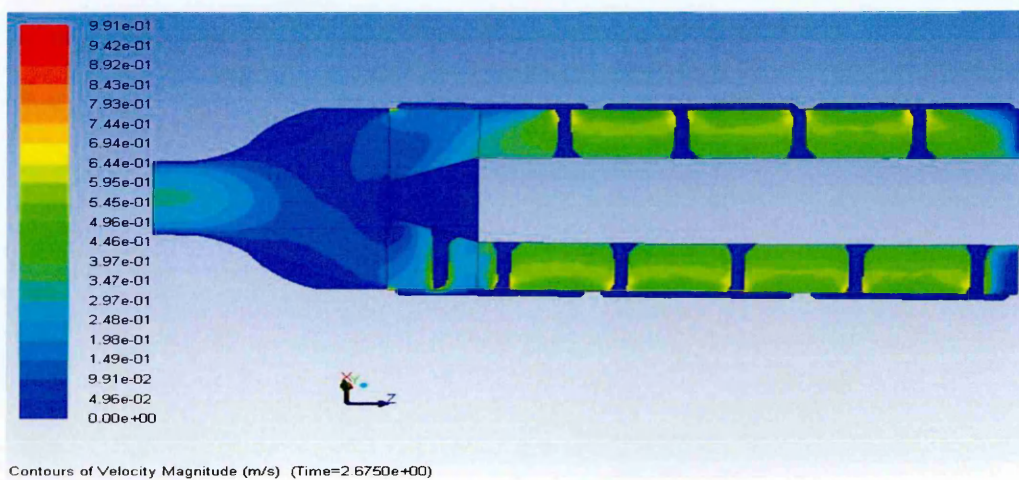
Figure A-A-96 Flow velocity during extrusion(sectional view)-feed rate 19 kgs^{-1}

168
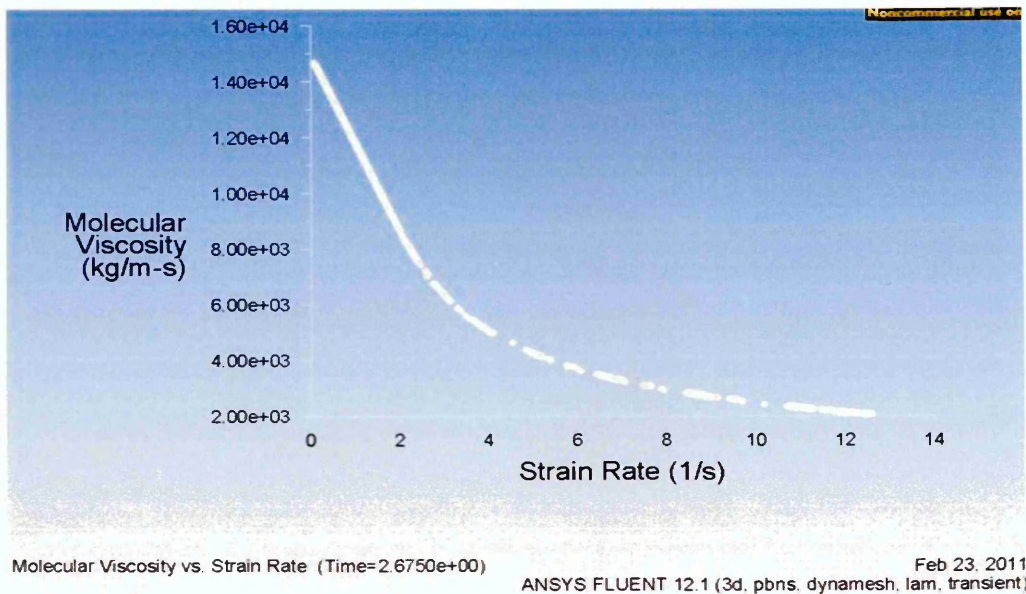
Figure A-A-97 Molecular viscosity vs. Strain rate- feed rate 19 kgs^{-1}

XI. CFD Simulation results of 600 mm extruder with varying Auger speed:-

a. Auger speed:-30 rpm

Extrusion pressure:
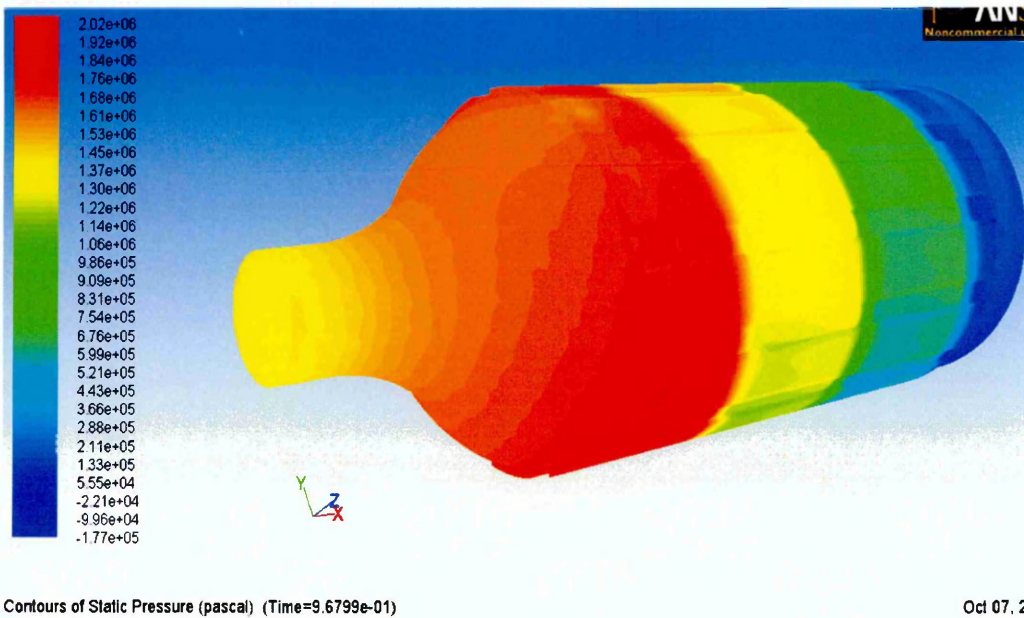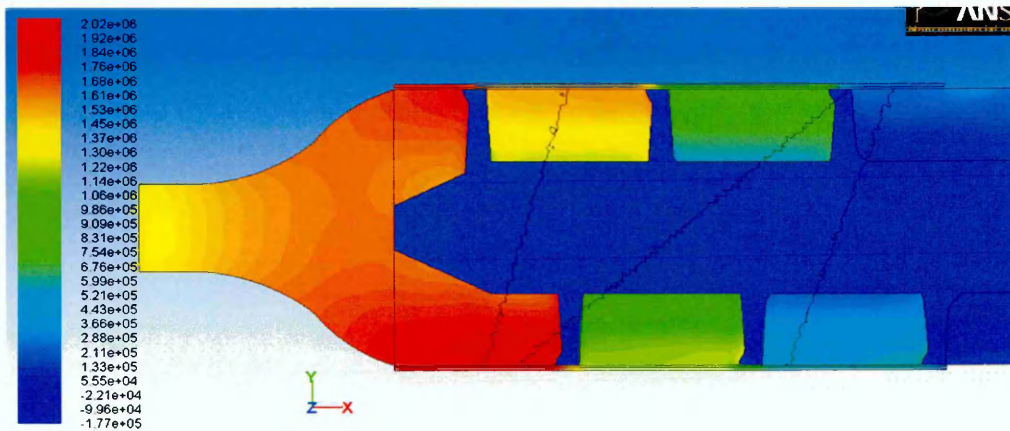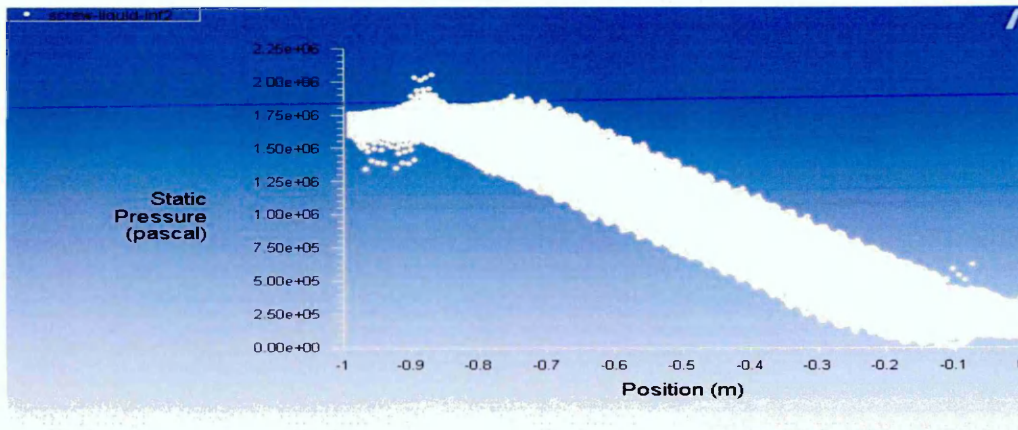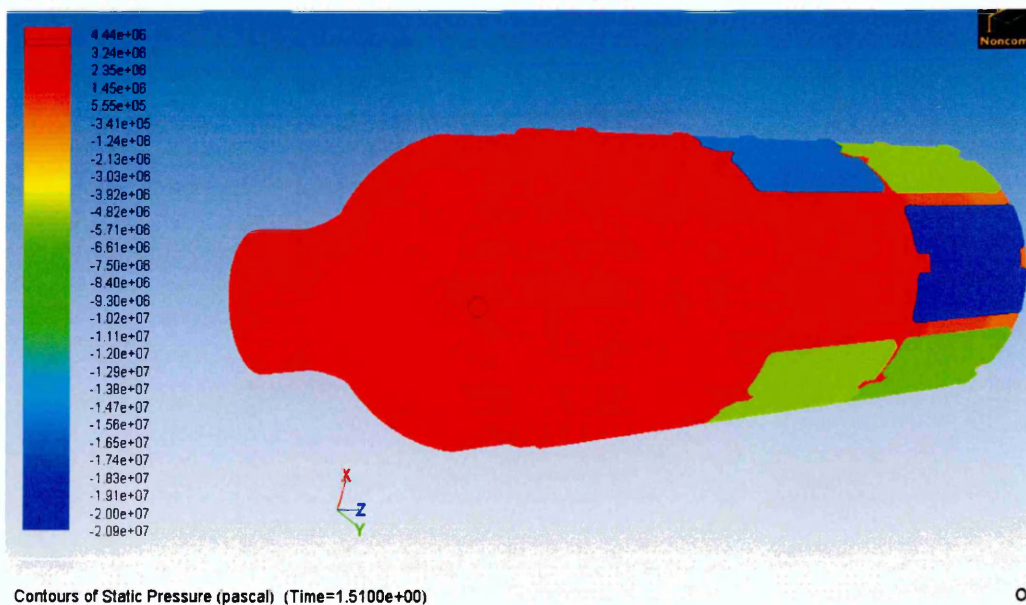

Figure A-A-98 Static pressure contour (full view) - auger speed 30 rpm

Contours of Static Pressure (pascal) (Time=1.5100e+00)   Oct 31, 2011
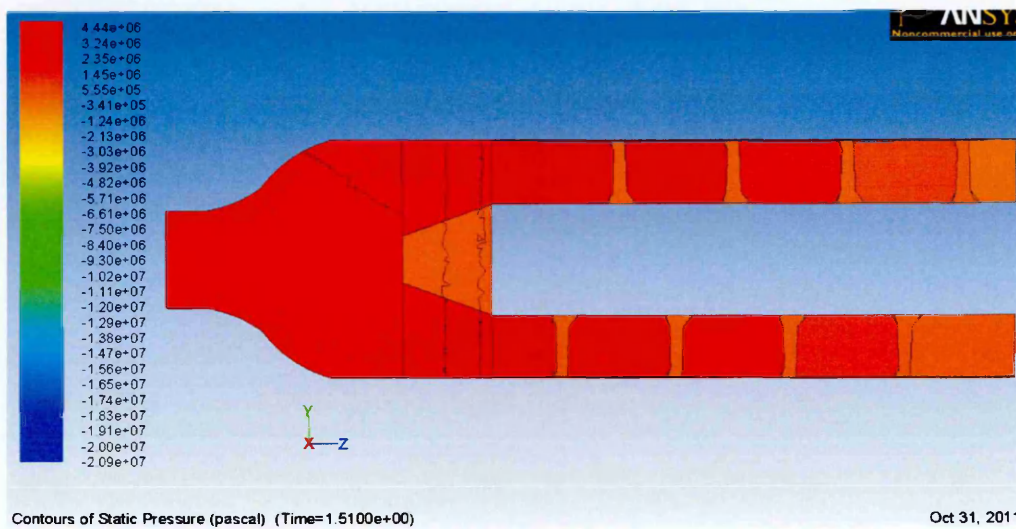
Figure A-A-99 Static pressure contour (sectional view) - auger speed 30 rpm

Static Pressure (Time=1.5100e+00)
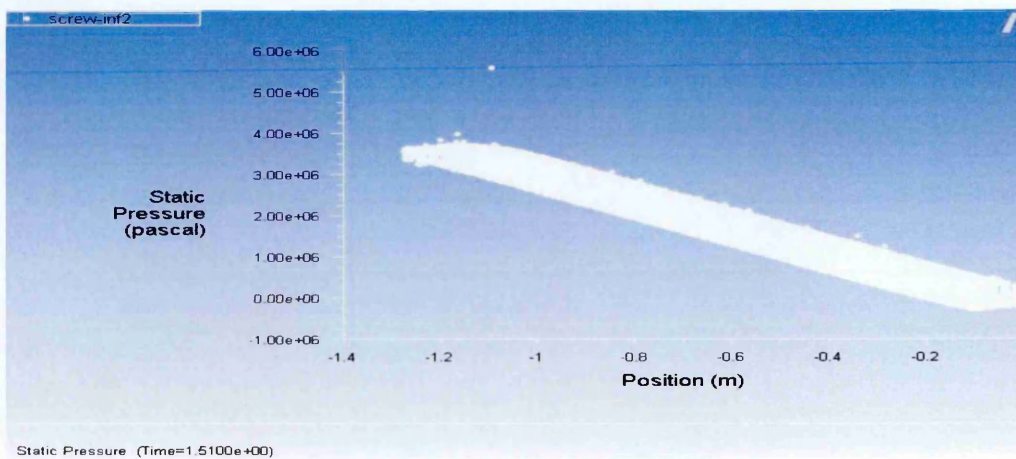
Figure A-A-100 Static pressure profile- auger speed 30 rpm

<u>*Material flow pattern:*</u>

Contours of Velocity Magnitude (m/s) (Time=1.5100e+00)   Oct 31, 2011
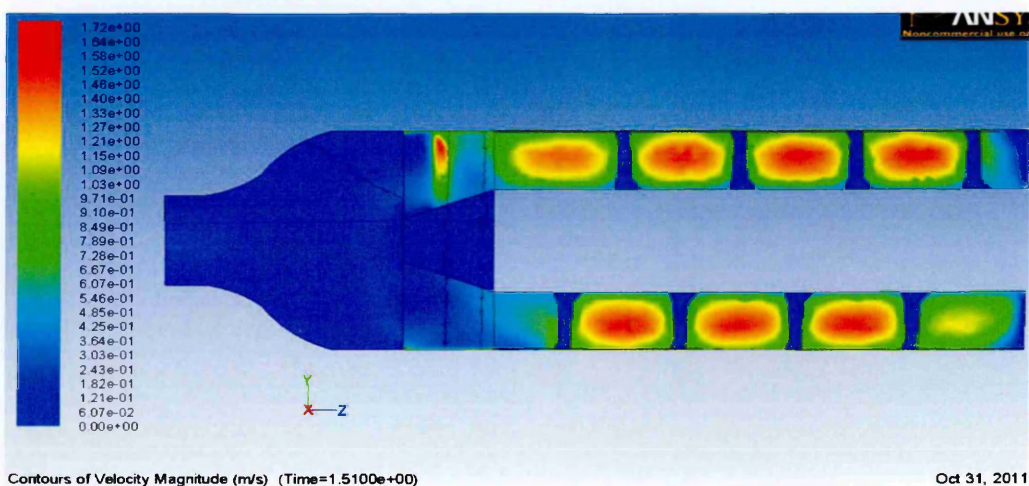
*Figure A-A-101 Flow velocity during extrusion(sectional view)-auger speed
30 rpm*
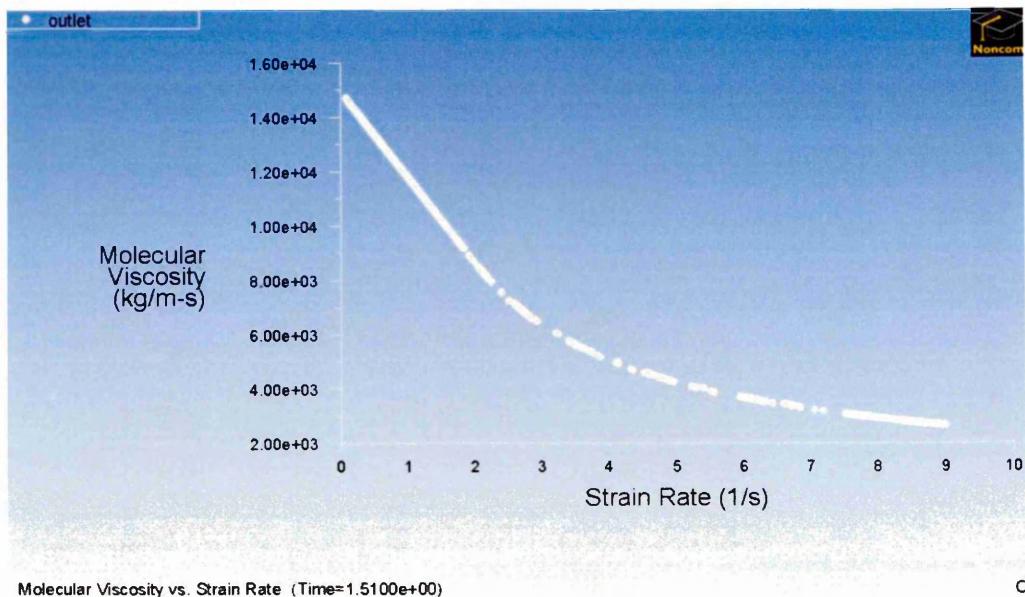
Figure A-A-102 Molecular viscosity vs. Strain rate- auger speed 30 rpm

XII.   CFD Simulation results of _Trial:1 experimental set up:-_

Extrusion Pressure:
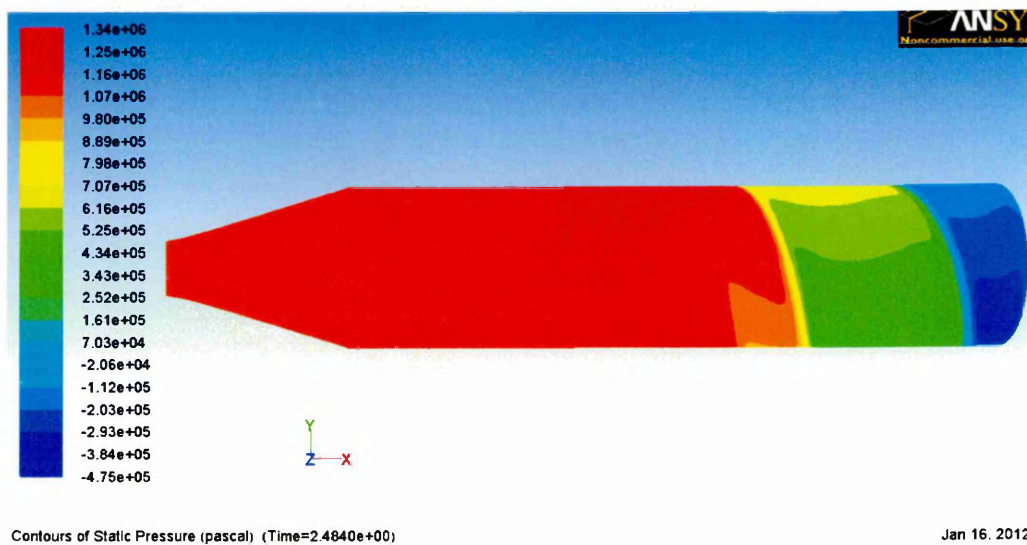
Figure A-A-103 Static pressure contour (full view)-scaled extruder-T1
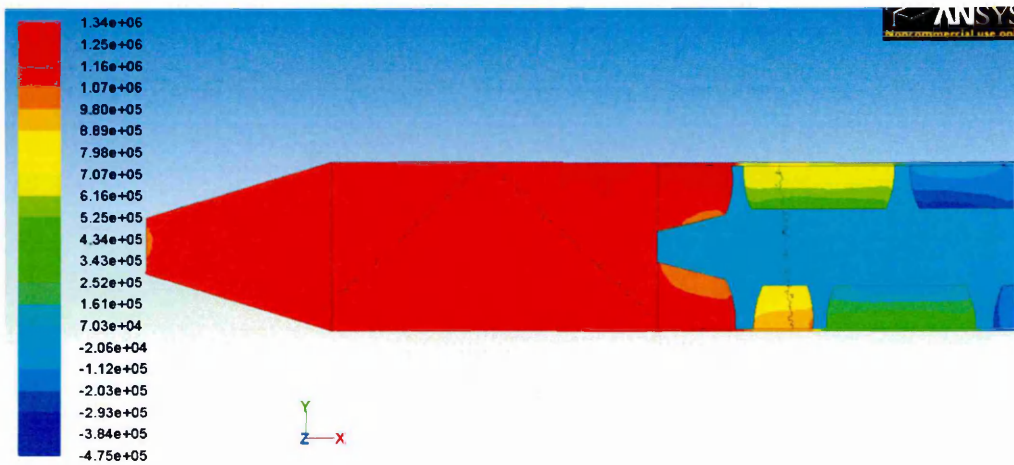
Contours of Static Pressure (pascal) (Time=2.4840e+00)   Jan 16, 2012

Figure A-A-104 Static pressure contour (sectional view)-scaled

extruder-T1

<u>Material flow pattern:</u>
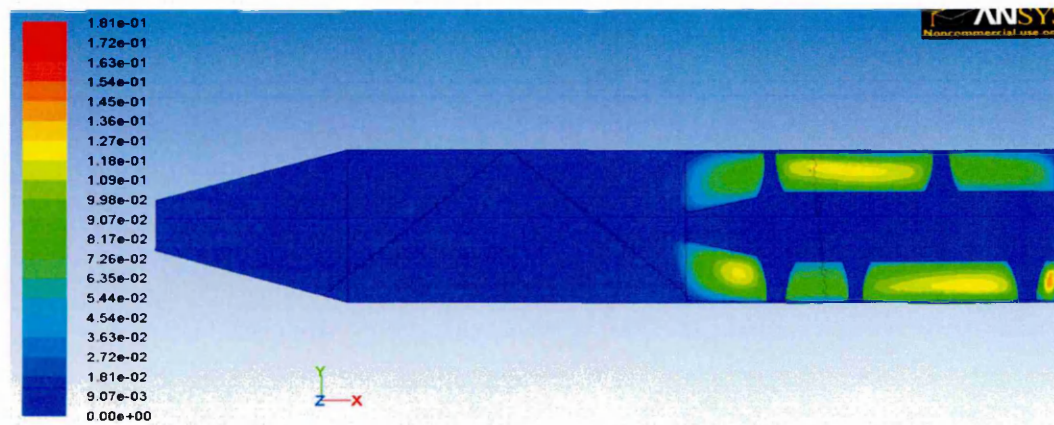
Contours of Velocity Magnitude (m/s) (Time=2.4840e+00)   Jan 16, 2012

Figure A-A-105 Flow velocity during extrusion (sectional view)-scaled

extruder-T1

<u>Viscosity profile:</u>
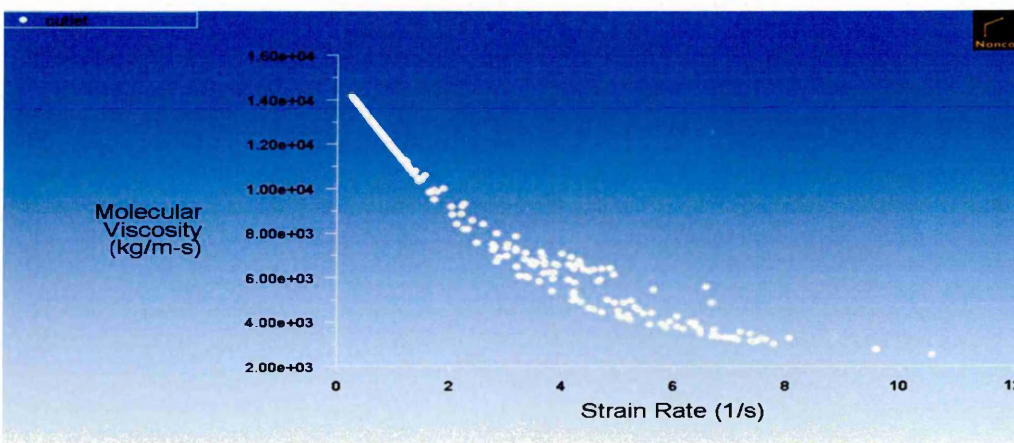
Molecular Viscosity vs. Strain Rate (Time=2.4840e+00)   J

Figure A-A-106 Molecular viscosity vs. Strain rate-*scaled extruder-T1*

172

Extrusion Pressure:

Contours of Static Pressure (pascal) (Time=2.4000e+00)   M

Figure A-A-107 Static pressure contour (full view)-scaled extruder-T2
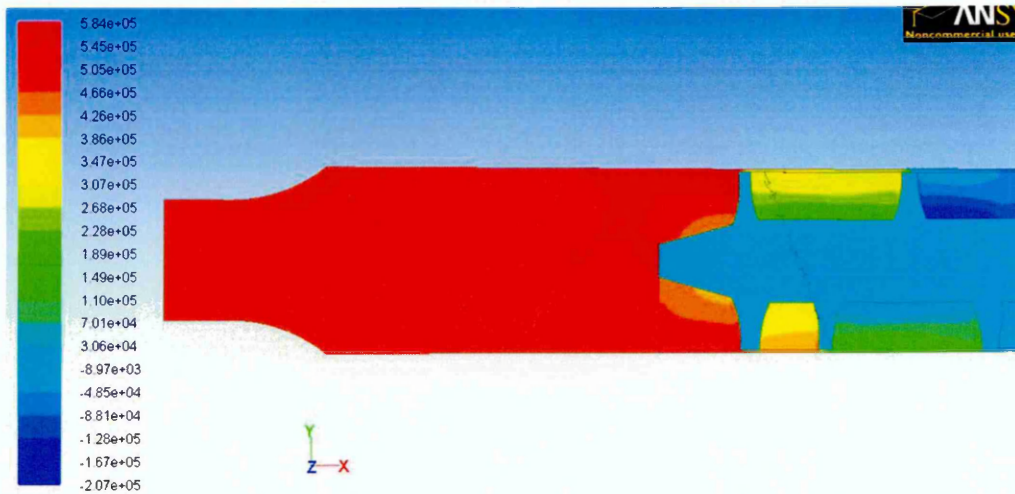
Contours of Static Pressure (pascal) (Time=2.4000e+00)   Mar 02. 201

Figure A-A-108 Static pressure contour (sectional view)-scaled
extruder-T2

Material flow pattern:
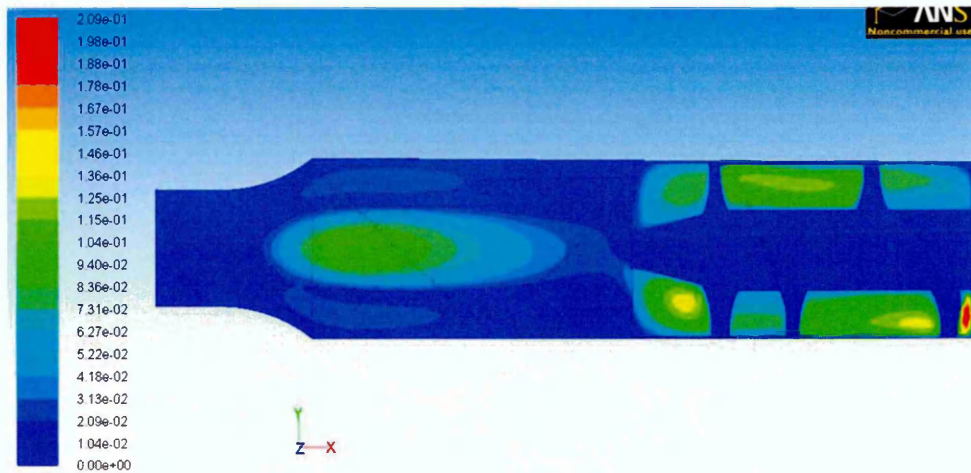
Contours of Velocity Magnitude (m/s) (Time=2.4000e+00)   Mar 02, 201

Figure A-A-109 Flow velocity during extrusion (sectional view)-scaled extruder-T2

Viscosity profile:
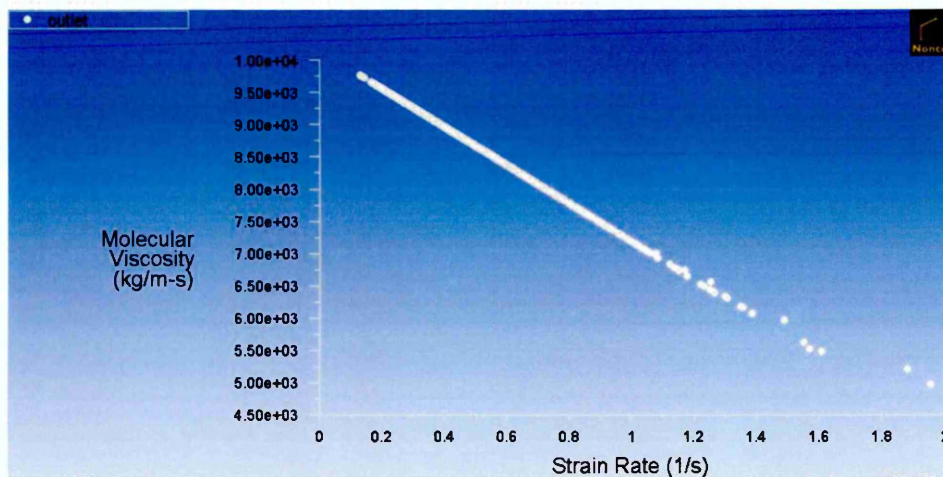
Molecular Viscosity vs. Strain Rate (Time=2.4000e+00)

Figure A-A-110 Molecular viscosity vs. Strain rate-scaled extruder-T2

I. **Stress distribution pattern in 430 mm extruder barrel-for applied load of 1.8 MPa :-**
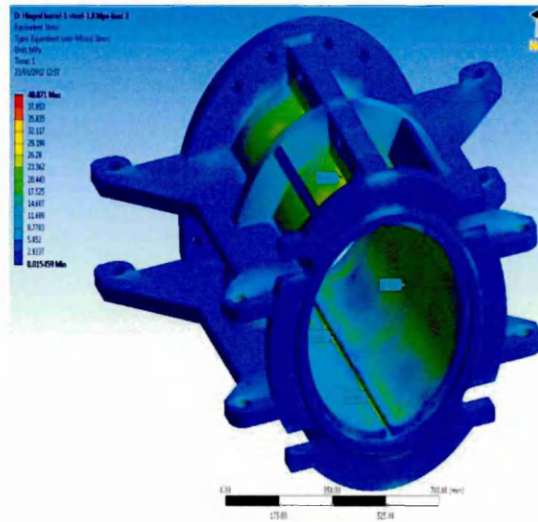
a) Structural steel
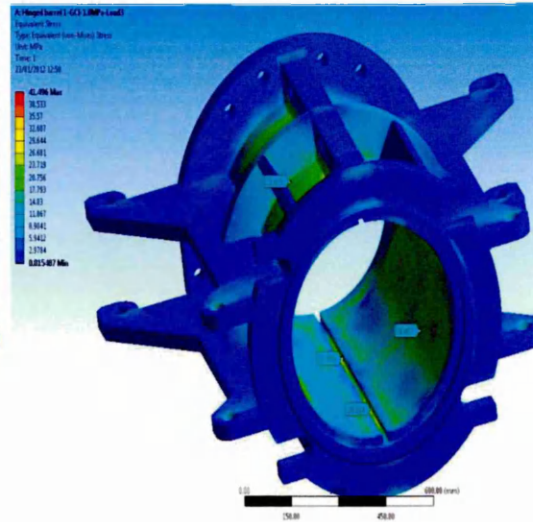
b) GCI
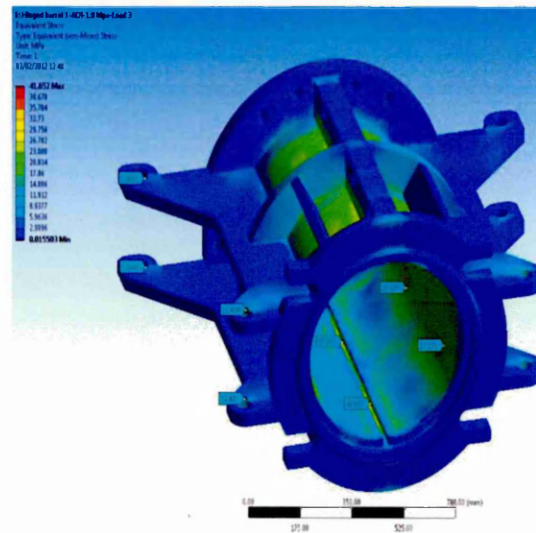
c) ADI

Figure A-B- 1 Stress induced in barrel @1.8 MPa load

II. Deformation pattern in 430 mm extruder barrel-for applied load of 1.8 MPa:-

a) Structural steel   b) GCI
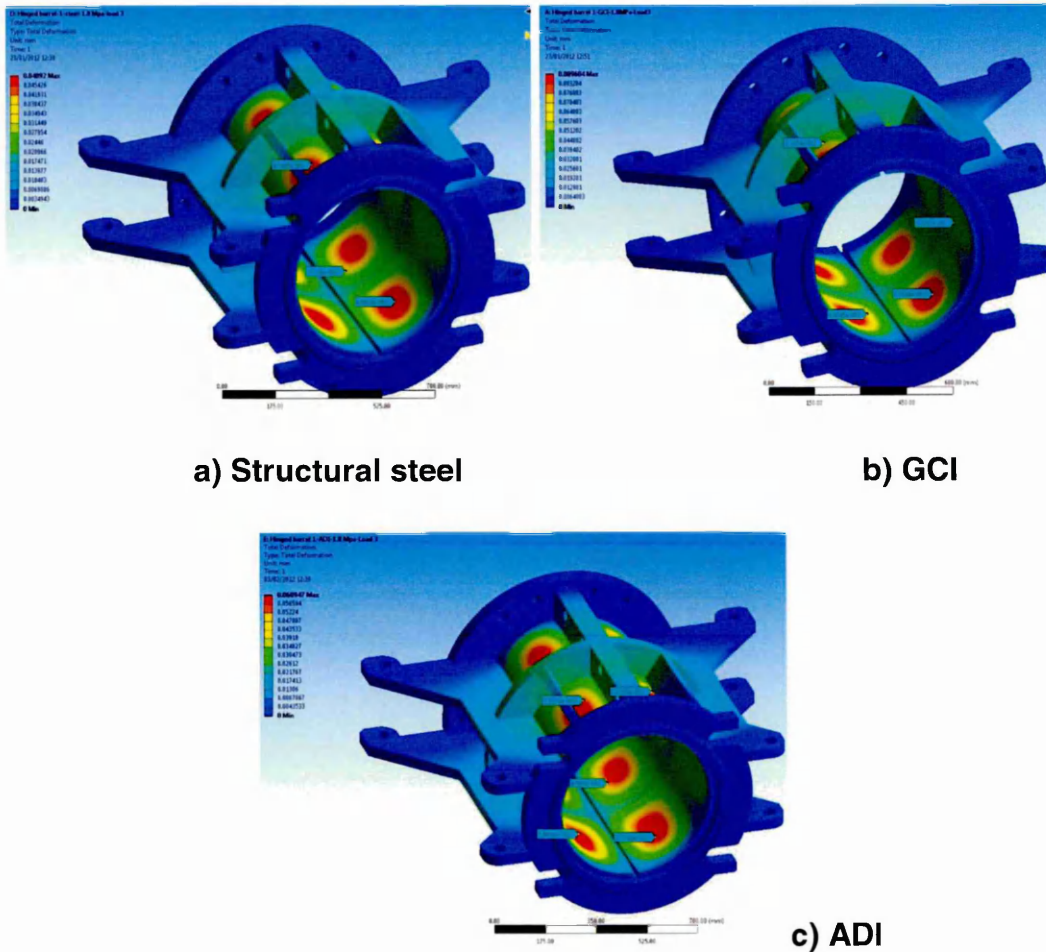
c) ADI

Figure A-B- 2 Deformation in barrel @1.8 MPa load

III. Stress distribution pattern in 430 mm extruder distance piece- for applied load of 1.8 MPa:-

a) Structural steel   b) GCI
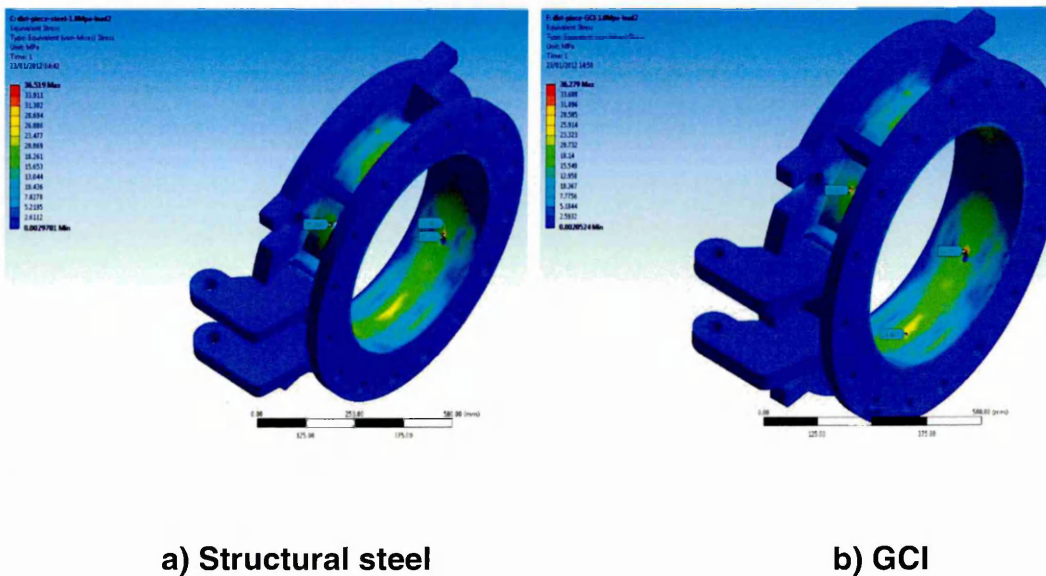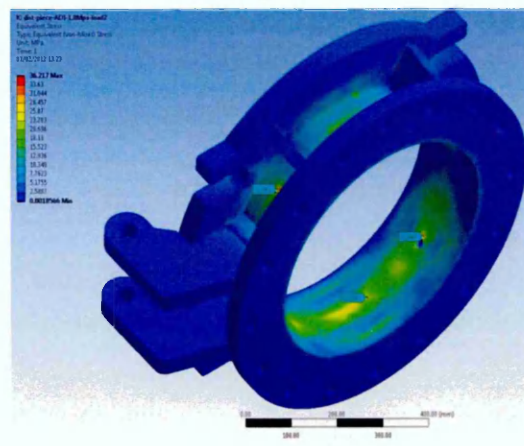
c) ADI

Figure A-B- 3 Stress induced in distance piece @1.8 MPa load

IV. Deformation pattern in 430 mm extruder distance piece -for applied load 1.8 MPa :-

a) Structural steel
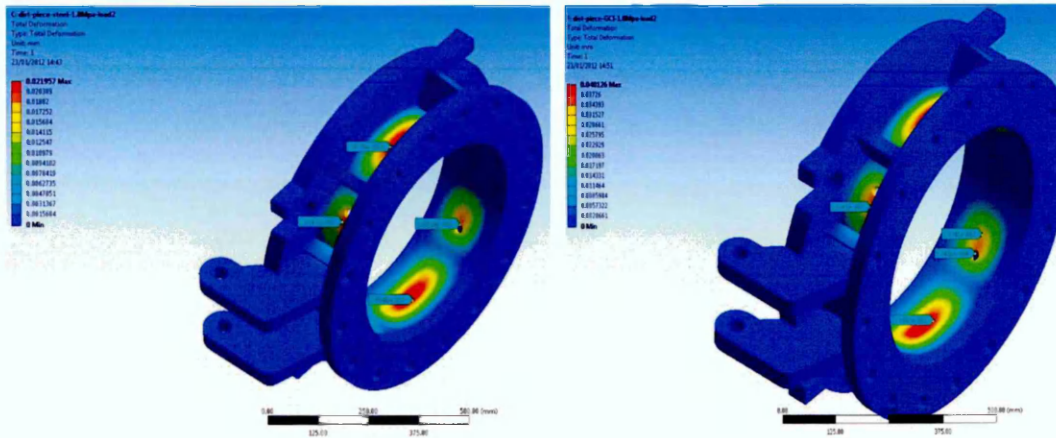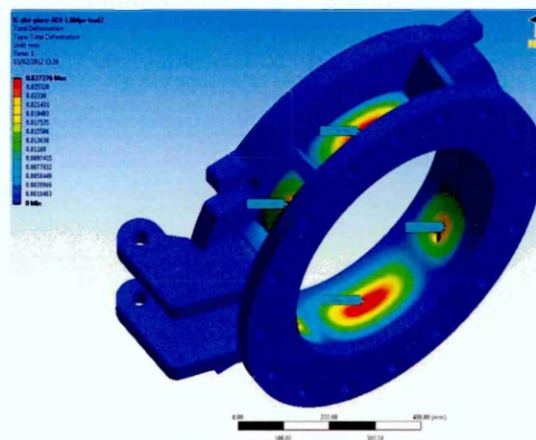
b) GCI

c) ADI

Figure A-B- 4 Deformation in distance piece @1.8 MPa load

V. <u>**Stress distribution pattern in 430 mm extruder liner- for applied load of 1.8 MPa:-**</u>
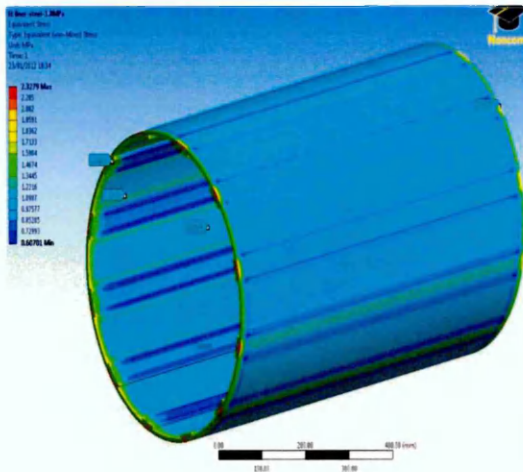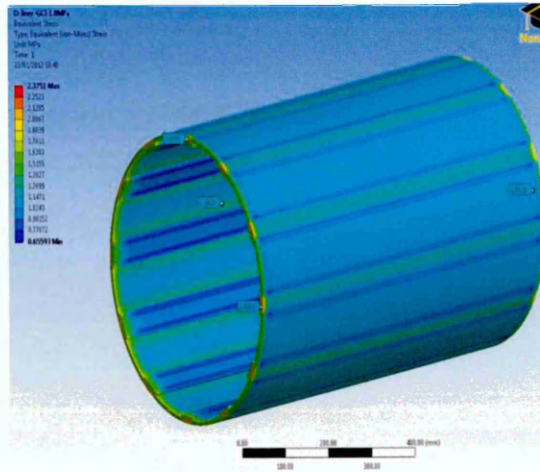
a) Structural steel   b) GCI
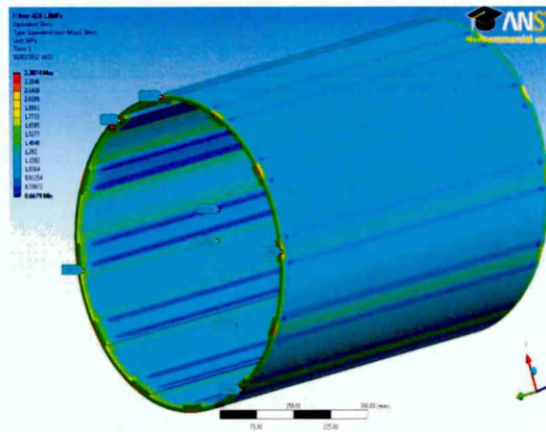
c) ADI

Figure A-B- 5 Stress induced in liner @1.8 MPa load

VI. <u>**Deformation pattern in 430 mm extruder liner -for applied load of 1.8 MPa:-**</u>
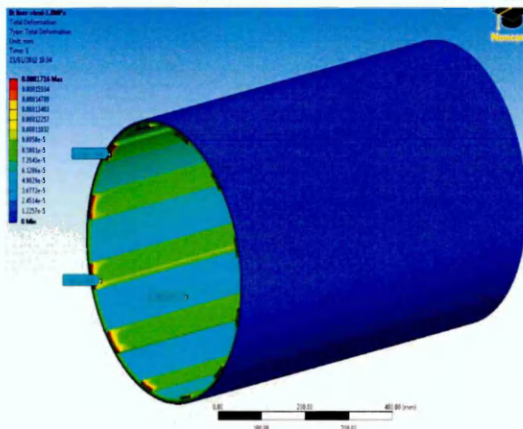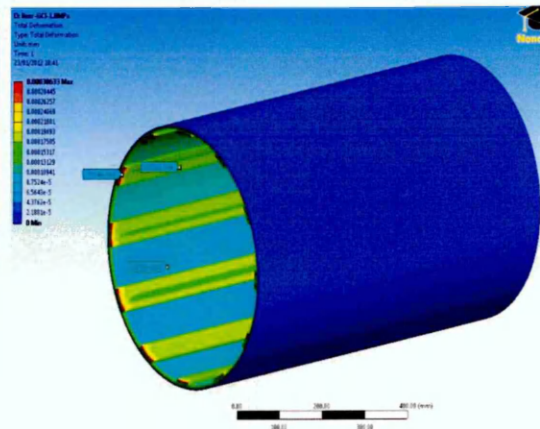
a) Structural steel   b) GCI
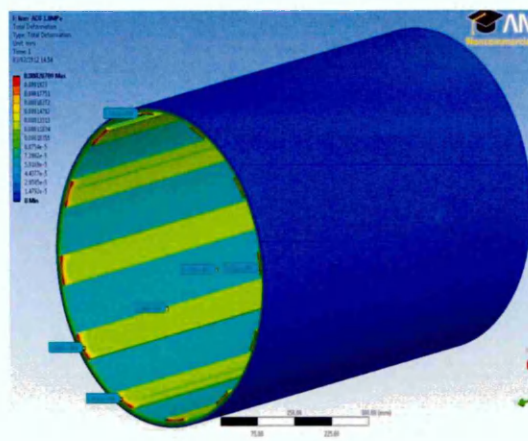
c) ADI

Figure A-B- 6 Deformation in liner @1.8 MPa load

VII.   Stress distribution pattern in 430 mm extruder auger shaft- for applied load of 1.8 MPa:-

a) Structural steel
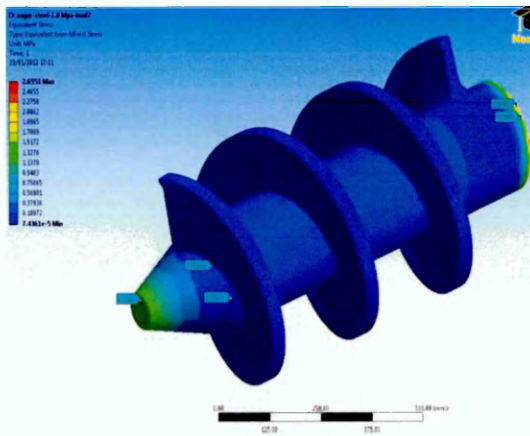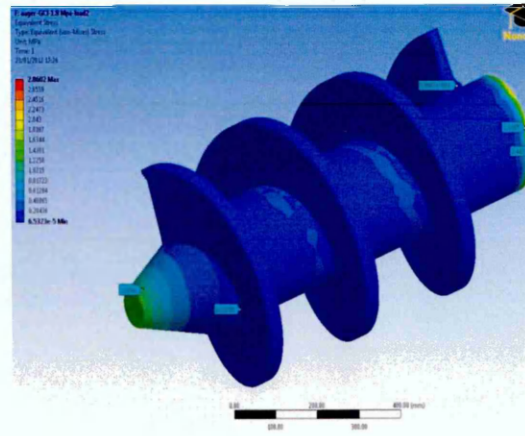
b) GCI
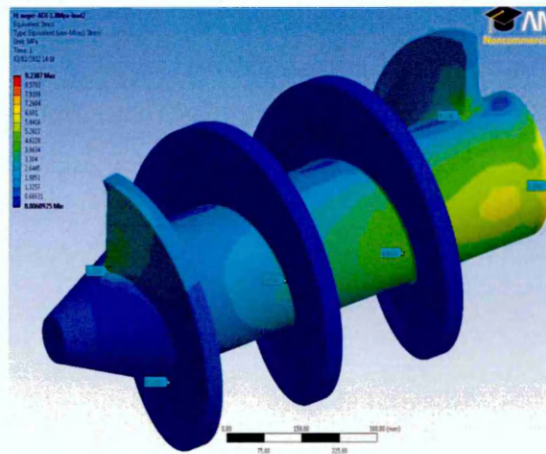
c) ADI

Figure A-B- 7Stress induced in auger shaft @1.8 MPa load

a) Structural steel   b) GCI

c) ADI
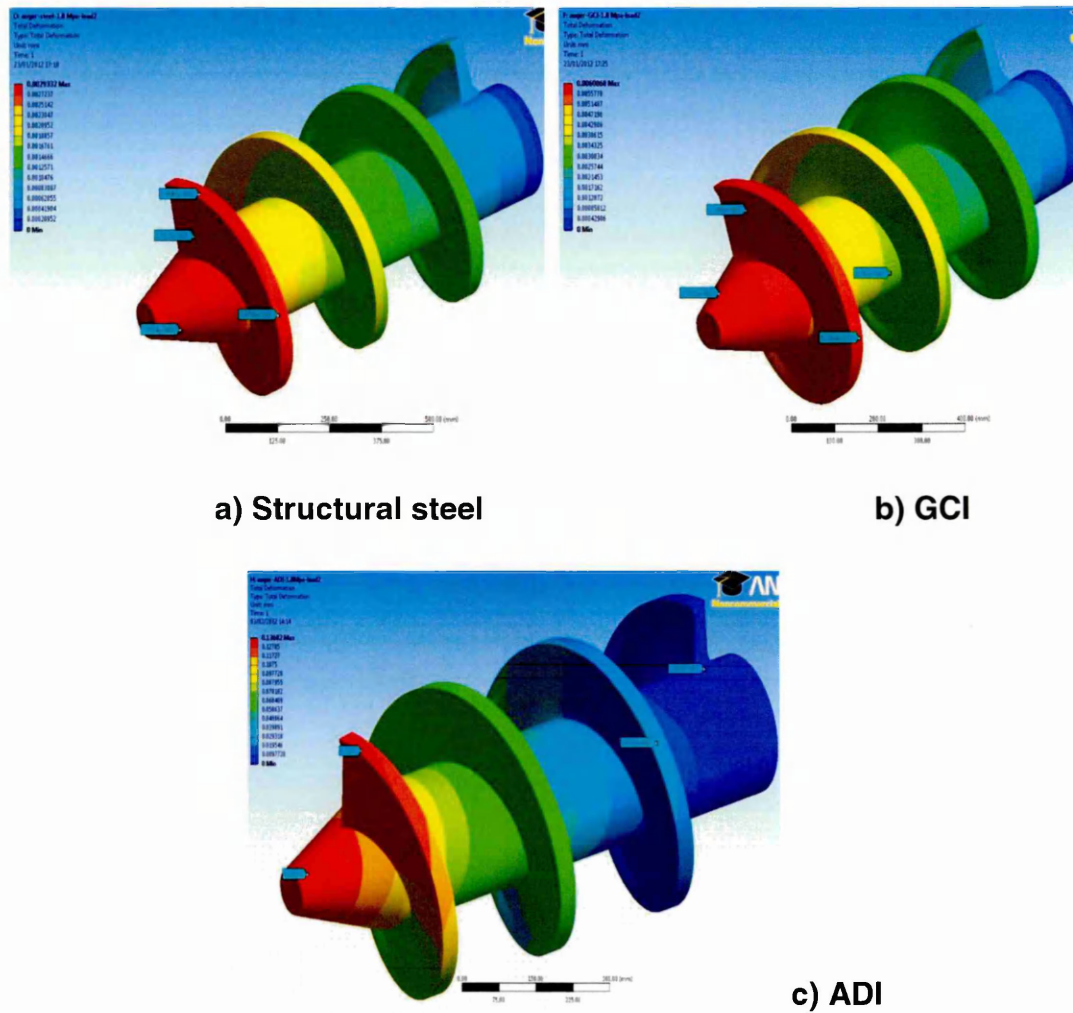
Figure A-B- 8 Deformation in auger shaft @1.8 MPa load

Appendix-C

Brick industry and the brick-making process

Prospects for global brick industry

Globally the ceramic industry is considered to be among the other major revenue yielding industrial sectors, which offers significant contribution to the economy by creating jobs and income. Brick being the favourable construction material, brick industry shares the major percentage of output produced within this sector. The global brick production has increased rapidly over the past few decades, due to increase in demand in the housing market from both developed and developing countries. Of the various countries that produce bricks, China remains the largest producer of bricks with an estimated production of more the 700 billion bricks in 2000 and showing an increasing trend for the future **[CESST, 2000]**. India remains in the second place with more than 140 billion bricks being produced per year **[Asian Institute of Technology, 2003]**. The other major producers include USA, which produced around seven to nine billion bricks during the year 2010 **[Madehow, 2012]**. Ceramic industries in European Union (EU) do play a significant role in the global market for producing quality ceramic products. It accounts for 25% of the total global production **[European ceramic Industry Association, 2012]**. The major producers in EU include U.K, Spain, Germany, France, Italy, Czech Republic, Poland and Hungary.

Given the scale of production capacities of brick industries globally, it is clearly understandable that the amount of energy consumed by brick industries is high. It is also considered to be one among the other major energy intensive industries that uses fossil fuels, coal and gas for its various operations.

U.K. Brick industry- future prospect and challenges

In 2010 the U.K brick industry was valued to be £395 million annually, and it was predicted to rise on an average of 4% over the next five years and is expected to reach £471 million by 2015 and is expected to grow further in the future **[AMA research limited 2011]**. Gas and coal are the major sources of fuel used in UK brick industries **[Department of Technology and Industry-2006]**, and the energy consumed by the industry accounts for 1.5% of the total energy consumed by all manufacturing industries and it is estimated to

be approximately 5.4TWh **[Brick Development Association, 2011]**. It accounts for more than 30% of the total cost incurred by the industry **[European Ceramic Industry Association, 2012]**.Though it appears to be less in value, considering the current global situation on the availability of fuel sources and the predicted future demand for bricks, it is a very significant amount.

The other major challenges faced by the brick industries globally and in the U.K include reduction in the level of energy consumption and pollutants (mainly CO_2, Hydrogen fluorides and particulates) released from its various processes. Through the use of advanced technologies, improved machines, operating procedures and energy regulation policies, the modern brick industries are considered to be more energy efficient compared to what was available in the early 1970's. A typical energy consumption pattern of UK brick industries from 1970-2010 is presented in Figure A-C- 1.
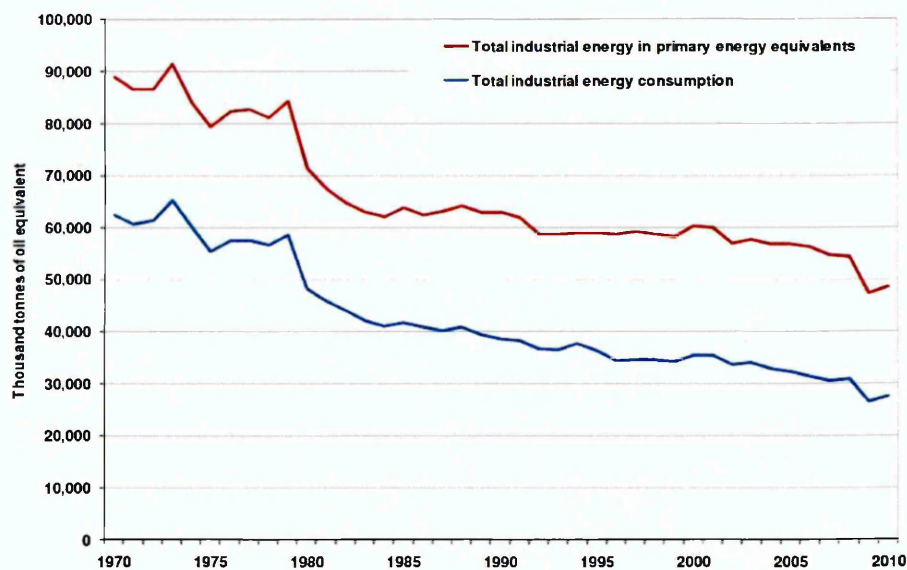
Figure A-C- 1 Energy consumption pattern of U.K brick industries

[Source: DECC, U.K 2011]

Though the energy trends indicate that there is a significant reduction in the energy consumed, the growing concerns about the climate change and implementation of new environmental legislations has left the UK brick industries to face a tougher challenge in-terms of reducing the energy usage

and its impact on environment. Hence it is worth looking at what makes this industry energy intensive, which will be dealt with, further in this chapter.

Brick manufacturing

The process of brick manufacturing is a very complex process. It involves the use of heavy and rugged high performance power consuming machines and tools, right from obtaining raw materials to the finished product. A simple overview of the various process involved in the brick manufacturing is discussed below.

Manufacturing of bricks briefly involves the following key processes:

- Mining raw materials
- Storage of raw materials
- Preparation of raw materials
- Shaping
- Surface treatment
- Cutting
- Drying
- Firing
- Packing and despatch.

Figure A-C- 2 shows a simple schematic representation of various steps involved in a typical brick manufacturing process.
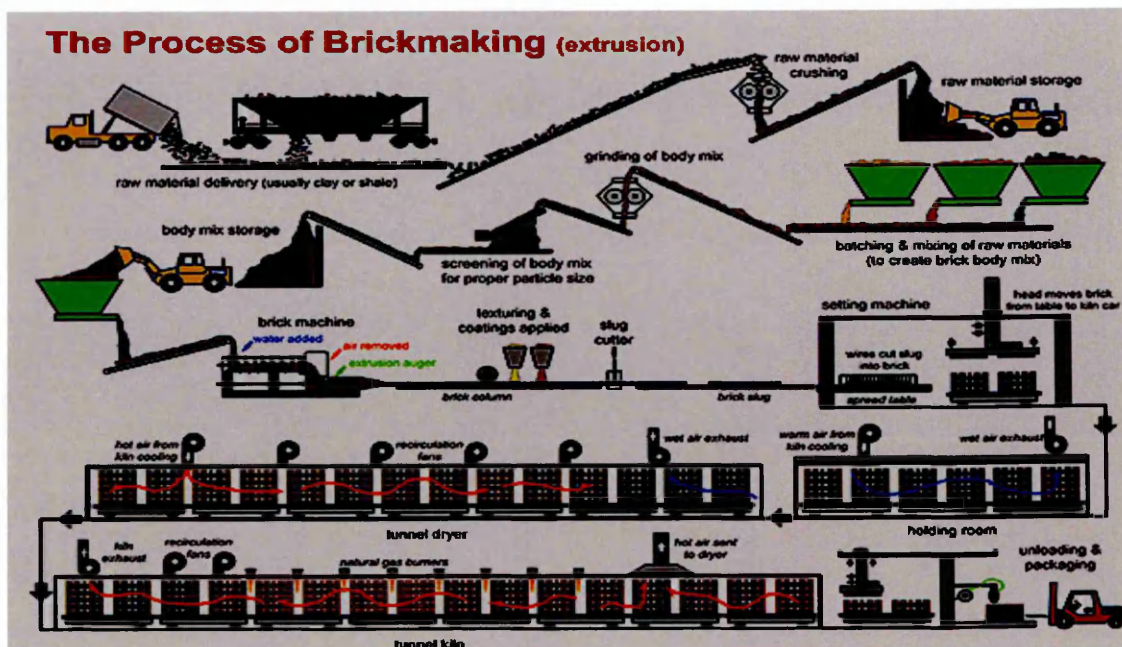
Figure A-C- 2 Typical brick making process flow diagram

[Source: Boral Limited 2002]

Mining raw materials

Clay and loam have been used for making bricks and other ceramic products for over one thousand years. It is formed by erosion and weathering of rocks, and gets deposited in different places due to the action of water and wind. Hence the major mineral constituents of clay are rock minerals **[Bender and Händle, 1982].** Depending upon the geographical location and age of deposit, the mineral and chemical composition of clay varies significantly and has a major influence on its flow characters during shaping and drying and in the aesthetics (like appearance and colour) of the final finished products.

Depending upon the raw material used and applications, bricks are broadly classified into three different types **[Petavratzi and Barton, 2007]**, namely:

• *Clay bricks (Burned bricks):-* This includes common building brick, facing brick, glazing brick, fire brick, flooring brick and Hollow brick etc.

• *Cementitious bricks:* - This includes bricks that are made up of cementitious material, which gets its hardness by chemical reaction- Example: - sand lime brick and sewer brick.

186

- **Adobe bricks**: - These types of bricks are sun dried bricks, unlike burned bricks which are dried in special chambers called Kilns (will be reviewed later in this chapter). The major constituent includes calcareous sandy clay or any alluvial desert clay with good plastic properties.

The chemical composition of typical pure clay will contain the following substances in respective proportions as indicated **[Petavratzi and Barton, 2007]**.

- Silica (50-60%)
- Alumina (20-30%)
- Lime (2- to 5%)
- Oxide of iron (5- 6%, but not greater than 7%)
- Magnesia (<1%)

It is clearly evident from the chemical composition that the major constituent of clay is silicates. Based on the mineralogical composition and presence of other chemical substances, clay minerals are classified into various groups as shown in Figure A-C- 3,
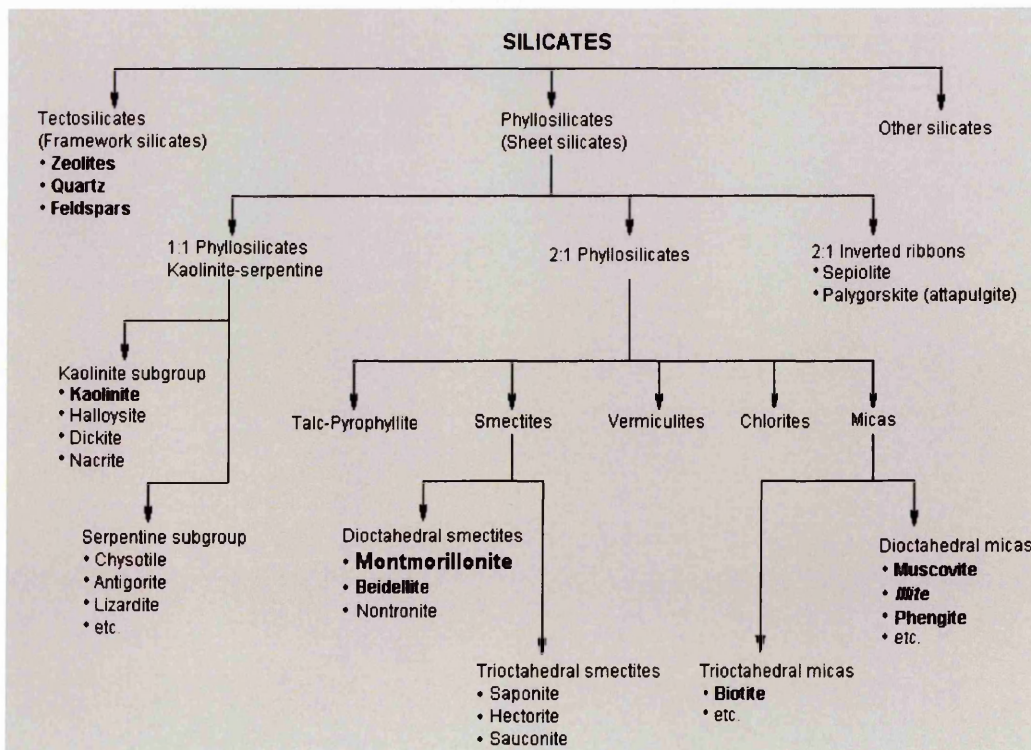
Figure A-C- 3 Classification of clay mineral groups

[Source: Punmia and Jain, 2005]

The major constituents of pure clay minerals are Kaolin and Shale and small amount of additives like manganese, barium. Other additives are blended with clay to produce different colours **[Punmia and Jain,2005].**

The major mineral constituent of the clay used in making bricks, in the United Kingdom, includes,

- Kaolinite.
- Illit.
- Illite.

The clay used in brick manufacturing is extracted from "Quarries". Quarry is a place where natural deposits of clay and mineral occur in significant proportion, considered to other geographical locations. It is essential to obtain approval from the government, local authorities and concerned environmental organisations before setting up a quarry. This is to ensure that quarrying operation is not affecting the surrounding localities, natural vegetation and do not possess any risk to humans or animals living in the nearby areas. Figure A-C- 4 shows the geographical location of various quarries, currently under operation in the U.K.
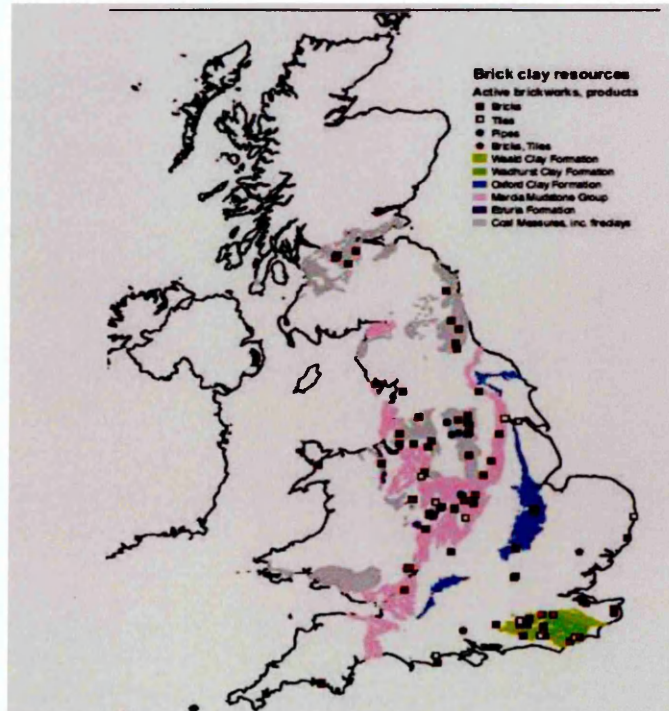
Figure A-C- 4 Quarries for brick clay in U.K

[DEFRA, 2007]

There are different ways of extracting clay from quarries. Depending upon the requirement and factors like economic and efficient operation of a quarry, there are two commonly used methods, namely a) Opencast mining b) Underground mining. Since open cast mining is accepted to be more economical compared to the other technique, it is widely used all over the world to extract clay used in brick making process. A few of the open cast methods includes Manual Digging, Mechanical extraction, Blasting, Hydraulic mining **[Bender and Händle, 1982]**.

Mechanical extraction is the most widely used method; a typical mechanical extraction using an excavator is shown in Figure A-C- 5.

Figure A-C- 5 Quarry operated with mechanical extraction process
[Source: lqsgroup]

Storage of raw materials

Clay extracted from quarries will be transported to the brick manufacturing facilities through suitable modes. Factories operating on a continuous and mass production process basis should be supplied with ample amount of raw materials, to meet their demands. Hence most of the brick manufacturing industries across the world store their raw materials within the factory or nearby area, enabling them for an easy and quick access during production. This is considered to be another main reason for such industries to be located near the quarries. There are different ways to store the raw material and the most widely used includes open-air storage, storage sheds, large volume feeders and silos.

189

Preparation of raw materials

The stored raw material is pre-processed before being used to make bricks. The pre-processing of brick clays mainly involves reduction of clay particle size to the required standards, blending of any additives as required for the products and process and adding or removing moisture to meet the required standard. The required size for clay particles is achieved by using bespoke mechanical equipment called pan mill. Size of clay particles and moisture content are two other important parameters that have influence on the flow characters of clay water mixture and hence in-order to have a smooth shaping process and better product, it is important to implement a controlled strategy at this stage of the production process. Recommended raw material size is 2-4 μm, before being mixed with water.

The flow character of clay and water mixture, used in brick making process and in other applications is defined by two variables namely Plasticity Index and Liquidity Index. The amount of water content determines the plasticity of clay during shaping process. Depending upon the type of shaping process the amount of water content varies. A typical stiff extrusion process has 7-14% of moisture content depending upon the clay type and extruding technique.

Shaping

Shaping is the next step involved in the brick making process. The required shape of a ceramic product, like brick, can be obtained through many techniques using manually operated and completely automated complex machines, commonly found in modern brick industries. It is a very important process which determines the shape of the ceramic body and also impacts the further processes involved, before the product is put into its final use. Based on the raw material conditions and product requirements, the most widely used and accepted shaping techniques are divided into four types, namely, Soft mud moulding, Extrusion, Pressing and Casting.

Soft mud moulding

It is one of the oldest and traditional methods of brick making. In simple terms it could be defined as filling up of lose clay with high plasticity, either

mechanically or manually, into a mould made up of wood or metal. Moulds made of up of wood were widely used. The clay-water mixture used in this technique is highly plastic, with water content approximately equal to 30% or even more sometimes, which gives the ability to have a dry shrinkage value between 6% - 8% [**Bender and Händle, 1982**], and also required to avoid insufficient strength of the product. The preferred or recommended plasticity value of clay water mixture used in this process is 4 mm - 6 mm residual height in the Pfefferkorn test. *(Pefefferkorn test is one among the other standard testing methods that are widely used and commonly accepted testing method in ceramic industries to measure the plasticity value of wet clay)* [**Wilkinson, 1960**].

Ceramic bodies like bricks, made out of soft-mud moulding are amorphous and solid in nature and offer a good protection during severe cold weather conditions. The different methods of soft-mud moulding techniques that were used are as follows,

1. Hand moulding

    A typical hand moulding process is shown in Figure A-C- 6.

Figure A-C- 6 Hand moulding process

[**Source: Bender and Händle, 1982**]

2. Mechanized moulding
   a. Soft-mud brick moulding machines with loose moulds

191

A typical brick production line with loose moulds setup is shown in Figure A-C- 7.
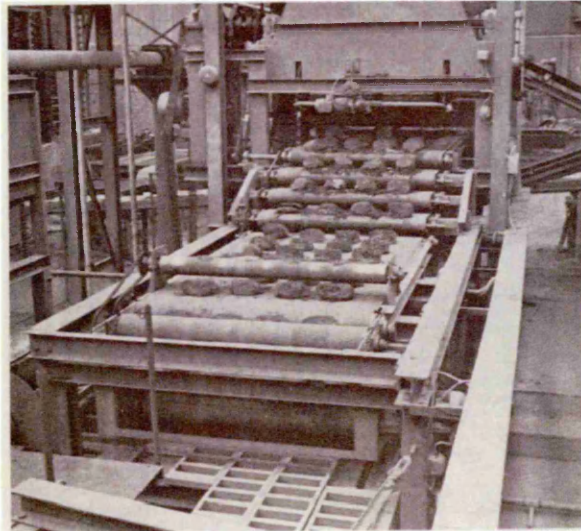
Figure A-C- 7 Mechanized soft moulding machine

[Source: Bender and Händle, 1982]

b. Mould-chain type soft-mud brick moulding

c. Mechanical soft-mud moulding

d. De-Boer soft-mud moulding:-

A typical De-Boer machine is shown in Figure A-C- 8
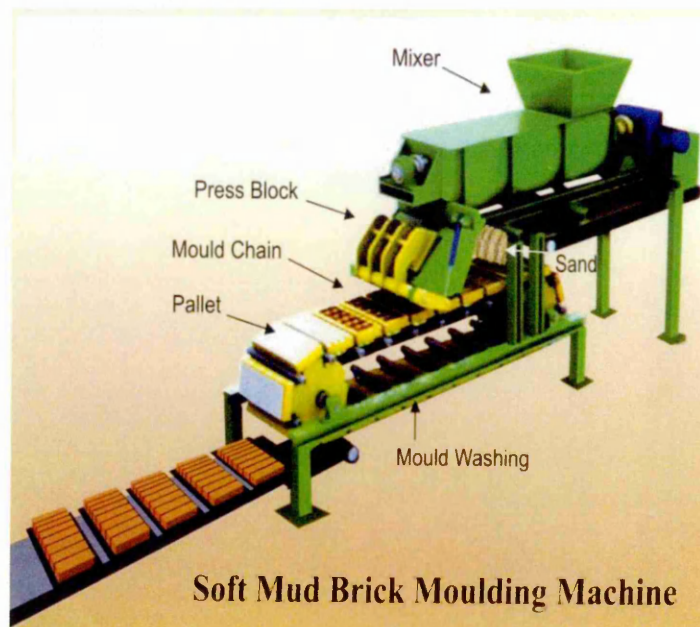
Figure A-C- 8 Typical De-Boer soft mud moulding machine

[Source: resourceefficientbricks, 2011]

e. The Aberson soft-mud moulding: A typical Aberson soft moulding machine is shown in Figure A-C- 9.
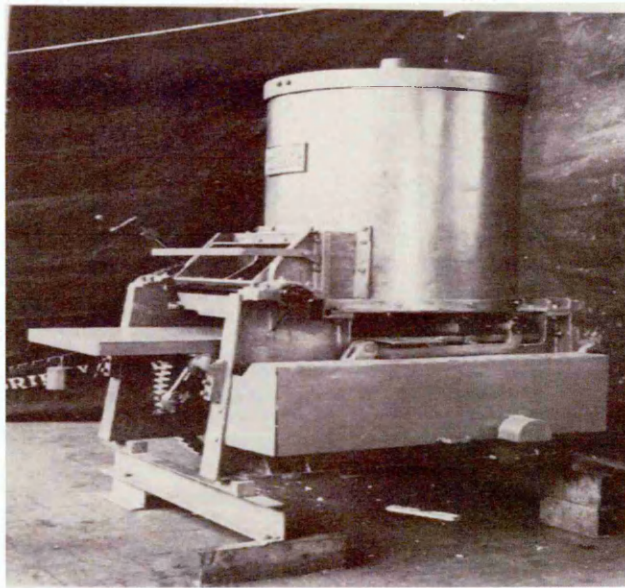
Figure A-C- 9 Soft moulding machine-Aberson type

[Source: Bender and Händle, 1982]

    f.   The Hubert soft-mud moulding.

A few among the main advantages of soft mud moulding includes lower power consumption compared to extrusion process, can be used for both small scale and large scale production and has a lower maintenance and operational cost.

Extrusion

Invented by Schlickeysen, more than 150 years ago **[Bender and Händle, 1982]**, extrusion is the most commonly used shaping techniques in large scale ceramic industries for manufacturing bricks, tiles and pipes etc. Vacuum extruder is one of the recent advancement from its predecessor, de-airing auger and it is an integrated unit that combines more than one operation involved in the ceramic product manufacturing, like mixing clay with water to prepare the "slip"(Plasticised clay), compress the slip to densify the mass and remove any trapped air with the application of vacuum, densify the slip further by forcing it through a chamber with auger shaft and then produce the required shape of the clay body by forcing it further through the die or mouth. The die or the extruder mouth resembles the required cross sectional shape of the final finished product. A typical vacuum type extruder, used in heavy clay industries, designed and manufactured by Craven Fawcett Ltd, U.K is shown in Figure A-C- 10.
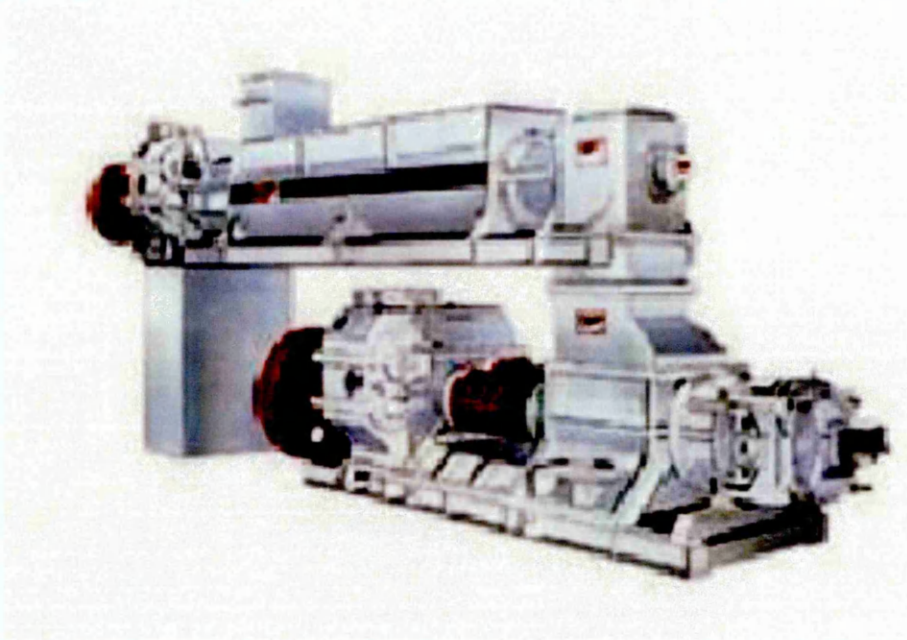
Figure A-C- 10 Vacuum extruder

[Source:-Craven Fawcett Limited, U.K]

The main aim of this research is to study in detail the flow process of wet clay within the extruder and assess its performance with respect to various design conditions. Hence a detailed review about the extruders, its performance characters and the process of extrusion is presented in Appendix- D.

Pressing

It is another type of ceramic product shaping technique, mainly used to manufacture tiles and bricks. In simple terms, the final shape of the ceramic body is achieved by applying mechanical compaction force to the raw material placed in an enclosed chamber called a die. A typical hydraulic pressing machine used for making tiles is shown in Figure A-C- 11.
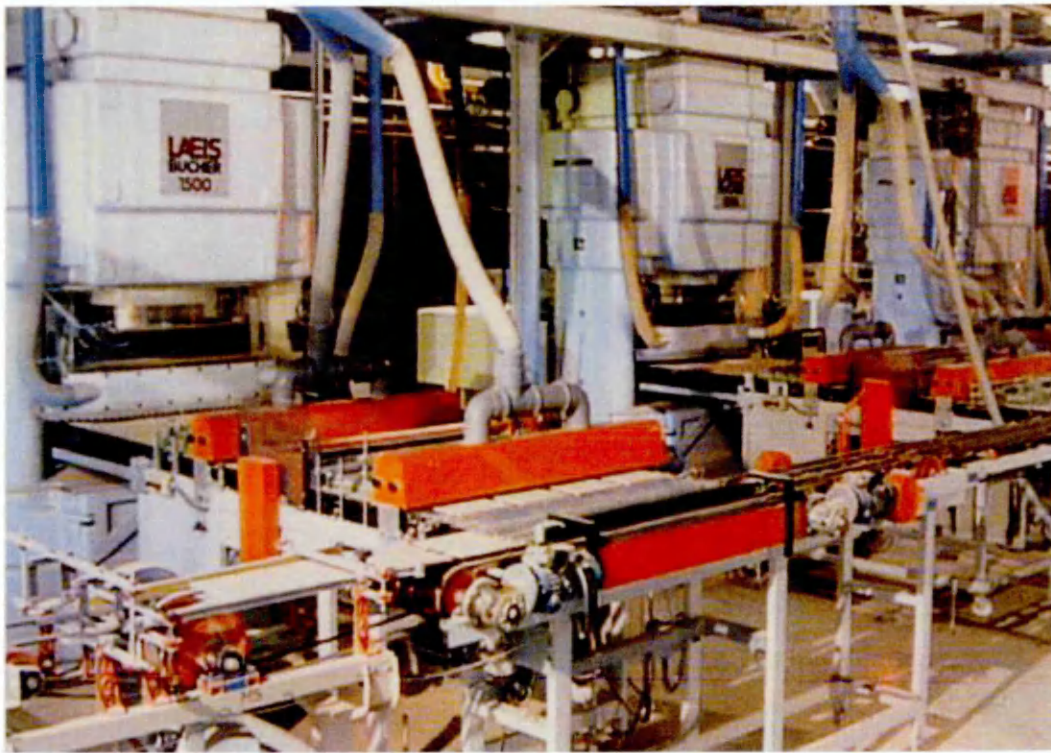
Figure A-C- 11 Hydraulic press type tile making machine

[Source:-American Ceramic Society]

Based on the pressing technique and raw material condition, the pressing process is classified into the following types,

1. Dry pressing
2. Isostatic Pressing
3. Semi-dry brick pressing
4. Tile pressing.

The shape and quality of the final product depends upon the pressure applied to compact the loose mass of clay and it varies with respect to the techniques used. Irrespective of the technique used, it is required to take a proper care regarding the pressure applied and die design, to have a better product. Most of the pressing techniques mentioned above involves three main steps - 1) filling the loose clay and water mixture (if required) into the bottom die cavity, usually attached to the bottom of the press, 2) applying pressure through the top die attached to a ram and 3) removing the formed product from the bottom die. The removal of final product from the bottom of die is an important step in pressing, as it often decides the final quality of the

product. If care is not taken at the design stage, it could result in major problems like cracking and irregular shape of final product. The achievable technical characteristics of the product, speed, simplicity and inexpensiveness of the overall production cycle has seen pressing technique to be used widely and extensively in ceramic industries.

Casting

It is similar to the casting technique applied in the manufacturing of metal components. Ceramic casting is another type of shaping technique, used mainly for making ceramic components like tableware, sanitary ware and advanced ceramics. There are different types of casting techniques used in the ceramic industries **[Händle, 2007]**, namely

1. Slip casting
2. Pressure slip casting
3. Capillary casting in plaster moulds
4. Pressure casting in polymer moulds.

The raw material condition and final product requirements determine the appropriate type of technique to be used. However the basic principle of manufacturing is same for all the above mentioned techniques. A suitable design of mould resembling the shape of the ceramic product will be made using Plastercine or Polymers or Acrylic or Plaster of Paris or clay and then the slip will be introduced into the mould. Slip in this case will be more like a thick liquid. This liquid mass will then be allowed to dry for a sufficient period, before it is removed. Depending upon the size and thickness of the product, the drying time varies from hours to days. The main advantages include the re-usability of the moulds, geometrical accuracy of components produced and adaptability to large scale production.

Electrophoretic shaping

Invented in the year 1809 **[Bender and Händle, 1982]**, it is a type of ceramics shaping technique, developed to a commercial scale for special requirements. This technique involves the use of electric field, applied to the raw materials, to achieve a preferred orientation of the clay particles in the

196

finished product. Since it is of not much relevance to this research work, it has not been discussed in this work. However if the reader is interested in exploring further about this technique, it is recommended to refer the above stated reference.

Summary of Shaping methods and its applications:

The shaping process in ceramic manufacturing varies widely with respect to type of raw material, size of the industry and quantity to be manufactured. It is an energy intense process, which requires a special attention to improve the overall efficiency of the whole production cycle. Hence engineers and industrial experts in this sector take an extra care while choosing the appropriate techniques to meet their requirement. Table A-C- 1 provides the details of various shaping techniques and their applicability for producing ceramic components based on the raw material condition and shapes **[Bender and Händle, 1982]**.

Raw material condition, Requirements, Shapes.	Hand moulding	Extrusion	Ram Pressing	Rolling, Milling	Ramming	Dry pressing	Isostatic pressing	Electrophoresi	Casting	Vibration
Cohesive material processing	+	+	+	+	+	x	X	+	+	
Materials with Low plastic	x	x	-	x	x	++	+	x	x	x
Material with high water content	+	+	-	-	o	o	O	+	+	x
Material with low water content	-	+	x	x	+	++	+	o	o	x
Material with high compact stability	-	x	x	x	+	++	+		-	-
Deaerated material	x	++	+	+			X	+	+	x

	1	2	3	4	5	6	7	8	9	10
Uniform compaction		+	+	+	x	x	++		x	-
High throughput	+	++			-		-		-	
Non standards material, in low numbers	+ +	x	+	+	++		X		+	
Products with certain texturation	+	+	+	+	x			x	+	
Product without texturation	-				x	+	++			
Dimensionally stable products	-		x			++	+			
Smooth surfaces	-	+	+	+	+	+	X	+	+	+
Rough surfaces	+	x	x	x	x	x	+		x	
Massive blocks	+	++			+	+	+		-	x
Tiles	+	+	+	+		++	+	+	x	x
Extruded products	-	++	o			o	O	x	o	
Compacts for presses & rollers		++						x		x
Roofing tiles	x		++							
Holloware	-		x		x	x	X		++	
Tableware			+	++		x	+			
+= Applicable; - = Inapplicable; x=Applicable with certain conditions										

Table A-C- 1 Various shaping techniques and their applicability

[Source: Bender and Händle, 1982]

Surface treatment

It is the process of introducing texturing, glazing, colour and coating to a ceramic product, to enhance the appearance of the product and make it appealing. Surface treatment is done mainly to give a specific profile or a colour to the ceramic products, especially bricks. Coloured bricks, textured bricks and profiled bricks are a few examples. There are many types of

surface treatment techniques been developed and used, such as Sanding, Profiling, Peeling, Colouring, Glazing, Coating, Brushing and Addition of Combustible materials.

During earlier days, ceramic products with different colours and shapes were of great appeal to the consumers. This led to the development and introduction of new techniques in surface treatment, by both small scale and large scale industries, to capitalise on the demand. But the increase in raw material cost has led small scale industries to concentrate less on this process and this factor helped the large scale industries to increase their market share.

Cutting

With the invention and advent of the extrusion technique in ceramic-brick manufacturing, which produces continuous mass of compacted green clay or wet clay, it was required to introduce a cutting system into the production process, especially in brick manufacturing, to produce bricks with certain length and width. The main function of the cutting system is to continuously cut the compacted mass that comes out of the extruder mouth to the required size. During the earlier days, it was done manually which is now replaced by far advanced, efficient and automatic mechanical cutters. A typical cutter system installed in a brick production line is shown in Figure A-C- 12.
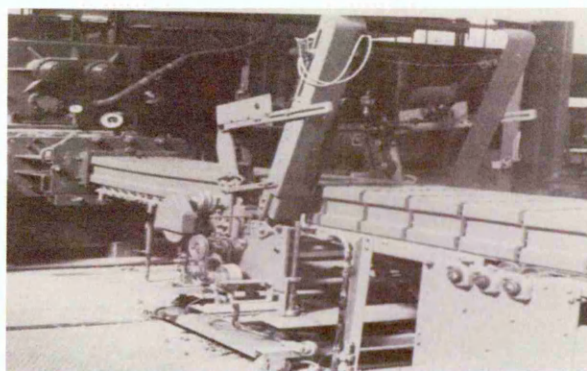
Figure A-C- 12 Typical cutting system used in a brick production line

[Source: Bender and Händle, 1982]

199

The cutting systems currently used in the ceramic industries are classified into two main groups -

1. Depending upon the cutting direction- Vertical cutters, horizontal cutters and segmental cutters.
2. Depending upon the type of cutter and application- column controlled cutters and fixed cycle cutters.

The most commonly used cutting tool is a thin metal wire of gauge size varying from 0.5 mm to 1.6 mm, depending upon the thickness of the compacted clay **[Madehow, 2012]**. In some special cases knives are used as a cutting tool. The appropriate cutting system and cutting tool depends upon the ceramic material processed, speed and economy of the overall production cycle.

Drying

Drying is defined as the process of removing water or moisture content from the compacted or shaped ceramic product. Drying is completed before the ceramic product is fired to achieve the final colour and strength. Drying also prevents the development of crack in the product during firing. The process of drying can be achieved either by applying mechanical forces or using thermal energy. The most common in practice is drying by using thermal energy, where a hot medium like gas or air (mostly air) is used to heat the wet ceramic product under a controlled atmosphere and remove the water in the form of vapour. It is to be noted that after drying, the ceramic product still retains some moisture in it and it is soluble in water. The two common types of drying system used in the ceramic industries are Tunnel dryers and Automatic Chamber dryers. The tunnel drying system is a single stage process, whereas the automatic chamber drying system involves more than one stage. Automatic transfer cars are used to transfer the ceramic product through the various stages of drying process. A typical tunnel drier is shown in Figure A-C- 13.
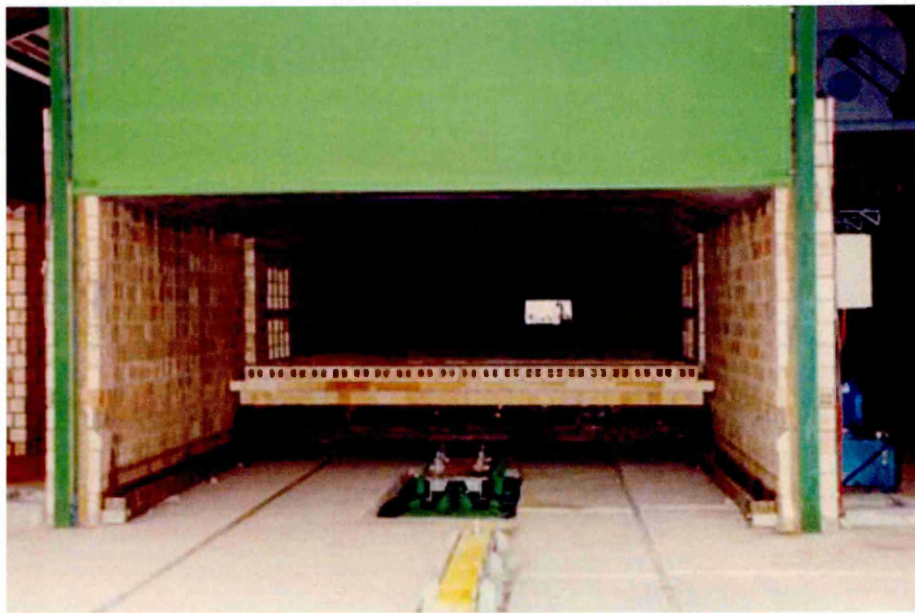
Figure A-C- 13 Tunnel dryer

[Source: Cereamtechno, 2013]

Firing

Firing is the final process involved in the manufacturing of ceramic products used in structural applications. It helps the ceramic product to achieve required compressive strength, build strong cohesion between the particles and introduces colouring. Since it is the final process, any additives that are required to produce a ceramic product with certain features must be added before the firing stage, mostly at the raw material preparation stage.

The firing of green bricks (wet bricks) vaporises the water content left after the process of drying and induces chemical reaction that involves production of gases. Most of the gaseous products are hazardous in nature for both the environment and to the humans (CO_2 and Hydrogen Fluoride). Flu gas treatment is another important area involved in the design of efficient, cost effective and environmental friendly ceramic industries. Since it is of not much interest pertaining to this research work, it is not reviewed in detail.

The process of firing takes place in a closed and controlled chamber called a "Kiln". Since the invention of kilns for firing process there have been many developments to increase the efficiency and safety of this process. Though there are different types of kilns, which are operational in ceramic industries

worldwide, one type of kiln which is very common and used in brick manufacturing is "Tunnel Kilns". Tunnel Kilns are further sub divided into different types based on the firing arrangement. The features like economical operation, faster heating time, increased capacity and safe design has offered the advantage for tunnel kilns to be preferred over the other types. Typical types of tunnel kilns are shown in Figure A-C- 14 and A-C- 15.
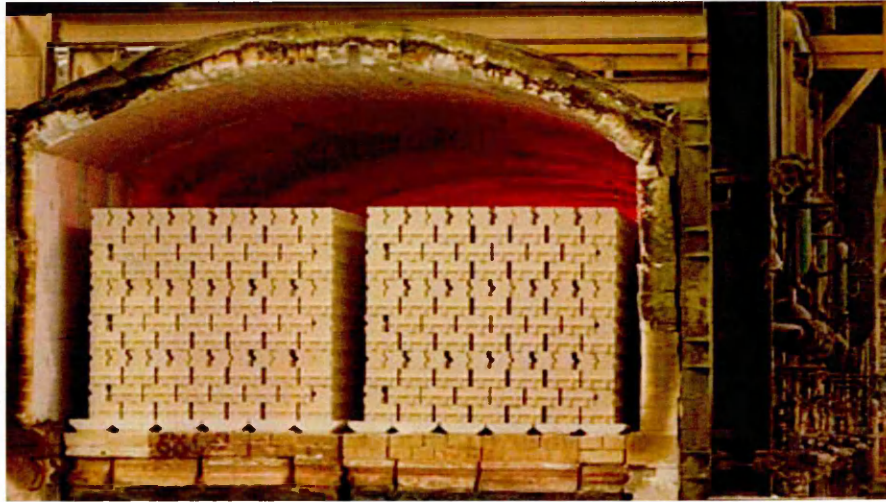
Figure A-C- 14 Tunnel kiln-Type I

[Source: Shinagawa Refactories, 2013]

Figure A-C- 15 Tunnel kiln-Type 2

[Source: West Lothian Archaeology Group, 2013]

Packing and Dispatch

The final stage involved in ceramic (brick) manufacturing process is storing the product that comes out of the kiln in an appropriate place and keeping it

ready for final inspection and dispatch. Considering the number of products that are produced, it is physically impossible to check the products individually for the required quality and hence random visual inspection techniques are used at every stage during the production process, to make sure the product meets the required standard. The products that pass the quality check will then be stored appropriately before being packed and transported to the end users. The products that fail the quality check are either re-used along with virgin raw materials for making new products or as aggregates. So in simple terms, there is no waste of product, but the energy consumed is still lost and hence products with defects are not preferred by the industries. Packing involves the use of wooden pallets or boards made up of plastic, onto which the bricks are arranged in a specific pattern to ensure that the load is evenly distributed and suitable provisions will be provided to withstand the weather conditions and avoid damage during transportation. Mechanical or automatic wrapping machines are widely used in packing applications.

Conclusion

It is clearly understood from the above discussion that the ceramic industry, especially brick manufacturing, involves the use of both heavy and light duty mechanical and electrical systems to achieve the required objectives. Considering the demand for bricks and the volume of production, it is impossible to replace it with a human workforce and also it is not good practice, hence the use of power consuming machines is inevitable. So for the longer sustainability of the brick industries in terms of its power consumption and environmental impact, it is necessary to identify and undertake suitable developmental work in all possible areas of the manufacturing cycle on a regular basis. With the availability of advanced computing methodologies and simulation based techniques, improvement in certain processes and in design of machines used in brick manufacturing can be accelerated. This research work is one such effort to demonstrate the application of CFD and FEA techniques towards improving the process of brick making in heavy clay industries.

Appendix-D

Extruder and the process of extrusion

Introduction

Shaping is an important function in the process of brick making or in any ceramic product manufacturing. It is also a major power consuming processes. Most of the brick industries in the U.K and worldwide uses combined de-airing type extruder to perform this function. As discussed in previous chapter, due to certain inherent functional aspects, these types of extruders are used widely. The aim of this chapter is to review the history of machines used in extrusion process, general design principles applicable in the design of combined de-airing auger extruders and the flow parameters that govern the design and power consumption of extruders together with the process of shaping.

Developments in extruder

A wide variety of mechanical systems have been developed and used for the purpose of shaping ceramic products since the earlier days. However only a few of them were very successful in achieving the intended functional requirements and used widely. This includes the following,

- Piston extruder
- Expression rolls
- Electrophoretic extruders
- Auger extruders

Piston extruders

The use of piston extruders began in the year 1807, with the invention of a hand operated piston extruder used in making drainage pipes **[Händle, 2007]**. As the name suggests, the working mechanism of this machine is mainly based on a piston moving inside a closed chamber that pushes the clay material through the die or mouth, predominantly in a vertical direction. The main problems faced with this type of machine includes filling up of raw material after every cycle of operation and removal of air entrapped in the raw material. Even though design changes were made to overcome these problems, to gain acceptance in the ceramic industries for manufacturing

structural ceramic products, the piston extruders played a less significant part in ceramic industries. A simple vertical piston extruder developed and used in the year 1880 is shown in Figure A-D- 1.
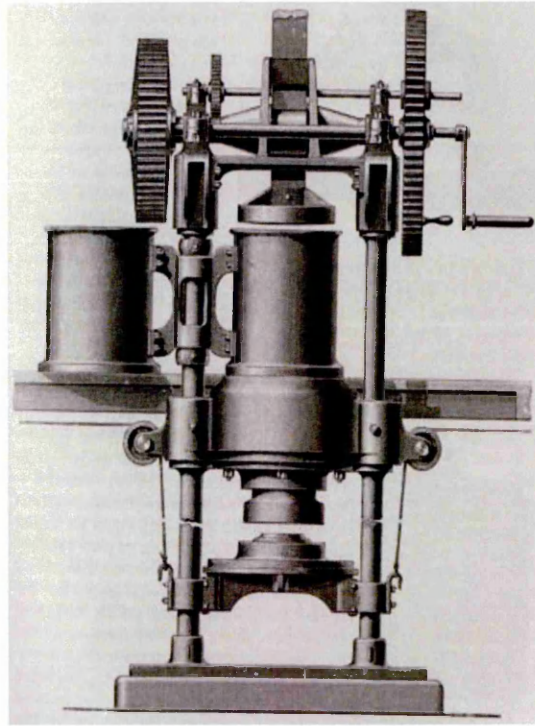
Figure A-D- 1 Piston extruder

[Source: Händle, 2007]

Expression rolls

The process of extruding a continuous column of clay by pushing it through a die through a connecting element called a pressure head was born with the introduction of Expression Rolls in 1830 **[Händle, 2007]**.The first machine designed by the Englishmen Ainslie **[Händle, 2007],** served as a blue print for future machines built using the same principle. Expression rolls capable of extruding both in vertical and horizontal direction were built and used in ceramic industries, especially for making thin tiles. "Europresse" is one of the most notable developments from the earlier designs of expression rolls. It is also called as augerless extruder or rotor type extrusion machine. This type of machine was used for extruding ceramic product with more than one layer (multilayer) and each layer will be made up of different or same raw material. Due its technical advantage and less defect in the extruded product it gained

its popularity in fine and advanced ceramic industries. A typical Europresse type Expression Roll machine is shown in Figure A-D- 2.
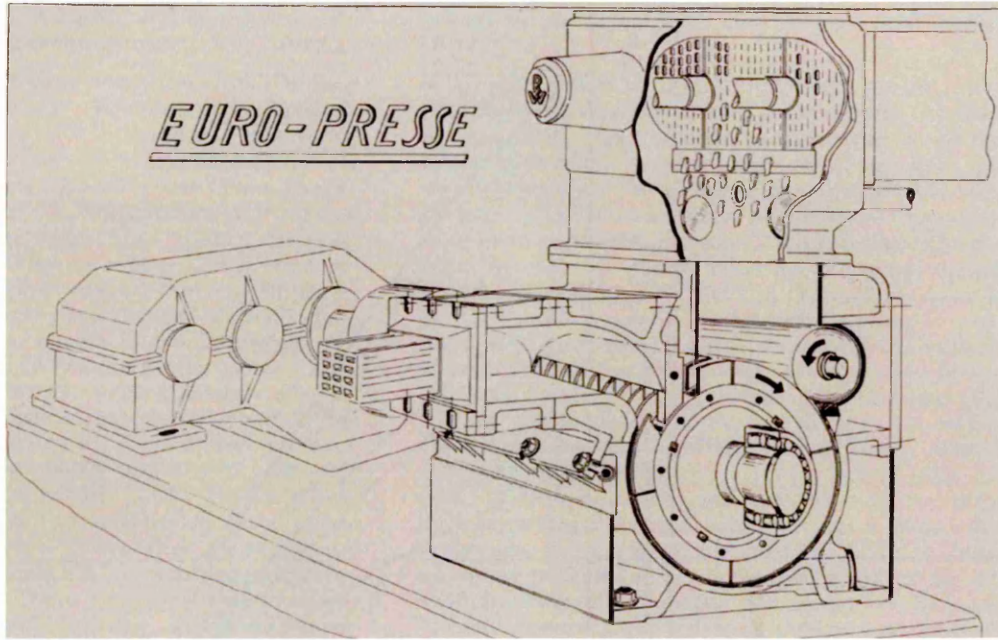
Figure A-D- 2 Europresse extruder

[Source: Bender and Händle, 1982]

Electrophoretic extrusion

Electrophoretic extruder is similar to Expression Roll machine; it was introduced and used in ceramic industries by 1977. The machines were built based on the principle of "Electrophoresis" and is used for special applications in ceramic industry. Due to the complexity involved in the design and operation of these machines it was seldom used in the structural ceramic industries. A typical electrophoretic extruding system is shown in Figure A-D- 3.
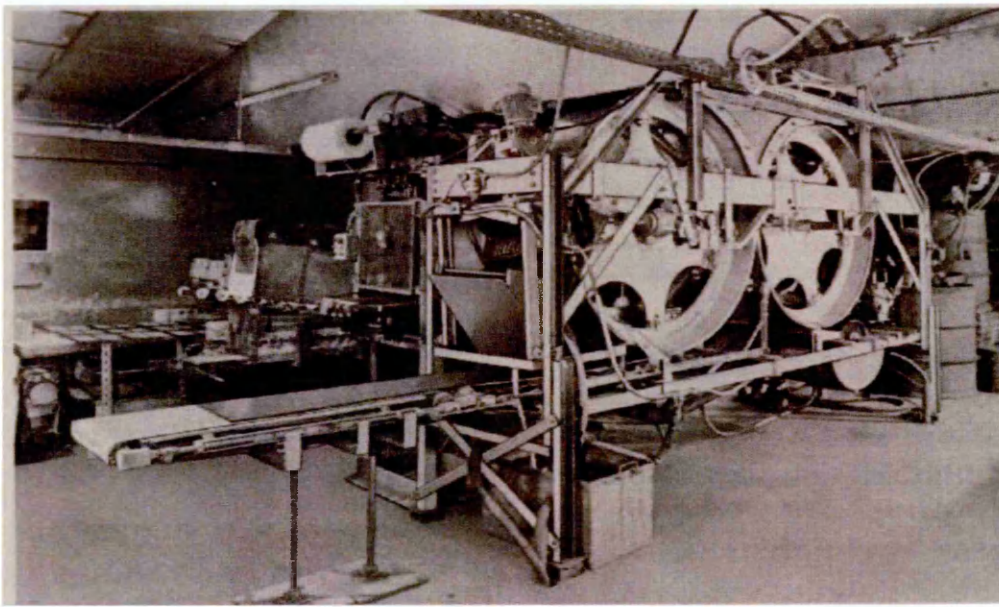
Figure A-D- 3 Electrophoretic extruder

[Source: Bender and Händle, 1982]

Auger extruders

The use of auger extruders in the process of shaping structural ceramic products began in the year 1855, with the introduction of Carl Schlickeysen's "Patent Brick Making Machine"- an upright machine for extruding clay columns **[Händle, 2007]**. Thereafter, driven by market requirements and demands, the auger extruders underwent a series of rapid development processes in various aspects to make it a more operator friendly system and meet the mass production requirement. Auger extruders capable of extruding both in vertical and horizontal direction were developed and used for specific purposes. Even though there were different types of auger extruders developed and they all can be grouped into the following three categories,

- Auger extruder without de-airing
- Auger extruder with vacuum device installed in extrusion barrel
- Combined de-airing extrusion units consisting of auger extruder, vacuum chamber and mixer.

Auger extruders can also be classified into different types based on the process and design features. The various types that fall under such classification includes,

208

- Range of application.
- Product to be extruded - bricks, tiles and pipes etc.
- Auger shaft arrangement and direction of column exit- upright extruder, horizontal extruder, vertical extruder, hinged type extruder.
- Extruder barrel diameter.
- Number of auger shafts- single auger shaft extruder, combined single auger de-airing extruder, twin shaft extruder, multiple shaft extruder.
- Consistency of the body to be processed.
- Extruder barrel design- cylindrical, conical, combined (cylindrical/conical), enlarged barrel, expanded barrel, stepped barrel, noodle barrel.
- Design and mounting of augers-progressive pitch, acute or decreasing pitch, linear pitch, combined pitch.
- Special extrusion methods-twin layer extrusion, multiple column extrusion, hot extrusion and vacuum extrusion.
- De-airing device used.
- Design of the extruder elements- auger, housing, infeed device and barrel liners etc.
- Design of the de-airing mixer.
- Design of combined de-airing extrusion unit- configuration of mixer and auger shafts, method of connection between the extruder and mixer and the construction of de-airing mixer.

The most important types in the above said classifications are based on application and consistency of the body to be processed, which is elaborated below.

Extruder classification based on application

Based on the shaping effects, body composition, degree of fineness of the raw material, throughput and extrusion pressure the extruders are classified into three categories namely, extruders used in heavy clay industries, fine ceramic industries and advanced ceramic industries. Auger extruder in heavy clay industries is used for direct shaping process to achieve the final shape of the product, example brick and pipe. Whereas in fields like advanced

ceramics and fine ceramics, it is used for homogenising, de-airing and improving the plasticity and density of the clay material before the final shape of product is acquired through other means.

Extruder classification based on body to be processed

The raw material to be extruded varies hugely with respect to products or even for the same product it might vary in mineral composition and moisture content. This influences the extrudability of the material and also the function of the extruder to a greater extent. Based on the moisture content and pressure developed during extrusion the extruders can be classified into three categories namely low, medium and high pressure extruders. Table A-D- 1 provides a rough guide on the classification of extruders based on process.

Type of extruder		Low pressure	Medium pressure	High pressure	
Description of extruder		Soft	Semi-stiff	Stiff	
Parameter	Dimension	1	2	3	4
Moisture content	% (dry basis)	10-27	15-22	12-18	10-15
Extrusion pressure	Bar	4-12	15-22	25-45	up to 300
Penetrometer	Nmm^{-2}	<0.20	0.20-0.30	0.25-0.45	0.30

Table A-D- 1 Extruder classification based on process parameters

[Source: Händle, 2007].

It is recommended to refer "Extrusion in Ceramics", mentioned in the reference section of this report, for more details on the classification of auger extruders.

De-airing extruder

Of the various development works that were undertaken with respect to the design of an extruder system, the most notable and successful work includes

the development of de-airing extruders. De-airing is the process of removing air particles trapped in the clay-water mixture, before being extruded into continuous column. This helps to increase the plasticity of the mixture and extrude a dense mass. Failure to do so will cause problems like lamination, void formation and blistering. The earlier designs of extrusion system had the de-airing units located separately from the extruder. This type of design offered certain process advantages like multiple de-airing and less sophistication in design. The main disadvantages were blockage, back pressure and uneven de-airing. This led to the development of combined de-airing extruders or vacuum extruders around 1935 **[Händle, 2007]**. In simple terms a vacuum extruder incorporates the mixing, de-airing and extruding unit in a single system, arranged sequentially. Compare with other earlier designs of extruders, vacuum extruders possessed a numerous advantages. Like better efficiency, adoptability for mass production requirement (modern vacuum extruders are capable of extruding 15000-20000 bricks per hour), manoeuvrability and quality of extrudate. These factors favoured it to gain its popularity in structural ceramic industries in a very short time. Based on the design, arrangement of pug mill, extruder and extruding direction, the vacuum extruders can be classified into different types. The basic building blocks of any vacuum extruder include pug mill or the mixing chamber, primary compression zone, vacuum chamber, extruder, die and drive system. An overview of each component is presented below. A typical vacuum extruder designed and built by Craven Fawcett Limited, U.K is shown in Figure A-D- 4 for the purpose of understanding.
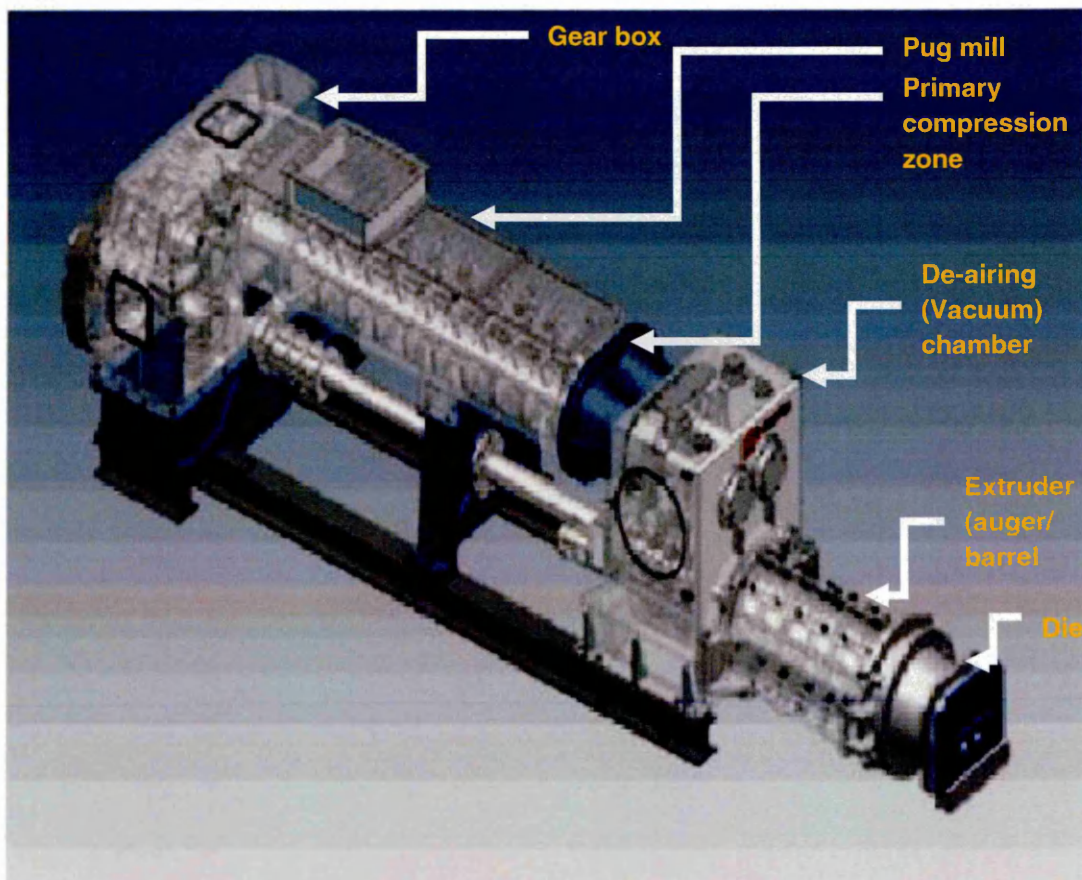
Figure A-D- 4 Vacuum extruder-Centex model

[Source:-Craven Fawcett Limited, U.K]

Pug mill

Pug mills or the mixing chamber is a semi enclosed metal chamber, mostly u-shaped, placed before the vacuum chamber. It will be either in line with the extruder or placed above the extruder (most of the extruders designed and manufactured by C.F Ltd, have the pug mill aligned parallel to the extruder's axis of rotation). It is where the right sized clay particles (usually >2 μm and <4 μm) that comes out of a rotary silos is mixed with water, supplied through controlled pipe lines. A rotary silo is a rotating drum made up of wire meshes of different size, used to filter the over sized clay particle. A fairly homogenised mixture of clay and water is acquired through the rotating shaft equipped with paddle or knife like structures placed in this chamber. Most of the machines used in Europe consist of a twin mixing shaft arrangement in this chamber. Though a 100% homogenised mixture cannot be achieved through this type of arrangement, it is accepted in the industries as a better and more efficient system compared to the earlier systems. This type of

design offers a great flexibility in controlling the moisture content either automatically or mechanically, with respect to the quality and stiffness of the extrudate. A typical pug mill with a twin shaft mixer arrangement is shown in Figure A-D- 5.
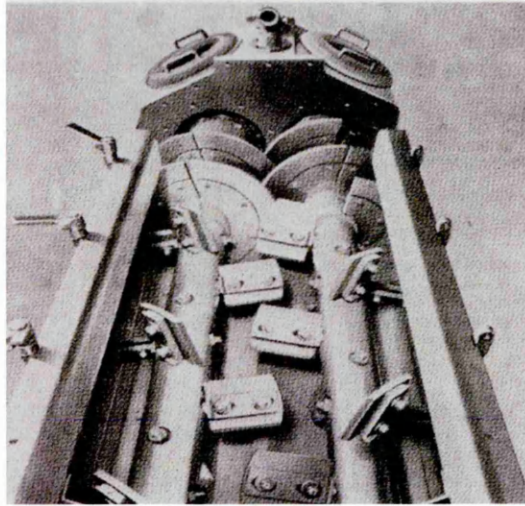
Figure A-D- 5 Mixing chamber

[Source: Bender and Händle, 1982]

Primary compression zone

The connecting element between the vacuum chamber and the mixing unit is called the primary compression zone, and it is shown in Figure A-D- 4. In industries this unit is designed with various shapes and accessories attached to it, depending upon the requirement. In most of the design there will be a twin conical chamber fitted with small augers in each chamber. The main function of this unit is to compress the loose wet clay transported from the pug mill into a mass of substance with medium density called "slip" (as mentioned in Appendix- C). This helps in creating a bond between the loose clay and water and removes the trapped air content to a certain extent. The compressed mass is then cut into suitable lengths using a cutter arrangement placed at the downstream side of the chamber, in order to maximise the efficiency of the de-airing process that follows.

De-airing (or) vacuum chamber

The concept of de-airing and the need for it was been discussed earlier in this chapter. The process of de-airing is achieved by many ways; however in

modern combined de-airing and vacuum extruders, this is achieved by using a vacuum pump mounted on top of an enclosed chamber; typical arrangement of a vacuum chamber is shown in Figure A-D- 4. The slip, after being sliced to the required length from the preliminary compression zone is made to fall into the vacuum chamber by the action of gravitational force; the vacuum created in this chamber facilitates the air, from the slip, to escape in the direction of suction. The de-aeration depends on few factors like the vacuum created, specific surface area of slip and on the duration of the vacuum **[Bender and Händle, 1982]**. The de-aired mass of clay will then enter the charging zone or the extruder section.

Extruder

The extruder used in modern machines is a simplified version of earlier designs and resulted from the process of continuous development. The extruder section is sub-divided into two main zones namely a charging and compression zone. The main elements that contribute to these zones include auger shaft, barrel, and barrel liners. Figure A-D- 6 shows a typical barrel and an auger shaft used in one of C.F Ltd's vacuum type de-airing extruder system.

Barrel   **Auger and shaft assembly**
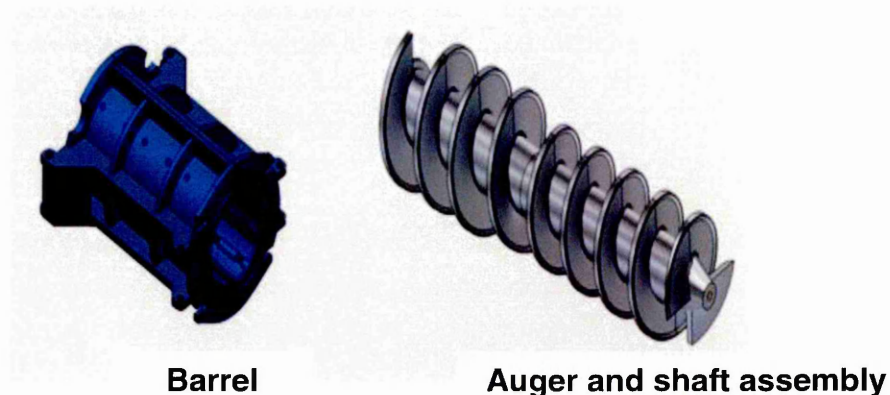
Figure A-D- 6 Components of an extruder system

Charging zone is where the severed slip from the mixing chamber gets accumulated before it enters into the compression zone. To ensure a uniform feed of clay during the process of continuous extrusion, maintaining a certain level of clay in this zone is important. This is achieved by using sensors and other suitable means of measuring. An excess accumulation of clay in this

214

zone could cause deaeration problems and cause severe damage to the machine by means of overloading.

The auger is an integral element between the charging and compression zones. The slip from the charging zone is carried forward by these augers and in order to accommodate the uncompacted nature of the clay and achieve reliable throughput, the diameter of auger in the charging zone will be slightly larger than the diameter of auger in compression zone. Suitable design provisions are available in modern extruders, to prevent the clay from sticking and rotating along with auger (paddle shaft is one such example).

The extended auger shaft from the charging zone is enclosed within a cylindrical barrel along with liners, which constitutes the compression zone. The uncompacted mass of clay that enters the compression zone is mixed well to achieve a good homogenised mixture of clay and water and then will be pressed together to form a compacted mass. Any air entrapped further will be removed because of this pressing action and suction pressure created by the vacuum pump in the charging zone.

Die

The die or mouth is the final element in an extruder system. A continuous mass of clay is produced because of the rotation of the auger shaft within extruder section will force the compacted clay to pass through the openings in the die section. The opening at the downstream side usually resembles the required cross sectional shape of the extruded product. The earlier designs of extruder, used in commercial scale include a pressure head, connecting element that links the extruder with the die (similar to those used in expression rolls, discussed earlier). The compacted clay will be pushed into the die or mouth through the pressure head to acquire the intended final shape of the extruded product. A careful consideration to the flow conditions and extensive field knowledge has led the design engineers to integrate the pressure head and die into a single unit. A further brief review about the flow process and related flow parameters for the die section of an extruder is presented later in this chapter. Other significant design advancements in the die design includes dies with core used for manufacturing perforated bricks

215

and hollow blocks etc, and dies with external lubrication arrangement, used for extruding slip with very less moisture content.

Drive system

The power required to rotate the auger and shafts in the mixing chamber is obtained through the drive system. The drive system has undergone a series of many notable developments that includes the use of steam power, electrical motors and the most recent advancement is the use of planetary gear boxes. As discussed earlier, the drive system design is another category for classifying extruders. Most of the modern combined de-airing type extruder drive system comprises an electric motor combined with a gear box. The electrical motor (mostly squirrel cage motor, due to the flexibility of speed control) acts as the primary power source which drives a gear unit, designed suitably to achieve the required speed with respect to the extrusion rate required. The electric motor will be coupled to the gear box either directly or through stepped pulley and belt drive arrangement or through a clutch system. The gear box will be directly coupled to the shafts in the extruder and mixing chamber.

Usually a common drive system exists for both the shaft, but there are extruders with separate drive units for auger and mixing chamber. The advantage in the latter case is it offers better control of the extrusion process and reduces complexity in design requirements; the main disadvantage includes the capital and running cost incurred.

Process of stiff extrusion

The technical aspects of a stiff extrusion process are very sophisticated and during years of its extensive use in industries, only a very little understanding has been developed by experts to make any conclusive remarks about the flow process that occurs inside the auger/barrel and die sections. Smooth extrusion depends on many factors like the clay particle size, moisture contents, efficiency of the de-airing system, drive elements and its control systems, extrusion pressure, die design, pitch and profile of the auger, clearance between auger tip and the barrel and most importantly the plasticity of the slip (clay-water mixture).The main performance parameters

of a de-airing type vacuum extruder includes extrusion rate, extrusion pressure, material flow velocity at the die section and power consumption. The geometric and operating parameters that have direct influence on the performance includes auger speed, auger diameter, uncompacted density of clay, material of construction of augers and moisture content of the clay. A brief overview about extruder's performance characters is presented further in this chapter.

Extrusion rate

It is quantified by the amount of bricks produced per unit of time (usually rate per hour). As mentioned earlier in this chapter, modern vacuum extruders are designed to produce more than 12,000 bricks per hour and this depends upon two main factors- the auger pitch and plasticity of the clay. Since the moisture content is controlled by product requirement and other factors, it is relevant in this context to just to talk about the dependency of extrusion rate on auger pitch. Figure A-D- 7 shows the various auger geometrical variables necessary for determining the extrusion rate.
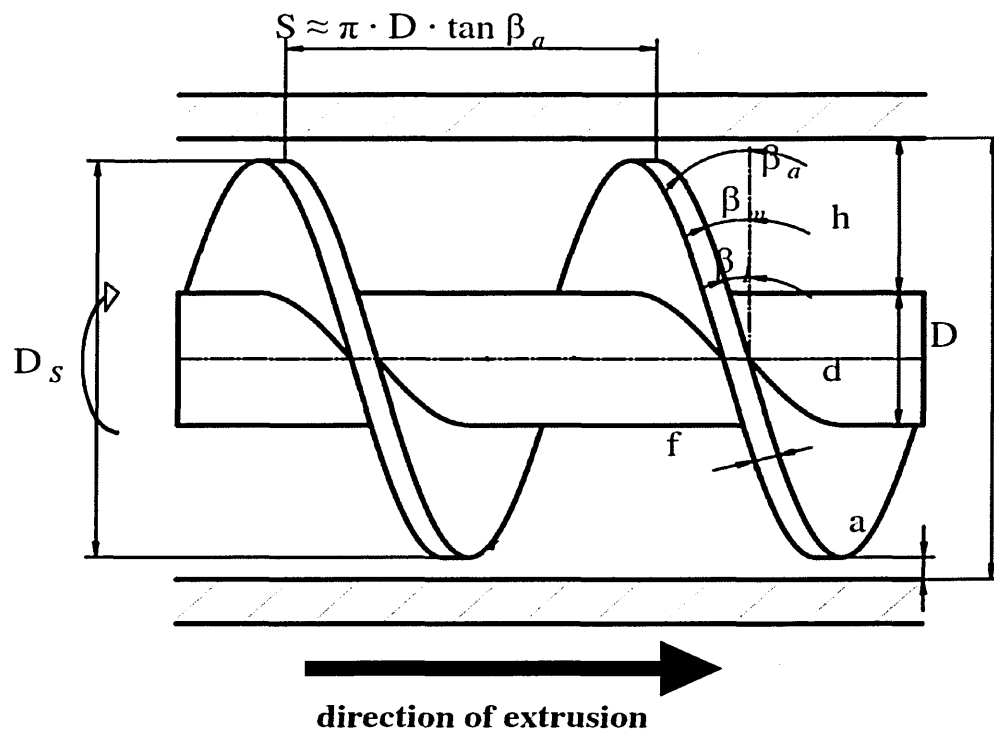

$$S \approx \pi \cdot D \cdot \tan \beta_a$$

direction of extrusion

Figure A-D- 7 Auger geometrical parameters

[Source: Händle, 2007]

217

Where,

D_s =Diameter of the auger

f   =Flight thickness or auger blade thickness

a   =Clearance between the auger and barrel

d   =Hub diameter

D   =Barrel diameter

h   =area of effective gap between hub and barrel

β   =helix angle or angle of inclination

S   =Pitch distance or effective distance which can be determined using Equation A.D.1

$$S = \pi * D * \tan \beta a - A.D.1$$

Where, D- diameter of the barrel, βa- Helix angle measured at the tip of the auger.

Using the above formula, once the auger pitch has been determined, the swept volume of the auger or the volume of the material discharged per revolution of the auger shall be determined by Equation A.D.2.

$$Vs = S * h - A.D.2$$

Where, Vs = Swept volume (m³).

The final, volumetric extrusion rate of an auger shall be determined using Equation A.D.3.

$$Q_v = \frac{Vs \times n}{60} \left(\frac{m^3}{sec}\right) - A.D.3$$

Where, Q_v= Volumetric discharge rate, n = auger speed in rpm.

It is a common practice in the industries, to express the discharge rate in terms of mass of clay extruded per unit time. This shall be obtained by including the density of the final clay column in the above equation as shown in Equation A.D.4.

$$Q_m = \frac{Vs \times n \times \rho}{60} \left(\frac{Kg}{sec}\right) - A.D.4$$

Where, Q_m= discharge rate, ρ=density of extrudate

It is clearly evident from the above presented equations that the discharge rate of an extruder depends on the geometrical and operational parameters of auger. Hence in actual scenarios the required discharge rate is obtained by making necessary adjustments to one of the above referred parameters on a trial and error basis.

Extrusion pressure

Extrusion pressure is another important flow parameter that has a more significant role in determining the shape, stiffness and quality of the extrudate (extruded product). The clay material from the charging zone will flow through the auger convolutions and will fill the extruder and barrel chamber slowly. The decrease in flow area between the die and auger-barrel chamber facilitates the material to build up in this zone and impart pressure on the extruder and die sections gradually. The extrusion pressure developed during extrusion depends mostly on the clay moisture content, extrusion speed, yield point of the material and throughput. The pressure raises from a negative value (at the entrance of the extruder- charging zone) to a maximum value at the tip of the auger and then gradually decreases to reach atmospheric pressure or value equal to the condition at the downstream side of the die **[Bender and Händle, 1982]**.Figure A-D- 8 shows the pressure profile observed in a typical vacuum type de-airing extruder.
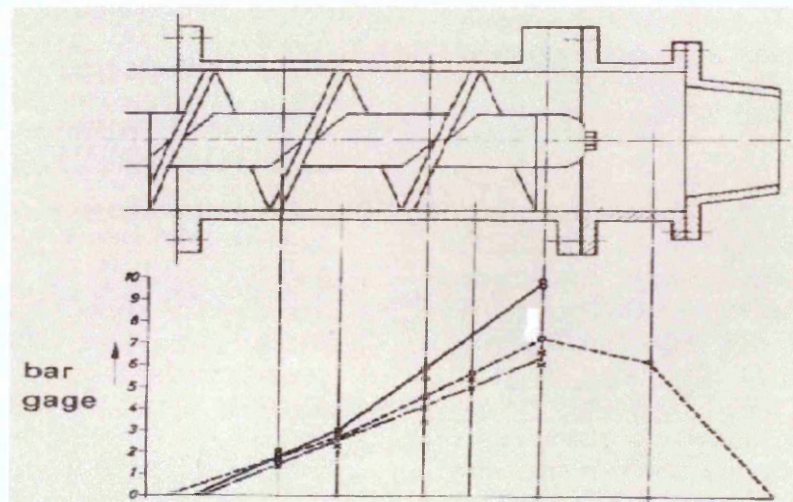

Figure A-D- 8 Vacuum extruder pressure profile

[Source: Bender and Händle, 1982]

219

It is clearly understood form the graph that the front side of an auger will always be subjected to high pressure and in turn a high wear rate occurs. Hence a greater care is required in designing the auger profile and selecting suitable material of construction. Even though the pressure is dropping in the die section, the design should be able to accommodate the stress and heat induced, due to the loss in pressure. While using dies with core in stiff extrusion process, the dies are designed with sufficient strength and flexibility to accommodate any stress and forces induced due to the extrusion process. Significant scientific works dealing with the flow of clay and assessing the performance characters of an extruder system is reviewed in Chapter 2.

Power

Stiff extrusion is a high pressure extrusion process; extruders used in this process are always robustly built to withstand this pressure, stress and wear induced. This makes them to be a significant power consuming device used in brick making process. The power consumption depends upon both operational and performance characters discussed above. Within the industries, through repeated lab based experimental works and data obtained from field, guidelines on power consumption pattern are prepared for the use of design engineers and it varies with respect to machines and manufacturers. Due to the complexities involved in the process of extrusion and extruder design, there is a lack of specific data or an empirical method that provides an overall picture about the power consumption pattern of any extruder system.

Quality of extrudate

The quality and nature of the extruded product determines the clay preparation, extrusion technique and equipments required. Stiff extrusion is renowned for producing complex shapes with sharp edges and smooth surfaces. The quality of a stiff extruded clay column depends upon one or many of the process and operational parameters discussed above. A Clay column with right stiffness and free of defects is what required at the end of process. The stiffness of the material is determined by the extrusion pressure and by achieving a suitable extrusion pressure for a given raw material

220

condition, column with unique density and mechanical properties can be produced through stiff extrusion process (density of the loose clay at the charging zone will be typically around 1600 kgm^{-3} and the density of extruded column varies between 2100 kgm^{-3} to 2800 kgm^{-3} **[Händle, 2007]**). Predominant problems that occur in the extruded products include texturation (alignment of clay particles- important for uniform mechanical properties in all direction), void formation (inclusion of air bubbles, which in turn induces crack during firing process) and lamination.

Conclusion

The use of extruders and the evolution of vacuum extruders in the brick industry were reviewed in this chapter. The process and operational parameters that are necessary to assess the performance of an extruder system was also reviewed. Through the various facts presented above, it is evident that the development processes that were undertaken to enhance the design of the extruder system were through empirical methods or repeated field trials and there is a lack in application of advanced computing tools towards the design and development of extruders used in the stiff extrusion process. Through the introduction of such tools towards the design and development of extruders will not solve the entire problem and the challenges faced by the brick industry, it will help to speed up the process in certain areas that will help in the efficient and sustainable operation.